AUGUST 2023

Ph.D. in Civil Engineering

RUYA MEHDI ZAINALABDEEN ZAINALABDEEN

REPUBLIC OF TÜRKİYE

GAZİANTEP UNIVERSITY

GRADUATE SCHOOL OF NATURAL & APPLIED SCIENCES

FLOW COEFFICIENT MODELING USING THE FUZZY SMRGT METHOD COMPARED WITH ANFIS AND ANN METHODS: AN EXAMPLE OF THE AKSU RIVER BASIN

Ph.D. THESIS

IN

CIVIL ENGINEERING

BY

RUYA MEHDI ZAINALABDEEN ZAINALABDEEN

AUGUST 2023

FLOW COEFFICIENT MODELING USING THE FUZZY SMRGT METHOD COMPARED WITH ANFIS AND ANN METHODS: AN EXAMPLE OF THE AKSU RIVER BASIN

Ph.D. THESIS

in

Civil Engineering

Gaziantep University

Supervisor

Asst. Prof. Dr. Ayse Yeter GÜNAL

by

Ruya Mehdi Zainalabdeen ZAINALABDEEN

August 2023

FLOW COEFFICIENT MODELING USING THE FUZZY SMRGT METHOD COMPARED WITH ANFIS AND ANN METHODS: AN EXAMPLE OF THE AKSU RIVER BASIN

submitted by **ZAINALABDEEN, Ruya Mehdi zainalabdeen** in partial fulfillment of the requirements for the degree of Master of Science in **Civil Engineering, Gaziantep University** is approved by,

Prof. Dr. Mehmet İshak YÜCE
Director of the Graduate School of Natural and Applied Sciences. ………..............

Prof.Dr. Nildem TAYŞİ
Head of the Department of Civil Engineering ………..............

Asst. Prof. Dr. Ayse Yeter GÜNAL
Supervisor, Civil Engineering
Gaziantep University ………..............

Exam Date: 23 AUGUST 2023

Examining Committee Members:

Prof. Dr. Zeynel Fuat TOPRAK
Dicle University ………..............

Prof. Dr. Aytaç GÜVEN
Gaziantep University ………..............

Prof. Dr. Kasim MERMERDAŞ
Harran University ………..............

Prof. Dr. Mustafa GÜNAL
Gaziantep University ………..............

Asst. Prof. Dr. Ayşe Y. GÜNAL
Gaziantep University ………..............

I hereby declare that all information in this document has been obtained and presented in accordance with academic rules and ethical conduct. I also declare that, as required by these rules and conduct, I have fully cited and referenced all material and results that are not original to this work.

Ruya Mehdi Zainalabdeen ZAINALABDEEN

ABSTRACT

FLOW COEFFICIENT MODELING USING THE FUZZY SMRGT METHOD COMPARED WITH ANFIS AND ANN METHODS: AN EXAMPLE OF THE AKSU RIVER BASIN

ZAINALABDEEN, Ruya Mehdi zainalabdeen
Ph.D. in Civil Engineering
Supervisor: Asst. Prof. Dr. Ayse Yeter GUNAL
August 2023
203 pages

Estimating the flow coefficient is a vital hydrological procedure that holds considerable importance in flood prediction, water resource management, and flood mitigation. It is hard to accurately determine the flow coefficient without a good understanding of the river basin's hydrology, climate, topography, and soil characteristics. The latest flow coefficient modeling literature describes several methods. Most of these methods use opaque, non-generalizable methodologies. Therefore, this research employed three distinct methodologies; specifically, the Adaptive Neural Fuzzy Inference System (ANFIS), the Simple Membership Function and the Fuzzy Rules Generation Technique (SMRGT) are all examples of fuzzy inference systems, and the Artificial Neural Network (ANN), to achieve its objectives. The Aksu river basin in Antalya, Turkey, was chosen as the study area. The models underwent multiple permutations of precipitation, temperature, relative humidity, wind speed, land use, slope, and soil properties data tailored to the particular study region. The study analyzed the results using various performance metrics of the model, such as mean absolute error, Nash-Sutcliffe efficiency coefficient, root mean square error, and correlation coefficient. The results indicate that the SMRGT method resulted in a remarkable degree of accuracy in forecasting the flow coefficient, as demonstrated with the minimal RMSE and MAE values and high correlation coefficient values.

Key Words: Hydrological analysis, Flow coefficient, ANFIS, SMRGT, Neural network, Fuzzy logic.

ÖZET

BULANIK SMRGT YÖNTEMİ KULLANARAK AKIŞ KATSAYISINI MODELLEME VE ANFİS VE ANN YÖNTEMLERİYLE KARŞILAŞTIRILMASI: AKSU NEHRİ HAVZASI ÖRNEĞİ

ZAINALABDEEN, Ruya Mehdi zainalabdeen
Doktora Tezi, İnşaat Mühendisliği
Danışman: Dr. Öğr. Üyesi Ayşe Yeter GÜNAL
Ağustos 2023
203 sayfa

Akış katsayısının tahmini, taşkın tahmini, su kaynakları yönetimi ve taşkın azaltmada büyük önem taşıyan hayati bir hidrolojik prosedürdür. Nehir havzasının hidrolojisi, iklimi, topografyası ve toprak özellikleri iyi anlaşılmadan akış katsayısını doğru bir şekilde belirlemek zordur. En son akış katsayısı modelleme literatürü birkaç yöntemi açıklamaktadır. Bu yöntemlerin çoğu opak, genelleştirilemez metodolojiler kullanır. Bu nedenle, bu araştırma üç farklı metodoloji kullanmıştır; özellikle Uyarlanabilir Sinirsel Bulanık Çıkarım Sistemi (ANFIS), Basit Üyelik Fonksiyonu ve Bulanık Kural Oluşturma Tekniği (SMRGT), ve Yapay Sinir Ağı'na (ANN). Çalışma alanı olarak Antalya ilindeki Aksu Nehri Havzası seçilmiştir. Modeller, belirli çalışma bölgesine uyarlanmış yağış, sıcaklık, bağıl nem, rüzgar hızı, arazi kullanımı, eğim ve toprak özellikleri verilerinin çoklu permütasyonlarına tabi tutuldu. Çalışma, ortalama mutlak hata, Nash-Sutcliffe verimlilik katsayısı, ortalama karesel hatanın kökü ve korelasyon katsayısı gibi modelin çeşitli performans ölçümlerini kullanarak sonuçlar analiz edildi. Sonuçlar, minimum RMSE ve MAE değerleri ve yüksek korelasyon katsayısı değerleri ile gösterildiği gibi, SMRGT yönteminin akış katsayısını tahmin etmede dikkate değer bir doğruluk derecesi ile sonuçlandığını göstermektedir.

Anahtar Kelimeler: Hidrolojik analiz, Belirsizlik, Akış katsayısı, ANFIS, SMRGT, Sinir ağı, Bulanık mantık.

To My

Father and mother which they span there live for me. Also, to my husband Erkan Kahveci who give the time and support to reach this level from the knowledge

ACKNOWLEDGEMENTS

I would like to thank my supervisor, Asst. Prof. Dr. Ayşe Yeter GÜNAL for her guidance and support throughout the study. I am thankful for her encouragement and motivation. A special thanks to Prof. Dr. Zeynel Fuat TOPRAK, who has the spirit and substance of a genius: he consistently and convincingly conveyed a spirit of adventure and enthusiasm for science in terms of research related to teaching. This study would not have been possible without his guidance and consistent assistance. I would like to express my love and gratitude to my family for their support, always best wishes.

TABLE OF CONTENTS

LIST OF TABLES

Page

LIST OF FIGURES

Page

LIST OF SYMBOLS/ABBREVIATIONS

ANFIS	Adaptive Neural Fuzzy Inference System
AI	Adaptive Integration
A	Area
ANN	Artificial Neural Network
BDD	Basic Defuzzification Distributions
BOA	Bisector Of Area
BP	Back-Propagation
CT	warm and dry tropical air
CDD	Constraint Decision Defuzzification
COG	Center Of Gravity
C_I	Core value
°C	Celsius
CVX	Coefficient of Variation
CSX	Coefficient of Skewness
C	Flow Coefficient
DEM	Digital Elevation Model
EM-DAT	Emergency Events Database
EPA	Environmental Protection Agency
EUW	Extended Unit Width
ECOA	Extended Center Of the Area
EQM	Extended Quality Method
FL	Fuzzy Logic
FIS	Fuzzy Inference System
FOM	First Of Maximum
FCD	Fuzzy Clustering Defuzzification
FM	Fuzzy Mean

FM	Fuzzy Mean
FRS	Fuzzy Rules
FFNN	Feed Forward Neural Network
FLSR	Fuzzy Least Square Regression
GIS	Geographic Information Systems
GLSD	Generalized Level Set Defuzzification
GL	Groundwater Level
GRNN	Generalized Regression Neural Networks
GBELLMF	Generalized Bell Membership Functions
IPCC	Intergovernmental Panel on Climate Change
I	Rainfall Intensity
ICOG	Indexed Center Of Gravity
IT	Information Technology
IV	Influence Value
KM	Kilometers
LU	Land Use
LOM	Last Of Maximum
LMBP-NN	Levenberg-Marquardt Back-Propagation Neural Network
MAE	Mean Absolute Error
MASW	Multiple Analyses of Surface Wave
MLR	Multiple Linear Regression
M5T	M5 Decision Trees
MFL	Mamdani Fuzzy Logic
MM	Millimeters
MFS	Membership Functions
MNLR	Multiple Nonlinear Regression
ML	Machine Learning
MT	Moist Tropical
MK	Mann-Kendal
NF	Neuro Fuzzy
NSE	Nash-Sutcliffe Efficiency Coefficient

nu	Right-angled triangles
O	Two Intersecting Neighbor Membership Functions
OAT	Once At Time
POSs	Precipitation Observation Stations
pimf	π shaped membership function
QM	Quality Method
Q	Flow Rate
q	Drainage Area Yield
RSS	Residuals Sum of Squares
Rh	Relative humidity
RMSE	Root Mean Square Error
R^2	Coefficient of Determination
RME	Rock Mass Excitability
RCOM	Random Choice Of Maximum
r	Correlation Coefficient
S	Slope
SMRGT	Simple Membership functions and fuzzy Rules Generation Techniques
SCS-CN	Soil Conservation Service – Curve Number
SVM	Support Vector Machine
SFM	SMRGT Fuzzy Modeler
SLIDE	Semi-Linear Defuzzification
TS	Takagi-Sugeno
To	Soil Dominant Vibration Period
TABB	Turkish Disaster Database
TSMS	Turkish State Meteorological Service
UW	Unit Width
Vs	Seismic Wave Velocity
WFM	Weighted Fuzzy Mean
Ws	Wind Speed

$\mathbf{X_{nor.}}$	Normalized Data
$\mathbf{X}$	Original Data
$\mathbf{X_{min}}$	Minimum of the Original Data
$\mathbf{X_{max}}$	Maximum of the Original Data
$\mathbf{Z}$	Standardized test statistic
$\boldsymbol{\sigma}$	Standard deviation
$\boldsymbol{\alpha}$	Alpha

CHAPTER I

INTRODUCTION

1.1 Background

Water is considered to be one of the most remarkable substances on Earth. Approximately 71% of the planet's surface is covered by water, with the remaining 29% being comprised of land. Water is considered to be one of the most crucial natural resources that are currently available. It is a fundamental requirement for all stages of human life, both in terms of its presence and quality.Worldwide water usage increased by a factor of ten in the year 1900. It is projected that by the year 2025, there will be a 70% increase in domestic water consumption, a 20% increase in industrial water consumption, and a 17% increase in agricultural water consumption. The escalating rates of water consumption have led to a rapid depletion of clean water sources, primarily due to the effects of industrialization and pollution. Presently, an estimated 20% of the global population, which amounts to approximately 6 billion individuals, is believed to be devoid of access to potable water. The per capita water supply was 16,800 m3 in 1950, and it declined to 7,300 m3 by 2000. By the year 2025, it is estimated that the worldwide populace will attain 8 billion individuals, while the anticipated per capita water usage is expected to decline to roughly 4,800 cubic meters. The reduction in consumption is anticipated to lead to a diminution of water resources. It is projected that numerous water sources will be polluted by the year 2025. Consequently, water sourced from these locations will become unsuitable for consumption (Onur et al., 2016).The occurrence of severe water-related incidents has intensified the magnitude of human casualties and financial damages attributed to human activities. There exist several factors that could contribute to the escalation of hazards associated with water. Furthermore, it is probable that climate change and anthropogenic actions will augment the probability of hazardous events that carry substantial societalimplications, such as desertification, river depletion, reservoir capacity reduction, and dam failure. The urbanization of flood-prone areas is also influenced by population growth and economic expansion. Insufficient control over water resources, in conjunction with inadequate emergency management organizations and infrastructure, diminishes a community's capacity to endure perilous occurrences, thus amplifying the risk to human life and assets.

1.2 The Hydrological Cycle and Water Circulation

The field of study concerned with the dynamics and transport of water is commonly referred to as "hydro-mechanical." The applications of this system that involve the utilization of techniques related to fluid mechanics are commonly referred to as "hydraulic." Hydrology is the scientific discipline that is concerned with the study of the movement, path, circulation, properties, and composition of water on Earth. Hydrology is a fundamental and applied scientific discipline that encompasses the examination of the attributes, spatial arrangement, physical and chemical attributes, and the hydrological cycle of water in the terrestrial, subsurface, and atmospheric domains, as well as their interrelationships with the biotic and abiotic components of the environment. This depiction of hydrology encompasses various scientific disciplines. In contemporary times, the demarcation between hydrology and other scientific disciplines has become increasingly challenging. For instance, meteorology pertains to the study of water in the atmosphere, oceanography focuses on water in the sea, and geology concerns itself with groundwater.Water is a vital resource for the growth and well-being of human societies worldwide, owing to its indispensability in sustaining all forms of life as a result of the natural cycle. Nevertheless, individuals persist in squandering water as though it were an inexhaustible resource that replenishes itself perpetually. Nonetheless, the availability of water is limited, and its depletion can occur expeditiously due to inappropriate utilization and pollution. The escalating urbanization, industrialization, and agricultural expansion in developing nations are amplifying the demand for freshwater resources. The impact of global warming on the worldwide water cycle suggests that the future availability of potable water may be more uncertain than ever before (Onur, 2015).

Throughout history, human populations have established settlements in various geographical locations according to their specific requirements. Over time, the progression and development of humanity have coincided with the ongoing flow of life. The direction of this flow is primarily oriented toward fulfilling human needs. As a result, settlements and major urban centers have been established and progressed in areas with abundant water resources, including oceans, lakes, and rivers. Prominent instances include significant urban centers like Venice, Paris, New York, and Istanbul (Yenigün ve Gümüş, 2009).

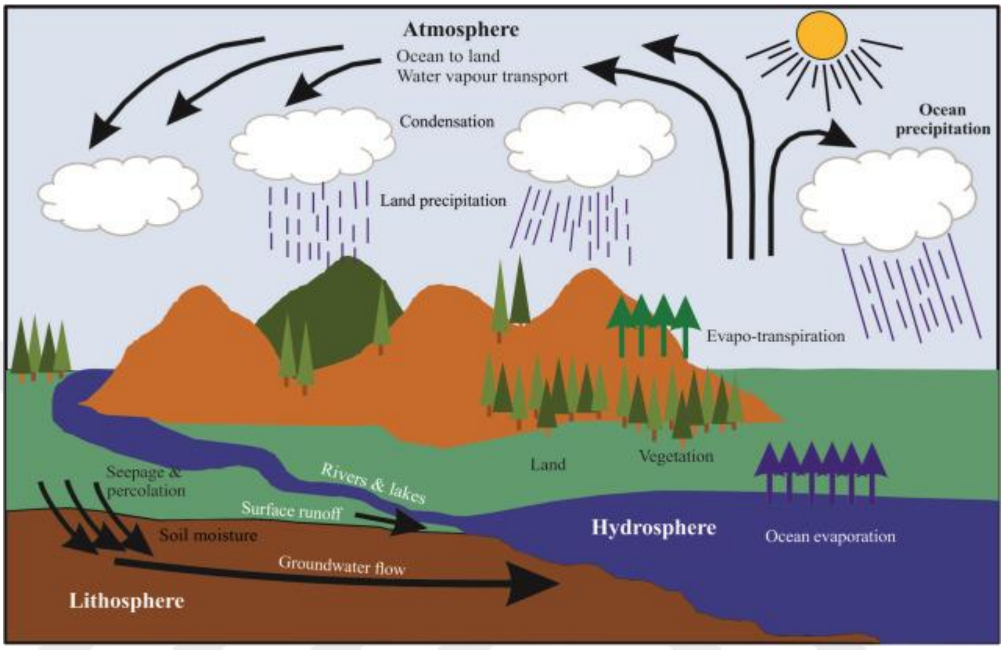

Figure 1. 1 Hydrological Cycle (Singh and Singh, 2021)

The river is a hydrological feature characterized by the continuous movement of a significant volume of water from areas of higher elevation to lower elevations, driven by the force of gravity. The topography of the earth's surface has not always been uniform. The subject exhibits a tendency towards a specific orientation. Initially, the water exhibits a downhill flow in the form of minor streams. As tributaries flow downstream, they confluence to create larger rivers that exceed their individual sizes. As a result of this hydrological process, waterways ultimately converge with large bodies of saltwater, such as seas or oceans. The formation of a lake occurs when water enters a restricted region characterized by a sharp incline in topography.

The hydrologic cycle is a fundamental process that illustrates the uninterrupted movement of water across the diverse constituents of the Earth's climatic structure. Water is sourced from various locations such as the oceans, atmosphere, and subterranean reservoirs. The interdependence of the climate system relies on the transfer of water between distinct basins during various stages. Water evaporates from the earth's surface and both oceans, circulating as water vapor throughout the planet's atmosphere. Water vapor undergoes a process of gradual condensation within the Earth's atmosphere, ultimately resulting in its precipitation as various forms of frozen or liquid precipitation, such as sleet, snow, hail, and rain. The aforementioned form of precipitation has the potential to descend upon exposed bodies of water, undergo absorption by flora, and subsequently transform into either surface runoff or groundwater recharge. Percolation of water through the land surface can lead to its infiltration into subsurface regions, where it can be incorporated into the groundwater reservoir prior to resurfacing as streamflow or, in coastal regions, undergoing mixing with saline water. In the end, the water is returned to the ocean and undergoes evaporation, thereby completing the water cycle (Thomas Pagano and Sorooshian, 2002). The estimated quantity of water produced on the surface of the Earth on a yearly basis is roughly 577,000 cubic kilometers. An estimated volume of 74,200 km^3 and 502,800 km^3 of water undergoes the process of evaporation from the terrestrial surface and the world's oceans, respectively. The quantity of water that precipitates in the atmosphere is equivalent to the amount of water that falls on land and sea, with 119,000 km^3 and 458,000 km^3, respectively. The hydrological phenomenon of the river's water capacity is determined by the variance between the amount of precipitation and evaporation from the land. The total volume of water capacity is estimated to be 44,800 km^3/year, with 42,700 km^3/year being attributed to river water and 2100 km^3/year to groundwater runoff that eventually reaches the ocean. The aforementioned are the principal sources of freshwater that sustain human existence and commercial operations. The hydrological cycle is illustrated in Figure 1.1, highlighting its crucial steps. Precipitation is a crucial component of the hydrological cycle and serves as the primary source of water for the earth's surface, as evidenced by the field of hydrology. The quantity of precipitation that is retained by plants, such as vegetation and trees, is contingent upon various factors, including their respective classifications, developmental phases, and degree of vegetative coverage, as well as the magnitude and length of rainfall events.

Several flow processes can be identified, including Horton overland flow. This phenomenon transpires when the intensity of precipitation surpasses the soil's capacity for infiltration, leading to the accumulation of water on the ground surface.

Horton overland flow is a phenomenon that is commonly observed in regions characterized by arid and semiarid climates, where there is a high amount of precipitation and limited vegetation cover. Saturation overland flow is a distinct form of flow that arises when the soil reaches its saturation point due to the ascent of groundwater to the surface of the land. Overland flows that are saturated are frequently observed in regions with high precipitation. Stream flows occur as a result of the gradual transformation of surface water flow into a minor stream. Upon entering the catchment drainage system, water is conveyed through channels. The phenomenon of fluid flow is not confined solely to the Earth's surface but instead occurs subsurface as well. The subsurface is infiltrated by water through two distinct mechanisms, namely matrix and macro pore flow. These mechanisms are both categorized as forms of unsaturated underground flow. In the event that the saturation conductivity of a given layer is comparatively lower than that of the overlying layer, it will result in the occurrence of perched subsurface flow. The velocity of groundwater movement within saturated zones can vary, exhibiting either a high or low rate of flow.

The initial stage of any hydrological investigation involves the acquisition of essential data, including but not limited to current measurements, evaporation rates, precipitation levels, and temperature readings. It is imperative that hydrological processes remain as close to their natural state as possible. Thus, it is imperative to furnish ample instruments and metrics.

1.3 Flow Coefficient Definition and its Importance

The flow coefficient, also known as the runoff coefficient, is a unitless variable that ranges from 0 to 1. The rainfall-flow relation was originally suggested by Kuichling (1889). Wong (2002) stated that this concept has been used over 100 years. Hundreds of methods have been used for obtaining the best result for flow estimation from rainfall data. Most of these approaches are empirical. Drainage area, main channel slope, drainage density are some of the input requirements of various geomorphologic parameters for these empirical approaches. Chow (1962) and Haan et al. (1994) stated that they are used rather arbitrarily. The simplest linear method relates the flow rate to the basin area and rainfall intensity through the flow coefficient. The main purpose of study of Sen and Altunkaynak (2006) is to understand the relationship between rainfall intensity i and flow rate Q on a monthly basis. This can be explained as follows

$$Q=CiA \tag{1.1}$$

The variable C represents the flow coefficient. With the exception of drainage area, all the variables encompassed in this formulation possess hydrological attributes that are representative of the natural water cycle within a given geographical region. By performing the operation of dividing both sides of Equation (1.1) by the variable A, it is possible to formulate the expression in relation to hydrological variables. Therefore, the revised formulation is as follows:

$$q=Ci \tag{1.2}$$

The variable q represents the drainage area yield, which is defined as the depth of direct runoff over a catchment per unit area. The runoff coefficient may be characterised as a numerical ratio;

$$C=q/i \tag{1.3}$$

The classical 'rational technique' assumes a constant value, which is determined by the features of the drainage basin (Dooge, 1957). Both variable q and variable i exhibit stochastic characteristics, indicating that variable C is likely to have a similar behaviour. However, it is common in hydrological practises to treat C as a constant and regard it as a deterministic value. According to Chow (1962), the key factors in establishing the C value for basin characteristics are vegetal cover, soil type, and the percentage of impermeable land.

Higher values of the coefficient signify that a larger proportion of precipitation transforms into runoff, while lower values indicate that a greater proportion of precipitation infiltrates into the soil and recharges groundwater. The value of the flow coefficient is influenced by various factors, including but not limited to soil type, land use, slope, vegetation cover, and antecedent moisture conditions. The flow coefficient plays a crucial role in flood control and the design of hydraulic structures such as culverts, bridges, and dams. The flow coefficient holds significant importance in flood management, as it serves as a predictive measure for the peak flow rate of a river or stream in the event of a storm. The aforementioned data is utilized for the purpose of devising a comprehensive strategy for ensuring sufficient drainage and effective management of erosion. In the process of designing a hydraulic structure, the flow coefficient is utilized to approximate the volume of water that will traverse the structure, thereby aiding in determining its size and capacity (Chow et al., 1988; Singh, 1995; USDA Natural Resources Conservation Service, 1986).

Estimating the flow coefficient is hard because there are so many factors that affect runoff and how they interact with each other. Flow coefficients can be estimated in a number of ways, from simple empirical equations based on land use and soil type to more complex physically based models that simulate the hydrological processes that lead to runoff. In the past few years, machine-learning algorithms like artificial neural networks and fuzzy logic have been used more and more to estimate flow coefficients. This is because they can take into account the complex relationships between different factors and make accurate predictions (Sevgin, 2021, Firat, 2007, Karakaya, 2018). A number of situations in civil engineering necessitate the determination of the flow coefficient. For starters, it is necessary-have a metric when planning drainage systems, which are vital to controlling floods in populated areas. For the purpose of assessing the drainage system's capacity and making sure it can handle peak flows during heavy rainfall events, an accurate estimation of the flow coefficient is required. Damage to infrastructure and property, as well as human lives, can result from flooding if drainage systems are not adequately planned for and sized. Additionally, the flow coefficient is used in the design of water supply systems, such as pipelines and canals, to determine the flow rate and capacity of the system. Accurate flow coefficient estimation is necessary to ensure that the system can meet the demands of the users and to prevent overloading or underutilization of the system.

The flow coefficient holds significant importance in the development of erosion control strategies, including retaining walls, riprap, and gabions, that are implemented to safeguard riverbanks, shorelines, and other vulnerable regions. If engineers can precisely estimate the flow coefficient, they have the capacity to design structures that can endure the erosive impacts of water and furnish sufficient safeguards against erosion. The flow coefficient holds significant importance in the management of floodplains and the establishment of zoning regulations. The precise estimation of flow coefficient can aid in the identification of regions that are susceptible to flooding, as well as in the determination of measures for mitigating floods and policies for land use that can decrease the likelihood of flood damage.

1.4 Climate Change

The hydrology and water resources are being significantly impacted by climate change, leading to changes in the availability, quality, and distribution of water worldwide. These changes in temperature and precipitation patterns are primarily responsible for alterations in the water cycle (Huntington, 2006). The changes mentioned have significant consequences for water management, food security, energy production, and ecosystem services. Climate change has a significant impact on hydrology and water resources, primarily by altering the water cycle. As temperatures rise, the Earth's surface experiences an increase in water evaporation, resulting in a higher concentration of water vapor in the atmosphere. According to the IPCC (2014), the rise in water vapor can lead to an increase in both the frequency and intensity of precipitation events. Consequently, certain areas may experience more frequent and severe flooding. Changes in precipitation patterns, such as reduced rainfall or increased rainfall variability, may lead to longer and more severe droughts in other regions (Barnett et al., 2005).

Variations in precipitation timing, intensity, and duration can have an impact on the accessibility of water for agricultural, hydropower, and residential purposes. Elevated temperatures have the potential to induce alterations in the schedule of snowmelt and the quantity of snow accumulation in mountainous areas, thereby influencing the timing and magnitude of water availability for irrigation and residential purposes. This event may have noteworthy consequences for areas that rely on snowmelt and glaciers as their primary source of water (Immerzeel et al., 2010).

The impact of climate change extends to the susceptibility of societies and physical structures to hydrological anomalies, including but not limited to floods and droughts. It is anticipated that numerous regions will experience a rise in the frequency and severity of extreme weather phenomena, thereby jeopardizing the safety and livelihoods of millions of individuals. The occurrence of floods and droughts can result in substantial harm to infrastructure, including but not limited to roads, bridges, and buildings, thereby influencing the economy and social stability.

Floods have the potential to result in waterborne illnesses, displacement, and fatalities, particularly in regions that are densely populated and situated at lower elevations (IPCC, 2014).

Advancements in hydrological modeling, remote sensing, and data assimilation methodologies have enhanced our comprehension of the effects of climate change on hydrology and water resources. Satellite data has the potential to be utilized for precipitation and evapotranspiration estimation, thereby offering significant insights into water resource management and emergency preparedness. Hydrological models have the potential to simulate the effects of forthcoming climate scenarios on water quality and availability. This information can be utilized to make informed decisions regarding water management and adaptation strategies (IPCC, 2014).

1.5 Purpose and Scope of the Thesis

This research aims to compare three distinct methodologies, namely ANFIS, SMRGT, and ANN, to determine the flow coefficient in Antalya's Aksu River basin. The study region was selected due to its high potential for floods and the importance of accurate flow coefficient estimation in managing water resources and mitigating flood damag-es. The models were developed using various data, including precipitation, tempera-ture, relative humidity, wind speed, land use, and soil properties, tailored to the par-ticular study region. The research carried out a comparative examination of the out-comes, considering diverse performance metrics of the model, such as MAE, NSE, RMSE, and R^2. The study's findings will contribute to more accurate flood prediction, water resource management, and flood mitigation strategies, benefiting the residents and stakeholders in the Aksu River basin and potentially other flood-prone regions. Additionally, the innovative modeling techniques employed in this study serve as a foundation for future research in other river basins facing similar challenges.

The objective of the study is to apply and compare the performance of three well-established methodologies, namely Fuzzy SMRGT, ANN, and ANFIS, for accurately estimating flow coefficients in the Antalya River Basin, and to evaluate the suitability of these methodologies in a real-world river basin context, considering factors such as da-ta availability, basin characteristics, and modeling requirements.

Previous studies (Smith, 1995; Jang, 1993; Abrahart & See, 2000) have primarily relied on traditional statistical approaches, which not adequately capture the complex nonlinear patterns exhibited by flow data. By introducing these advanced modeling techniques, this research attempts to overcome established approaches' shortcomings and provide more accurate estimations of flow coefficients. The innovative contribution of this study lies in its integration of fuzzy logic, genetic training, neural networks, and adaptive inference systems. This approach considers uncertainties and linguistic variables associated with flow coefficient estimation, which need to be adequately ad-dressed in previous studies.

Furthermore, incorporating ANN and ANFIS models enables the capturing of nonlinear relationships, resulting in improved accuracy. Fuzzy SMRGT models provide a robust framework for handling uncertainty and variability in the Antalya River Basin context.

Additionally, the innovative modeling techniques employed in this study serve as a foundation for future research in other river basins facing similar challenges. The implementation of Fuzzy SMRGT, ANN, and ANFIS approaches for flow coefficient estimation in the Antalya River Basin has certain limitations that should be consid-ered; the accessibility and quality of data are critical factors in estimating accuracy limited or unreliable data for critical variables hinder the model's performance. The model's applicability to other river basins varies due to differences in hydrological characteristics and environmental factors. Factors such as varying flow patterns, land use, and water management practices significantly impact the model's effectiveness in different contexts. The calibration and validation of the model are essential to ensure reliable results, as improper parameterization or validation processes lead to biased estimations.

Furthermore, the inherent uncertainties and assumptions associated with the models should be acknowledged, as they influence the reliability of the estimations. Despite these limitations, integrating Fuzzy SMRGT, ANN, and ANFIS approaches improve flow coefficient estimation in the Antalya River Basin and other similar river basins facing similar challenges. Further research and validation in different geo-graphical contexts are necessary to assess this approach's applicability and effectiveness.

The research compares three distinct methodologies, namely ANFIS, SMRGT, and ANN, for estimating the flow coefficient in Antalya's Aksu River basin. Acknowledging the models' limitations and their broader applicability is crucial. One limitation is that the comparison of methodologies is confined to the specific study region of Antalya's Aksu River basin. The hydrological characteristics of different regions vary, and therefore, the performance of these models differs in other geographic locations. To apply the findings to other river basins, it is necessary to consider those regions' unique environmental and hydrological conditions.

Moreover, the reliability and accuracy of the model's quality and availability of input data are crucial. The study utilizes diverse data sets, including precipitation, temperature, relative humidity, wind speed, land use, and soil properties, explicitly tailored to the Aksu River basin. However, in regions where data availability or quality is different, the performance of these models needs to be improved. Additionally, while the study employs quantitative performance metrics such as MAE, NSE, RMSE, and R^2 to compare the models, other factors like interpretability, computational efficiency, and ease of implementation are also considered in practical applications.

The current research presents a novel approach utilizing an Artificial Neural Network (ANN), Adaptive Neural Fuzzy Inference System (ANFIS), Simple Membership functions, and fuzzy Rules Generation Techniques (SMRGT) models to describe the nonlinear connection between influencing factors and flow coefficients properly. In addition, empirical measurements and comparison analysis are included in the study to support the proposed model. Relying exclusively on climate, topography, and soil characteristics of the river basin as input and subsequently evaluating the effectiveness of the employed methodology about its predictive aptitude. Another objective of this investigation is to present a novel approach, Fuzzy SMRGT, which precisely assess the river flow coefficient.

1.6 Organization of the Thesis

This thesis will be organized into the following sections:

Chapter 1- Introduction: Provides an introduction to the research topic, encompassing a concise outline of the study's range and particular aims. The introduction of the thesis includes a presentation of its objectives and organization.

Chapter 2- Literature review: This chapter provides an extensive examination of the pertinent literature relevant to Fuzzy logic, Simple Membership functions and fuzzy Rules Generation Technique (SMRGT), ANFIS, and ANN in flow coefficient modeling, and other techniques employed in hydrological modeling.

Chapter 3-Study area: The study area is comprehensively introduced, encompassing various aspects such as geography, climate, meteorology, geology characteristics, and water resource management in the Aksu River Basin.

Chapter 4- Methodology: elucidates the requisite procedures and analyses conducted through the utilization of Simple Membership functions and fuzzy Rules Generation Technique (SMRGT), as well as the Adaptive Neuro-Fuzzy Inference System and Artificial Neural Network techniques, in the construction of the models.

Chapter 5 - Results and Discussion: This chapter presents a comprehensive analysis and processing of the hydrological results obtained from the study area.

Chapter 6- Conclusions: The final chapter presents comprehensive findings and ramifications of the investigation.

CHAPTER II

LITERATURE REVIEW

2.1 Introduction

Studies have indicated that the flow coefficient's value is subject to variation across different studies, even within the same area, due to the influence of diverse factors. Hence, in the determination of flood flow rate, it would be more suitable for numerous researchers to employ analytical techniques on smaller geographical areas rather than the entirety of the region. According to Beven et al. (1979), hydrological models are mathematical or symbolic representations that depict anticipated or acknowledged functions of the distinct components of a hydrological cycle. Schultz (1993) posits that hydrological modeling is a reliable analytical tool for the study of hydrological systems. It is commonly employed by hydrologists and water resource engineers to develop integrated approaches for the effective management of water resources. Hydrological modeling techniques have been extensively employed for diverse objectives since the 1970s. The majority of modeling tools, however, have been primarily designed for implementation in wetland scenarios. In regions characterized by aridity and aridity transitioning to semi-aridity, there exist distinctive challenges that have not been adequately addressed. The progress of model development is intricately linked to the advancement of computational capabilities. During the 1930s, the initial event-based models were formulated and implemented through manual computation. Prior attempts have been made in Turkey to create a record of flood occurrences. However, the extent of data coverage and availability was restricted. The extant databases exhibit an inadequate representation of flood information with respect to both the quantity of entries and the granularity of data pertaining to discrete flood occurrences. A comprehensive and meticulous record of previous flood data can enhance the efficacy of preventive measures in the Republic of Turkey. The severity of a flood can be influenced by a variety of factors, including natural factors such as weather patterns, rainfall, sudden changes in air temperature, and rapid snowmelt. Additionally, topographic factors such as catchment shape, size, slope, and elevation, as well as soil properties, land use properties, and human-induced factors such as urbanization, hydraulic engineering practices, and unplanned infrastructure practices can also play a role.

2.2 Various Applications of Fuzzy Logic Method

A multitude of scholars spanning different time periods has conducted a wide range of investigations on the coefficient of river flow, utilizing diverse methodologies and models. Fuzzy logic models have been employed in various fields, such as civil engineering, water resources, and water management, as evidenced by a multitude of prior studies.

The concept of fuzzy logic denotes a fundamental change in the approach to computer logic. It facilitates computational and logical processes in a manner analogous to its facilitation of human behavior. Lutfu Askerzade published the initial documentation on the principles of fuzzy logic in 1965, as cited by Zadeh (1965). Zadeh posits that a significant portion of human cognition is characterized by vagueness and ambiguity. Zadeh (1965) commenced a novel examination of systems that incorporate uncertainty. Zadeh argues that restricting the attributes of assets and objects to binary values of zero and one is inadequate, given the multitude of gradations, continuums, and antitheses that exist in the actual world between these two extremes. (Karatas, 2018). Nevertheless, these concepts faced criticism from the Western world. This philosophical approach offers a straightforward and modern resolution to intricate and multifaceted issues across a wide range of disciplines and domains, including but not limited to science, mathematics, and engineering. According to Freksa et al. (2001), the frequency fuzzy logic theory posits that while facts may be fuzzy, their rules must not be ignored. Mamdani and Assilian first introduced the implementation of fuzzy logic in the control system of a steam engine in 1975.

The fuzzy logic method, introduced by Zadeh in 1965, has garnered significant attention and interest from scholars, researchers, and professionals across various disciplines. Kaufmann (1975) provides additional data in conjunction with exemplifying use cases. The employment of the method in civil engineering has demonstrated its efficacy in addressing issues characterized by the uncertainty of the vagueness type. During the early 1970s, the scientific and engineering community acknowledged the appropriateness and possibilities of the said implementation, as noted by Brown (1979) and Alley et al. (1979). Several civil engineering applications of this method have been developed thus far.

Following the successful implementation of fuzzy logic applications in Japan, fuzzy systems have been rapidly adopted worldwide, particularly within the engineering and industrial domains, since 1990. Several prominent corporations, including Chrysler, Canon, Mitsubishi, Boeing, General Motors, Allen, and Bradley, have implemented fuzzy systems within their operational procedures (Saka, 1999).

Fuzzy logic is a computational technique employed to represent imprecision inherent in a given system. There are various explanations for these uncertainties. Instances of measurement issues, slight fluctuations in values, potential data loss, and other uncertainties may arise (Cimen, 2002).

Several types of research were carried out to delineate the diverse origins of uncertainty in the field of civil engineering. Brown (1980) made a distinction between objective and subjective uncertainty and proposed the integration of subjective uncertainty with objective possibilities. Ayyub and Ibrahim (1990) and Alvi and Ayyub (1990) have suggested the usefulness of existing uncertainty events in the field of structural engineering. Several measures have been proposed in the literature to quantify uncertainty, such as the Hartley measure (1928), Shannon entropy (1948), U-uncertainty, dissonance in evidence, and degree of fuzziness.

The differentiation between system models and vagueness models was explored by Ben-Haim (2001). The individual asserted that the theory of fuzzy logic could be perceived as a fusion of two distinct concepts as it endeavors to develop a system that lacks a model and incorporates data that may possess ambiguity, imprecision, or uncertainty. Systems that demonstrate a level of robustness against erroneous changes are those whose performances are comprehensible and manageable. Robust systems are characterized by their ability to maintain consistent output despite variations in input under the assumption that the system operates within a range of uncertain conditions. The argument put forth suggests that fuzzy systems exhibit robustness owing to their ability to incorporate uncertainties in both input and output variables into the system structure. This stands in contrast to conventional systems analysis, which typically involves formulating a mathematical model based on a set of assumptions and subsequently accounting for uncertainties in individual parameters of the model. The study performed by Nayak et al. (2004) involved an analysis of the suitability of the FL method for real-time flood modeling, as well as an examination of the relationship between precipitation and flow. The study incorporated hourly flow and precipitation variables of the Narmada basin in India into flow estimation models, resulting in the creation of a fuzzy rule-based flood prediction model. It was discovered that the FL method could be effectively applied to the analysis of precipitation flow.

A workshop on the applications of fuzzy logic in civil engineering was held at Purdue University in 1985, with sponsorship from the National Science Foundation. The study's participants have identified several potential and current applications, including but not limited to nuclear power plants, dam safety screening, construction safety, wildlife quality, construction management, implementation of structures, facilities, and systems, damage analysis, and process and control of water and reservoir systems.

The utilization of fuzzy logic modeling was suggested by Esendal (2007) as a means to investigate the seasonal fluctuations in the water level of Throat Lake. The functions of the variables encompassed precipitation, flow, evaporation, and irrigation water demand. Empirical data were gathered during the period spanning from 1966 to 2000. Upon comparing the outcomes, it was found that the correlation coefficients exhibit a satisfactory level on average. The results produced by fuzzy logic were deemed reliable.

The planning of the Grand River basin in Ontario, Canada, was carried out by Alley et al. (1979) through the application of fuzzy logic. Fuzzy logic was taken into consideration for the purpose of analyzing the survey responses of local politicians and other relevant stakeholders. The decision-making process was augmented with non-quantitative and qualitative considerations, as well as the viewpoints of relevant stakeholders. The available alternatives were evaluated, compared, and ranked using a dominance matrix. The alternatives were assessed based on their cost-effectiveness.

A study was done by Keskin et al. (2004) in Turkey to estimate daily pan evaporation through the utilization of fuzzy models. By employing meteorological information, a technique was devised for approximating the daily pan evaporation. The researchers utilized an Artificial Neural Network (ANN) and multiple linear regression models to approximate pan evaporation based on a range of meteorological variables.

In their study, Mahabir et al. (2003) applied the FL method to forecast seasonal flow and implemented it in the Lodge Creek and Middle Creek basins. The Lodge Creek basin was the focus of a study wherein a prediction model for FL was developed based on rules. The study conducted a comparative analysis between the results obtained and the statistical-based studies previously recommended for the basins under consideration. The findings revealed that the FL method outperformed conventional methods.

The sudden destruction of dams can result in significant floods that may endanger human life and property. The potential failure of dams may result from various factors, including but not limited to unexpected floods, insufficient foundations, seismic activity, faulty construction, and project-related issues. Accurate estimation of flood flows and levels plays a crucial role in the development of emergency and early warning systems. Various empirical and numerical models have been employed to assess the flood resulting from the failure of a dam. Nonetheless, Demirpence (2001) employed a fuzzy logic model to ascertain the highest flow rate of the dam's filling that would result from its collapse. The principal benefit of employing a fuzzy logic model lies in its utilization of solely user-defined variables and uncomplicated rules to define information. The researcher conducted a comparative analysis between fuzzy logic and multiple linear regression models by utilizing correlation coefficients in his investigation.

Toprak and Akkoyun (2008) employed the fuzzy logic approach to categorize marble blocks. A model was developed which utilized the characteristics of marble blocks as input and expert classification as output. The authors assessed the efficacy of fuzzy models in block classification by employing diverse statistical techniques to compare their outcomes with actual data.

Gokay (1998) introduced a novel approach to evaluations by utilizing the fuzzy logic technique. The present study applied the Rock Mass Excitability (RME) approach to assess the suitability of fuzzy rock engineering classifications by elucidating the fundamental principles of the fuzzy logic method. The findings suggest that the fuzzy logic approach exhibits satisfactory dependability across all rock engineering classification schemes.

Achari et al. (2020) focused on the Athabasca River located in Alberta, Canada, where a novel technique was employed to forecast the river's flow. A single-input ANFIS model was utilized to estimate the delivery durations among four stations. The outcomes of this approach were juxtaposed with those of the non-sequential and multi-input ANFIS model for all four hydrometric stations. It was observed that the novel approach yields precise measurements over extended distances and has the capability to forecast flow patterns for prolonged durations.

Anusree and Varhese (2016) conducted a study to quantify the flow in their methodology, utilizing data from the Caruvannur River located in the Thrissur region. The authors employed various techniques, including multiple nonlinear regression (MNLR), artificial neural network (ANN), and adaptive neuro-fuzzy inference system (ANFIS), in their study. The models were developed based on the precipitation data collected from nine distinct precipitation stations. The researchers generated various combinations of precipitation, flow, and temporal data. The evaluation of the models was conducted using the Root Mean Square Error (RMSE) coefficients and Nash-Sutcliffe coefficients. The researchers noted that the ANFIS model yielded more reliable estimations compared to the ANN and MNLR techniques.

Bardzadeh et al. (2018) utilized data preprocessing techniques on ANFIS to develop a more sophisticated flow prediction model. The enhancement of the model was achieved through the amalgamation of the Wave Form Multi-Resolution Analysis and the ANFIS model. Monthly flow data were obtained from the Ellen Brook River and Western Railway Parade stations located in Austria. Subsequently, the wavelength coefficient was integrated with a Neuro-fuzzy model. The models formulated for the subsequent phase are founded on the Takagi-Sugeno-Kang fuzzy inference mechanism. The ANFIS model and WNF models were found to yield dependable outcomes, particularly in evaluations conducted over extended periods of time.

Unes et al. (2019) employed Neuro-Fuzzy (NF) and SVM methodologies and obtained daily rainfall and flow hydrological data from Muskegon. The authors conducted an analysis of precipitation and temperature data from the US basin, utilizing NF and SVM methods, over a period of 1397 days. The model's outcomes were contrasted with the daily observations obtained from the basin. Based on the comparative analysis, it was observed that the Support Vector Machine (SVM) approach exhibited a low error rate in the estimation of precipitation-flow. Moreover, it has been discovered that the Support Vector Machine (SVM) technique can serve as a substitute for traditional approaches utilized in the estimation of precipitation-flow.

Keskin and Taylan (2009) utilized ANFIS and ANN techniques to predict the river discharge of the Manavgat basin located in the southern region of Turkey. The flow of the Manavgat watershed was estimated by utilizing data from the Dalaman, Alara, and Goksu watersheds, which are geographically distinct. The ANFIS and ANN models consist of three inputs and one output. The results of the assessment suggest that the Adaptive Neuro-Fuzzy Inference System (ANFIS) model outperforms the Artificial Neural Network (ANN) model in the context of monthly flow measurements. The ANFIS model was utilized to predict missing or unmeasured data, as per their findings.

The study conducted by Onur et al. (2016) aimed to develop a novel predictive model that utilizes both present and past data to forecast the anticipated water level in the Istanbul-Terkos Dam lake. The ANFIS method was utilized to develop a modeling mechanism based on data from the previous 12 years of the Terkos dam. The objective was to derive precise prediction values for future use. Upon reviewing the values, it was found that the hybrid functions exhibited lower errors. However, they were still deemed insufficient. The reason for this phenomenon can be attributed to the distinction between the feedback methodology and the hybrid approach.

Liong et al. (2000) conducted a study to assess the suitability of the fuzzy logic approach for estimating water levels in Dhaka, Bangladesh. A fuzzy rule-based outflow model was devised and sensitivity analysis was conducted on the input variables in order to accomplish this task. The present study involved the development of a novel model, which was subsequently subjected to evaluation through the reduction of input variables. The obtained outcomes are juxtaposed with the antecedent predictive model of Artificial Neural Network (ANN) in the corresponding area. The study resulted in the development of a superior model utilizing fuzzy logic, which exhibited greater efficacy and success, while employing a reduced number of input variables in comparison to prior prediction models.

Saplioğlu and Grass (2010) partitioned the Bridge River into measuring boxes that spanned 500x500 meters. The slope, geological structure, and vegetation data in each box have been effectively managed. A fuzzy logic model was employed to detect the flow data of each box. The study employed Thiessen polygons to identify the properties of rainfall stations that impact the basin. The researchers acknowledged the presence of missing data in precipitation stations that impact the basin. To address this issue, they employed various statistical techniques such as multiple regressions, artificial neural networks, harmonic averaging, and weighted averaging methods to identify and mitigate the gaps in the data. Subsequently, utilizing flow and precipitation data, the researchers determined the quantity of flow that can be generated independently as a consequence of individual precipitation events. During this phase, the employment of flow measurement stations was implemented, and it was deemed that the surface flow and base flow measurements were efficacious in the preceding days when the data was not solely attributable to precipitation. The researchers utilized the Artificial Neural Network (ANN) approach to address the issue of incomplete data by expanding the dataset and constructing a model.

In Ozger's (2009) study, a comparison was made between the Mamdani and Takagi-Sugeno (TS) fuzzy systems for the purpose of predicting flow values. The Takagi-Sugeno methodology employed linear functions of the inputs to determine the output in the context of fuzzy inference systems, while Mamdani utilized fuzzy subsets to establish the output. Both of these methods were utilized in the Frat River of Turkey. The author failed to consider additional variables, such as precipitation, in the estimation of flow using both methods. The author conducted an analysis of the advantages and disadvantages of both models. Empirical evidence suggests that the Mamdani fuzzy Inference System exhibits superior performance compared to the Takagi-Sugeno system.

Ying et al. (2006) conducted a thorough examination of a fuzzy set. Fuzzy logic is distinct from the classical or crisp methodology in that the constituents of the set can possess diverse levels of membership, as opposed to being limited to binary values of 0 or 1. In the context of fuzzy sets, a node may be regarded as possessing a degree of membership, and this degree of membership can be translated into a membership function or a universe of membership values. Several steps must be considered when implementing fuzzy logic in practise. The initial step in fuzzification involves the conversion of precise or classical data into fuzzy or Membership Functions (MFs). The outcome of the Fuzzy Inference process is a fuzzy result, which is obtained by integrating membership functions and Fuzzy rules. Thirdly, the process of defuzzification is utilized to determine all the outputs that are associated.

In their publication, Palanisamy and Sundaravadivelu (2000) introduced a new methodology for forecasting waves through the utilization of fuzzy logic. The objective of their research was to establish a precise and dependable technique for predicting waves, which could be utilized in the fields of coastal engineering and marine operations. The proposal put forth a model based on fuzzy logic that utilizes meteorological and oceanographic data that has been previously gathered to make precise forecasts of wave direction, wave period, and significant wave height.

Fuzzy logic-based approaches have been extensively used in various hydrological applications, including flood prediction, water resource management, and groundwater simulation. In their review article, Kambalimath and Deka (2020) explore the potential use of fuzzy logic in the field of hydrology. The study conducted by Nurul et al. (2020) used a fuzzy inference system to model rainfall-runoff. The quality of groundwater was simulated and analysed in a study conducted by Nayak et al. (2004) using a fuzzy inference system. Another study conducted by Dhaoui et al. (2023) supports these findings. The authors of this study utilised fuzzy-based modelling techniques to analyse hydrological time series. In contrast, Santos and Silva (2014) utilised various artificial neural network methods and wavelet transforms for the purpose of predicting daily streamflow. Pesti et al. (1996) used these systems to evaluate drought, while Abebe et al. (2000) used them to predict rainfall patterns and reconstruct missing precipitation data. Vernieuwe et al. (2005) utilised this method to simulate the temporal patterns of rainfall streamflow in their research. The research conducted by Jiang et al. (2008), Mao and Wang (2002), and Nayak et al. (2005) is examined to explore the field of flood forecasting and risk assessment.

2.3 Modeling of the Flow Coefficient

The flow coefficient can be described as the proportion of the volume of water that is superficially drained during rainfall to the overall volume of precipitation that occurs over a specific time. Bedient et al. (2013) and Júnior (2015) have established this definition. A flow coefficient is a crucial tool utilized in hydrological investigations of engineering projects located in both urban and rural regions (Sen & Atunkaynak, 2006). It serves to quantify the volume of water discharged from specific precipitation events and provides insight into the influence of natural geomorphological features on the flow. Furthermore, the utilization of flow coefficients is advantageous in facilitating comparisons with other watersheds, thereby enhancing comprehension of the diverse ways in which various landscapes convert precipitation into rainfall events (Blume et al., 2007; Che et al., 2018). Precipitation is a crucial element in the assessment and computation of the flow coefficient. This term encompasses both sporadic rainfall events and periods during which multiple instances of precipitation take place (Júnior, 2015; Campos & Machado, 2018). As precipitation levels rise, they reach a point where the initial losses and infiltration capacity are reached. According to Tucci (2000), the flow coefficient is elevated due to the escalation of runoff. Apart from the precipitation attributes encompassing intensity, duration, and distribution, the occurrence and magnitude of runoff are influenced by distinct physical features of watersheds, including but not limited to soil composition, vegetation, gradient, catchment area, and permeability. The comprehension of the flow coefficient is a crucial aspect in the development of hydraulic structures employed for the purposes of water retention, irrigation, and preserving against inundation.

Kisi and Sanikhani (2018) conducted a study to investigate the use of deep learning models for predicting the flow coefficient. The research findings showed that the models accurately predicted the flow coefficient by combining meteorological and hydrological factors. The authors emphasized the importance of accurately predicting the flow coefficient in relation to the construction of water supply infrastructures such as pipelines and canals. This is crucial to ensure that these infrastructures can meet the needs of users without experiencing overload or being underutilized.

As per Bayazit's (1995) findings, the range of flow coefficients is generally observed to be between 0.05 to 0.50. The coefficient for monthly flow is determined by dividing the average monthly runoff depth by the total monthly precipitation depth. The seasonal flow coefficient pertains to the proportion of flow depth to precipitation depth for a specific season, such as spring or summer. The computation of the flow coefficient involves the division of the mean annual flow depth by the aggregate annual precipitation depth. The flow coefficient for a given event pertains to the direct flow occurring during the said event. The term in question was initially introduced at the beginning of the 20th century, as evidenced by the work of Sherman (1932). Hydraulic structures continue to be frequently employed in engineering design.

According to Savenije (1996), the flow coefficient (runoff coefficient) is the critical variable in water reuse. It is useful for seeing how the moisture recycling in a basin has changed over time and for gauging the significance of that change. An increase in the flow coefficient over time is a strong indicator of degraded land.

Two different methods are used to calculate the percentage of rainfall that contributes to streamflow. The event scale analysis of flow and rainfall records is the first method that can be used. The second method involves keeping a continuous record of the soil moisture conditions of the catchments (Merz et al., 2006).

In semiarid regions, the most critical mechanism for maintaining rainfall on catchment is moisture recycling, which occurs primarily through evapotranspiration from vegetation. It is also the most essential component in maintaining the flow of the river. In semiarid regions, the way land is used and the amount of precipitation are closely related. More than ninety percent of the moisture in the Sahel, which is located in Africa, is recycled. This indicates that more than 90 percent of the precipitation that fell in the Sahel region has evaporated (Savenije, 1995). Because of this, natural resource management must take into account the feedback mechanism between land use and climate. Each moisture particle can be used multiple times in catchments with low flow coefficients. Runoff from the catchments increases as a result of deforestation, agricultural development, urbanization, drainage, or anything else, reducing the capacity of the catchments to absorb evapotranspiration. As a result, precipitation has been decreasing (Savenije, 1996).

Rainfall is currently regarded as an exogenous variable by a significant number of hydrologists. The researchers postulated that the phenomenon is significantly influenced by extrinsic variables. The proportion of total adverted moisture attributable to exogenous sources may be significant; however, the catchment's ability to recycle water is determined by its land use. Moisture recycling plays a crucial role in regions characterized by semiarid and arid climates, where the availability of fresh water is limited (Savenije, 1996).

There exists a common misconception that a high flow coefficient confers benefits to the expansion of water resources. There exists a discourse surrounding the impact of forests on hydrological systems, particularly with regard to their water consumption and the consequent reduction in catchment runoff. This assertion is partially inaccurate. Afforestation or deforestation does not have any impact on the overall quantity of moisture transported from the ocean. Consequently, the overall amount of water flowing off the land surface remains constant. While the flow coefficient may exhibit an increase, there is a concomitant decrease in precipitation, yet the overall total runoff remains unaltered. The argument possesses a certain degree of validity. Afforestation has the potential to augment the water content of a catchment due to the possibility of increased moisture content along the boundaries of the catchment resulting from reforestation on the mountain ranges that border it. This situation has the potential to enhance the transport of moisture through advection. Consequently, this advection process will lead to a rise in precipitation levels within the neighboring catchment areas. (Savenije, 1996).

In sensitive areas, the conservation of forest, vegetation cover, and evaporation capacity are crucial for the management of water resources. Retaining moisture, soils, and nutrients are the three most essential watershed activities for maintaining rainfall (Savenije, 1996). Current hydrologists continue to struggle with determining the typical rainfall-runoff relationship for a given catchment. Due to the complexity of the rainfall-to-runoff transformation process, semi-arid and arid catchments face heightened difficulty. It is also impacted by rapid, continuous changes in land use and land cover resulting from numerous human and economic activities (Parida et al., 2006). The flow coefficient proposed by Merz et al. (2006) was calculated based on hourly measurements of both runoff and precipitation, including rain and snow, in order to estimate the flow rate. The objective of this study was to investigate the spatiotemporal variability of runoff coefficients by analyzing a dataset of 50,000 events obtained from 337 catchments located in Austria, with areas ranging from 80 to 10,000 km^2. The subject of the investigation was examined over a period of nine years, commencing in 1981 and concluding in the year 2000. The findings indicate a significant correlation between the spatial distribution of the runoff coefficient and mean annual precipitation, whereas land use and soil type exhibit a relatively weak correlation with the runoff coefficient. The beta distribution has been utilized to fit the temporal distribution of runoff coefficients effectively. The utilization of distribution parameters has facilitated the demonstration of spatial patterns that exhibit conformity with the six distinct climate zones of Austria.

In each of the regions, event flow coefficients increase with event rainfall depths and preceding rainfall. However, the differences in event flow coefficients between regions are more significant than those between events of various sizes (Merz et al., 2006). They analyzed the flow coefficients of various types of flooding. According to the results, flow coefficients rise for flash floods, short rain floods, long rain floods, rain on snow floods, and snowmelt floods, respectively. In addition to event characteristics, the climate and runoff regime through the seasonal water balance are the primary determinants of the event flow coefficient. The influence of soil and land use on the flow coefficient is marginal (Merz et al., 2006).

Despite the fact that the flow coefficient is the most crucial concept in hydrology science, most regional scale studies have only considered a small number of events. Cerdan et al. (2004), on the other hand, studied 345 rainfall-runoff events in various size catchments in France. The results showed that the flow coefficient decreases with increasing catchment area. They also stated that numerous studies on the flow coefficient of plot scale exist. However, scaling these estimates to the catchment area can be difficult. Dos Reis Castro et al. (1999), the flow coefficients of catchments with different basin areas on the basaltic plateau in southern Brazil were investigated. Naef (1993) examined several large floods in 100 Swiss catchments and stated that the interactions between watershed circumstances and flow coefficient are incredibly complex. As a result, they can be regarded as random numbers. By classifying catchments according to shared physical characteristics, they could account for the observed variations in flow coefficients. The SCS curve number method and the Lutz (1984) method, popular in Germany, are two examples of predictive empirical equations for the event flow coefficient. This makes it difficult to determine when they can be used (Blöschl, 2005).

The fuzzy logic approach is based on linguistic expressions that are vague or imprecise in nature. The findings of Mahabir et al. (2003) and Sen and Altunkaynak (2004) suggest that fuzzy logic modeling techniques exhibit greater efficacy than regression equations. The hydrological variables are linguistically categorized into subgroups based on fuzzy logic principles. Each subgroup is assigned a label consisting of fuzzy terms such as "low," "medium," and "big." Consequently, the variable is not regarded as a constituent of the overall quantity in question. Conversely, within partial groups that allow for greater explication of subordinate relationships among multiple variables, imprecise terminology is employed.

Kisi and Shiri (2009) presented a methodology based on fuzzy logic to forecast the flow coefficient (runoff coefficient) in regions with high humidity. The authors have emphasized the difficulties in forecasting the flow coefficient owing to the intricate interdependence of physical mechanisms, such as infiltration, evaporation, and transpiration. The authors expounded on the utilization of a fuzzy logic-derived methodology to depict the intricate connections between meteorological and hydrological factors that impact the flow coefficient. The authors in two catchments located in Turkey implemented the proposed methodology. The outcomes were then compared to those obtained through conventional regression-based techniques. The findings indicate that the approach based on fuzzy logic exhibits superior performance in forecasting the flow coefficient in both catchments.

For more than a century, the rational method has been employed to compute the runoff resulting from precipitation. It continues to be employed for a multitude of objectives. This approach produces acceptable outcomes, particularly in limited catchment regions. The conventional employment of the rational method involves the computation of runoff through the unaltered multiplication of the mean precipitation and flow coefficients. The conventional rational approach fails to consider the intrinsic unpredictability associated with precipitation data. It can be inferred that computations involving perturbation theory consistently yield results that exceed those obtained through a purely classical methodology. Two apparent challenges in the classical regression methodology are the requirement for fundamental assumptions and the existence of data uncertainty. The utilization of a fuzzy approach in deriving rainfall-runoff relationships results in more precise estimations compared to those obtained through classical regression techniques. This approach results in reduced prediction inaccuracies (Sen and Altunkaynak, 2006).

Precise determination of the flow coefficient holds significant importance in the development of erosion control strategies alongside the design of water supply and drainage systems. The estimation of the flow coefficient for small catchments was examined through continuous simulation modeling in a study conducted by Ghosh et al. (2017). The research has demonstrated that precise determination of the flow coefficient plays a pivotal role in the development of erosion mitigation strategies, including the implementation of retaining walls, riprap, and gabions. These measures are commonly employed to safeguard riverbanks, shorelines, and other erosion-prone regions. The research conducted by Sen and Altunkaynak (2006) aimed to utilize the fuzzy logic approach for the purpose of approximating the flow rate and flow coefficient pertaining to the drainage region of Istanbul. The process of comparing and assessing outcomes is achieved through the utilization of diverse methodologies. The researchers arrived at the conclusion that the employment of the FL model is uncomplicated in the computation of flow rate and flow coefficient.

In their study on the flow coefficient, Mimikou and Rao (1983) designed a regional monthly rainfall-runoff model for the Aracthos River Basin in Greece. The model has a structure that can be applied to both linear and nonlinear rainfall-runoff characteristics of the basins. Two parameters were used in the model: the degree of the model k and n that controls the rainfall-runoff process of the basin. The main aim of the model was to be used in other basins where flow data is not available and to be generalized.

2.4 Various Applications of the SMRGT

The present study introduces a novel approach, namely Simple Membership functions and fuzzy Rules Generation Technique (SMRGT), which is utilized for the purpose of modeling open canal flow. The proposed technique is based on a limited set of numerical values assigned to all membership functions associated with input and output variables. The present methodology was initially introduced by Toprak in 2009 and was regarded as a groundbreaking investigation in this particular domain. The selection of the crucial numerical values was determined by the defuzzification technique and the configuration of the membership function, which may be in the form of a triangular or trapezoidal shape. The principal objective of this study was to tackle two prominent concerns in flow modeling, namely, the enhancement of an open channel's cross-sectional configuration for a specified flow and the development of MFs and FRs to yield optimal outcomes in fuzzy modeling. Toprak et al. 2017 conducted a comprehensive investigation into the benefits and drawbacks of this approach, as well as its pragmatic implementations.

Toprak et al. (2013) In light of the anticipated escalation of water stress and scarcity in numerous regions globally, it is imperative to promptly and expeditiously manage and diminish water losses in water networks without prioritizing cost avoidance. The "simple membership functions and fuzzy rules generation technique" was employed to estimate the losses in drinking water networks. The research was conducted in the urban center of Diyarbakir, Turkey. The study spanned a period of three years, during which monthly data was gathered from 43 areas. The data encompassed various factors such as population, water usage, water supply, and water losses. Upon comparison with the available empirical data, it was observed that the fuzzy model yielded dependable and credible outcomes.

Coskun et al. (2014) developed the SMRGT Fuzzy Modeler (SFM), which is a computerized system for generating fuzzy models using the SMRGT approach (SMRGT Fuzzy Modeler). The SFM Software was tested using Vertebral Column Data, which was obtained in digital format from the School of Information and Computer Science at the University of California. The rules were formulated based on factual data obtained from the Machine Learning repository. The SMRGT technique necessitates a minimum of three membership functions, while the SFM program requires a minimum of two fuzzy values for each variable. The software utilized in the study was created through the implementation of the Java programming language, utilizing the NetBeans 6.9.1 development platform. The rule base in SFM software was generated using two distinct methods, namely the 'Nearest Entry' and 'MF Boundaries' techniques, with the latter being employed more frequently. The study's findings indicate that the precision of fuzzy models derived through the SMRGT approach was slightly inferior to those derived through the SVM and ANN approaches when applied to the identical dataset, as per the author's conclusion.

In research done by Yalaz et al., (2015), the fuzzy time series data were generated using the simple membership function and fuzzy rule generation technique (SMRGT) and the fuzzy least square regression (FLSR) method, which is a simple linear regression technique. Two distinct data sets were employed. They compared the performance of traditional and fuzzy linear regression on a dataset using different measurement principles. As a result, they observed that for three of the eight performance criteria used, the SMRGT model performed better than the linear regression model, while for the remaining five criteria, the SMRGT values were comparable to the linear regression values.

Altas (2017) employed the SMRGT technique to assess the water surface profile in unconfined waterways across diverse hydraulic scenarios. The SMRGT model was selected for the study due to its ability to produce more realistic outcomes and its relative simplicity compared to other conventional methods. The evaluation of the model was conducted through the application of empirically derived datasets that encompassed the geometric characteristics of the floor sill, its height, and the distance from its top. These variables were considered independent inputs for the model. The model's outcomes are compared with the actual data. The findings indicate that the model exhibits a significant capability in assessing the water surface profile within open canals.

The flow coefficient was evaluated by Karakaya (2018) through the utilization of the SMRGT (Simple Membership Functions and Fuzzy Rules Generation Technique) approach. The study area selected for this research was the campus of Sirnak University. The SMRGT technique was employed to ascertain the fuzzy sets and fuzzy rules base accurately. The flow coefficient evaluation model comprises three sub-models. The initial sub-model was developed by considering the meteorological attributes of the designated region, while the subsequent two models were constructed by separately incorporating the land use conditions and soil characteristics. According to the author, the model can be validated for all hydrological, land use, and soil characteristics with a minor modification in the boundary conditions of the models. Consequently, the researcher arrived at the conclusion that the employment of the fuzzy SMRGT technique is a highly pragmatic and efficacious approach for the computation of the flow coefficient.

Bayri (2018) The SMRGT method was employed to classify experimental data pertaining to SPT Pulse Counts, Seismic Wave Velocity (Vs), Groundwater Level (GL), and Soil Dominant Vibration Period (To) in the Dardanelles Region. A classification system was utilized to create a risk map for different ground types, taking into account variables such as seismic properties, grain size, and penetrability. The research employed 151 geotechnical drilling and geophysical investigations, along with seismic fracture size, Multiple Analyses of Surface Wave (MASW), and micro tremor size for 110 points each. The study's author arrived at the conclusion that the fuzzy logic approach is both uncomplicated and lucid, rendering it suitable for employment in this category of examination.

Unes et al. (2020) attempted to estimate river flow utilizing various methodologies, including multiple linear regression (MLR), artificial neural networks (ANN), M5 decision trees (M5T), adaptive neuro-fuzzy inference systems (ANFIS), simple membership function and fuzzy rule generation technique (SMRGT), and Mamdani-fuzzy logic (M-FL). The Stillwater River has been selected as the designated study area within the Sterling region of the United States. In all models, the input variables were identified as the water temperature, daily precipitation, and river discharge. The researchers conducted a statistical evaluation of the results obtained from the models and compared them to the recorded values. The researchers computed the correlation coefficient (R^2), Mean Square Error (MSE), and Mean Absolute Error (MAE) for every model. It was determined that the M-FL model and SMRGT model yielded superior outcomes compared to alternative models.

Fatih Sevgin (2021) determined the flow coefficient of the Kalecik basin. The utilization of fuzzy logic was favored over alternative methodologies in the research because the flow coefficient employed in the computation of the flood flow rate is indicative of the underlying causal relationship between the events. The hydrological event's physical attributes and level of uncertainty were given due consideration. The SMRGT model was the preferred choice of the author due to its novelty and ability to determine both factors concurrently. The basin maps were generated by employing both the Digital Elevation Model (DEM) and Kriging method.

2.5 ANFIS and ANN Applications in Hydrology and Flow Prediction.

Several research studies have been carried out to investigate the utilization of ANFIS in the prediction of streamflow and flow coefficients. The architecture of ANFIS, along with its model inputs, is a defining characteristic. As such, a critical inquiry in the application of ANFIS to flow modeling pertains to the optimal architecture for accurately mapping the process. The selection process requires the selection of a suitable input vector in addition to the hidden units and weights. In contrast to physically-based models, the exogenous variables that impact the system are not predetermined. Hence, the process of choosing an appropriate input vector that facilitates the ANFIS in accurately mapping to the intended output vector is a complex undertaking. Most of the applications that were reported were developed through a process of experimentation and refinement.

M. Kisi (2009) introduced a new approach for the estimation of the flow coefficient in watersheds, utilizing an adaptive neuro-fuzzy inference system (ANFIS). The ANFIS model proposed in this study employed antecedent and consequent fuzzy sets, as well as adaptive learning algorithms, to estimate the flow coefficient using multiple input parameters. The ANFIS model's ability to accurately estimate the flow coefficient was assessed on three separate watersheds in Turkey. The findings indicate that the model's correlation coefficients were high, and its accuracy was satisfactory. The research findings suggest that the implementation of the ANFIS model holds great potential in accurately predicting watershed flow coefficients.

In Bisht and Jangid (2011), the ANFIS and Multi Linear Regression (MLR) techniques were employed for the purpose of flow estimation in river systems. The researchers noted that artificial neural network (ANN) models and fuzzy logic models demonstrate potential for use in estimating river flow. The models developed were utilized for training and testing the data of the Gadavri River. Upon comparison of the outcomes, it was observed that ANFIS models exhibit superior performance in contrast to conventional models like MLR.

He et al. (2014) used three different data-based methods, ANN, ANFIS, and Support Vector machines (SVM), in their study. They analyzed the river flow values of the riverside mountain region in northwest China with different combinations and chose the most appropriate input variables. The training and verification tests have compared the performance of the ANFIS, ANN, and SVM models. The three models used were suitable models for river flow estimation.

The study of Fırat (2007) selected the Seyhan basin, located in the southern region of Turkey. The Uctepe flow station provided the daily river flow data, which consisted of 5114 data points. The estimation of daily river flow was conducted through the utilization of various methods, including the Artificial Neural Network (ANN), Adaptive Neuro-Fuzzy Induction System (ANFIS), Feed Forward Neural Network (FFNN), and Generalized Regression Neural Networks (GRNN). Upon conducting a comparative analysis and performance evaluation of the outcomes, it was determined that the ANFIS model exhibited greater efficacy in comparison to the GRNN and FFNN models.

CHAPTER III

MATERIALS AND METHODS

3.1 Study Area and Data Used

Turkey is susceptible to various flood hazards, including flash floods and overbank floods, due to its diverse topography and geographical location. The most severe flood events in Turkey have historically occurred along the coasts of the Black Sea and the Mediterranean Sea, mainly caused by heavy rainfall along the mountains that run parallel to the coast. Although coastal flooding is infrequent, the majority of flood incidents happen along the coast. The melting of snow in the mountainous areas in Turkey's eastern region is another significant factor leading to increased streamflow and flooding. Overall, the Black Sea, Mediterranean, and Eastern Anatolian regions are the most at risk of flooding in Turkey.

In the previous half-century, Turkey has experienced significant ramifications from flood occurrences, which have been identified as the second most detrimental natural catastrophe within the nation. The Emergency Events Database (EM-DAT) and the Turkish Disaster Database (TABB) have documented a total of 1076 flood occurrences in Turkey spanning from 1960 to 2014. According to Koc and Thieken (2018), the floods have led to an estimated 795 fatalities and incurred economic losses of approximately 800 million dollars. Throughout history, floods have caused significant social, economic, and environmental consequences, resulting in severe and far-reaching impacts on individuals and communities. The escalation of flood losses on a global scale has been observed in recent times, which can be attributed to a multitude of factors such as extreme weather events, urbanization, and inadequate disaster response measures. Unplanned urbanization and land use practices upstream of catchment areas and along riverbanks have contributed to an increase in the frequency of flood incidents and associated damages in Turkey. The aforementioned trend underscores the pressing necessity for efficacious flood risk management tactics and appropriate land-use planning to alleviate the possible detriments resulting from floods. Consequently, the federal administration has enforced an all-inclusive plan for flood management that encompasses both physical and non-physical remedies to alleviate the mounting consequences of flood occurrences. The accessibility of flood event data is highly advantageous in facilitating a comprehensive analysis of flood attributes and a locality's vulnerability, augmenting the accuracy of models, and exploring flood risk evaluation research. The Turkish State Meteorological Service (TSMS) assumes the responsibility of predicting and documenting meteorological perils, such as floods. The TSMS compiles a record of meteorological hazards that have a significant impact on daily life or result in damage. The TSMS data set categorizes heavy rainfall and flooding events as a singular meteorological hazard type. The TSMS dataset provides a record of incidents, including information on the date, location, and extent of direct damage. The document presents a thorough compilation of catastrophic events that have occurred since the year 1975. The dataset in question is not publicly accessible. However, it is possible for academic institutions to make a request for its use in research endeavors. As per the findings of the Turkish State Meteorological Service (TSMS), the year 2020 observed a total of 297 occurrences of flooding. Since the turn of the millennium, there has been a rise in the frequency of flood events. Over the course of the last ten years, it has been observed that there has been an average of 100 or more instances of flooding occurring on a yearly basis (as depicted in Figure 3.1). The localities of Giresun, Van, Antalya, and Bursa encountered the most substantial precipitation and flooding events during the year 2020, as illustrated in Figure 3.2. In 2020, Turkey experienced a rise in heavy precipitation and flooding in its coastal regions of Marmara, the Black Sea, and the Mediterranean.

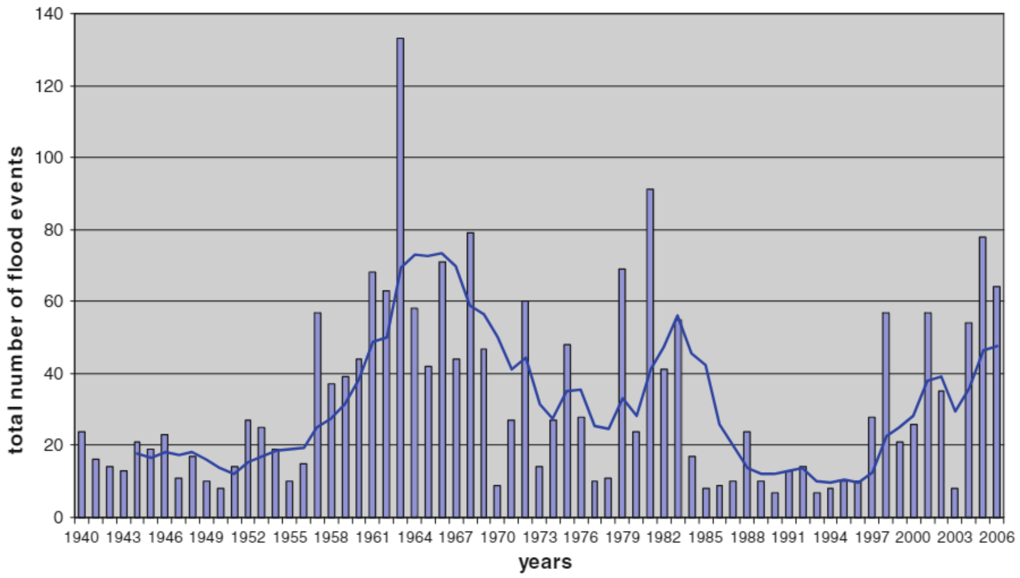

Figure 3.1 Distribution of flood disasters in Turkey (1940-2006), (AFAD, 2006).

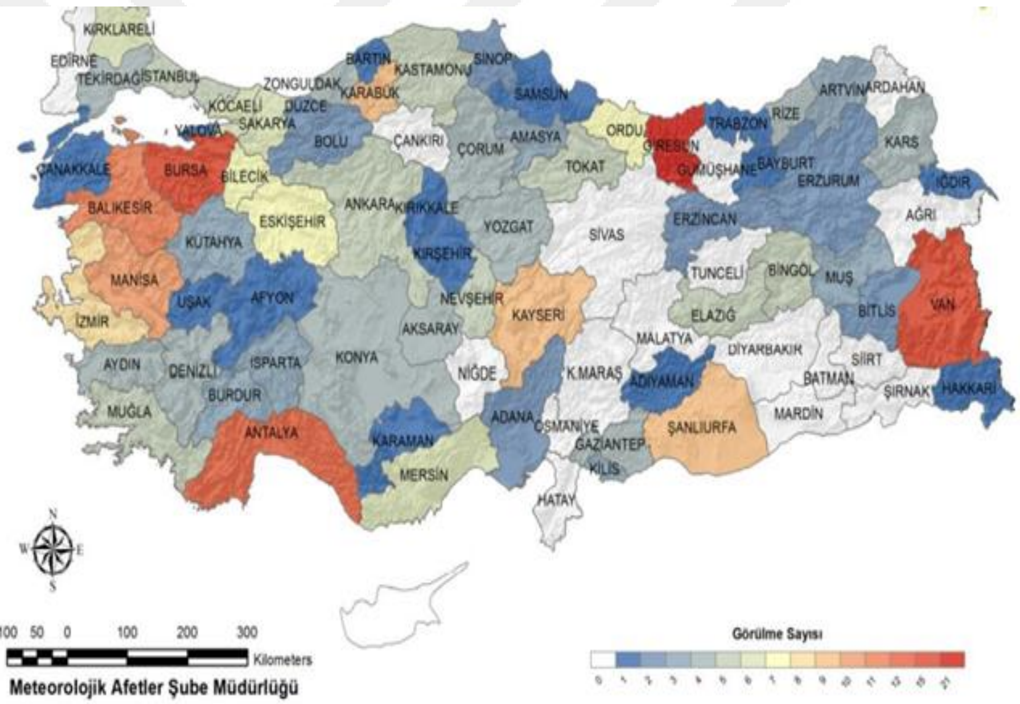

Figure 3.2 Flood events in Turkey in 2020 (AFAD, 2020).

3.1.1 Antalya Basin

The Antalya basin is located in the Mediterranean area and is characterized by the presence of numerous watercourses such as Bogacay, Kirkgozler, Duden, Aksu, Koprucay, Manavgat, Karpuz, Alara, Kargi, Oba, and Dim, which discharge into the Mediterranean Sea. The geographical coordinates of its location fall within the range of 36° 30’ to 38° 28’ North Latitudes and 30° 10’ to 32° 22’ East Longitudes. The basin encompasses the central regions of the Antalya and Isparta provinces, as well as multiple districts within these provinces, such as Bucak and Aglasun districts of Burdur, Serik, Manavgat, Alanya, Gundoğmuş, Akseki, Korkuteli districts of Antalya, and Atabey, Egridir, Sutculer, Gelendost, Yalvac, Senirkent, and Uluborlu districts of Isparta province. The geographical location of the area under discussion is characterized by its mountainous terrain, with the Sultan Mountains situated to the north, the Taurus Mountains to the east, the Beydalar and Katranc Mountains to the west, and the Antalya Gulf to the south, thereby rendering it enclosed by mountain ranges on all sides. The land area of the region in question is approximately 2,500.036 square kilometers, which constitutes roughly 2.56 percent of the total land area of Turkey. Mountains are a defining feature of the eastern, western, central, and northern regions. Consequently, the basin is situated at an average altitude exceeding one thousand meters. The altitude in question is in close proximity to the average elevation of Turkey, which is 1132 meters. Located in the eastern region, Dedegulda boasts the highest elevation of 2935 meters. The regions situated towards the south exhibit predominantly low-lying terrain, characterized by an average altitude of approximately 100 meters. The mean elevations of the plains exhibit variations ranging from 800 m to 1250 m towards the western and northern regions of the basin. Floods are typically observed to occur in the Bogacay and Aksu streams. Precipitation is a significant element that contributes to the occurrence of floods. Furthermore, the melting of snow during the spring season results in a rise in the flow rates of streams. Moreover, the southwest wind produces substantial waves along the coast. The Antalya Basin exhibits two distinct climatic patterns, namely a conventional Mediterranean climate in the coastal region and a continental climate in the upstream region of the basin. There is a decreasing trend in the amount of precipitation as one moves from the southern to the northern regions. While the coastal region experiences an annual total precipitation of 1000 millimeters, the northern portion of the basin receives only 600 millimeters. The presence of mountains in the northern region of the basin restricts the quantity of precipitation that can accumulate in the area. The season of winter is commonly characterized by the highest levels of precipitation. On average, Antalya, Manavgat, and Alanya receive 1030.5 mm, 1038.3 mm, and 1041.8 mm of precipitation, respectively, annually. The mean yearly precipitation in the elevated regions of the basin ranges from 500 to 750 millimeters. Intense precipitation events result in an increased volume of runoff on the earth's surface. The Antalya Basin does not face any issues pertaining to water scarcity. The streams of Pupa, Hayran, Yalvac, and Korkuteli, along with the aforementioned coastal streams, are located upstream of the basin. The aforementioned basin encompasses the bodies of water known as Eridir, Kovada, and Kestel lakes. To clarify, Mamak Lake is a seasonal body of water that is present only during specific periods. Groundwater reservoirs are present in the plains of Boacay, Manavgat, Alanya, Korkuteli, Bozova, Hayran, Gelendost, Uluborlu, and Senirkent (Topraksu, 1970).

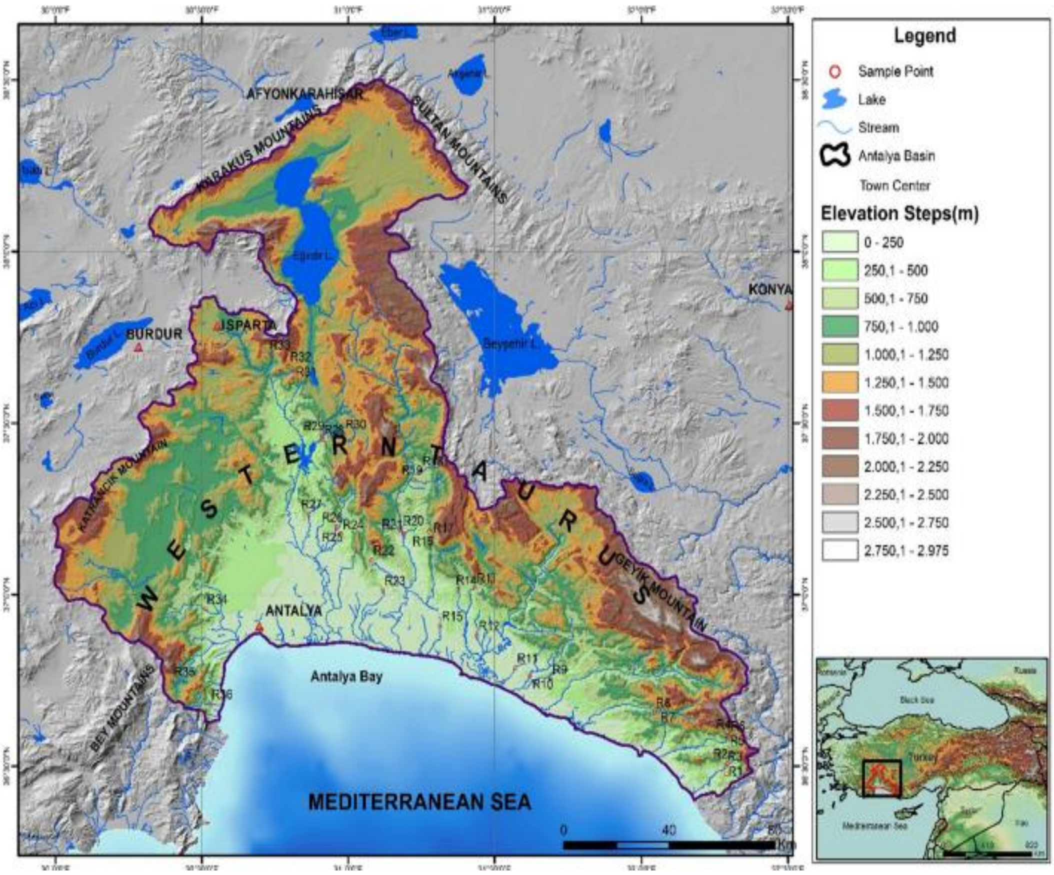

Figure 3.3 Map of the Antalya basin (Celekli et al., 2021)

3.1.2 Aksu River Basin

A basin refers to a topographically delineated region of land that serves as a conduit for various substances such as water, sediment, dissolved materials, heat, and biota towards a shared outlet along a stream channel. The term catchment or watershed is commonly used to describe a geographical region that is demarcated by natural boundaries, such as mountain ridges or other topographical features, which serve to distinguish it from neighboring areas. The convergence of precipitation runoff within a given basin occurs at a singular juncture in the hydrological network, commonly manifested as a river or stream, which ultimately discharges into the ocean or other aqueous reservoirs (Murthy, 2000). The importance of water resources has gained paramount importance in contemporary times owing to the surge in global population and the phenomenon of global warming. The significance of water resources in Turkey has experienced a notable increase, aligning with the prevailing global trend. The management of basins and rivers, encompassing hydrological modeling, has emerged as a critical concern in Turkey. The proficient administration of water resources is a crucial factor in providing sustainable development, alleviating the unfavorable consequences of climate change, and preserving ecological equilibrium. The utilization of hydrological modeling presents a significant asset in the management of water resources, as it empowers decision-makers and policy planners to make well-informed judgments grounded on dependable data and forecasts. Advanced computer technology is frequently utilized in engineering to simulate real-world scenarios and offer solutions through mathematical models. Consequently, the utilization of modeling presents a potent approach to tackling engineering issues. Recent technological advancements have had a positive impact on hydrological models, leading to the development of more accurate solutions. Although these models can offer significant advantages, a considerable proportion of them necessitate a substantial quantity of parameters that require precise calibration to achieve precise simulations. Hence, the adjustment of these parameters is of utmost importance to ensure the model's ability to yield dependable outcomes (Gunal, 2015).

The geographic location of the research site falls within the range of 36°-38° north latitudes and 30°-31° east longitudes. This area is classified as one of the ten sub-basins of the Antalya Basin, which is recognized as one of the 25 prominent basins in Turkey based on its hydrographic features. The present sub-basin is situated within the geographical confines of the Mediterranean Region. The Aksu River, serving as the principal waterway in the region, spans approximately 145 kilometers in length and measures 100 meters in width at its estuary, boasting a depth of 3 meters . In certain regions within the delta, the river's depth is limited to a degree that prohibits the passage of vessels with a draught exceeding 0.30 m. The confluence of the river's estuary and the oceanic swells leads to the formation of turbulent waves. The basin encompasses a drainage area of roughly 7505 km^2 and is flanked by the Mediterranean Sea to the south, the Korkuteli and Duden Stream sub-basin to the west, the Buyuk Menderes Basin and Akarcayi Basin to the north, the enclosed Konya Basin to the northeast, and the Koprucayi sub-basin to the east.

The northern boundary of the basin is formed by the Karakus and Sultan Mountains, which run parallel to the Isparta dirsegi. To the east, the basin boundary starts from the northwest extension of the Dedegol Mountains and follows the Kuyucak Mountain water section towards the Aksu/Isparta district center before terminating in the Mediterranean to the west of the Serik district center in the south. The southern boundary of the basin is formed by the Mediterranean coast, with the boundary extending northwest from the Aksu district center to the fields of Antalya in the west. The Cubuk strait begins at Karlik Mountain in the east and follows the water part lines until it reaches the eastern end of the Katrancik Mountains. From there, it proceeds northwards, encircling the back of Celtikci from the east and reaching the west of the Aglasun district towards the Burdur city center. It then turns to the northeast and encloses the Isparta plain from the west and north. The boundary line proceeds eastward from Yayla Mountain and the Isparta provincial center, passing over Davraz Mountain to reach the north of the Egirdir district and extending towards Barla Mountain. From there, the waterway heads westward again and reaches the west end of the Karakus Mountains. The boundary line then proceeds northeast and reaches the Sultan Mountains, following the range to delineate the boundary. Within the basin, there are several prominent settlements, including Aksu (Antalya), Aglasun (Burdur), Sutculer (Isparta), Isparta provincial center, Gelendost (Isparta), Yalvac (Isparta), Uluborlu (Isparta), and Senirkent (Isparta). However, the most significant settlement in the basin is undoubtedly the Isparta province center.

The Aksu River Basin is one of the lower sub-basins of the Antalya Basin, which is one of the 25 major hydrographic basins in Turkey designated by the Ministry of Forestry and Water Affairs. The Aksu River is of great importance to the region since it is the main river that recharges Karacaoren-1 and Karacaoren-11 Dams Lake. Surface waters in the study area include Kovada Lake and the Karacaoren-1 Dam, with Kovada Lake situated in Turkey's Lake Area and within a Turkish National Park. The lake is shallow, with a depth of 6-7 m and a size of 8 km^2, and it is built on allochthones limestone. Groundwater flow and rainfall are critical sources of recharge for the lake. The Karacaoren-1 Dam, built between 1977 and 1990 for irrigation, flood prevention, and energy production, is situated in the Middle Mediterranean basin. The local government had planned to use water from the Karacaoren-1 Dam Lake to meet Antalya's drinking and municipal water needs. However, due to pollution of the drinking water sources, the plans to use water from the Karacaoren-1 Dam Lake for drinking and municipal purposes are questionable. The Aksu River and precipitation primarily recharge the Karacaoren-1 Dam Lake. Settlement areas in the basin region include agricultural and animal husbandry areas as well as refinery plants.

The Aksu River basin exhibits two distinct climatic classifications, namely a Mediterranean climate and a continental climate. The northern region of the basin is characterized by a Central Anatolia continental climate, featuring arid summers and frigid winters with substantial snowfall. The majority of the area typically experiences minimal levels of precipitation throughout the annual cycle. The southern region of the basin is characterized by a Mediterranean climate. The Mediterranean climate is typified by a seasonal pattern of arid summers and temperate, damp winters. The basin's elevation varies from 0 meters to 2835 meters above the mean sea level. The regions situated in the northwest and northeast, characterized by mountainous terrain, exhibit more significant elevations and correspondingly lower temperatures, accompanied by heightened levels of precipitation and snowfall. Conversely, the southern plains experience comparatively warmer temperatures, with elevated levels of precipitation and evaporation.

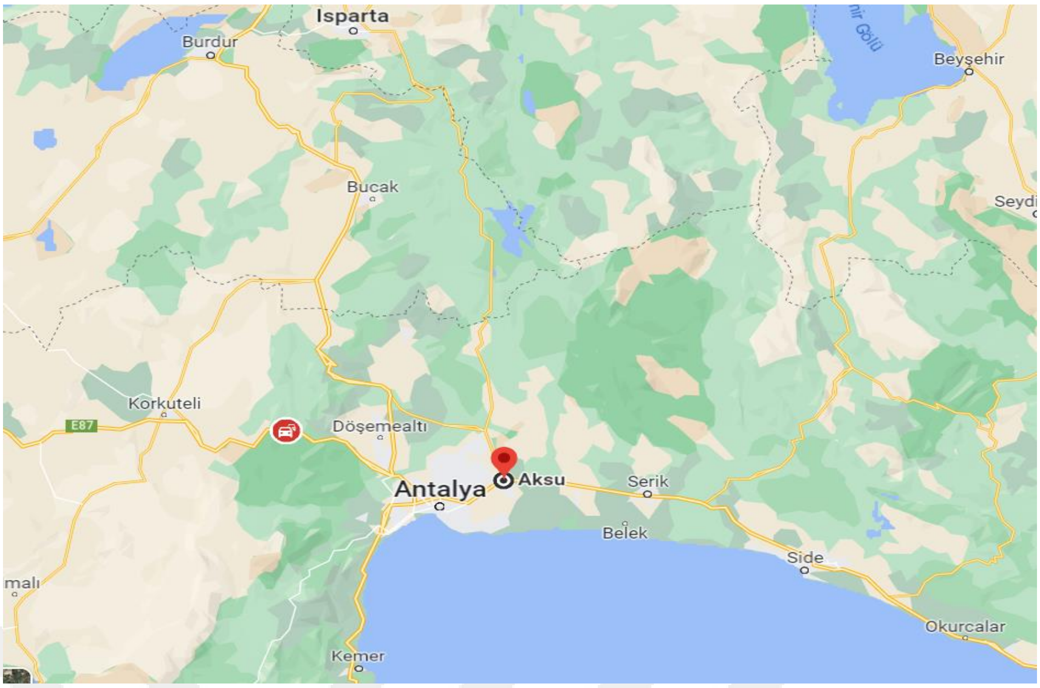

Figure 3.4 Location of the study area from GeoMapApp.

3.1.3 Water Resources Management in Aksu River Basin

The Aksu River Basin's water resource management entails the proficient utilization and preservation of the water resources accessible within the region. The Aksu River Basin, situated in the southern region of Turkey's Antalya province, accommodates a range of agricultural, industrial, and tourist pursuits. The sustainability of these activities is contingent upon a dependable provision of water. The management of water resources within the Aksu River Basin is a multifaceted undertaking, as it is beset by a range of challenges, including but not limited to climate change, water scarcity, and pollution. In order to tackle these obstacles, a range of tactics have been employed, such as the implementation of water preservation techniques, the management of groundwater resources, and the treatment of wastewater. The Aksu River Basin can be managed effectively through the implementation of a comprehensive water management plan that considers the diverse water users in the region. An effective strategy ought to encompass provisions that guarantee the enduring utilization of water resources, curtail superfluous dissipation, and safeguard the integrity of water. Furthermore, the implementation of advanced technologies such as remote sensing, geographic information systems (GIS), and machine learning (ML) can facilitate the effective management of water resources in the Aksu River Basin. The implementation of these technologies can furnish precise and current data regarding the water resources within the region, thereby facilitating well-informed decision-making and strategic planning. The implementation of efficient water resource management practices is imperative for the sustained expansion and advancement of the region. It is a complex task that requires the collaboration of various investors, including government agencies, water users, and the local community, to ensure the sustainable use of water resources for future generations.

Figure 3.5 Location of the Study Area (Aksu river basin).

3.1.4 Precipitation

The Aksu River Basin in Antalya, Turkey, is an important water source for the region, and the precipitation patterns in the area play a crucial role in determining the availability and distribution of water resources. The precipitation in the Aksu River

Basin shows a marked temporal variation, with distinct wet and dry seasons. The rainy season in the area generally occurs between November and April, with the heaviest precipitation occurring between December and February. During this period, the region receives about 70% of its annual rainfall. The dry season, on the other hand, occurs between May and October, with little to no rainfall. The total annual precipitation in the basin ranges from 500 to 2000 mm, with an average of about 1000 mm. The precipitation in the Aksu River Basin shows a significant spatial variation, with different areas receiving varying amounts of rainfall. The highest precipitation is generally observed in the mountainous areas of the basin, where the terrain is steep, and the elevation is high. The lower slopes and the valley areas, on the other hand, receive lower amounts of precipitation due to their relatively flat terrain and lower elevation. The spatial variation in precipitation is also influenced by the prevailing wind direction, which brings moist air from the Mediterranean Sea towards the mountains, resulting in orographic precipitation.

The hydrological regime of the Aksu River Basin holds significant implications for the management of water resources in the area. The fluctuation in precipitation patterns across seasons results in significant variability in the accessibility and allocation of water resources within the basin over the course of the year. In the wet season, the basin experiences a substantial influx of water, which, if not adequately controlled, may result in detrimental consequences such as flooding and soil erosion. In contrast, the basin may encounter a dearth of water during the arid season, particularly in the valley regions and lower altitudes. The heterogeneity in precipitation patterns can result in differential susceptibility to water scarcity across regions, thereby impacting the accessibility of water for various applications such as irrigation, domestic consumption, and industrial activities. In response to the aforementioned challenges, diverse water management strategies have been formulated and implemented in the Aksu River Basin. These strategies encompass the construction of dams and reservoirs, the exploitation of groundwater resources, and the advocacy of water conservation and efficiency measures. The implementation of the dam and reservoir infrastructure has facilitated the management of water flow within the basin, mitigating the potential for inundation and furnishing a dependable supply of water for agricultural and residential purposes. The utilization of groundwater resources has additionally served as a supplementary measure to complement surface water resources, thereby furnishing an alternative water source during instances of arid conditions. The implementation of water conservation and efficiency strategies, such as the advocacy of drip irrigation and the adoption of water-saving technologies, has resulted in a reduction in water demand within the region, thereby enhancing the efficacy of water utilization. The hydrological regime of the Aksu River Basin is significantly influenced by precipitation patterns, which are a key determinant of the accessibility and spatial allocation of water resources within the area. The management of water resources in the basin is confronted with considerable difficulties due to the fluctuations in precipitation over time and space. As a result, it is imperative to devise diverse approaches to guarantee dependable and enduring water provision for the area. Comprehending the precipitation patterns and their ramifications for water management is imperative for ensuring the sustained feasibility of the water resources in the Aksu River Basin. Climate change has had a significant impact on extreme meteorological events in certain geographic regions, with a notable example being the recent increase in extreme precipitation in various parts of the world. This has resulted in inadequate infrastructure systems due to the severity of the precipitation. Precipitation is a crucial component of climatic parameters and atmospheric circulation, as it is responsible for the presence of water on land and serves as the primary source of flow. Hence, the factor of precipitation holds the highest significance. The data of the precipitation stations and their locations are obtained from the Turkish State of Meteorological Service (TSMS). 31 precipitation observation stations (POSs) with (1793) records of monthly precipitation data for 20 years are used. The precipitation showed an increase in (Oct., Nov., Dec., Jan., and Feb.) and the minimum precipitation recordings showed in (June, July, August. and Sep.). The maximum monthly precipitation was (907.2 mm) recorded in (Nov. 2001). While the minimum record for most of the years was (0.1 mm) showed especially in August. The annual average rainfall was 963.60 mm based on 19 years of Aksu meteorological station measurements. The maximum annual rainfall was 1891.8 mm in 2001.

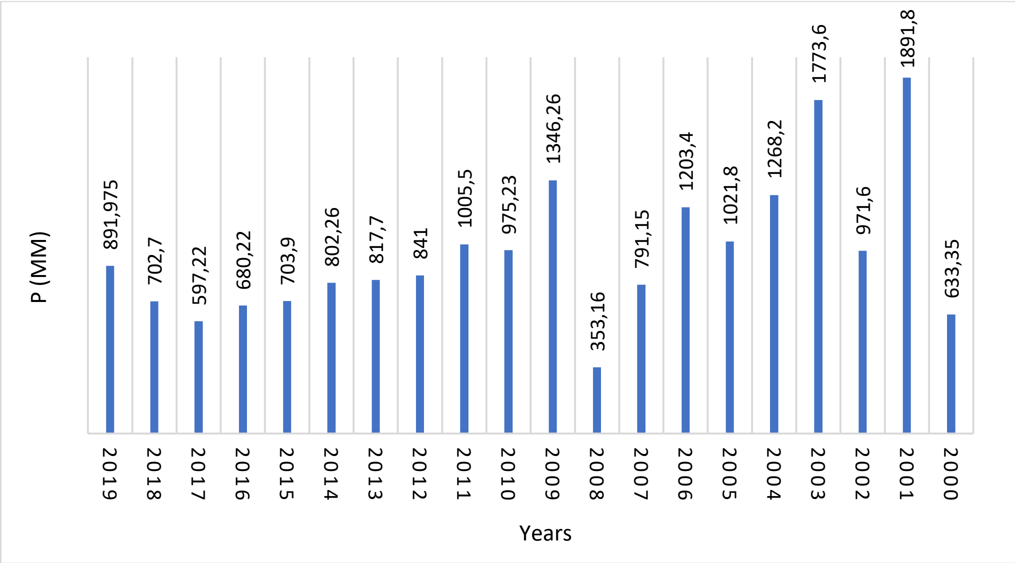

Figure 3.6 The annual precipitation of the Aksu river basin from 2000 to 2019.

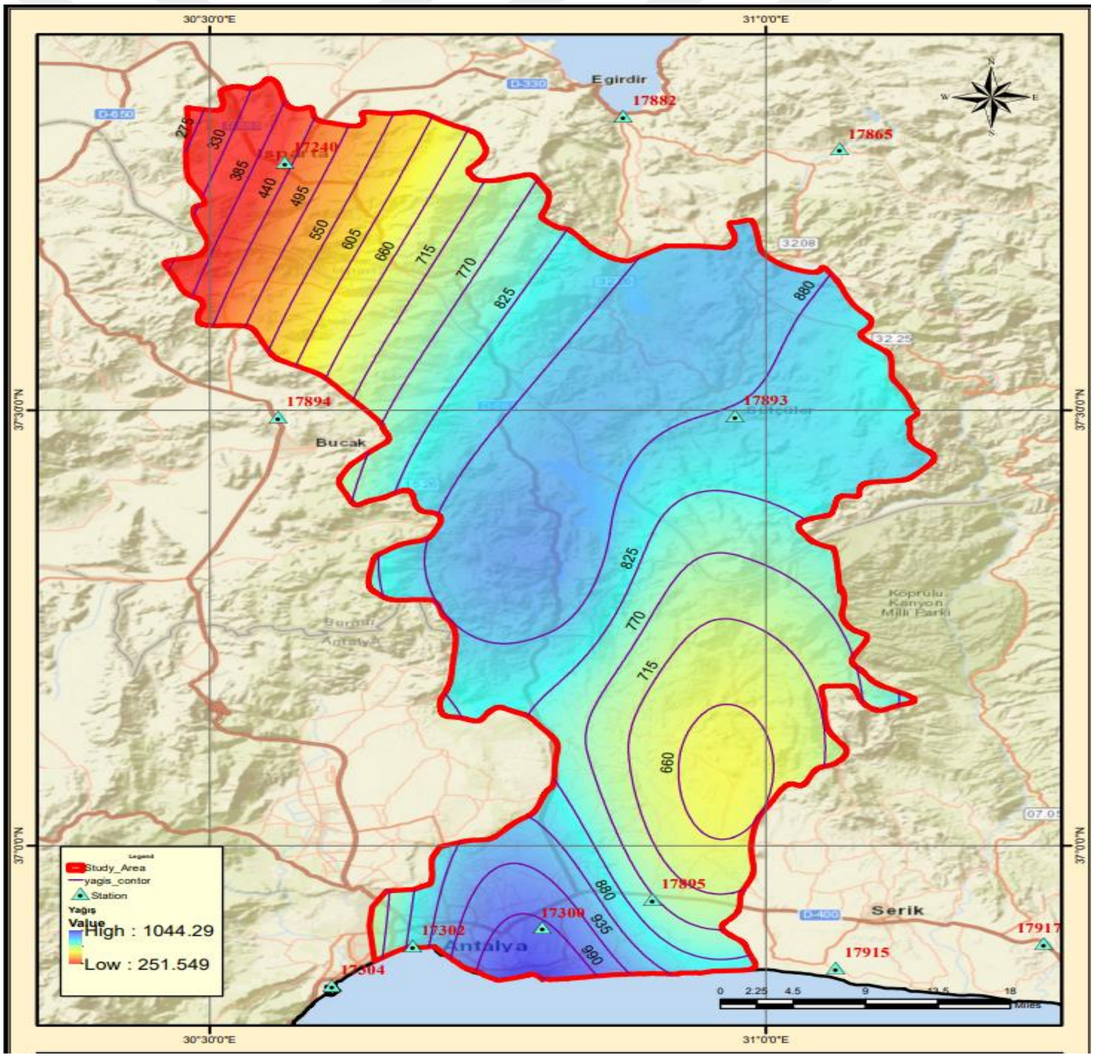

Figure 3.7 Precipitation map of the study area.

3.1.5 Coverage of vegetation

Because the climate, soil, and topography conditions are favorable for plant life, the Aksu basin has diverse vegetation and a perennial plant basis. Many years of plants have resulted in a Mediterranean maki community at elevations ranging from the sea to 0-600 m. The region's most important tree, red cam (Pinus brutia), is found at elevations ranging from 0 to 1200 m. The cedar (Cedrus) and karacam (Pinus nigra) form the foundation at elevations of 1000-1400 m. Fir (Abies) and Juniper grow to heights of 1400-1700 m. (Juniperus). Furthermore, willow (Salix), poplar (Populus), wild igde (Hippophae), wild pear (Pyrus pyraster), elm (Ulmus), maple (Acer), and zinc (Platanus) trees can be found on almost every side of the basin.

The coverage of vegetation in the Aksu River Basin is an essential factor in hydrological processes and water resources management. Vegetation plays a crucial role in regulating the water cycle by intercepting rainfall, reducing runoff, and enhancing infiltration. The vegetation cover in the basin is affected by several factors, including climate, land use, and management practices.

In the Aksu River Basin, the dominant vegetation type is Mediterranean shrubland, which includes species such as maquis, phrygana, and garrigue. These vegetation types are adapted to the region's hot and dry climate and are characterized by low shrubs, herbs, and sparse tree cover. However, the vegetation cover in the basin has been impacted by anthropogenic activities, including urbanization, agriculture, and deforestation. Vegetation cover can have significant impacts on hydrological processes, such as infiltration, evapotranspiration, and runoff. Vegetation cover can enhance infiltration by increasing soil porosity and reducing soil compaction. This can lead to increased groundwater recharge and sustained streamflow during dry periods. Vegetation cover can also reduce runoff by intercepting rainfall, reducing surface erosion, and increasing water storage in the soil.

Moreover, vegetation cover can affect water quality by filtering out sediments and pollutants from runoff and reducing the impacts of erosion. Vegetation cover can also help regulate stream temperature by providing shading and maintaining cooler water temperatures, which is essential for the survival and distribution of aquatic organisms. Real-time information on vegetation cover can provide valuable information for hydrological and water resources management applications, such as flood forecasting, water quality monitoring, and erosion control. This data can also help improve the accuracy and reliability of hydrological models to predict future water availability and quality in the Aksu River Basin.

3.1.6 Temperature

Aksu River basin climate, which is located in the southern part of the Taurus Mountains in the Mediterranean Region, is influenced by topography as well as the air masses that are effective in the region. Since the end of October, the region has been influenced by a warm and humid air mass originating in the Central Mediterranean. Heavy precipitation in the winter months occurs as a result of the cold air from the north and warm air from the south. The north part of the basin has a Central Anatolia continental climate condition with hot, dry summers and cold, snowy winters and a Mediterranean climate is observed in the south part of the basin. The Mediterranean climate is characterized by dry summers and mild, moist winters.

During the summer season, the region is subject to the influence of both moist tropical (MT) and warm and dry tropical air (CT) originating from the African and Arabian regions. A total of 6996 temperature data points were analyzed at the Aksu meteorological station. The data revealed a noticeable rise in temperature during the months of July and August, whereas the lowest temperature readings were observed in December and January. In August of 2012, the highest monthly temperature on record was documented at 31.4°C. Conversely, the lowest recorded temperature of -5°C was observed during the months of December 2016 and January 2017. The mean temperature recorded at the Aksu meteorological station over a period of 19 years was 16.03 °C. In the year 2010, the highest recorded temperature on an annual basis was 16.92 °C. The Aksu River Basin is located in the Mediterranean region of Turkey, which experiences a typical Mediterranean climate with hot and dry summers and mild and rainy winters. The region is known for its agricultural activities, including citrus and banana cultivation, which can be impacted by temperature changes. Temperature plays a critical role in hydrological processes, such as evapotranspiration, which is the process by which water is lost from the soil and vegetation to the atmosphere through the combined processes of evaporation and transpiration. High temperatures can increase the rate of evapotranspiration, leading to reduced soil moisture and water availability for plants and other organisms in the Aksu River Basin.

The quality of water can be impacted by temperature as it can have an effect on the proliferation and dispersion of aquatic organisms, including bacteria and algae. Elevated temperatures have the potential to facilitate the proliferation of specific varieties of algae and bacteria, thereby inducing alterations in the quality of water and heightening the likelihood of detrimental algal blooms and waterborne illnesses. Furthermore, the effectiveness of water management techniques, such as irrigation and water treatment, can be influenced by temperature. Elevated temperatures have the potential to augment the rate of water loss via evaporation and transpiration, thereby diminishing the effectiveness of irrigation systems and intensifying the requirement for water. Elevated temperatures have the potential to diminish the effectiveness of water treatment systems, thereby augmenting the likelihood of waterborne illnesses.

The utilization of real-time temperature data can offer significant insights for hydrological and water resources management purposes, including but not limited to flood prediction, irrigation planning, and water quality surveillance. The utilization of this data has the potential to enhance the precision and dependability of hydrological models that are employed for the purpose of forecasting forthcoming water availability and quality within the Aksu River Basin. In addition, the consideration of temperature data holds significant importance in the management of hydrological and water resources within the Aksu River Basin. The data can serve as a valuable resource for enhancing decision-making processes and optimizing the efficiency of water management strategies within the area. The availability of current weather information can offer significant perspectives on the effects of temperature on hydrologic phenomena and water reserves in the Aksu River Basin.

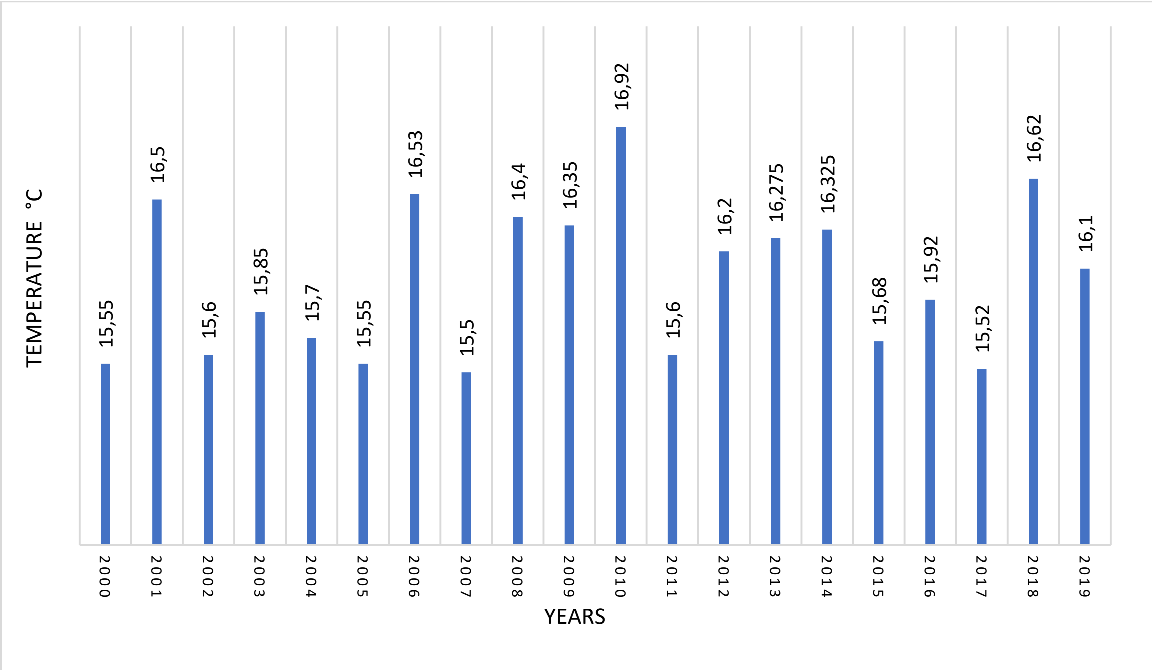

Figure 3.8 The average annual temperature of the Aksu river basin from 2000 to 2019.

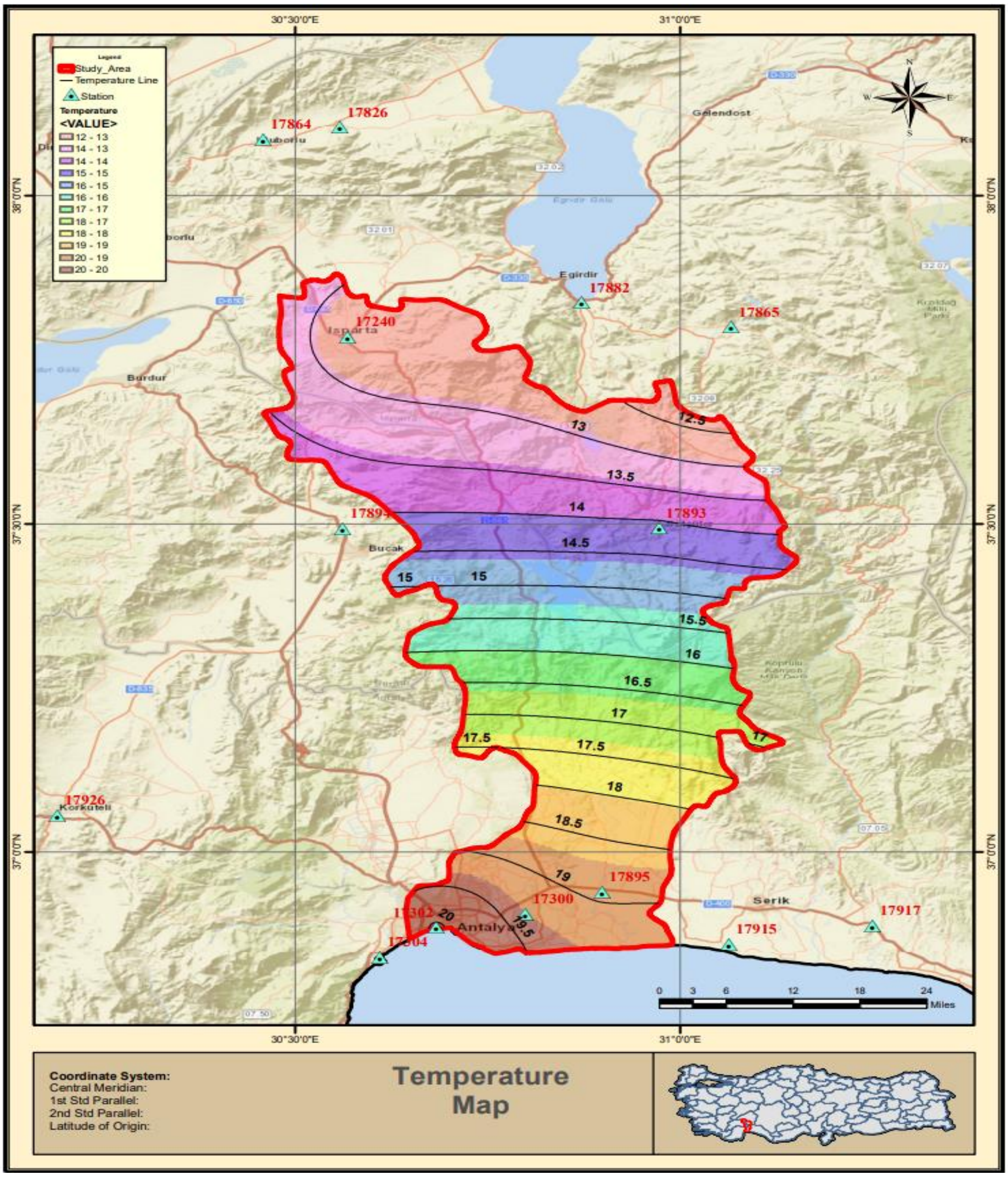

Figure 3.9 The Temperature map of the Aksu river basin.

3.1.7 Relative Humidity

The Aksu River Basin's hydrological processes and water resources can be impacted by humidity, which is a significant climatic factor. The variability of relative humidity in the area over the course of a year can hold significant implications for water resource management and agricultural practices.

The largest city in the Aksu River Basin, Antalya, exhibits a range of relative humidity levels based on historical weather data. Specifically, the relative humidity fluctuates between 47% in July and 75% in December (World Weather Online, n.d.).

Elevated levels of humidity have the potential to augment the pace of evapotranspiration, culminating in a decline in soil moisture and the accessibility of water for flora and fauna inhabiting the Aksu River Basin. The effectiveness of water management techniques, such as irrigation and water treatment, can also be influenced by humidity levels. Elevated levels of humidity have the capacity to augment the likelihood of the proliferation of fungi and other diseases that are transmitted through water. This study analyzed 6680 data points of humidity from the Aksu meteorological station. The findings indicate an increase in humidity during the months of January and December, while the lowest humidity readings were observed in July and August. In January 2017, the highest level of monthly humidity was recorded at 97.7%, while the lowest level was observed in December 2017 at 2.4%. The mean humidity on a yearly basis was 63.3%. In 2002, the highest recorded annual humidity was 67.4%, while the lowest was observed in 2013 at 58.85%.

In addition, humidity can affect the accuracy and reliability of hydrological models used to predict future water availability and quality in the Aksu River Basin. Humidity data can be used to estimate the potential for evapotranspiration, which is a critical component of hydrological models. Real-time humidity data can provide valuable information for hydrological and water resources management applications, such as irrigation scheduling and water quality monitoring. This data can also help improve the accuracy and reliability of hydrological models to predict future water availability and quality in the Aksu River Basin.

In the Aksu River Basin, the management of hydrological and water resources necessitates careful consideration of humidity as a significant factor. The data can serve as a valuable resource for enhancing the decision-making process and optimizing the efficacy of water management strategies within the locality. The availability of up-to-date meteorological information can offer significant advantages in comprehending the effects of moisture levels on hydrologic phenomena and water reserves within the Aksu River Basin. The vegetation cover in the Aksu River Basin can also be affected by humidity. Elevated levels of humidity have the propensity to augment the likelihood of fungal and bacterial ailments, thereby exerting an adverse influence on the growth and viability of plants. Furthermore, elevated levels of humidity have the potential to augment the prevalence of pest populations, including mites and insects, thereby exerting a deleterious influence on the overall well-being of vegetation. The effects of these impacts can hold significant consequences for agricultural practices and the provision of ecosystem services by flora, including but not limited to soil stabilization and carbon sequestration.

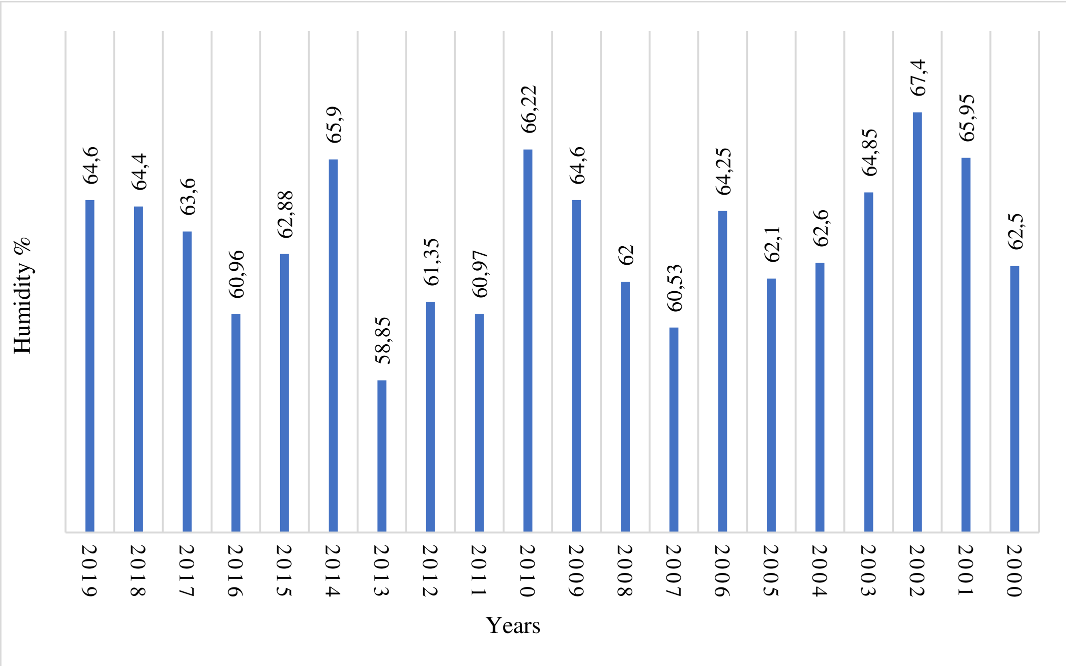

Figure 3.10 The average annual humidity of the Aksu river basin from 2000 to 2019.

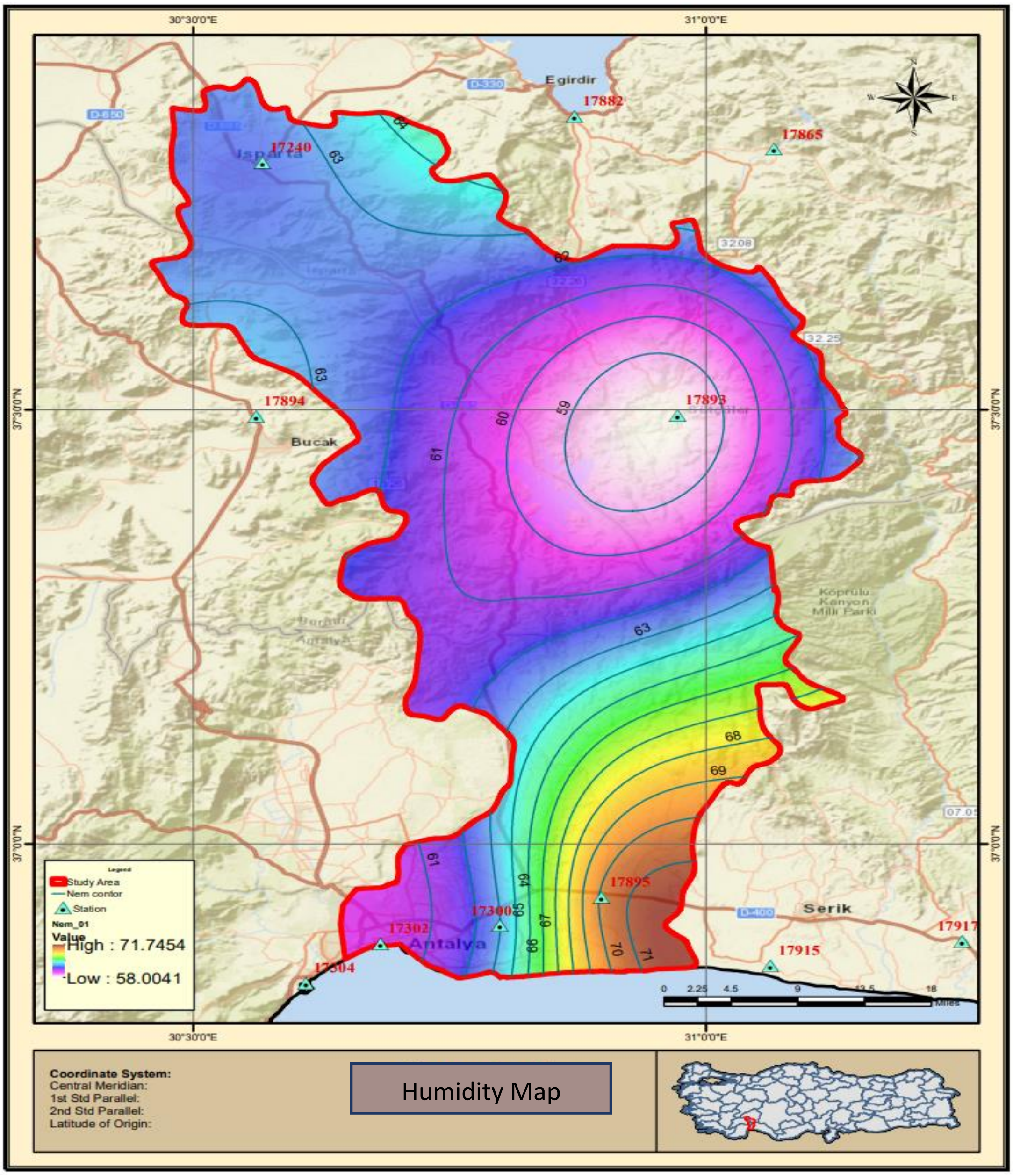

Figure 3.11 The Humidity map of the Aksu river basin.

3.1.8 Wind Speed

According to historical weather data, the average wind speed in the Aksu River Basin ranges from 3.1 meters per second (m/s) in July to 4.6 m/s in February (World Weather Online, n.d.). The highest recorded wind speed in Antalya was 25.9 m/s, which occurred in March 2010 (Turkish State Meteorological Service, n.d.).

Wind speed can have essential implications for hydrological processes, such as evapotranspiration and the distribution of precipitation. In addition, wind speed can influence the effectiveness of irrigation and water management practices in the Aksu

River Basin. It is important to note that wind speed can vary significantly depending on the location and time of day. Real-time weather data can provide more accurate and up-to-date information on wind speed in the Aksu River Basin.

For this study, (2122) of wind speed data have been considered from the Aksu meteorological station; it is recognized that the wind speed increased in (Jan., Feb., and March), while the minimum wind speed recordings showed in (Oct., Nov., and Dec.). The maximum monthly wind speed was (5.7 m/s) recorded in Feb. 2003, and the minimum record was (0.1 m/s) in Oct. 2006. The annual average speed was 1.93m/s. The maximum annual speed was 2.27 m/s in 2016, and the minimum was 1.08 m/s in 2004.

The wind speed information in the Aksu River Basin is significant because it can impact hydrological processes and water resources management in the region. For example, high wind speeds can increase the rate of evapotranspiration, which can have implications for water availability and agricultural production. Moreover, wind speed can also influence the distribution of precipitation, particularly in areas with orographic precipitation patterns. Orographic precipitation occurs when moist air is forced to rise over a mountain range, causing the air to cool and condense, leading to precipitation. The speed and direction of wind can affect the distribution of this precipitation, which can impact water availability and quality in the Aksu River Basin.

In addition, wind speed can impact the effectiveness of irrigation and water management practices in the region. High wind speeds can increase water loss through evaporation and transpiration, which can reduce the efficiency of irrigation systems. This can result in reduced crop yields and increased water demand, which can exacerbate water scarcity issues in the basin area. Real-time wind speed data can provide valuable information for hydrological and water resources management applications, such as flood forecasting, irrigation scheduling, and water allocation. This data can also help improve the accuracy and reliability of hydrological models used to predict future water availability and quality.

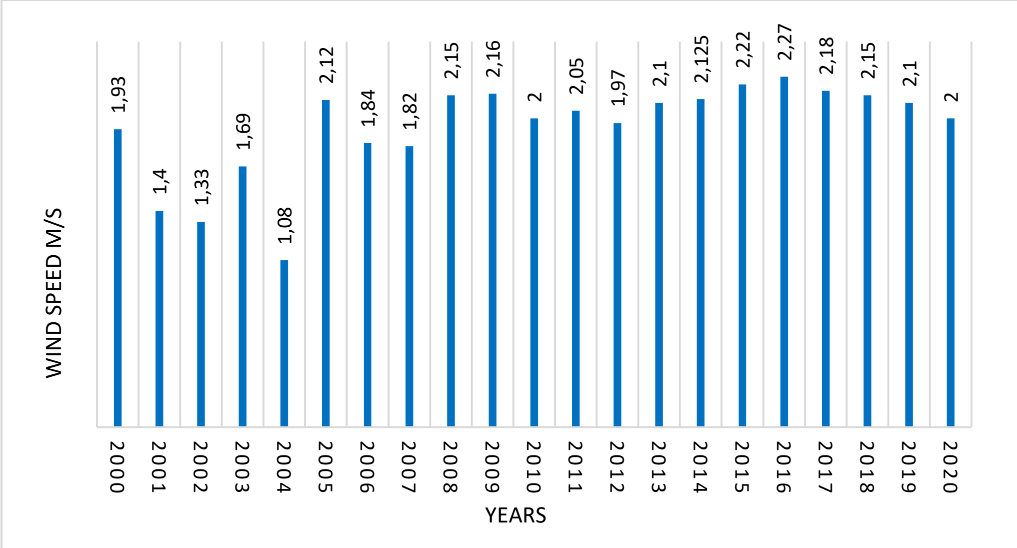

Figure 3.12 The average annual wind speed of the Aksu river basin from 2000 to 2020.

3.1.9 Slope

The slope information of the Aksu River Basin is an essential factor in understanding its hydrological characteristics. The basin has a complex topography with steep slopes and rugged terrain. The elevation ranges from sea level to 3,086 meters above sea level at the summit of Mount Tahtalı. The slope of the Aksu River Basin varies from gentle to steep, with the steepest slopes located in the mountainous areas of the basin. The average slope of the basin is around 7%, with some areas having slopes as steep as 30%. The steep slopes of the basin contribute to the rapid water runoff during rainfall events, leading to flash floods.

The Aksu River is the main river in the basin, and it flows for approximately 115 km before emptying into the Mediterranean Sea. The river has a steep gradient, with an average slope of around 0.5% and a maximum slope of around 2.5%. The steep slope of the river contributes to its high velocity and the erosion of its banks. The slope information of the Aksu River Basin in Antalya plays a critical role in understanding its hydrological processes, including runoff, erosion, and sediment transport. It is important to monitor and manage the basin's slopes to minimize the risk of floods, erosion, and other related hazards. Because water accumulates steadily as it transfers along the slope from high to low, and flooding typically occurs in the lower region, slope length is a factor that influences both floods and the probability of flooding. Begarello and Ferro (2010) stated that when the slope length increases the flow volume and speed also increase. The slope length increases as the volume of water, flow speed, and inertia force increase. In other words, the farther the flow is from the watershed line, the greater its kinetic energy and, thus, the higher its velocity, increasing flood risk. The slope causes easier draining of the water that passes through the flow. The slope generally shows an increase when the soil's ability to infiltrate is insufficient against the flow. The Aksu River Basin has a morphology of mountainous areas, plains, and coastal plains, with the highest parts in the north and the lowest parts along the narrow coastline in the south. The Aksu Basin encompasses a significant portion of the land, with approximately 70% of the area characterized by a low slope, 21.47% of the land exhibiting a medium slope, and roughly 9% featuring a high slope. The data indicates that the Aksu stream basin falls within the category of low-slope terrain. The Aksu Basin exhibits an average elevation of 1664 meters. The basin is comprised of 46.14% shaded altitude in the northeast and 52.46% sunny altitude in the south-west.

Table 3. 1 Slope proportion of the basin

Slope	Values (%)
0-10	39.55
10-20	30.51
20-30	21.47
30-40	7.34
40-50	1.13

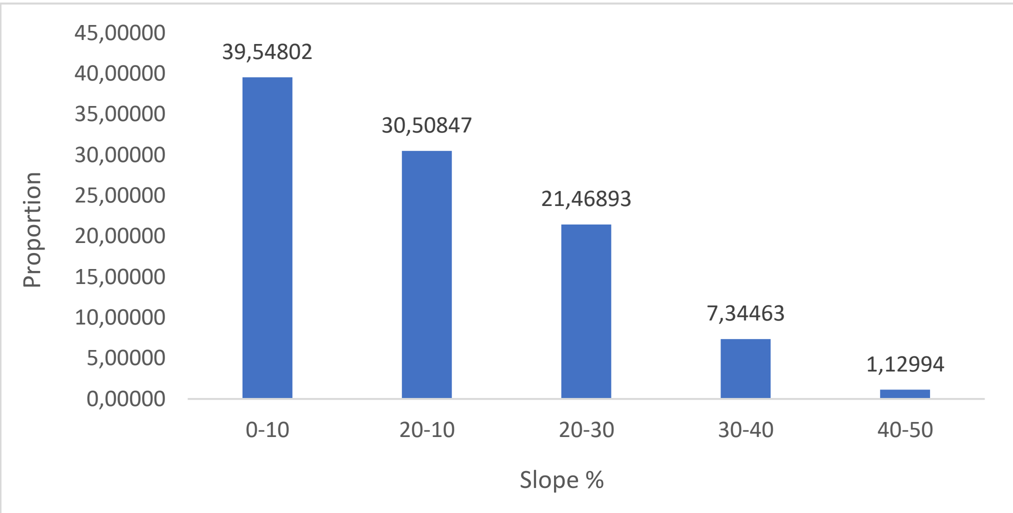

Figure 3.13 Slope proportions of the basin.

3.1.10 Land use

The variability observed in the flow coefficient values may be associated with modifications in land use practices, as well as other factors such as soil attributes (e.g., porosity and stratification), topographical features (e.g., river channel slope and gradient), and precipitation regimes (e.g., magnitude, duration, and intensity). Theoretical studies conducted by Huff et al. (2000) and Crouzeilles and Curran (2016), as cited by Zhang et al. (2017), suggested that larger watersheds display increased heterogeneity in various aspects such as landscape, topography, climate, geology, and vegetation. As a result, larger watersheds exhibit a greater ability to mitigate disruptions, such as alterations in land use, which leads to decreased susceptibility to modifications in forest cover as compared to their smaller counterparts. Catchments, which are small watersheds, demonstrate a greater degree of homogeneity in terms of relief, soil, and geology. The homogeneity of the catchment area eliminates the influence of these factors on the response of the catchment, as noted by Cerdan et al. (2004) and Merz et al. (2006).

The hydrological processes of the basin are significantly influenced by the diverse land use and land cover pattern it exhibits. The Aksu River Basin in Antalya exhibits diverse land uses, such as agriculture, forest, urbanization, and water bodies, as evidenced by the available land use and land cover data (refer to table 2). The basin is characterized by a predominant utilization of agricultural land, which encompasses roughly 44% of the entire region. The predominant agricultural produce grown within the basin comprises of citrus fruits, bananas, and various types of vegetables. The utilization of irrigation is imperative for the majority of agricultural pursuits in the basin, with the Aksu River serving as a primary source of water for such purposes. Approximately 25% of the basin area is covered by forest land, primarily situated on the slopes of the mountains. The preservation of forested regions is crucial for the maintenance of biodiversity, soil integrity, and carbon storage. The process of urbanization holds a notable presence in the basin, especially in the regions adjacent to the coast. Urbanization has led to the transformation of agricultural and forested land into residential and commercial zones, encompassing approximately 24% of the basin area. Watercourses, comprising of rivers, streams, and reservoirs, occupy an estimated 7% of the basin's total area. The Aksu River holds a significant position as the primary river in the basin and serves as a crucial water resource for the area.

Table 3. 2 Land Use details of the basin

Land Type	**Range %**
Pasture- Low agricultural	3
residential and industrial zone	24
Natural and forest	25
High agricultural	41
water body	7

The land use type is classified into five classes based on its permeability, beginning with the least permeable. These areas are: "natural and forestry," "pasture-low agricultural," "wetland," "high agricultural areas," and "residential and industrial zone. Land use data were obtained from the Directorate of Agriculture and Forestry. The use of impermeable materials in residential areas increases the amount of precipitation that passes through the flow, such as asphalt, parquet, and concrete on floors.

Apart from the aforementioned classifications of land use and land cover, the Aksu River Basin encompasses regions characterized by bare soil, wetlands, and rock outcrops. The Aksu River Basin in Antalya exhibits a varied land use and land cover pattern, underscoring the significance of adopting sustainable land use strategies to safeguard natural resources and ensure the region's enduring sustainability (Atayeter, 2000).

3.1.11 Soil Properties

The dominant soil types in the Aksu River Basin in Antalya are generally classified as Brown Forest Soils, Regosols, and Leptosols (Atayeter, 2000).

1. Brown Forest Soils: These are the most common soil type in the basin and are found in the mid to upper slopes of the mountainous areas. These soils are characterized by a thick organic layer and a high content of clay and silt. They are generally well-drained and moderately fertile.

2. Regosols: These are soils that are found in areas where the soil has been recently deposited by erosion or other processes. They are characterized by a lack of well-defined soil horizons and a low organic matter content. Regosols are often found in areas of recent landslides, river terraces, or other forms of soil movement.

3. Leptosols: These are shallow soils that are found on steep slopes and rocky areas. They are characterized by a thin layer of soil overlying bedrock and a low fertility level. Leptosols are often found in areas of high erosion rates and are not suitable for agriculture.

In addition to the above-mentioned soil types, there are also other soil types found in the basin, such as Arenosols, Gleysols, and Fluvisols. These soils are generally found in areas of the basin that are influenced by specific factors such as waterlogging, flooding, or sand deposition. The soil types in the Aksu River Basin in Antalya are diverse and are influenced by various factors such as topography, geology, climate, and vegetation cover. Understanding the soil types is important for sustainable land use practices and soil conservation efforts in the basin (Atayeter, 2000).

The soil is an important component that can withstand the effects of rain in the flow. The permeability and aeration capacity is changing due to polarisation, which varies depending on the soil type, which can reduce and reproduce the violence and effect of floods relatively. In this context, the most risk-bearing territories are Alluvial, Chestnut Color, Red Sea Territories, and Coluval territories, which are the most common soil groups downstream of the Aksu basin. Other soil in the basin has also been classified into risk classes based on its permeability (Atayeter, 2000).

Soil texture, structure, and composition can all affect water infiltration rates and soil water holding capacity in the Aksu River Basin. Infiltration rates can impact the amount and timing of water available for plant growth and recharge of groundwater resources. Soil water holding capacity can impact the potential for waterlogging and drainage problems, which can negatively impact agricultural activities and ecosystem services provided by soils.

Soil fertility is also an important factor to consider in hydrological and water resources management in the Aksu River Basin. Soil nutrients, such as nitrogen and phosphorus, can impact plant growth and productivity and can also impact water quality through leaching and runoff of excess nutrients into surface and groundwater resources.

Soil erosion is another important factor that can affect hydrological processes and water resources in the Aksu River Basin. Soil erosion can lead to sedimentation of water bodies, which can negatively influence aquatic habitats and water quality. Soil erosion can also reduce the productivity of agricultural lands and increase the potential for flood and landslide hazards (Atayeter, 2000).

3.1.12 Effect of Above-Mentioned Factors in Flow Coefficient.

The flow coefficient, also known as the runoff coefficient, is a critical parameter in hydrology that represents the proportion of rainfall that becomes runoff. Precipitation, temperature, humidity, wind, land use, slope, and soil permeability can all have an impact on the calculation of the flow coefficient. Here is a brief overview of how each of these factors can affect the flow coefficient:

1. Precipitation: The amount and intensity of precipitation can impact the flow coefficient by affecting the amount of water that infiltrates the soil and the amount that becomes runoff. Heavy rainfall events can lead to increased runoff, while lighter rainfall events may allow for more infiltration and less runoff.

2. Temperature: Temperature can impact the flow coefficient through its effect on soil moisture and evapotranspiration. Higher temperatures can lead to increased evapotranspiration, which can reduce the amount of water available for runoff.

3. Humidity: Humidity can impact the flow coefficient through its effect on evapotranspiration. Higher humidity can reduce the rate of evapotranspiration, leading to more water being available for runoff.

4. Wind: Wind can impact the flow coefficient by affecting the distribution of precipitation and the rate of evapotranspiration. Strong winds can cause precipitation to be more evenly distributed over a larger area, potentially

reducing runoff. Wind can also increase the rate of evapotranspiration, leading to less water being available for runoff.

5. Land use: Land use can impact the flow coefficient by affecting the amount of impervious surfaces, such as buildings and pavement, in an area. Areas with high amounts of impervious surfaces tend to have higher flow coefficients because less water is able to infiltrate into the soil and more becomes runoff.

6. Slope: Slope can impact the flow coefficient by affecting the rate of runoff. Steeper slopes tend to have higher flow coefficients because water is able to move more quickly over the surface, while gentler slopes allow for more infiltration and less runoff.

7. Soil permeability: Soil permeability can impact the flow coefficient by affecting the rate of infiltration. Soils with higher permeability allow water to infiltrate more quickly, potentially reducing the amount of runoff.

Comprehending the interplay among these variables can provide valuable insights for making informed decisions regarding water resource management, encompassing irrigation scheduling, storm water management, and erosion control.

3.2 Methodology

The primary source of uncertainties in civil engineering structures can be attributed to the lack of clarity and precision in defining system parameters. Ambiguity can arise due to multiple factors, such as physical unpredictability, statistical uncertainty resulting from incomplete information used to define parameters, and model uncertainties that arise from simplifying assumptions in analytical and predictive models, as well as the use of idealized representations of real-world phenomena. The issue of uncertainty stemming from imprecision is a commonly encountered phenomenon in scholarly literature. The lack of clarity is frequently noted in the delineation of diverse factors, including but not limited to the structural efficacy, caliber, debilitation, proficiency, and expertise of laborers and engineers, ecological ramifications of undertakings, and the conditions of pre-existing edifices. Moreover, establishing the interdependencies among the variables of challenges, particularly in intricate systems, can present a formidable task.

The fundamental aim of system modeling is to establish a structured framework that facilitates the prediction of the system's output in response to various circumstances. Attaining complete precision in ascertaining the outcome of a non-deterministic model is considered to be an unachievable feat. On the other hand, deterministic methodologies are unsuitable for the purpose of representing non-deterministic systems. In the realm of system modeling, non-deterministic models are prioritized over deterministic methodologies in the analysis of non-deterministic systems. In conventional pursuits, the creation of verbal representations is considerably less complex than the attainment of accurate quantification. Unlike linguistic terms, computers utilize numerical values and are incapable of conducting direct manipulations on them. Zadeh's theory of fuzzy logic enables the computational manipulation of linguistic values by electronic devices. Hence, the application of fuzzy logic in computer-based modeling of non-deterministic systems is a feasible approach. According to Toprak (2009), the application of deterministic and analytical models for the purpose of modeling social and natural phenomena presents a formidable challenge within the realm of engineering. A range of modeling techniques, including analytical, probabilistic, statistical, and stochastic dynamical modeling, require a model consisting of a series of hypotheses, as well as data that can be utilized for the purpose of verification. Hypotheses are constructed with the purpose of conceptualizing a phenomenon in an idealized manner. The formulation of hypotheses initiates a filtering mechanism that may result in the exclusion of imprecise segments of essential information. The process of converting a given set of input variables into an output using a set of fuzzy rules (FRs) is known as fuzzy inference.

Furthermore, another modeling technique that has been widely adopted since their introduction by McCulloch and Pitts (1943) and Metropolis et al. (1953) is artificial neural networks (ANNs). This increased utilization can be attributed to significant advancements in computational methodologies that focus on self-organizing capabilities and parallel information processing systems, particularly during the 1980s. Rumelhart et al. (1986) introduced a pioneering learning algorithm called backpropagation (BP) that was explicitly developed for neural networks consisting of units that bear resemblance to neurons. The methodology employs an iterative process to adjust the weights of the connections within the network. This adjustment aims to minimize a metric that measures the difference between the observed output vector of the network and the target output vector. During the late 1980s, artificial neural networks (ANNs) were extensively utilized in the domain of machine intelligence to understand complex and nonlinear phenomena. This phenomenon was apparent in the scholarly contributions of Lippmann (1987), Wasserman (1989), Zurada (1992), and Haykin (1994).

3.2.1 Why Fuzzy Logic?

The concept of Fuzzy Logic constitutes noteworthy progress in the field of computer logic. It enables computational and logical procedures in a way that is similar to how it facilitates human behavior. In 1965, Lutfi Zadeh published the primary documentation on fuzzy principles. Zadeh's introduction of the fuzzy logic method in 1965 has attracted considerable attention and interest from scholars, researchers, and professionals in diverse fields. The application of this approach in the field of civil engineering has exhibited its effectiveness in resolving problems that involve ambiguity or indistinctness. In the early 1970s, scholars in the scientific and technological fields recognized the feasibility and potential of the aforementioned implementation, as evidenced by the works of Brown (1979) and Alley et al. (1979). This method has been utilized to create numerous applications in the field of civil engineering. The utilization of this methodology has demonstrated efficacy in the analysis of construction failures, management of construction activities, assessment of safety measures in construction processes, decision-making in construction projects, evaluation of bids, assessment of the effectiveness of existing structures, and other relevant applications within the realm of structural engineering. Furthermore, it has been employed in the scrutiny and evaluation of hazards in the field of engineering, the design of watercourses, and other associated areas.

The utilisation of fuzzy logic, a mathematical methodology, is implemented to address scenarios that encompass indistinctness or imprecision. The previously mentioned methodology provides a mechanism for dealing with scenarios characterised by a dearth of certainty. The application of fuzzy logic methodology enables the representation of diverse linguistic concepts, including but not limited to high, low, medium, always, and few. The expansive range of fuzzy theory offers an inferential structure that enables optimal cognitive performance. In contrast, the traditional approach of utilising binary sets clarifies discrete events that may or may not be realised. The imprecise nature of real-world phenomena often limits the accuracy of engineering approaches. Consequently, the fuzzy method has gained widespread recognition as a well-established approach.

The fuzzy logic approach is founded on the concept of relative graded membership, which is a fundamental characteristic of cognitive functions and reasoning processes. Fuzzy sets possess significant utility owing to their ability to effectively model imprecise or uncertain data, as illustrated in Figure 3.14, a frequently encountered phenomenon in real-world scenarios. Fuzzy logic systems are advantageous in two specific situations: (1) when dealing with complex systems that are not fully understood and (2) when a quick estimate of a solution is sufficient.

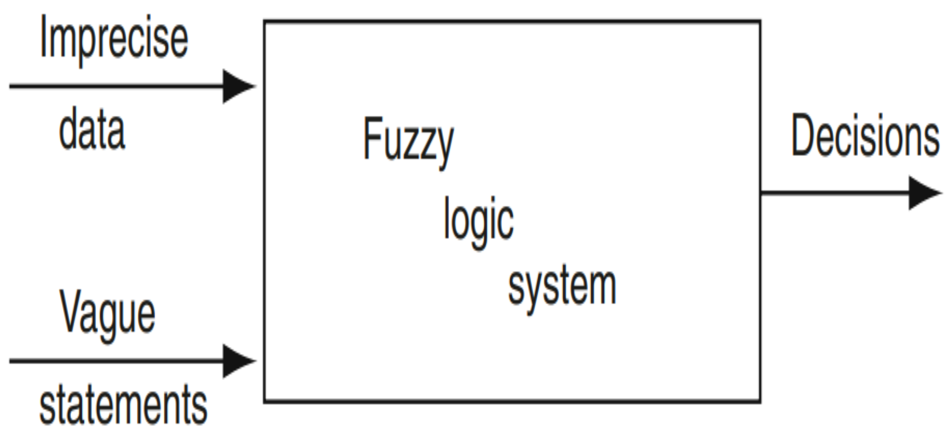

Figure 3.14 A system based on fuzzy logic that is capable of processing imprecise data and ambiguous statements to generate decisions.

The application of fuzzy logic theory can prove to be advantageous in the assessment of specific conventional systems that are relatively less intricate. For example, it is not always imperative to obtain precise solutions for certain problems. When faced with ambiguous, unclear, or poorly understood inputs, it can be essential to have a fast and approximate solution to generate initial design decisions, provide an initial assessment for a more precise numerical process to reduce computational costs, or address situations where the inputs remain unclear, vague, or not understood. The utilization of fuzzy logic is a popular method in scenarios where uncertainty is present, as it possesses the ability to facilitate adaptable and intuitive reasoning and decision-making. This is especially useful when faced with data that is either incomplete or imprecise. Fuzzy logic is distinguished from conventional Boolean logic by its ability to handle partial truths and uncertainties. While Boolean logic operates solely on binary values of true or false, fuzzy logic assigns degrees of membership to linguistic variables. This makes it more suitable for situations that are characterized by uncertain or ambiguous data, as well as multiple possible outcomes.

Fuzzy logic has the ability to incorporate non-linear relationships between variables and can proficiently represent complex and paradoxical phenomena. The adaptability of this feature renders it suitable for diverse pragmatic contexts, encompassing control systems, pattern recognition, decision-making, and artificial intelligence, among others. Furthermore, the implementation of fuzzy logic facilitates the incorporation of human knowledge and expertise into the decision-making process, which is a pivotal element in fields such as medicine, engineering, and finance.

3.2.2 The Significance and Function of Fuzzy Logic in the Field of Hydrology

The academic literature has established the intricate and uncertain nature of hydrological phenomena. Although a comprehensive dataset is typically required to accurately represent a hydrological phenomenon, the underlying mechanism of such an event can be sufficiently comprehended through human perception and reasoning. The complexity inherent in hydrological phenomena mandates the utilization of approximate reasoning (Fuzzy) in order to construct coherent and solvable models (Sen, 2002). The field of hydrology requires the implementation of a systematic model that can effectively integrate and communicate human knowledge, as well as integrate supplementary data sources such as field measurements and regulatory guidelines. Historically, there have been multiple attempts to convert nonlinear hydrological processes into linear systems as a result of mathematical constraints and requirements. An efficient model is expected to demonstrate a significant level of accuracy in defining the fundamental characteristics of the hydrological phenomenon while also being susceptible to mathematical scrutiny.

Fuzzy modeling is a mathematical methodology that functions autonomously from formulaic expressions, which are founded on rational principles. Fuzzy systems and models are distinct from mathematical models in their ability to integrate both linguistic and numerical information. The incorporation of professional assessments and quantitative data derived from a variety of instruments are regarded as crucial reservoirs of knowledge for hydrological systems. Traditional approaches do not take into account linguistic information. In contrast, the hallmark of fuzzy logic is the integration of data within a model's internal framework by means of fuzzy sets. The central focus of this inquiry pertains to the methodology employed by skilled hydrologists in converting their knowledge into a cohesive framework of principles, subsequently leading to the creation of a mathematical model or equation, as stated by Sen (1999).

3.2.3 Process for generating a membership function.

Membership Functions (MFs) are numerical values that are assigned to elements of a universal set within a predetermined range to indicate the degree of membership of those elements in the set. A mathematical function that assigns greater values to higher degrees of set membership is referred to as a membership function (MF).

The assessment of the imprecise characteristic of a fuzzy set entails the examination of its membership functions. The elements of the set are methodically organized, irrespective of their discreteness or continuity. Graphical representations can also be utilized to construct membership functions. A multitude of geometric shapes can be integrated into the visual representations. There are restrictions on the acceptable formats that can be utilized. The careful examination of the form of the membership function is a fundamental principle that necessitates due consideration. The regulations developed to account for the vague attributes of an application demonstrate a level of vagueness in their formulation. The notion of set membership was introduced by Zadeh (1965) as a means of arriving at sound decisions in situations where ambiguity is a factor.

The development of a lexicon of terms to describe the various characteristics of a membership function is beneficial, as it encompasses all the information provided in a fuzzy set. For the sake of simplicity, it is assumed that the functions illustrated in the figures are continuous. Nonetheless, the terms used are relevant to both discrete and continuous fuzzy sets. As illustrated in Figure 3.15.

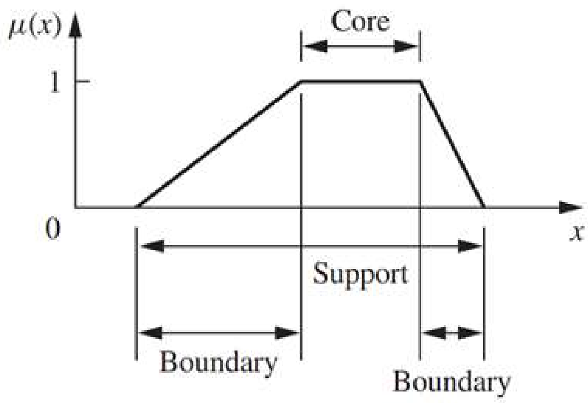

Figure 3. 15 Core, support, and boundaries of a fuzzy set.

(1) Core: The fundamental membership function of set A in Fuzzy is established by identifying the subset of the universal set that demonstrates a total membership value of 1 in set A. The core is defined as the set of elements whose membership function, denoted as μA (x) =1, attains a value of 1.

(2) Support: This statement concerns the act of providing support for a membership function that is linked to a fuzzy set A. This support is given when a portion of the universal set is determined to have a membership degree greater than zero in set A. The support set is characterised as a set of elements that exhibit a membership value greater than zero, denoted as μA (x) > 0.

(3) Boundary: The presence of partial membership in a particular region of the universe suggests the existence of a boundary for the membership function of a fuzzy set A. It is composed of constituent elements that possess memberships that vary between the values of 0 and 1, where 0 < μA (x) < 1.

The user has the option to select the configuration of the membership function, or alternatively, they may opt to generate it using machine learning techniques such as artificial neural networks and genetic algorithms, among others. A range of curves and shapes can be employed, although triangular or trapezoidal membership functions are commonly utilized owing to their simplicity of depiction. The study has shown a preference for the utilization of triangular membership functions.

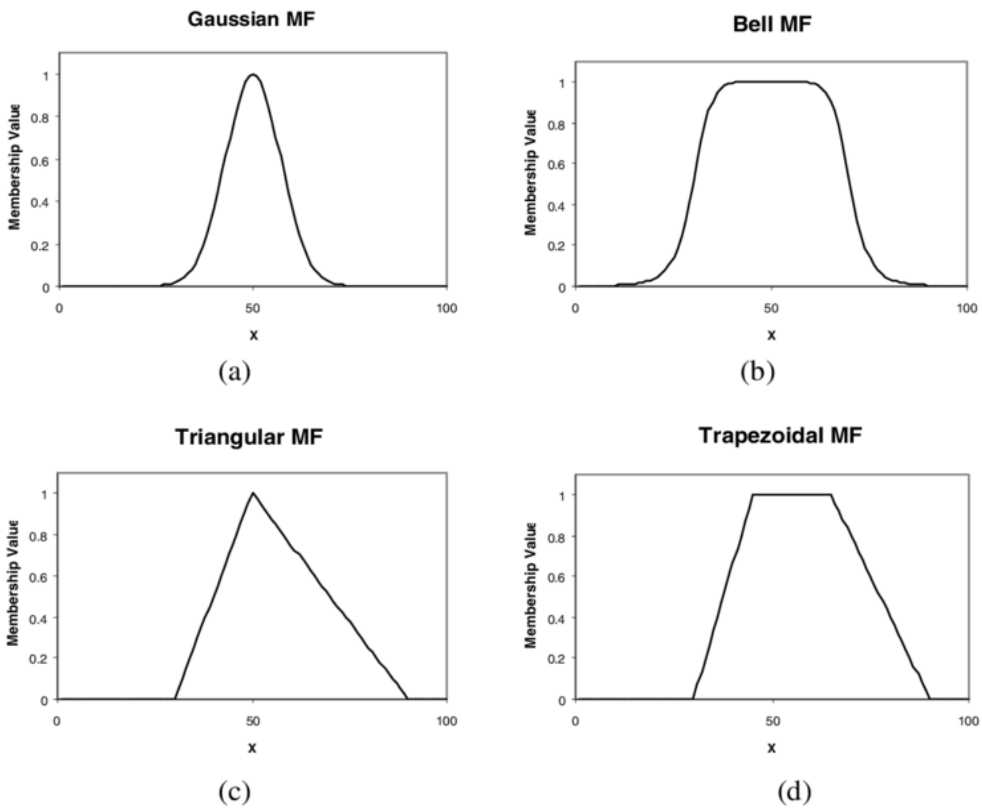

Figure 3.16 Commonly used MF shape (Ansari et al. 2004)

3.2.4 Fuzzy Set

A fuzzy set is a collection of elements that exhibit varying degrees of membership within the set. In contrast to classical or crisp set theory, wherein a member's membership in a set is negated if it is complete or exhaustive, the members of this set are considered members regardless of the completeness or exhaustiveness of their membership. Elements can belong to multiple fuzzy sets within the same universe, as their membership is not required to be mutually exclusive. The process of assigning numerical values to the fuzzy set yields a result that is bounded by the interval of 0 to 1. If a particular entity, represented as x, is a component of a fuzzy set A in the universe, then the associated mapping can be denoted as $\mu A\ (x) \in [0,\ 1]$. The graphical representation presented in Figures 3.17 and 3.18 delineates the process of mapping memberships.

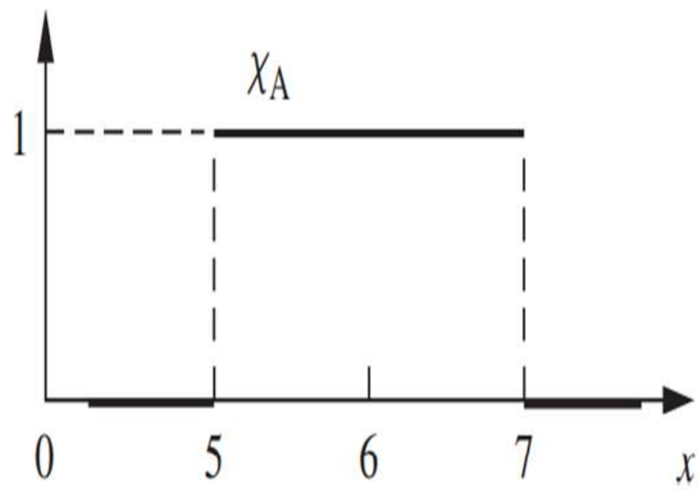

Figure 3.17 Classic (crips) set.

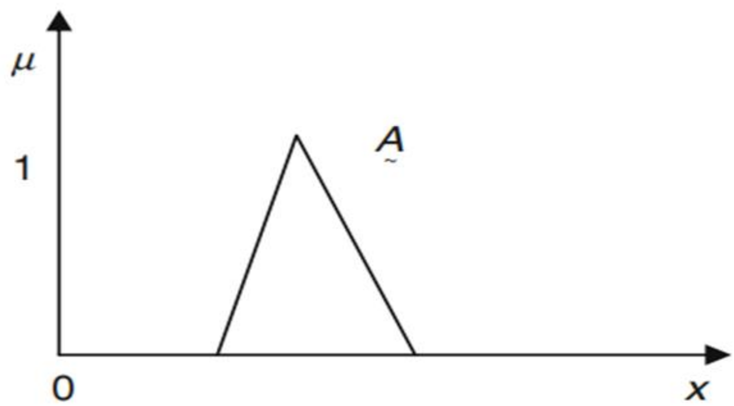

Figure 3.18 Fuzzy set.

Fuzzy sets consist of four fundamental components:

1. Fuzzy rule base: This segment delineates the collection of regulations and conditional IF-THEN statements that the user furnishes to manage the decision-making mechanism, predicated on linguistic information.

2. Fuzzification of input data: This section concerns the conversion of precise numerical inputs into fuzzy sets. Crisp inputs refer to accurate sensor readings that are conveyed to the control system for further analysis, including but not limited to temperature and pressure.

3. Inference System: The system governs the level of the established fuzzy input for every rule and determines the rules to be executed based on the input.

4. Defuzzification of output data: The process of converting the imprecise sets generated by the inference engine into a precise value is known as defuzzification.

3.2.5 Fuzzification of Input Data

The notion of fuzzification carries considerable significance within the framework of fuzzy logic methodology. Fuzzification refers to the transformation of fuzzy sets into sets that are either more vague or crisp sets into sets that demonstrate fuzziness. Fuzzy values can be produced by recognizing the intrinsic uncertainties that exist in exact quantities. The categorization of precise and definitive values can be deemed as entirely stochastic and distinguished by a significant level of indeterminacy. The indeterminacy pertaining to the variables can be ascribed to the existence of vagueness and inaccuracy, which may have led to fuzziness. Linguistic variable conversion is exemplified by the act of an observer transforming a specific input value, such as 37 degrees Celsius, into a linguistic variable that conveys whether the temperature is considered warm or cool with respect to the human body. The process of fuzzification pertains to the depiction of a system's inputs and outputs through the utilization of natural language, thereby enabling the formulation of a composite system that incorporates rules.

3.2.6 Fuzzy Rules Base

The foundation of acquiring a fuzzy output in fuzzy logic is established by fuzzy rules. The rule-based system differs from the expert system in that it generates knowledge from sources beyond those of human experts. The system that operates on the basis of rules employs linguistic variables in both its antecedents and consequents. The antecedent establishes a condition that must be met for the consequent to follow. Consequents refer to the inferred output resulting from the satisfaction of antecedent variation. Fuzzy rules are typically expressed in a formulaic manner, whereby the rule takes the form of "if (input 1 is membership function 1) and/or (input 2 is membership function 2) and/or...then (output is output membership function)." The multi-input single-output system's fuzzy model is characterized by rules that possess multi-ancestor and single-subsequent parameters, as exemplified by the following:

Rule R_i: [IF x_1 is A_{i1} and IF x_2 is A_{i2} and...and if x_n is A_{in} THEN y is $B_{i;}$ i ¼ 1; 2; . . .; k]

where x_1, x_2,…,x_n are input variables and y is the output, A_{ij} (i = 1,…,k, j = 1,…,n) and Bi (i = 1,…,k) are fuzzy sets. For example:

Rule 1: If Temperature is High and Humidity is High Then Flow is Low.

Rule 2: If Precipitation is High and Temperature is Low Then Flow is High.

Rule 3: If Precipitation is High Then Flow is High.

Rule 4: If Precipitation is High and Humidity is Low and Temperature is Low and Slope is High Then Flow is Very High.

The generation of fuzzy rules and membership functions can be achieved via either human expertise or a rigorous identification methodology. The integration of linguistic variables as antecedents and consequences in a fuzzy rule-based system framework provides considerable advantages for the modeling of intricate and diverse systems. The portrayal of linguistic variables can be achieved through the utilization of fuzzy sets and their corresponding logical connectives. By leveraging the inherent characteristics and mechanisms of fuzzy sets, it is possible to break down and simplify any combination rule framework into a limited set of basic standard rules. The regulatory framework is based on linguistic principles and patterns that have their origins in vague sets and imprecise reasoning.

3.2.7 Fuzzy Inference System (FIS)

A Fuzzy Inference System (FIS) is a type of system that is frequently denoted as a fuzzy rule-based system within academic literature. This is an essential element of systems that rely on fuzzy logic. The act of decision-making constitutes an essential element within the broader framework of the system. The Fuzzy Inference System (FIS) is a computational framework that devises and executes rules to facilitate informed decision-making. The aforementioned is predominantly dependent on the concept of fuzzy sets, fuzzy IF-THEN rules, and fuzzy cognitive concepts. FIS employs IF-THEN constructs, incorporating "OR" or "AND" operators within the rule statement to establish the requisite decision rules. The Fuzzy Inference System

(FIS) conforms to a norm that enables the inclusion of imprecise and precise inputs while uniformly producing imprecise outputs.

The Mamdani method, which is a widely utilised fuzzy inference technique, was first introduced by Mamdani and Assilian in 1975. Sugeno (1985) proposed the Takagi-Sugeno-Kang approach, considered one of the two most significant fuzzy inference techniques. The primary distinction between the two methodologies pertains to the impact of ambiguous regulations. Mamdani fuzzy systems utilise fuzzy sets as the resultant of rules, whereas TS fuzzy systems assign rule outcomes as linear functions of input variables. The current body of literature exclusively employs Mamdani fuzzy systems as universal approximators within the realm of fuzzy systems. However, there is a lack of empirical substantiation regarding the effectiveness of TS fuzzy systems with a linear rule consequent in this capacity.

4.1.7.1 Mamdani Fuzzy Inference System

The Mamdani fuzzy inference system, which employs maximum-minimum operations, has been widely adopted in the field of fuzzy logic. Its initial application was in the control of steam engines. The Mamdani approach, which employs fuzzy logic, was developed by Ibrahim Mamdani et al. 1977, starting from the very basics. Owing to its user-friendly design, alignment with human cognitive processes, and comprehensible framework, this particular fuzzy inference technique has rapidly gained widespread adoption. Figure 3.19 illustrates the fundamental logic of the Mamdani fuzzy inference system. The Mamdani fuzzy inference system employs expert knowledge or sample data during the fuzzification process to establish membership functions for all inputs and outputs. The level of imprecision in the system's inputs and outputs is established by the pre-established quantity of clusters. Following the process of fuzzification, the fuzzy rules are subsequently redefined by referencing either an existing knowledge base or a database of examples. The process of combining the outputs of the fuzzy rules occurs after evaluating their efficacy. The utilization of a suitable clarifying agent produces clear and comprehensible results, while the lack of such an agent results in uncertain and vague outcomes. The process of constructing a Mamdani-type fuzzy logic model comprises five distinct steps:

i. Using fuzzy expressions to determine membership degrees between 0 and 1 for input variables.

ii. Establishing the rules.

iii. Implementation and/or.

iv. Combining fuzzy sets that represent outputs.

v. Defuzzification of fuzzy set outcomes.

The computational methodology employed in a Mamdani-type fuzzy inference system for Ci fuzzy set functions, as illustrated in Figure 3.7, entails the integration of two rules that encompass numerical variables (x and y). Equations 3.5 and 3.6 delineate the two principles utilised for ascertaining this system.

Rule 1: if $x = A_1$ and $y = B_1$ then $z = C_1$ (4.1)

Rule 2: if $x = A_2$ and $y = B_2$ then $z = C_2$ (4.2)

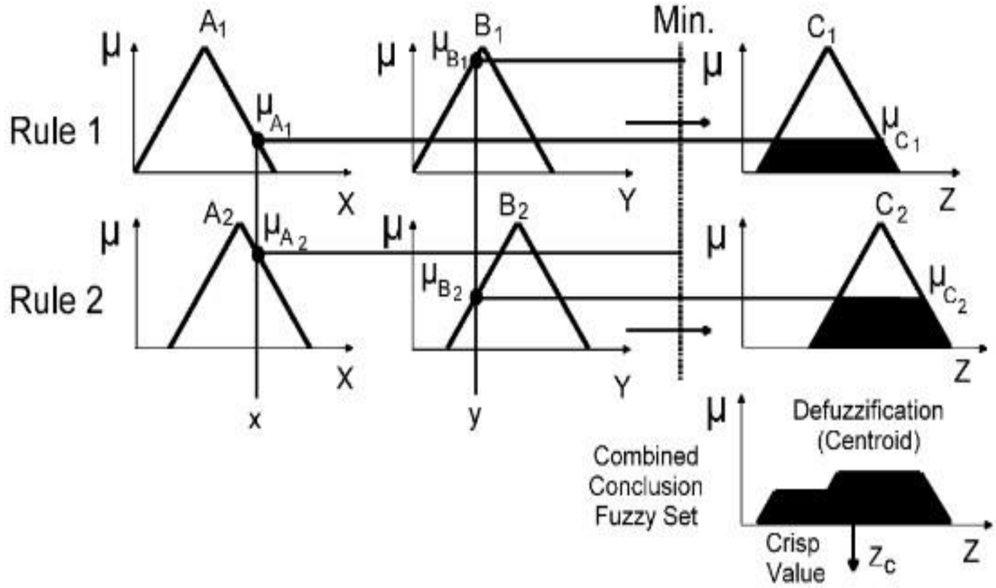

Figure 3.19 A schematic illustration of the Mamdani fuzzy inference system (Rustum et al., 2020).

The current study focused on the creation of the SMRGT forecasting model using the Mamdani fuzzy inference method. The approach mentioned above embodies a conventional application of fuzzy logic. The approach that has been put forward is consistent with the fundamental tenets of fuzzy logic as initially proposed by Zadeh in 1965. The methodology consists of linguistic expressions. Grima (2000) has asserted that the adaptability of this methodology has enabled its implementation in various fields of engineering. As per Yilmaz's (2015) findings, the Mamdani-type fuzzy logic methodology comprises a series of steps. These include the process of fuzzification of input variables, identification of rule bases, utilisation of fuzzy logic tools such as "and" and "or" operators, aggregation of outputs by merging all fuzzy sets obtained, and ultimately, defuzzification.

4.2.7.2 Sugeno Fuzzy Inference System

The Sugeno fuzzy model was introduced by Tagaki-Sugeno-Kang in 1985 as a variant of the Mamdani type model, achieved through the alteration of the rule structure of the Mamdani fuzzy inference system (Sivanandam et al., 2007). Zschorn (2006) asserts that the antecedent rules of the Sugeno fuzzy inference system are based on fuzzy sets. Hence, it is established that the inputs for every system necessitate blurring. In contrast to the Mamdani model, this model's output variable values are not fuzzy. According to Fırat's (2007) research, the output membership functions in Sugeno-type fuzzy logic models can be represented by either constant or linear functions. The aforementioned model can be classified as a zero-order model in the event that the output membership functions remain constant. Conversely, it can be categorized as a first-order Sugeno fuzzy model if it conforms to the structure of a first-order line equation. As a result, there is variation in the composition of rules. The fuzzy inference mechanism of the first-order Sugeno model is illustrated in Figure 3.8. The rules for a system with P inputs and one output of Sugeno type are as follows:

$$\mathrm{Pi} = \text{if Input1} = \mathrm{x} \text{ and Input2} = \mathrm{y} \text{ then } \mathrm{z} = \mathrm{c} \quad (4.3)$$

Or

$$\mathrm{Pi} = \text{if Input1} = \mathrm{x} \text{ and Input2} = \mathrm{y} \text{ then } \mathrm{z} = \mathrm{ax} + \mathrm{by} + \mathrm{c} \quad (4.4)$$

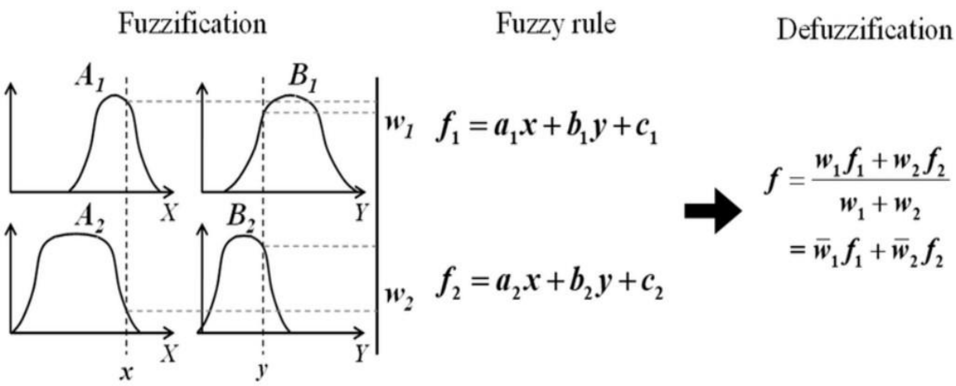

Figure 3.20 Sugeno inference system (Cho et al., 2020)

3.2.8 Defuzzification of Output Data

Defuzzification is a crucial step in fuzzy logic systems, whereby the imprecise output values derived from the rule-based inference process are transformed into a precise output value. The process of defuzzification is deemed necessary due to the fact that the outcome of a fuzzy logic system is a fuzzy set, which comprises a collection of membership values. Various techniques exist for defuzzification, with the centroid method being the most frequently employed. The method of centroid ascertains the crisp output value through the computation of the centroid of the fuzzy set pertaining to the output. The utilization of the center of gravity (COG) technique has been favored in this research due to its enhanced compatibility with the fuzzy SMRGT method, as noted by Toprak (2009). This approach is alternatively referred to as the center of mass and center of area technique. This particular defuzzification method enjoys widespread usage. The defuzzified output, denoted by z*, is expressed algebraically as follows:

$$z* = \int \mu(z).zdz / \int \mu(z)dz \qquad (4.5)$$

The steps for defuzzification using the centroid method:

1. Identification of the output fuzzy set with the highest membership value.
2. Calculation the centroid of the output fuzzy set.
3. The centroid value is the defuzzified output.

The utilisation of the centroid methodology is characterised by its straightforwardness in implementation and its ability to provide a desirable balance between accuracy and user-friendliness. However, it may not always be the most effective strategy for every situation. In certain situations, it may be more appropriate to utilise alternative defuzzification methodologies, such as the maxima or height techniques. The choice of the defuzzification method is dependent on the specific application and the specifications of the system. The process of choosing an appropriate defuzzification method is of utmost importance in ensuring accurate and meaningful results.

There are many other ways to defuzzify fuzzy output functions, such as AI (adaptive integration), BOA (bisector of area), SLIDE (semi-linear defuzzification), CDD (constraint decision defuzzification), FOM (first of maximum), ECOA (extended center of the area), EQM (extended quality method), FCD (fuzzy clustering defuzzification), QM (quality method), RCOM (random choice of maximum), FM (fuzzy mean), GLSD (generalized level set defuzzification), ICOG (indexed center of gravity), IV (influence value), LOM (last of maximum), MOM (mean of maxima), and WFM (weighted fuzzy mean), BDD (basic defuzzification distributions).

3.2.9 SMRGT Method Procedure

Toprak initially presented the SMRGT technique in 2009. The determination of membership functions (triangles/trapezes) and fuzzy rules necessitates the utilisation of the "center of gravity" method. The effectiveness of fuzzy modelling is heavily reliant on the establishment of membership functions (MFs) and fuzzy rules (FRs). This is particularly significant when utilising only the available data for modelling purposes. The academic literature has extensively explored the process of determining membership functions (MFs) and fuzzy rules (FRs) using various models such as genetic algorithms, artificial neural networks, and Kalman filters. Several studies have focused on the individual examination of membership functions and fuzzy rules, while others have investigated the joint determination of both MFs and FRs. Unfortunately, the methods utilised to determine membership functions (MFs) and fuzzy rules (FRs) require a significant amount of time and computational resources in comparison to other software packages or heuristic approaches. Moreover, notwithstanding the implementation of diverse research methodologies, academics are incapable of completely avoiding the trial-and-error methodology. As a result, the method of trial and error continues to be commonly employed. The selection of appropriate techniques for the determination of MFs and FRs necessitates the consideration of factors such as manageability, processing volume, and the reliability and validity of the results. The centroid method for determining the center of gravity is favored due to its greater compatibility with the fuzzy SMRGT method described by Toprak (2009). The aim of this methodology is to identify the center of gravity of the output and obtain the corresponding value for the said center of gravity, as stated by Sen in 2001. There are no limitations in the SMRGT model. The lower and higher boundaries of the model can both be selected by the user. The user may quickly determine the permissible value range for the model, which is represented by the aforementioned range. The Fuzzy SMRGT approach is preferred above other methods proposed in the literature because its implementation is easier to use and more reliable.

The current study focused on the creation of fuzzy models to accurately predict the flow coefficient within the Aksu River basin. Toprak's (2009) SMRGT methodology is utilised to determine the membership function and fuzzy rules base prior to the modelling process. The MATLAB R2019a software was employed thereafter. A compact subprogram can be utilised to execute MATLAB software. The implementation of the Centre of Gravity (Centroid Method) technique requires the determination of membership functions and the assignment of fuzzy rules. An essential benefit of this methodology is its ability to allow the model to simultaneously ascertain the fuzzy rules base (FRs) and membership functions (MFs) using a straightforward technique. On the contrary, as it depends solely on the expertise of experts, it allows for the development of the model even in the absence of any data.

Significant differences between SMRGT and other available methods include:

1. Model calibration does not necessitate the use of data.
2. The SMRGT approach is capable of simulating diverse hydrologic phenomena owing to its reliance on physical principles rather than empirical data. This statement suggests that the model exhibits a degree of generalizability.

3. It is unnecessary to invest in costly package programs in order to improve the model's performance.

4. The SMRGT modeling technique is characterized by its simplicity and the minimal resources it requires, as it solely relies on a single sheet of paper for its implementation.

5. The results exhibit a high degree of realism.

6. According to Toprak (2017), the SMRGT technique is a more contemporary approach compared to other techniques documented in the literature.

Moreover, this methodology demonstrates consistent performance across diverse datasets. If the model is applied to heterogeneous datasets, the error rate will remain constant. Therefore, the methodology was considered to be robust in terms of its results. The current investigation presents a novel approach and proposes a series of recommended procedures to achieve the most favorable results:

I. The independent and dependent variables that have an impact on the current event were identified. In the context of fuzzy systems, the independent variables are commonly referred to as inputs, while the dependent variables are referred to as outputs. For example:

Input (independent variables)	Output (dependent variables)
X, Y	**Z**

The determination of Xmin and Xmax values ought to be informed by expert recommendations, and the scope of these intervals may be modified to accommodate the particular circumstances under consideration. The XR value can be calculated using Equation 4.4.

$$X_R = (X_{\max}) - (X_{min}) \tag{4.6}$$

The present investigation consists of 5 models with different combinations of the inputs variable. The 1st model (SMRGT-1) employed temperature (T) and wind speed (Ws) as inputs, the 2nd model (SMRGT-2) employed land use (LU), and slope (S) as inputs, the 3rd model (SMRGT-3) employed precipitation (P), temperature(T), and relative humidity (Rh) as inputs, the 4th model (SMRGT-4) used precipitation

(P), land use (LU), and soil permeability (Sp) as inputs, the last model (SMRGT-5) used precipitation (P), temperature(T), and relative humidity (Rh), slope (S), and land use (LU) as inputs. At the same time, the dependent outcome is represented by the flow coefficient for all models.

II. Specify the variability domain, which includes limits on input and output variables. Upon analysis of the data gathered from the designated study region, it was determined that the precipitation ranges exhibited a minimum and maximum value of (200 – 2000) mm, land use (0 - 100)%, temperature (0 – 50) °C, wind speed (0 - 10) m/ s, relative humidity (0 - 100)%, slope (0-90)°, and soil permeability (0 - 100), respectively.

III. Choose the shape of the membership function (MF), such as triangular, trapezoidal, etc., as per the suggestion put by Toprak (2009). The utilization of triangular was preferred in models (SMRGT-1, SMRGT-2, SMRGT-3, and SMRGT-5), while trapezoidal membership functions were prioritized in model SMRGT-4. For each independent variable, the number of membership functions must be determined, with a minimum allocation of three MFs. The present study involves the construction of membership functions for each independent variable, comprising five distinct fuzzy sets denoted as (Very Low (VL), Low (L), Medium (M), High (H), and Very High (VH)), while only for SMRGT-1 they were (Very very low (VVL)Very Low (VL), Low (L), Medium (M), High (H), Very High (VH), and Very High (VVH)).

IV. Toprak (2009) suggests that it is advisable to employ a right-angled triangle for the initial and final membership functions while utilizing a trapezoidal shape or an isosceles triangle for the membership functions in between. The credibility of a fuzzy system relies on the distribution of data amidst the pivotal values of the initial and concluding membership functions for every autonomous variable. The implementation of the membership function and fuzzy rules set is essential in reducing the time required for trial and error. Table 3.3 displays the specific details of all SMRGT models.

Table 3. 3 The details of the SMRGT models

Models	No. of inputs	No. of MFs	No. of	MFs shape

			fuzzy rules	
SMRGT-1	Ws + T	7	49	Triangular
SMRGT-2	LU + S	5	25	Triangular
SMRGT-3	P + T + Rh	5	125	Triangular
SMRGT-4	P + LU + Sp	5	125	Trapezoidal
SMRGT-5	P + T + Rh + LU + S	5	3625	Triangular

V. In the current study, triangular membership functions (MFs) were selected for specific models, while trapezoidal MFs were chosen for others. The identification of the essential parameters, namely the key values (K1, K2, … KN) and the core value (Ci) of the membership functions, along with the unit width (UW), the symmetrically extended unit width (EUW) for each membership function, and the value (O) of the two intersecting neighbour membership functions, are fundamental stages in the examination of each variable. Moreover, the determination of right-angled triangles (nu) in the triangular fuzzy set has been established by utilizing the specified formulas illustrated in Figure 3.21. Furthermore, the process of establishing fundamental principles, standardizing unit measurements, and identifying pivotal values for both reliant and autonomous factors has been successfully executed.

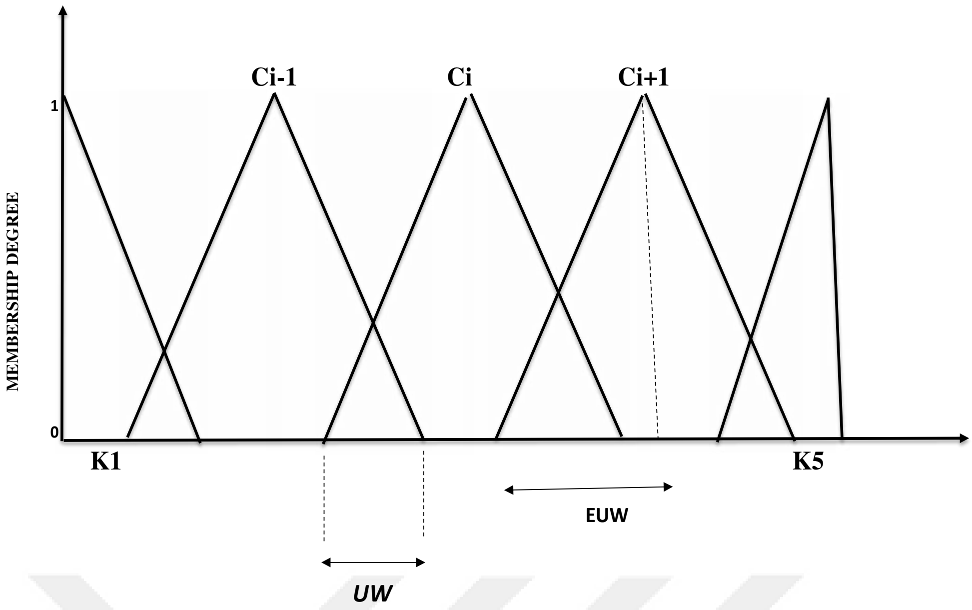

Figure 3.21 core values, key values, and unit width for the model.

$$Vr = X\max - Xmin \tag{4.8}$$

$$Ci = K3 = \frac{Vr}{2} - Xmin \tag{4.9}$$

$$UW = \frac{Vr}{nu} \tag{4.10}$$

$$O = \frac{UW}{2} \tag{4.11}$$

$$EUW = UW + O \tag{4.12}$$

$$K4 = Ki = Ci + 1 = \left(\frac{Ci - Xmin}{2}\right) + Xmin \tag{4.13}$$

$$K2 = Ci - 1 = Xmax - \left(Xmax - \frac{Ki}{2}\right) \tag{4.14}$$

$$K1 = Xmin + \left(\frac{EUW}{3}\right)$$

(4.15)

$$K5 = Xmax - \frac{EUW}{3}$$

(4.16)

In addition, MATLAB code can be used to calculate the key values of the models depicted in Figure 3.2.

```
[K,m,min,max] = keysCalculate ();
UW = (max - min) / (2*m - 2);
a = addvar(a,varType,varName,[min max]);
p1 = min -1;
p2 = min;
p3 = K(1) + UW;
a = addmf(a,varType,varNum,'1','trimf',[p1 p2 p3]);
p1 = K(1);
p2 = K(2);
p3 = p1 + 3*UW;
for i = 2: m-1
    a = addmf(a,varType,varNum,int2str(i),'trimf',[p1 p2 p3]);
    p1 = p3 - UW;
    p2 = K(i+1);
    p3 = p1 + 3*UW;
    if i == m - 1
        p3 = K(m);
    end
end
p1 = K(m) - UW;
p2 = max;
p3 = max + 1;
a = addmf(a,varType,varNum,int2str(m),'trimf',|[p1 p2 p3]);
b = a;
```

Figure 3.22 Generated MATLAB code for key values calculation.

VI. It was decided to ensure that the number of key values would align with the number of membership functions for each independent variable. The key values are utilized as the inputs for the fuzzy model. It is recommended to choose a commensurate quantity of membership functions (MFs) and fuzzy rules (FRs) when electing the outputs.

VII. Package programs, such as the MATLAB software, were designed to incorporate the concept of fuzzy sets.

VIII. The utilization of the Excel program can facilitate the execution of all procedures delineated in the preceding six articles. It is noteworthy that the aforementioned procedures solely pertain to the establishment (calibration) of the model.

IX. The pertinent software package was employed to generate the input and output data files using calibration data. Test data is employed to expeditiously generate input and output files in a comparable manner. In accordance with the established methodology, two sets of data files were produced, consisting of an input file and an output file, for both the calibration and testing phases. A fuzzy system was subsequently developed through the utilization of suitable software packages. A subprogram was utilized to streamline program execution and facilitate result evaluation. The SMRGT methodology, which has been developed recently, diminishes the dependence on the empirical approach.

X. In cases where the output membership functions display an excessive degree of intertwinement, it becomes imperative to undertake measures to reduce them. This can be achieved by consolidating two or more combined membership functions into a single function, as suggested by (Toprak, 2009& Toprak, 2017).

3.2.10 Artificial Neural Network (ANN)

Artificial neural network (ANN) models have demonstrated significant efficacy as prediction tools in the analysis of the correlation between rainfall and flow parameters. The findings derived from this research will offer significant assistance in informing decision-making processes within the realm of water resources planning and management. Furthermore, they assist urban planners and managers in the implementation of requisite strategies to mitigate the adverse effects of production. Consequently, they play a crucial role in averting harm to both public and private assets while also mitigating potential health and ecological hazards linked to inundation events. Moreover, there has been a substantial increase in the utilization of artificial neural network (ANN) models within the domains of science and engineering. The primary reason for their exceptional ability to effectively depict both linear and nonlinear systems is their capacity to eliminate the need for assumptions commonly required in conventional statistical methods. Artificial neural networks (ANNs) have proven effective in addressing a range of hydrologic issues. Riad et al. (2004) [1] and Lallahem et al. (2005) [2] utilized artificial neural networks (ANNs) in their research to forecast river flow. In their study, Smith and Eli (2003) [3] employed artificial neural networks (ANNs) to forecast the rainfall-runoff process. Furthermore, Maier and Dandy (1996) [4] employed artificial neural networks (ANNs) as a means of forecasting water quality parameters. In addition, artificial neural networks (ANNs) have been employed in diverse domains, including the estimation of evaporation (Sudheer, 2002) [5], forecasting rainfall-runoff patterns

(Minns and Hall, 1996) [6], predicting flood disasters (Wei et al., 2002) [7], and forecasting river time series (Hu et al., 2001) [8]. The hydrological applications make use of a multilayer feed-forward backpropagation algorithm, as described by Lippmann (1987) and Riad et al. (2004). [9]. A conventional neural network is comprised of multiple interconnected nodes, which are structured into an input layer, an output layer, and one or more hidden layers As illustrated in Figure 3.23.

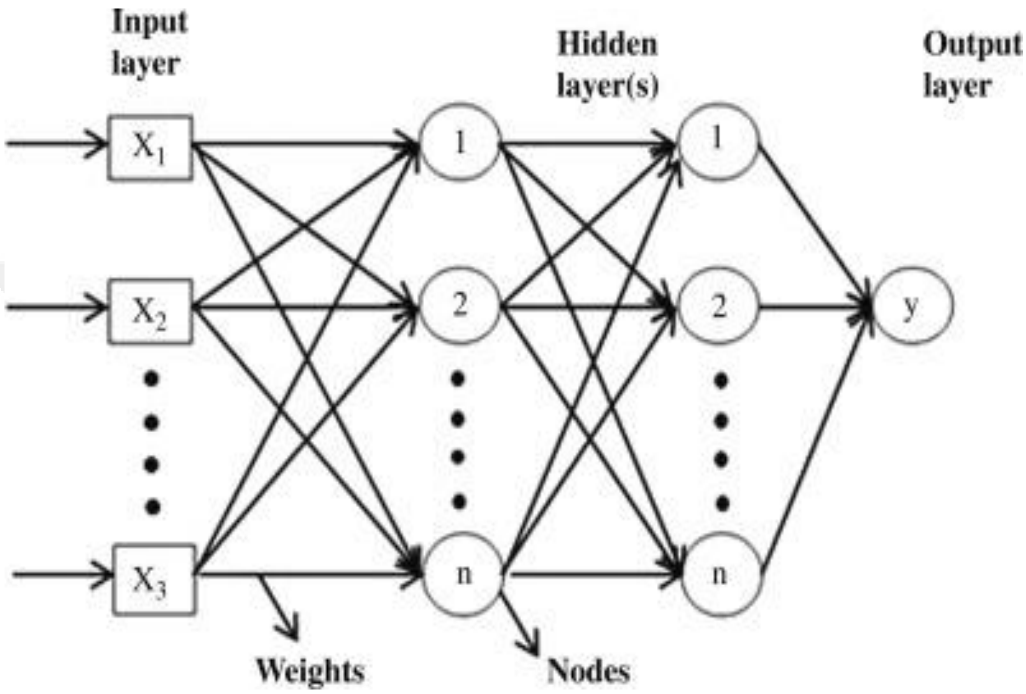

Figure 3.23 General Construction of ANN (Sairamya et al., 2019)

The present study utilized the Back Propagation (BP) algorithm for training, explicitly implementing the Levenberg–Marquardt optimization technique. The effectiveness of this particular optimization technique, as compared to conventional gradient descent techniques, has been suggested by a study conducted by Najjar and Ali [46]. The study's findings indicate that the Marquardt algorithm demonstrates a high level of efficiency when utilized for training neural networks that possess a relatively limited number of weights, typically falling within the range of hundreds. While the Marquardt algorithm necessitates greater computational resources per iteration, its efficacy remains unparalleled. This assertion holds particular validity in situations where a significant level of exactitude is necessary.

The present study employed the artificial neural network (ANN) methodology to forecast the flow coefficient. The analysis was performed utilizing the MATLAB software. The construction of the artificial neural network (ANN) models involved the utilization of an input layer comprising five neurons that represented variables such as precipitation, temperature, humidity, and wind speed. Furthermore, a solitary concealed layer comprising 20 neurons was employed. The determination of the number of neurons in the hidden layer was accomplished through an iterative process involving experimentation and evaluation. The output layer comprises a solitary neuron that is tasked with the prediction of the flow coefficient. Three artificial neural network (ANN) models were developed utilizing the Levenberg-Marquardt back-propagation training algorithm, explicitly employing the TRAINLM function in MATLAB. The Levenberg-Marquardt algorithm is a variant of the Gauss-Newton method, with additional details available in references [Hagan et al. 1994, Reynaldi 2012]. The initial model denoted as ANN-1, underwent training utilizing two distinct sets of inputs, namely temperature and wind speed.

The subsequent model, referred to as ANN-2, underwent training utilizing a dataset comprising three distinct inputs, namely precipitation, temperature, and humidity. The third model denoted as ANN-3, underwent training utilizing four distinct inputs, namely precipitation, temperature, wind speed, and humidity. The artificial neural network (ANN) model underwent training using a dataset comprising meteorological observations spanning a period of 16 years. The dataset was partitioned into three distinct stages: 70% for the purpose of training, 15% for validation, and the remaining 15% for testing. The application of the Min-Max scaling technique was employed to standardize the training, test, and validation datasets.

3.2.11 Adaptive Neuro-Fuzzy Inference System (ANFIS) Development

The Adaptive Neuro-Fuzzy Inference System (ANFIS) is a machine learning methodology that merges the strengths of neural networks and fuzzy logic. Jang (1993) introduced ANFIS as a method for effectively modeling intricate systems through the integration of both data-driven learning and human expert knowledge. The Adaptive Neuro-Fuzzy Inference System (ANFIS) has been employed in diverse domains, including control systems, pattern recognition, time-series forecasting, and optimization challenges (Shrivastava and Gupta, 2021).

The Adaptive Neuro-Fuzzy Inference System (ANFIS) utilizes imprecise rules to describe the relationship between the input and output of a particular system. The production of regulations is facilitated by a machine learning algorithm that integrates input-output data with human expertise in the form of linguistic variables and fuzzy sets. The ANFIS employs the aforementioned rules to generate outcomes for new input data. Jang (1993) posited that the ANFIS architecture is composed of five discrete layers, which include the input layer, membership function layer, normalization layer, fuzzy rule layer, and output layer.

The Adaptive Neuro-Fuzzy Inference System (ANFIS) has been extensively employed in the domain of hydrology for diverse purposes, including but not limited to flood prediction, modeling of rainfall-runoff, and forecasting of groundwater levels. Zhao et al. (2014) utilized ANFIS to construct a rainfall-runoff model for the upper region of a river basin in China. The model demonstrated a notable level of precision in forecasting streamflow. Haghighi et al. (2018) demonstrated the effectiveness of ANFIS in forecasting groundwater level in an Iranian aquifer, surpassing conventional regression models in terms of performance.

The Adaptive Neuro-Fuzzy Inference System (ANFIS) is a machine learning approach that combines the beneficial characteristics of neural networks and fuzzy logic, resulting in a resilient methodology. The effectiveness of this particular tool in simulating complex systems can be credited to its ability to incorporate both data-driven machine learning and human expert knowledge. The Adaptive Neuro-Fuzzy Inference System (ANFIS) has exhibited promising capabilities for a variety of hydrological applications, such as flood prediction and groundwater level estimation. Through the amalgamation of data-driven machine learning and expert human knowledge, the ANFIS model exhibits a notable degree of precision in forecasting the flow coefficient. The ANFIS model integrates input-output data and expert knowledge to produce fuzzy rules, facilitating the acquisition of knowledge regarding the underlying patterns and correlations between the input variables and the flow coefficient. The model subsequently utilizes the aforementioned fuzzy rules to generate outputs for new input data. The ANFIS model is designed to optimize the parameters of fuzzy rules, which results in improved precision of the model. The optimization procedure is frequently achieved through the utilization of a hybrid learning algorithm that combines backpropagation and least squares methodologies.

A standard set of IF/THEN rules for two inputs and one output in first-order Sugeno's system can be represented as follows:

Rule 1: If x is A_1 and y is B_1, then $f_1 = p_1 x + q_1 y + r_1$ (4.17)

Rule 2: If x is A_2 and y is B_2, then $f_2 = p_2 x + q_2 y + r_2$ (4.18)

Generally, ANFIS is composed of five layers:

1. **Input Layer:**

The nodes in the input layer function as a depiction of the input variables in the given system. Each input node is associated with a membership function that establishes a correlation between an input value and a fuzzy set. Given a set of n input variables, it is feasible to express the input layer as follows:

$$y_1 = x_1, y_2 = x_2 ... y_n = x_n \tag{4.19}$$

Where Input variables are denoted by x_1, x_2... xn, and their corresponding nodes in the input layer are denoted by y_1, y_2... yn.

2. Fuzzification Layer:

The nodes within this particular layer function as both multipliers and transmitters. This particular product denotes the degree of firing strength demonstrated by a specific rule. The function that represents the membership of a node (i) for a given input (j) is symbolized as Aij(x), with the parameters (pij) being explicitly defined. The notation used to represent the output of the fuzzification layer is as follows:

$$\mu_{ij} = A_{ij} (x_j), \quad \text{for i=1 to m and j=1 to n} \tag{4.20}$$

Where (m) is the number of membership functions per input variable and (μ_{ij}) is the degree of membership of the j^{th} input variable in the i^{th} fuzzy set.

3. Rule Layer:

The nodes situated within this particular layer perform computations to determine the firing strength of the i^{th} rule in relation to the overall firing strength of all rules s (Yılmaz, 2003).

$$\overline{W} = \frac{W1+W2+W3}{W1} \tag{4.21}$$

4. **Defuzzification Layer:**

This layer's nodes are adaptive with node functions.

$$\overline{W}if = \overline{W}\ (pix + qiy + ri) \tag{4.22}$$

Where i is the output of Layer 3 and {pi, qi,ri} are the parameter set. Parameters of this layer are referred to as consequent parameters.

5. **Output Layer:**

All inputs are combined at a single fixed node to produce the final output. We can model the output layer as s (Yılmaz, 2003):

$$f = \sum_{i=1}^{n} \overline{W}ifi \tag{4.23}$$

3.2.12 Normalization

The process of normalization involves the systematic structuring and optimisation of data within a database, with the aim of minimising redundancy and dependency among the data. The employment of a tool in the process of database design ensures consistent and systematic storage of information. The proposition of the relational model was initially put by Edgar F. Codd. Normalisation refers to the systematic organisation of a database's attributes, columns, and table relationships in a manner that enables integrity constraints to adequately enforce the dependencies between them. The process involves the application of formal rules, which may be in the form of synthesis for the creation of a new database design or decomposition for the improvement of an existing database design.

In order to mitigate the computational burden during preprocessing, the data is subjected to normalisation within the range of 0 to 1, utilising the subsequent equation:

$$Xnor. = \frac{X - Xmax}{Xmin - Xmax} \tag{4.24}$$

Where $X_{nor.}$ is the normalized data, x is the original data, X_{min}, and X_{max} are the minimum and maximum values of the original data, respectively.

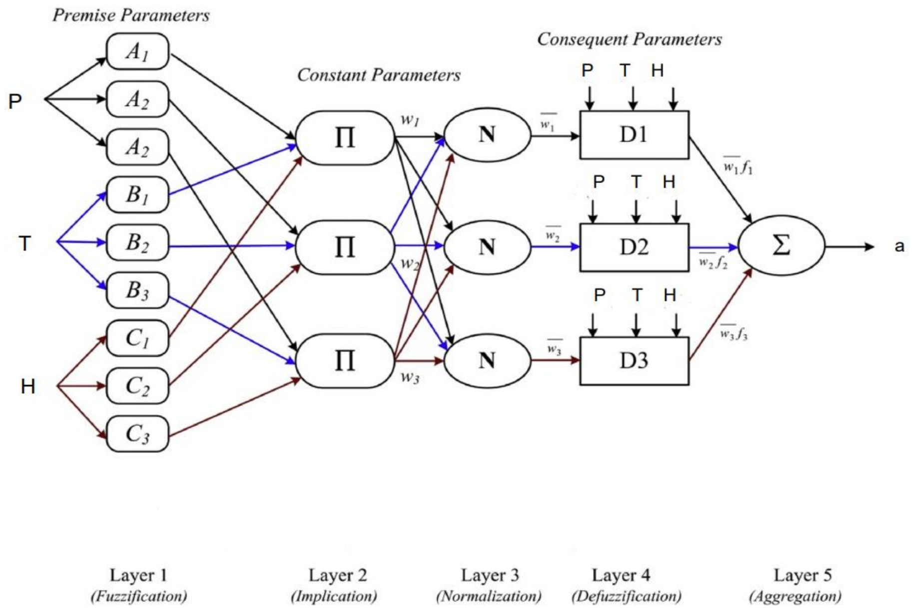

Figure 3.24 A framework of the ANFIS model.

3.2.13 Assessment Methods

The evaluation of the accuracy of relevant models is a pivotal step in any machine learning model. Assessing the predictive performance of a model is a pivotal stage in any machine learning procedure, as it establishes the effectiveness of the model. In the process of statistical analysis, multiple assessment measures such as MAE, RMSE, R^2, and MAPE are utilized to appraise the efficacy of the model. One of the performance metrics utilized to assess model performance is the R^2 coefficient, which denotes the precision level of the model. As per Atik's (2022) findings, a substantial coefficient value indicates a robust correlation between the two variables being examined. The Mean Squared Error (MSE), Root Mean Squared Error (RMSE), and Mean Absolute Error (MAE) are commonly used metrics to evaluate the accuracy of a model's predictions. These measures are indicative of the degree of error in the model's predictions, with lower values being indicative of better performance. It is important to note that these measures are inversely related to performance.

3.2.13.1 Mean Absolute Error (MAE)

The Mean Absolute Error (MAE) is a metric used to quantify the distance between two continuous measures. The MAE is a statistical metric that quantifies the average magnitude of the differences between the predicted and actual values in a given dataset. It is calculated as the arithmetic mean of the absolute differences between the predicted and actual values and represents the typical horizontal deviation from the line of best fit for the data. The horizontal distance between each data point and the line of best fit is a commonly observed measure, as noted by Salmasi (2021). The calculation involves the division of the aggregate data points by their arithmetic mean. The forecast error is a statistical metric that quantifies the discrepancy between an estimated value and the actual value of a time series. The MAE metric is frequently employed in regression and time series scenarios owing to its inherent comprehensibility. The minimum and maximum values for the MAE are 0 and infinity, respectively. According to Celestin (2020), a decrease in value results in an increase in effectiveness. The value of MAE is derived through the utilization of Equation 4.25:

$$MAE = \frac{1}{n} \sum_{1}^{n} |\mathrm{Si,actual} - \mathrm{Si,predicted}| \qquad (4.25)$$

Where n is the total number of data points.

3.2.13.2 Mean Absolute Percentage Error (MAPE)

The Mean Absolute Percentage Error (MAPE) is a statistical metric utilized to evaluate the accuracy of a forecasting system. According to Khatib et al. (2011), the MAPE statistic is utilized to mitigate the potential drawbacks of contrasting models that possess distinct unit values. The reason for the widespread use of MAPE is its simplicity in terms of explanation and interpretation. The MAPE is a metric used to evaluate the accuracy of a forecasting model. A lower MAPE value is indicative of a higher level of performance. The MAPE is a commonly employed metric for measuring the accuracy of models in the context of regression and time series tasks. Equation 4.26 is utilized to calculate MAPE:

$$MAPE = \frac{100\%}{n} \sum_{1}^{n} \left| \frac{(\mathrm{Si,actual} - \mathrm{Si,predicted})}{\mathrm{Si,actual}} \right| \qquad (4.26)$$

3.2.13.3 Root Mean Square Error (RMSE)

The quadratic metric known as root-mean-squared error (RMSE) is commonly employed in machine learning to assess the extent of a model's error by measuring the discrepancy between the predicted and observed values of the estimator (Karahoca et al., 2013). The RMSE is a statistical measure that quantifies the magnitude of the differences between predicted values and actual values, also known as estimation errors or residues. It is a representation of the variance of these estimation errors. To clarify, residuals serve as a metric for quantifying the discrepancy between the regression line and the observed data points, while RMSE provides a measure of the dispersion of these residuals. Stated differently, it denotes the level of data concentration in the vicinity of the optimal line of fit. RMSE can take on values between 0 and infinity. Equation 4.27 is utilized to calculate the RMSE:

$$RMSE = \sqrt{\frac{1}{n} \sum_{1}^{n} (Si, actual \; - \; Si, \text{predicted})\text{\^{}}2} \tag{4.27}$$

3.2.13.4 Coefficient of Determination (R^2)

The method of coefficient of determination is employed in predictive modeling for the purpose of forecasting and evaluating the prospective outcomes of a model. The R^2 functions as a means of evaluating the precision of the model, as stated by Gkountakou et al. (2020). The coefficient of determination method can be utilized to determine the extent of variability present in a given dataset. The coefficient R^2 is utilized in the model for the purpose of evaluating and interpreting data. It has a possible range of values between 0 and 1. As the model approaches a value of 1, its predictive accuracy increases. Formula 4.28 is utilized for the computation of R^2:

$$R^2 = 1 - \frac{\text{RSS}}{\text{TSS}} \tag{4.28}$$

Where RSS is the residual sum of squares, TSS is the total sum of squares.

3.2.14 Trend Analysis

There are several ways to perform trend analysis on a dataset, depending on the nature of the data and the specific research question. Here are a few standard methods:

1. Simple linear regression: This technique consists of fitting a straight line to the data points and estimating the rate of change over time using the slope of the line. Simple linear regression bases its predictions on the supposition that the relationship between the independent and dependent variables is linear

and that the residuals, the discrepancy between the observed and projected value, are normally distributed.

2. Polynomial regression: This method involves fitting a polynomial function to the data points, allowing for more flexibility in the shape of the trend line. Polynomial regression can be used to model trends that are not strictly linear but may be curved or oscillatory.
3. Moving averages: This method involves calculating the average value of the data over a rolling window of time. Moving averages can help to smooth out short-term fluctuations in the data and reveal longer-term trends.
4. Seasonal decomposition: This method involves separating the data into seasonal, trend, and residual components using mathematical models. Seasonal decomposition can be useful for identifying cyclical patterns in the data, as well as long-term trends.
5. Mann-Kendall test: This non-parametric statistical test is used to determine if a trend exists in a time-series dataset.
6. Time-series forecasting: This method involves using statistical models or machine learning algorithms to make predictions about future trends based on historical data. Time-series forecasting can be used to identify potential future trends, which can be valuable for decision-making and planning.

The choice of method for trend analysis depends on the specific research question, the nature of the data, and the underlying assumptions and limitations of the method.

3.2.14.1 Mann- Kendall Trend Test

Finding changes or trends in constituent concentrations over time is a key goal of many environmental monitoring projects. For identifying and estimating potential trends in the data, numerous statistical methods are already available. These comprise straightforward analyses of correlation and regression, time-series analysis, and nonparametric statistical techniques. The Mann-Kendell (MK) test is one of the most often used nonparametric tests for identifying temporal trends (Mann 1945; Kendall 1975; Gilbert 1987). Nonparametric techniques, often known as distribution-free techniques, are generally advised since they need little in the way of data assumptions. The MK test is helpful for examining data that are not normally distributed, censored, outlier-containing, or missing observations.The main goal of the MK test is to statistically evaluate whether there is a consistent trend, either increasing or decreasing, in the variable being studied over a specific time period. A monotonic upward (downward) trend refers to a consistent increase (decrease) in a variable over time, without necessarily following a linear pattern. The test is based on the idea that if there is no clear trend, the time series plot should show random fluctuations around a constant mean level. There should be no visually noticeable upward or downward pattern. The test focuses on comparing the sizes of the sample data rather than the specific values of the data. This means that it does not require the underlying data to follow a specific distribution. Each individual data value is compared to all subsequent data values. Hence, the test can be interpreted as a nonparametric test for the lack of slopes in the linear regression analysis of time-ordered data in relation to time, as demonstrated by Hollander and Wolfe (1973).

The computation of the MK test statistic (S) involves tallying the count of "concordant observations," wherein the series' later-in-time observation exhibits a greater value, and deducting the count of "discordant observations," wherein the later-in-time observation displays a lesser value. This procedure is performed for every pair of observations present in the dataset. The summation of discrepancies is represented by the variable S. S values that are positive denote a rise in the concentrations of constituents with the passage of time, while negative S values indicate a decline in the concentrations of constituents over time. The degree of the trend's potency is directly proportional to the magnitude of S. In other words, as the absolute value of S increases, the evidence supporting a genuine upward or downward trend becomes stronger. According to EPA (2009), it is not permissible to employ any detection instruments in the test by assigning them a shared value that is lower than the minimum recorded value in the dataset. The present investigation employed the Mann-Kendall test to perform a trend analysis on data pertaining to precipitation, temperature, humidity, and wind speed. The assessment of a statistically significant trend is conducted through the utilization of the Z value. The standardized test statistic Z is expressed as follows:

$$Z = \begin{cases} \frac{S-1}{\sqrt{VAR\,(S)}} & if\ S > 0, \\ 0 & if\ S = 0, \\ \frac{S-1}{\sqrt{VAR\,(S)}} & if\ S < 0. \end{cases} \tag{4.29}$$

This statistical measure is employed to evaluate the null hypothesis that posits the absence of any discernible trend. A Z-score with a positive value denotes an upward trend in the time-series, whereas a negative Z-score indicates a downward trend. Figure 3.25 displays the annual average wind speed (m/s), along with its corresponding trend line. The statistical significance of the observed positive trend (Z = 0.0525) was confirmed by the Mann-Kendall test, as shown in Table 3.4. A statistically significant trend is increasing, with a significance level of $P < 0.003$.

Table 3.4 Mann Kendall Test statistics for wind speed m/s.

Kendall's tau	0.381
S	165.000
Var(S)	3137.667
p-value (Two-tailed)	<0.003
Z	0.0525
α	0.05

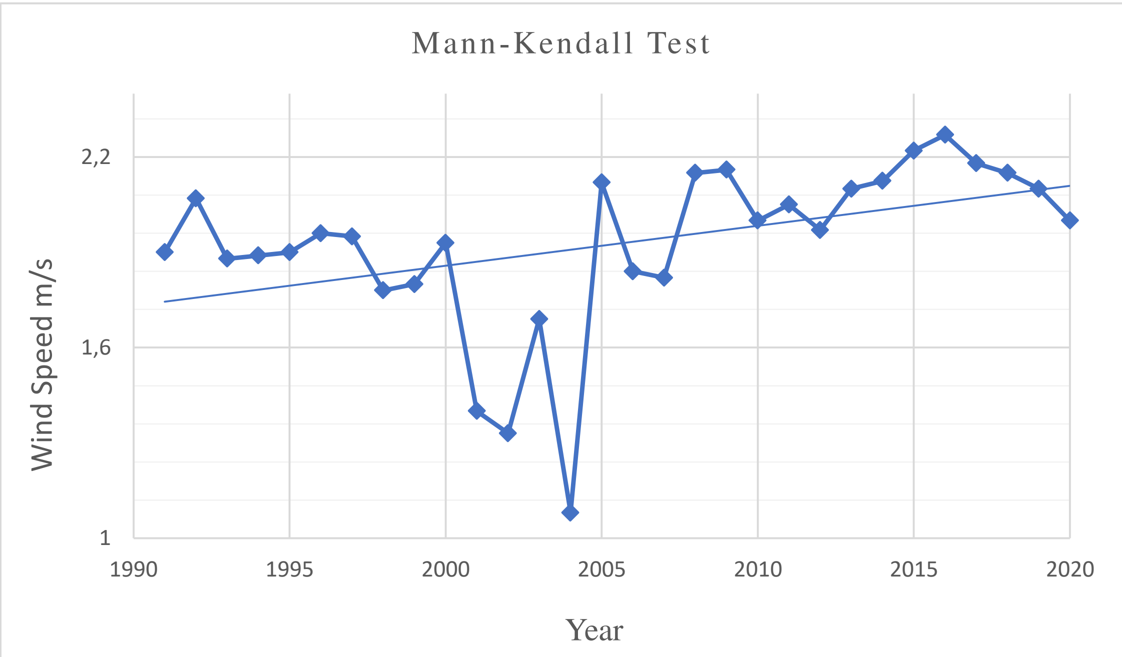

Figure 3.25 Annual average wind speed m/s trends.

Figure 3.26 displays the annual average precipitation (mm), along with the corresponding trend line. The statistical significance of the observed positive trend (Z = 0.045) was confirmed by the Mann-Kendall test, as presented in Table 3.5. There is a statistically significant trend that is increasing at a level of $P < 0.016$.

Table 3.5 Mann Kendall Test statistics for precipitation mm

Kendall's tau	0.320
S	130.000
Var(S)	2842.000
p-value (Two-tailed)	<0.016
Z	0.045
α	0.05

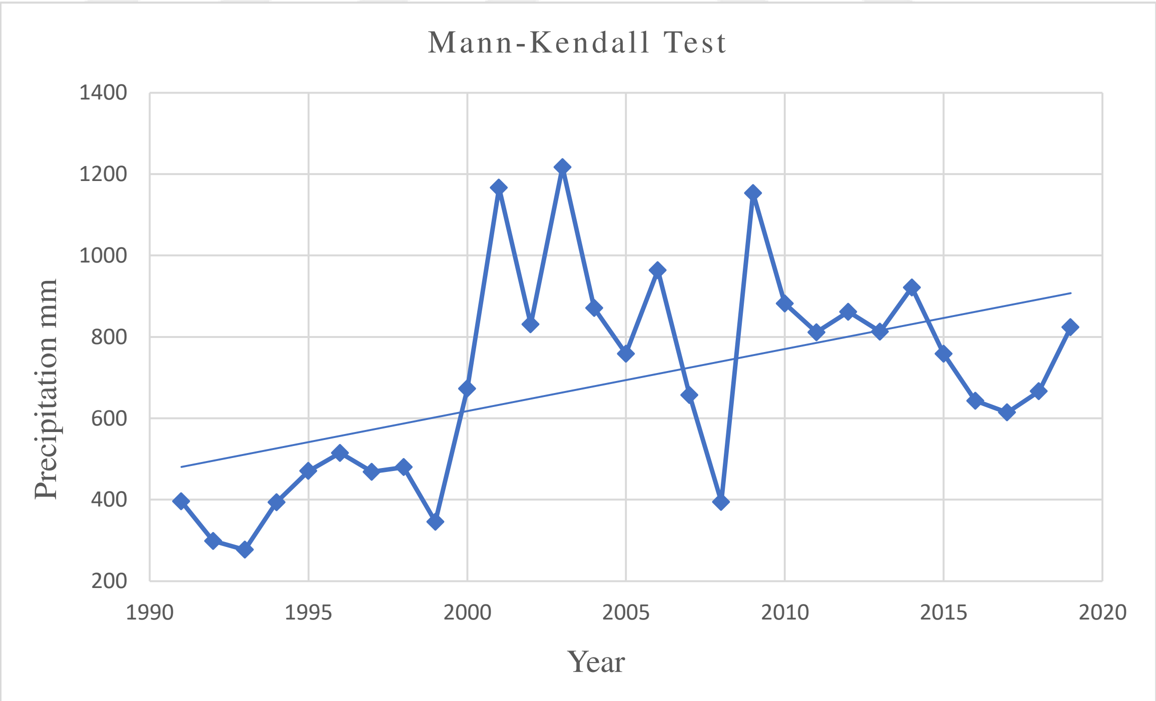

Figure 3.26 Annual average precipitation mm trends.

Figure 3.27 displays the annual average temperature (°C), along with its corresponding trend line. The statistical significance of the observed positive trend (Z = 0.087) was confirmed by the Mann-Kendall test, as presented in Table 3.6. There is a statistically significant trend that is increasing, with a significance level of P < 0.0001.

Table 3.6 Mann Kendall Test statistics for Temperature °C.

Kendall's tau	0.611
S	247.000
Var(S)	2838.333
p-value (Two-tailed)	< 0.0001
Z	0.087
α	0.05

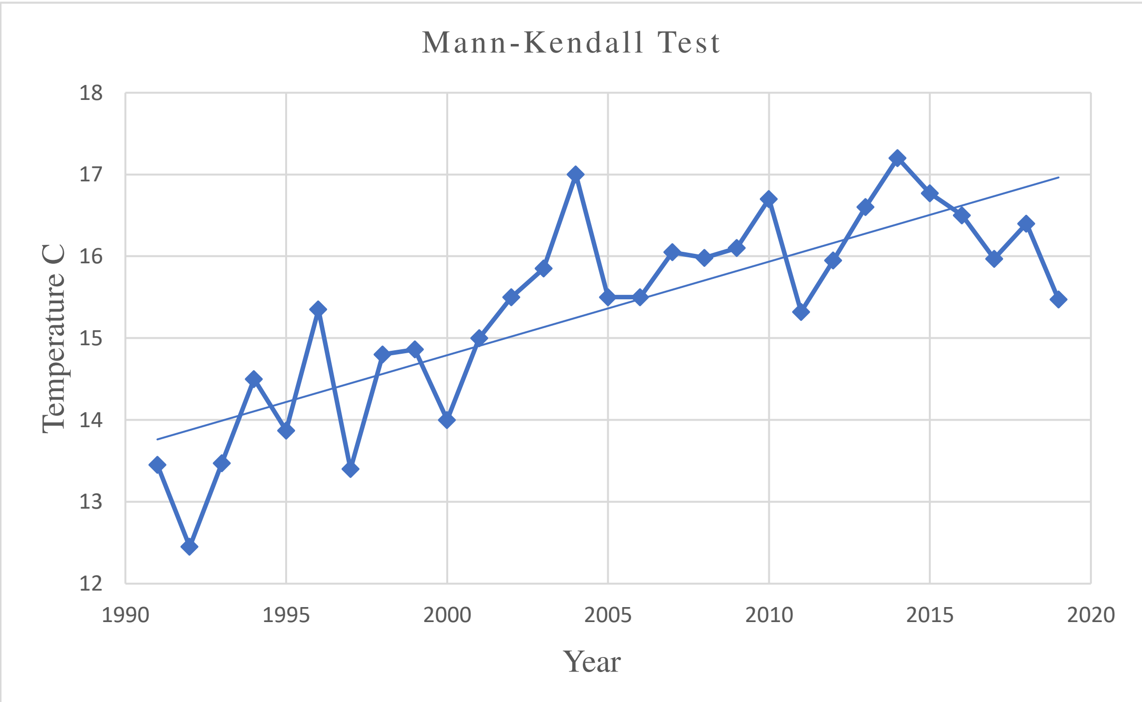

Figure 3.27 Annual average temperature °C trends.

Figure 3.28 displays the annual average humidity (%), along with its corresponding trend line. The statistical significance of the observed positive trend (Z = 0.015) was confirmed through the Mann-Kendall test, as presented in Table 3.7. There is a statistically significant trend that is increasing, with a significance level of P < 0.431.

Table 3.7 Mann Kendall Test statistics for humidity %.

Kendall's tau	0.106
S	43.000
Var(S)	2841.000
p-value (Two-tailed)	<0.431
Z	0.015
α	0.05

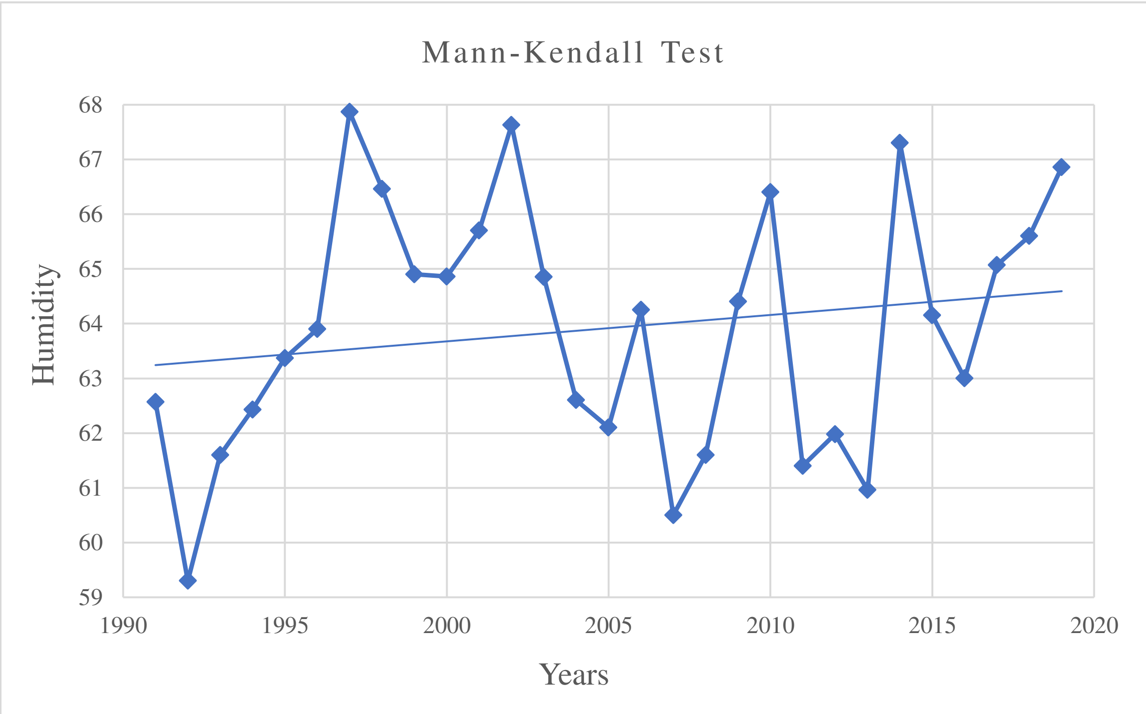

Figure 3.28 Annual average humidity % trends.

CHAPTER IV

RESULTS AND DISCUSSION

4.1 Introduction

In order to determine the primary factor influencing the flow coefficient in the designated study area, a correlation coefficient analysis was conducted utilizing the Origin Pro software. Figure 4.1 provided below depicts an illustration.

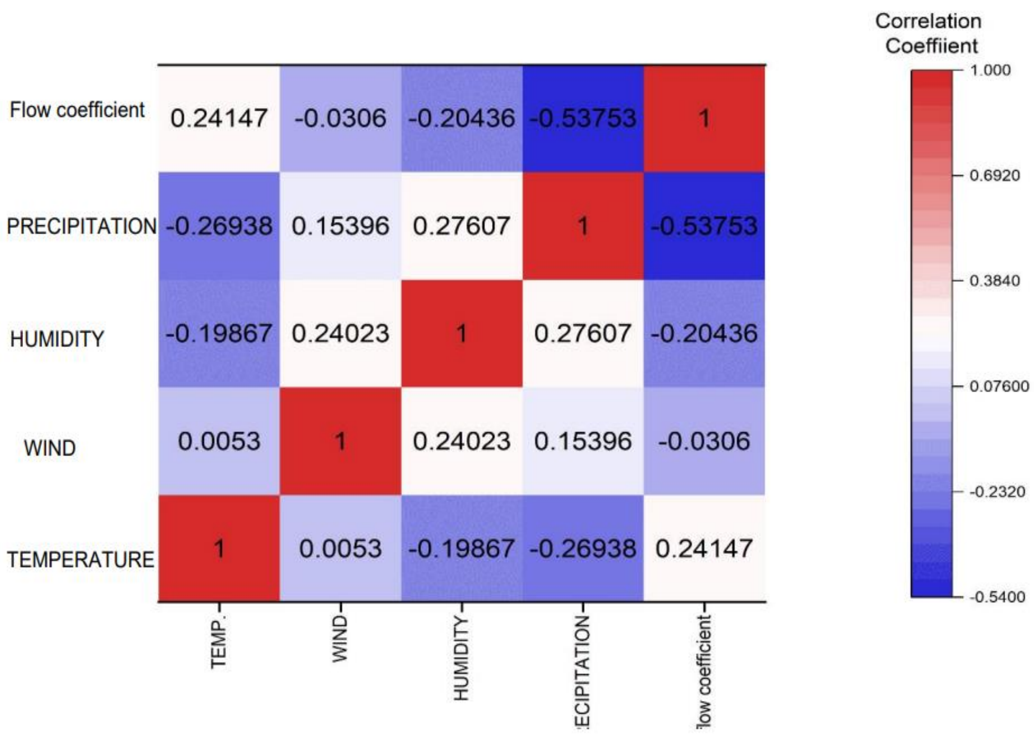

Figure 4.1 Correlation analysis of the data used.

The given correlation analysis indicates that temperature has the highest impact on the flow coefficient estimation, followed by wind, humidity, and precipitation in decreasing order of significance. Temperature is considered the most influential parameter because it affects the rate of evaporation and evapotranspiration, critical processes in the water cycle. Higher temperatures generally lead to increased evaporation, which reduces the amount of water available for surface flow. This, in turn, affects the flow coefficient estimation as it measures the proportion of rainfall that becomes a surface flow. The wind is the following parameter regarding its impact on the flow coefficient estimation. Wind can enhance evaporation by increasing the rate at which moisture is carried away from the surface. Higher wind speeds can accelerate evaporation and reduce the amount of water available for surface flow, thus affecting the flow coefficient.

Although less influential than temperature and wind, humidity still plays a role in flow coefficient estimation. Humidity represents the amount of moisture in the air, influencing the evaporation rates. Higher humidity levels tend to decrease the evaporation rate, resulting in higher surface flow and affecting the estimation of the flow coefficient. According to the correlation analysis, precipitation has the most negligible impact on the flow coefficient estimation. While precipitation directly contributes to the overall water input in the system, its direct influence on the flow coefficient is typically considered less significant compared to temperature, wind, and humidity. However, it is essential to note that the magnitude and intensity of precipitation events can still affect the flow coefficient, especially in areas with limited infiltration capacity.

These conclusions are based on the correlation analysis conducted and the parameters considered in that particular study. It is worth mentioning that the relative importance of these parameters may vary depending on the specific context, geographic location, and hydrological characteristics of the area under investigation. Other factors, such as soil properties, vegetation cover, and land use, can influence the flow coefficient estimation but may not have been included in the correlation analysis. The correlation analysis in the Aksu River Basin area indicates that precipitation has the most negligible impact on the flow coefficient estimation. Several possible reasons could explain this finding in the context of the Aksu River Basin:

Low Intensity and Duration of Precipitation: The region might experience predominantly low-intensity and short-duration precipitation events. If the rainfall is not intense and brief, the soil and vegetation can effectively absorb and retain most of the water, minimizing the amount of surface flow. In such cases, the correlation analysis may have revealed that precipitation has a relatively weaker association with the flow coefficient than other parameters.

High Infiltration Capacity: The Aksu River Basin might have soils with a high infiltration capacity, allowing water to penetrate the ground quickly. Soils that can absorb precipitation efficiently will have a reduced flow response, as a significant portion of the water is retained in the soil layers, contributing to groundwater recharge or plant uptake. Vegetation and Land Cover: Dense vegetation or land cover with high water-holding capacity, such as forests or wetlands, can contribute to increased evapotranspiration and enhanced water retention. Vegetation intercepts precipitation, slowing its direct contact with the ground and promoting more excellent water absorption. This can result in reduced surface flow and a lower sensitivity of the flow coefficient to precipitation.

4.2 Fuzzy SMRGT method application results

The present investigation employed the simple membership functions and fuzzy rules generation technique (SMRGT) to accurately predict the flow coefficient of the Aksu River basin in Antalya- Turkey. The input variables utilized in the study were based on the study area's distinct climatic and topographical characteristics. The first stage of developing the model entailed carrying out preliminary procedures. The initial step in establishing the model involved conducting introductory procedures. Independent (input) and dependent (output) variables have been identified during the introductory procedures. The utilization of membership functions facilitated the execution of a fuzzy process on both the input and output. Following this, fuzzy rules were formulated, and the centroid technique was adopted to convert fuzzy sets to crisp values, whereas the Mamdani approach opted for the fuzzy inference system stage. The SMRGT method established the membership functions and fuzzy rule base. The model is finalized once the procedures above have been executed and the resulting output has been acquired. The flow coefficient values were obtained as a percentage based on the results of the models. Five distinct models have been created based on various factors about the study area.

4.2.1 Model 1: SMRGT-1 (Wind speed and temperature):

The flow coefficient was calculated using temperature (T) and wind speed (Ws) data input variables. The Turkish State Meteorological Service has obtained a dataset that covers the period from 1990 to 2020. The dependent and independent variables in the SMRGT method have been identified. The experiment uses two independent variables: temperature (°C) and wind speed (m/s). These variables will be used as inputs. The output obtained is referred to as the flow coefficient, which is the dependent variable. The developed fuzzy model is illustrated in Figure 4.2.

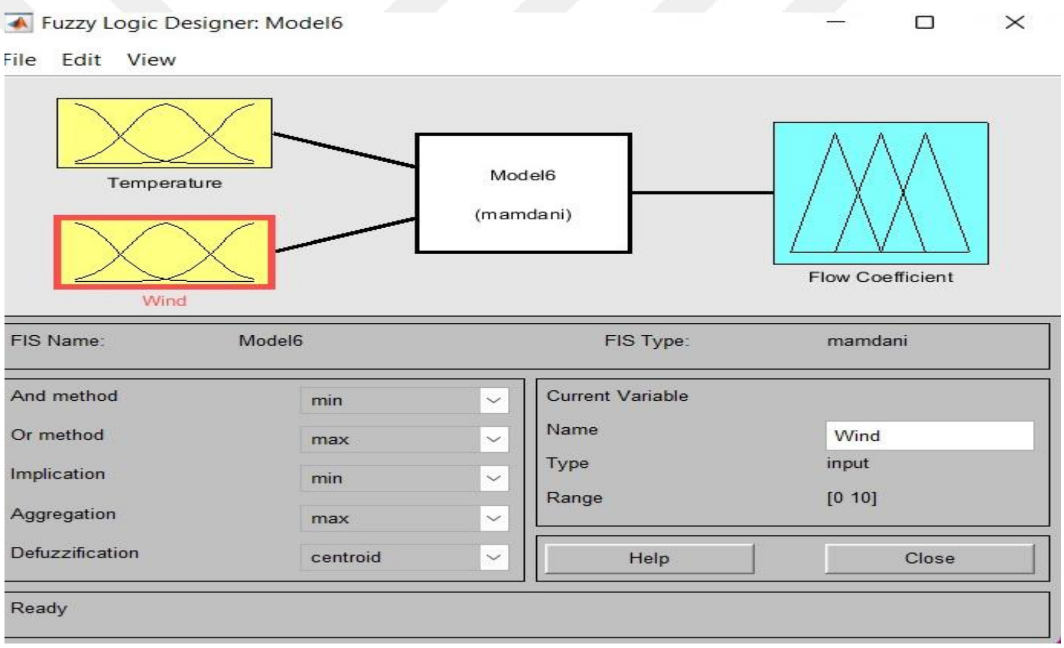

Figure 4.2 Inputs and output of the model.

A set of seven membership functions was created for each input variable. The corresponding key values for these membership functions were determined, as shown in Figure 4.3. This process resulted from the formulation of 49 fuzzy rules, as shown in Figure 4.4. The fuzzy rules base is established by factoring in physical conditions such as "IF," "and," and "THEN" (see Figure 4.5). The decision was made to use MATLAB software to execute the model.

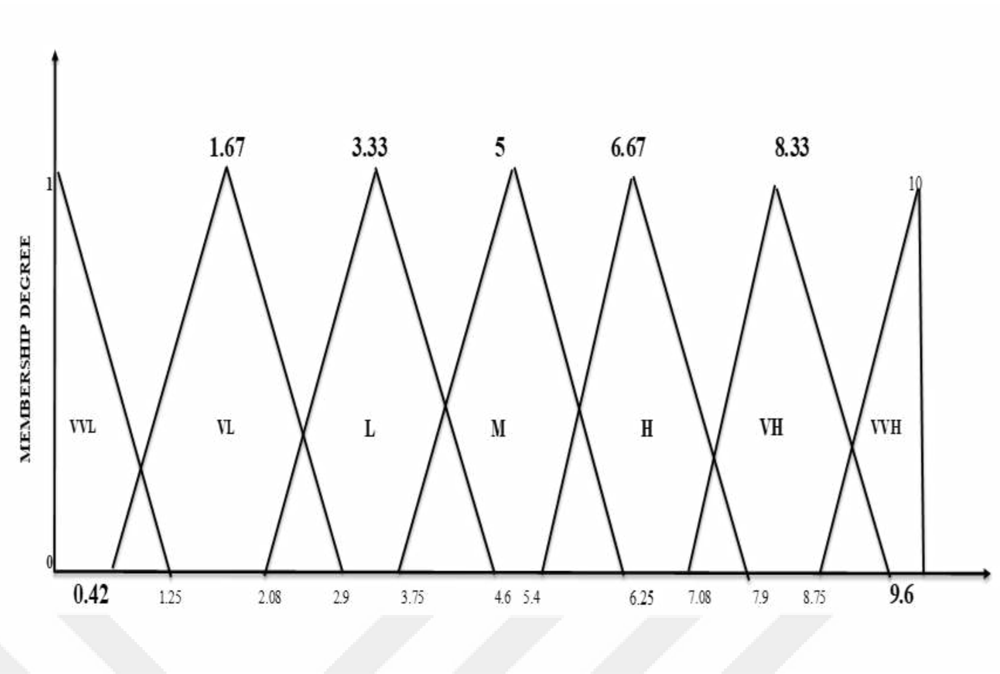

Figure 4.3 The key values of the wind MFs.

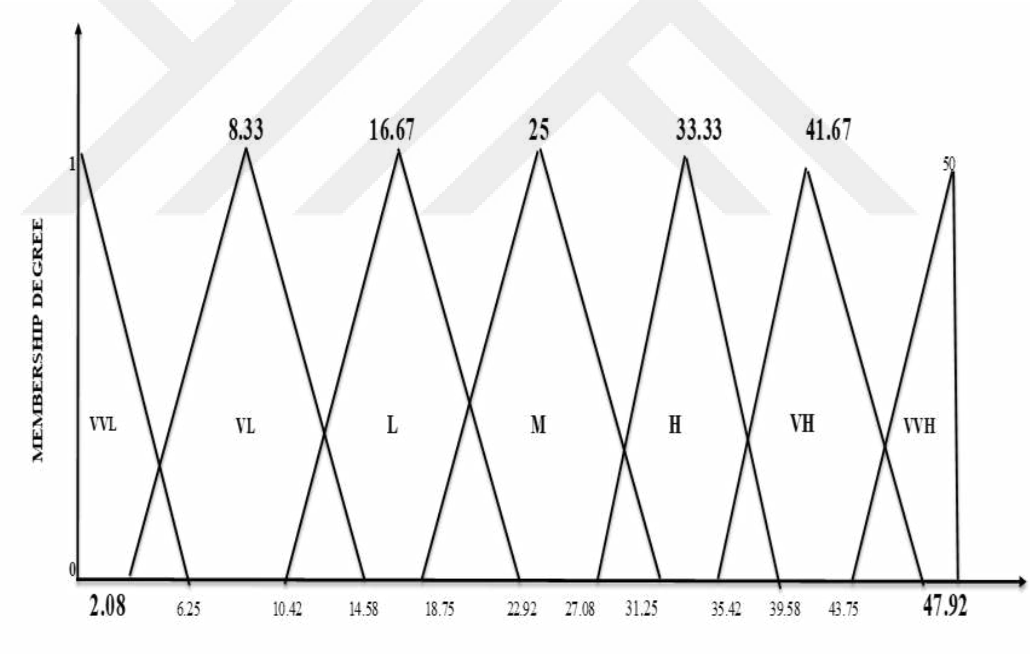

Figure 4.4 The key values of the temperature MFs.

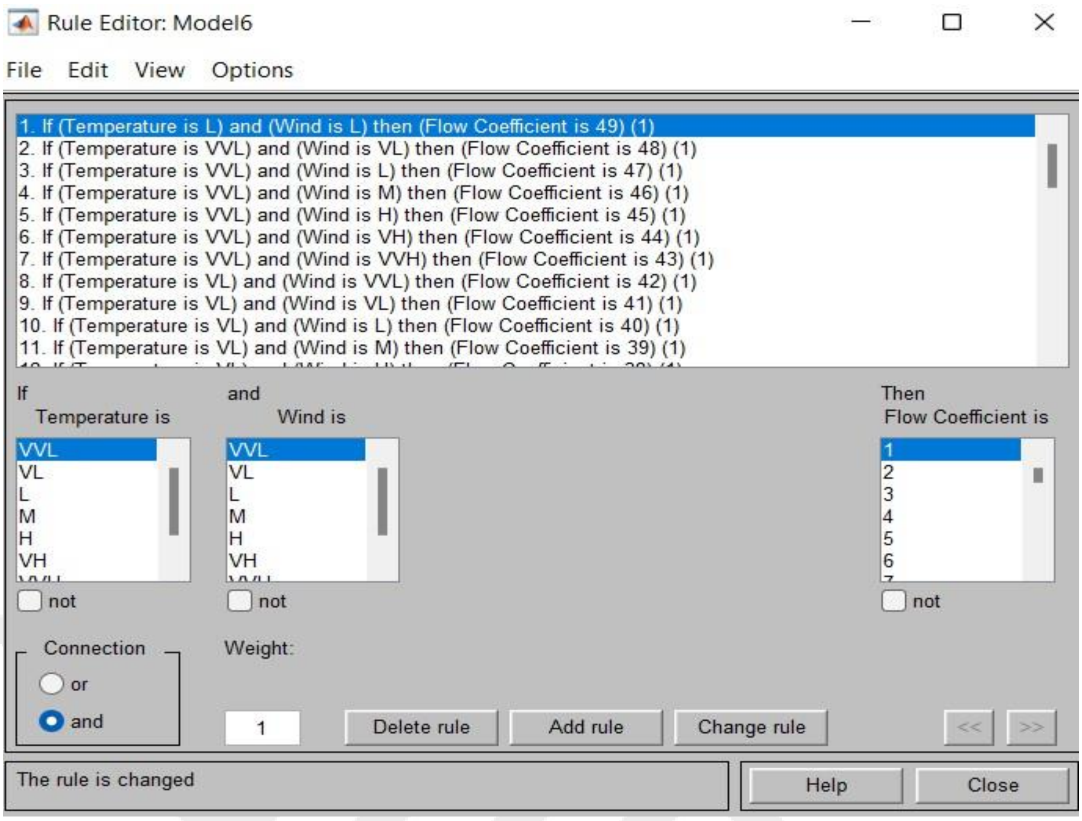

Figure 4.5 MATLAB view of the generated fuzzy rules.

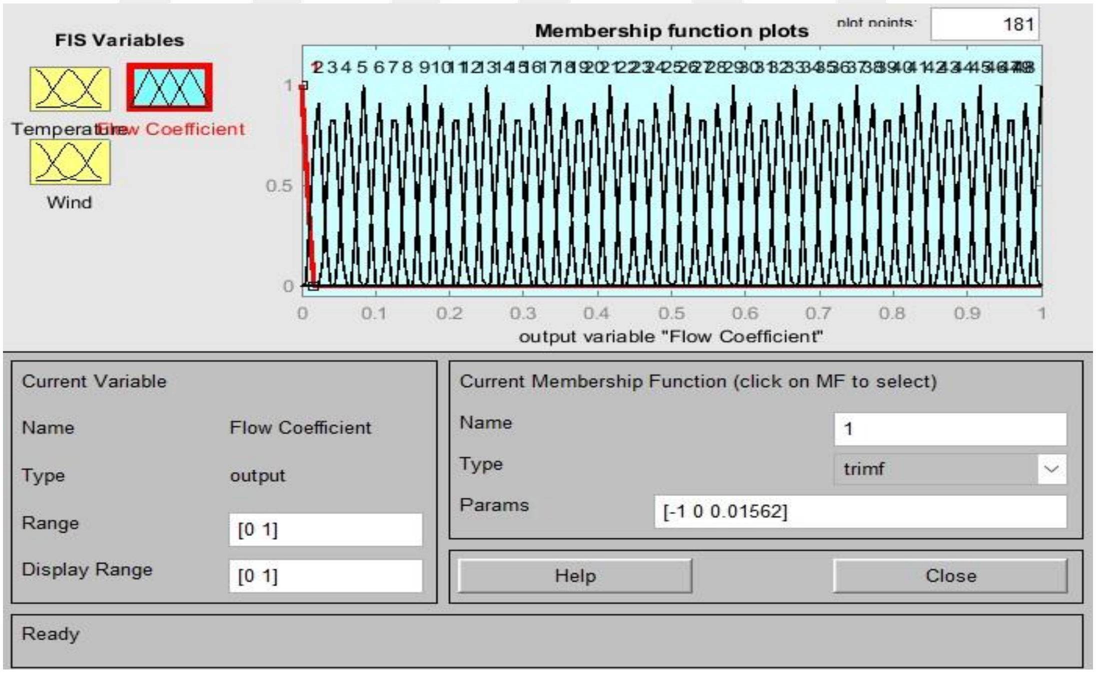

Figure 4.6 MFs of the output (flow coefficient).

Table 4.1 below displays the key values of each input variable, as determined by the equations provided in the preceding section. These key values were utilized as inputs for the model.

Table 4.1 key values of the input variables.

Model	**Input variables**	**K1**	**K2**	**K3**	**K4**	**K5**	**K6**	**K7**
SMRGT-1	T	50	41.67	33.33	25	16.67	8.33	0
	Ws	0	1.67	3.33	5	6.67	8.33	10

The fuzzy SMRGT-1 model is executed utilizing MATLAB software, deemed the most appropriate software package for this investigation. The program has been updated to include input and output files formatted with the (.dat) extension. Subsequently, the program denoted by the (.fis) file extension is loaded. The file with the extension ".m" is intended for the execution of the program that has been prepared. The model results can be obtained by executing the file with the (.m) extension. Implementing this procedure will minimize the trial-and-error process during program preparation.

Consequently, Figures 4.7 and 4.8 illustrate the upper and lower bounds of the flow coefficient, considering variations in temperature and wind speed. When the temperature reaches its lowest threshold of 2.08 °C and the wind speed is measured at 0.417 m/s, it becomes apparent that the flow coefficient attains a value of 0.98. Similarly, in instances where the temperature reaches its uppermost threshold of 47.9 °C and the wind velocity is measured at 9.58 m/s, the flow coefficient is determined to be 0.003. These examples prove that the model is operating mathematically and physically correctly. Furthermore, there exists a negative correlation between the output and inputs. Under the assumption that all precipitation effectively reaches the Earth's surface, it can be inferred that the flow rate will exhibit a significant increase during periods of cold weather and reduced wind velocity.

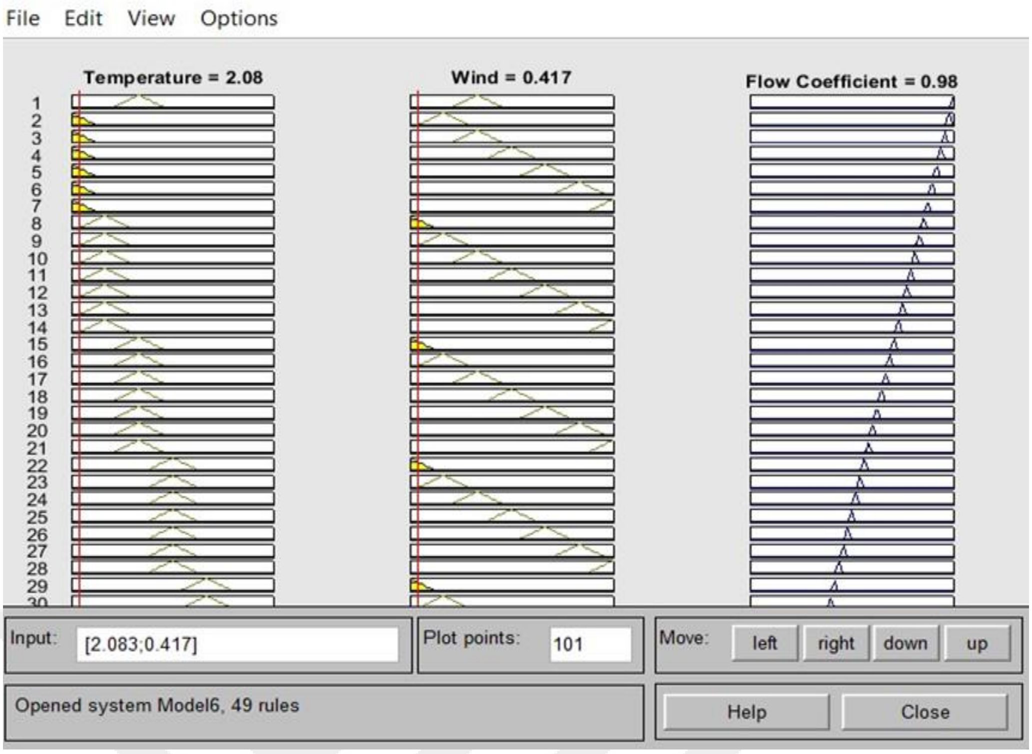

Figure 4.7 Graphical view of the rules (maximum value of output).

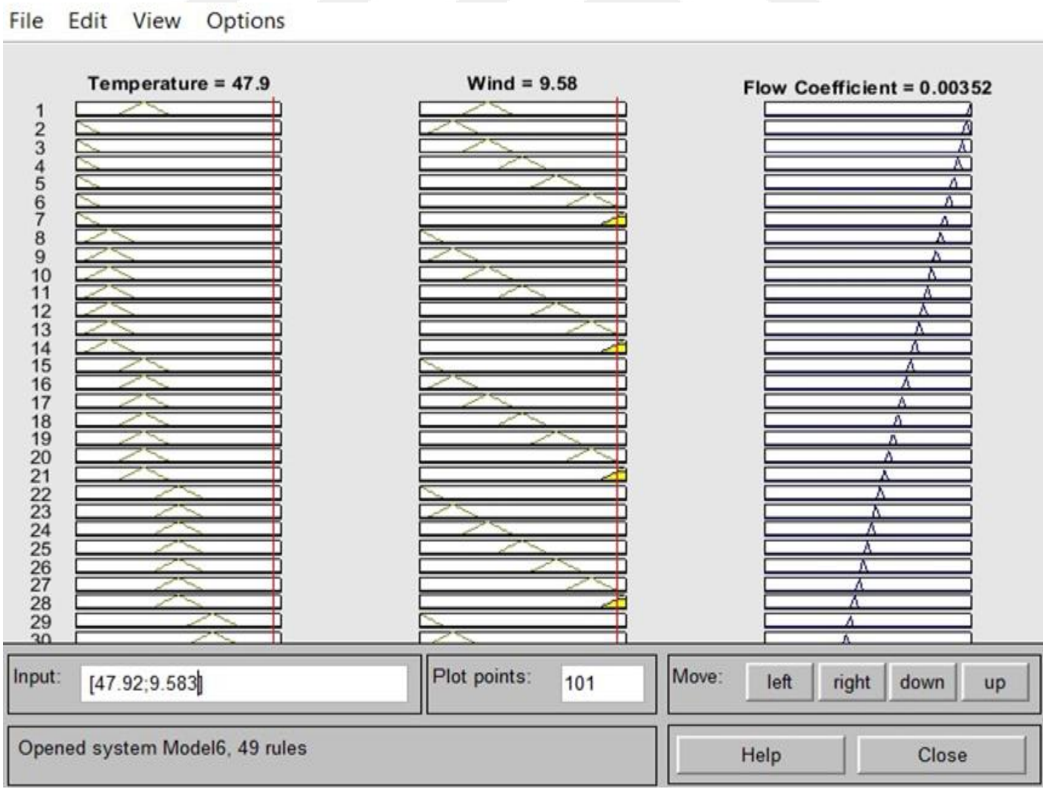

Figure 4.8 Graphical view of the rules (minimum value of output).

Table 4.2 displays key output values, the total number of fuzzy rules, and the creation of a fuzzy model.

Table 4.2 Generated fuzzy set.

Rules No	Temperature C		Wind m/s		Flow Coefficient	Flow Coefficient	MAPE
	Numerical	Verbal	Numerical	Verbal	(data)	(model)	
1	50	VVH	10	VVH	0.00	0.00	0.000
2	50	VVH	8.33	VH	0.01	0.02	1.168
3	50	VVH	6.67	H	0.03	0.04	1.186
4	50	VVH	5	M	0.04	0.06	1.180
5	50	VVH	3.33	L	0.05	0.08	1.165
6	50	VVH	1.67	VL	0.07	0.10	1.176
7	50	VVH	0	VVL	0.08	0.13	1.320
8	41.67	VH	10	VVH	0.16	0.15	0.149
9	41.67	VH	8.33	VH	0.17	0.17	0.002
10	41.67	VH	6.67	H	0.18	0.19	0.081
11	41.67	VH	5	M	0.19	0.21	0.152
12	41.67	VH	3.33	L	0.21	0.23	0.219
13	41.67	VH	1.67	VL	0.22	0.25	0.279
14	41.67	VH	0	VVL	0.23	0.27	0.356
15	33.33	H	10	VVH	0.31	0.29	0.130
16	33.33	H	8.33	VH	0.32	0.31	0.056
17	33.33	H	6.67	H	0.33	0.33	0.027
18	33.33	H	5	M	0.35	0.35	0.014
19	33.33	H	3.33	L	0.36	0.38	0.080
20	33.33	H	1.67	VL	0.37	0.40	0.119
21	33.33	H	0	VVL	0.38	0.42	0.174
22	25	M	10	VVH	0.47	0.44	0.122
23	25	M	8.33	VH	0.48	0.46	0.074
24	25	M	6.67	H	0.49	0.48	0.039
25	25	M	5	M	0.50	0.50	0.007
26	25	M	3.33	L	0.51	0.52	0.023
27	25	M	1.67	VL	0.53	0.54	0.052
28	25	M	0	VVL	0.54	0.56	0.093
29	16.67	L	10	VVH	0.62	0.58	0.130
30	16.67	L	8.33	VH	0.63	0.60	0.082
31	16.67	L	6.67	H	0.64	0.63	0.055

32	16.67	L	5	M	0.66	0.65	0.031
33	16.67	L	3.33	L	0.67	0.67	0.006
34	16.67	L	1.67	VL	0.68	0.69	0.017
35	16.67	L	0	VVL	0.69	0.71	0.047
36	8.33	VL	10	VVH	0.77	0.73	0.117
37	8.33	VL	8.33	VH	0.78	0.75	0.087
38	8.33	VL	6.67	H	0.80	0.77	0.068
39	8.33	VL	5	M	0.81	0.79	0.046
40	8.33	VL	3.33	L	0.82	0.81	0.026
41	8.33	VL	1.67	VL	0.84	0.83	0.008
42	8.33	VL	0	VVL	0.85	0.85	0.019
43	0	VVL	10	VVH	0.93	0.88	0.115
44	0	VVL	8.33	VH	0.94	0.90	0.092
45	0	VVL	6.67	H	0.95	0.92	0.073
46	0	VVL	5	M	0.96	0.94	0.055
47	0	VVL	3.33	L	0.98	0.96	0.040
48	0	VVL	1.67	VL	0.99	0.98	0.023
49	0	VVL	0	VVL	1.00	1.00	0.000

The outcomes of the model are compared to the available data. In order to assess the predictive performance of the model, several statistical parameters were used. These included the minimum value (Xmin), mean value (Xm), maximum value (Xmax), standard deviation (σ), coefficient of variation (Cvx), coefficient of skewness (Csx), correlation coefficient (r), as well as metrics such as Mean Absolute Relative Error (MARE), Mean Square Error (MSE), Mean Absolute Error (MAE), and Root Mean Square Error (RMSE). The results of the statistical comparison are displayed in Table 4.3. Low error rates and a high correlation coefficient suggest the potential for mathematically representing the statistical association between the model and the data.

Table 4.3 Statistical comparison of the SMRGT-1 model and data

Statistical Parameters and Errors	**Data**	**Model**
Max.	1.00	1.00
Min.	0.00	0.00
Mean	0.50	0.50

Standard Deviation	0.309	0.29

Continuous Table 4.3 Statistical comparison of the SMRGT-1 model and data

Skewness	0.00000000	0.00167
Coefficient of Variance (CV)	0.616	0.589
Correlation Coefficient (r)	0.99	
Mean Square Error (MSE)	0.05	
Mean Absolute Error (MAE)	0.02	
Mean Absolute Precentage Error (MAPE)	6.88	
Root Mean Square Error (RMSE)	0.02	

In addition, the comparison was visually represented using a scatter diagram and a series graph; each data point is represented as a dot on the graph, with one variable plotted on the horizontal axis and the other on the vertical axis. The passage mentions that the regression line (a line that best fits the data) intersects the horizontal axis at a 45-degree angle. This means the model's predictions are not consistently biased towards overestimation or underestimation. In other words, the model provides reasonably accurate estimations that are not systematically too high or too low compared to the actual data, as shown in Figures 4.9 and 4.10. The scatter plot shows a strong positive correlation between the observed and predicted data. Figure 4.11 visually represents the complex relationship between dependent and independent variables in a three-dimensional format.

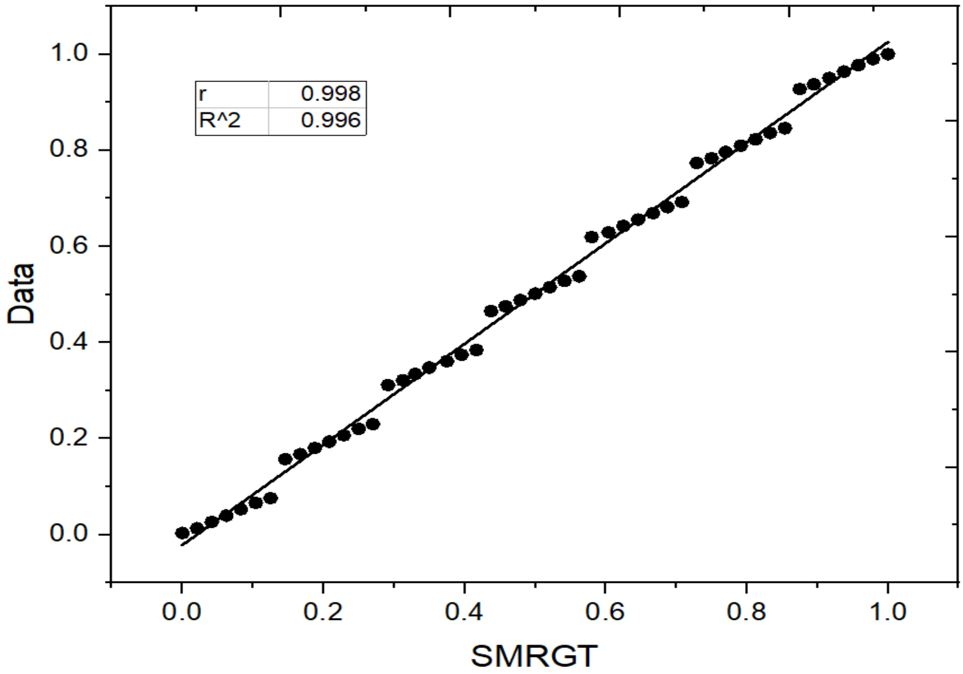

Figure 4.9 the series graph of the results.

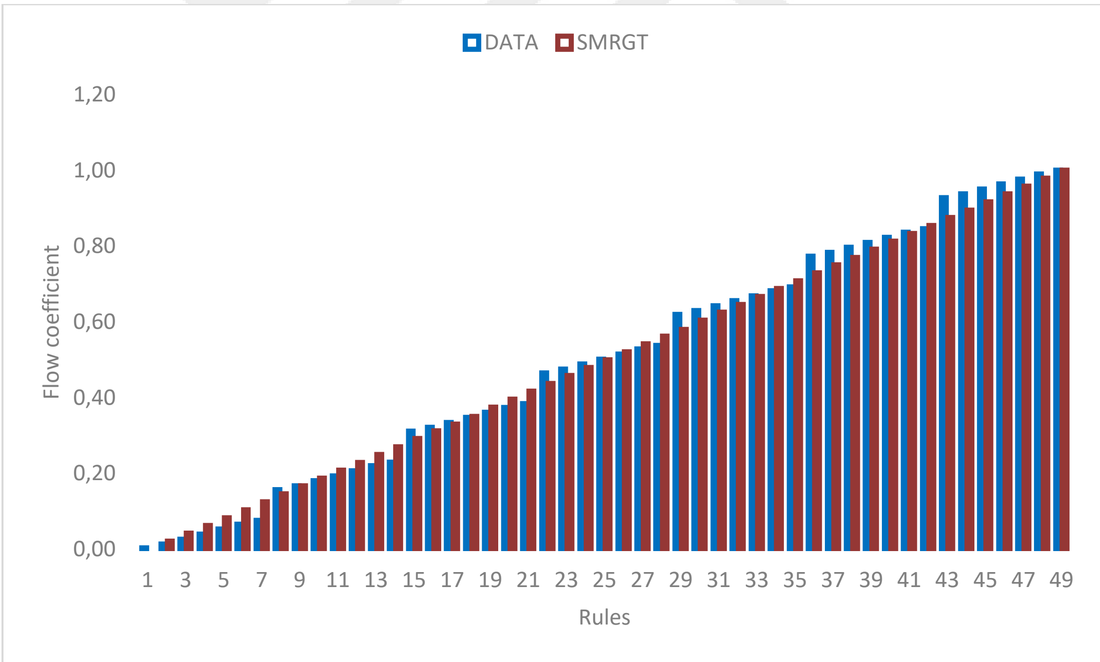

Figure 4.10 the series graph of the results.

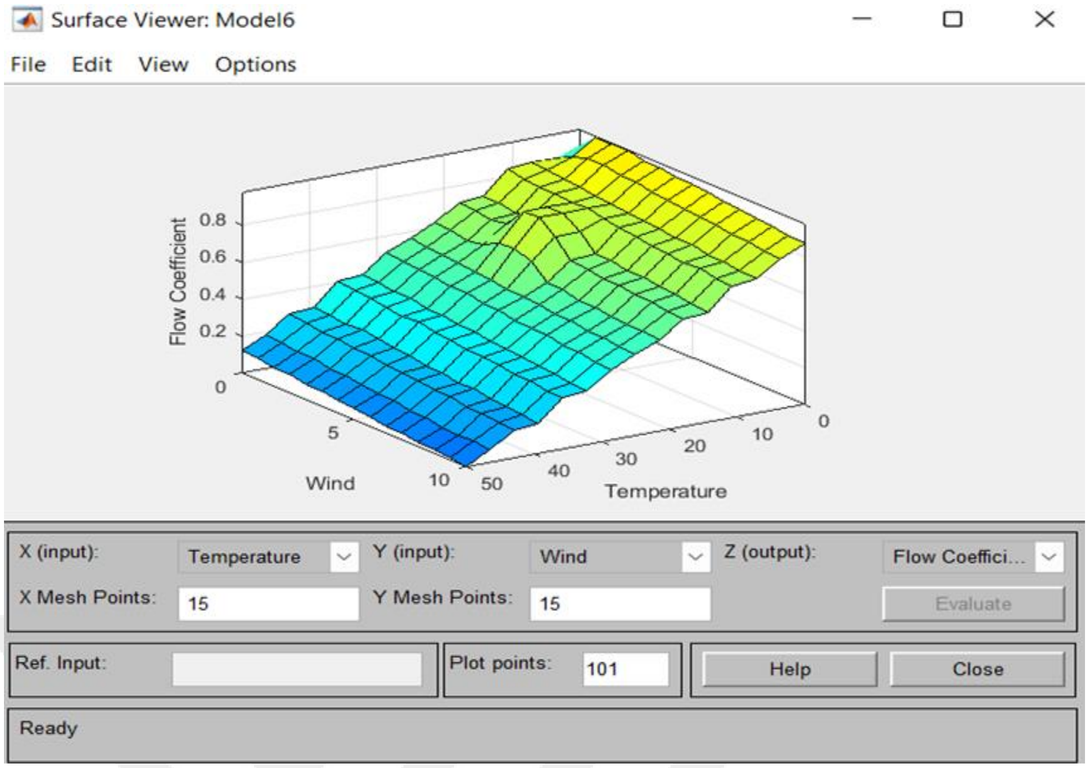

Figure 4.11 Variation of output as a function of inputs.

4.2.2 Model 2 : SMRGT-2

Land (LU) and Slope (S): The flow coefficient was calculated using Land Use (LU) and Slope (S %) data input variables. The SMRGT method has successfully identified the dependent and independent variables. The value that is commonly referred to as the flow coefficient is known as the dependent variable. The developed fuzzy model is illustrated in Figure 4.12.

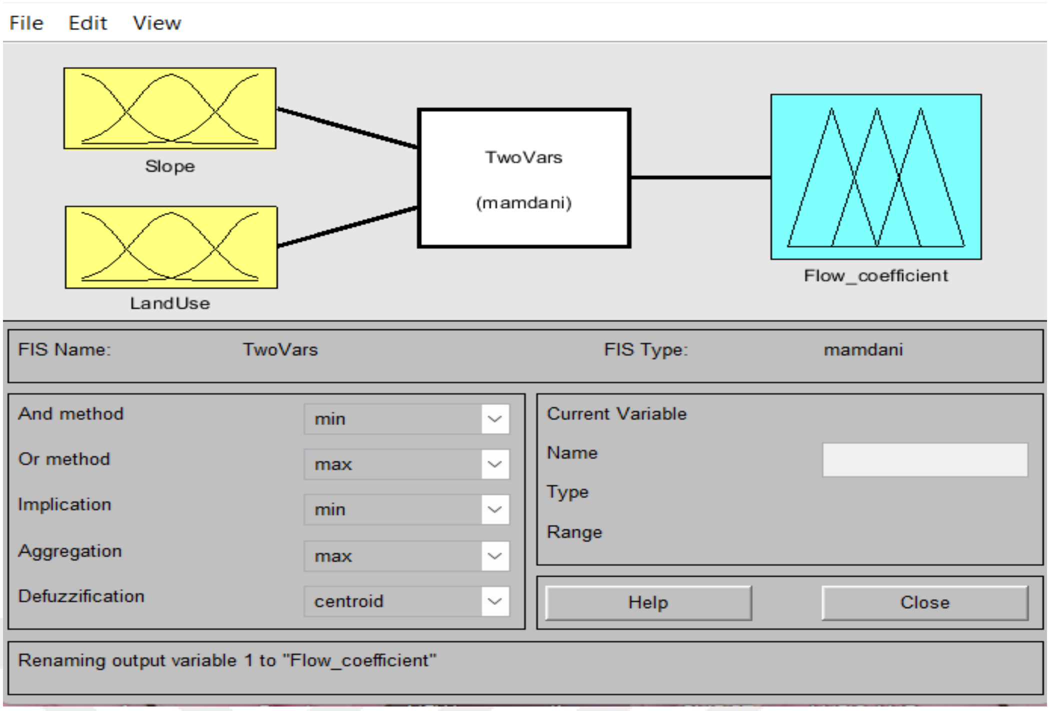

Figure 4.12 Inputs and output of the model.

Five membership functions were generated for each input variable. The key values for these membership functions were determined, as shown in Figure 4.13. The process created 25 fuzzy rules, as shown in Figure 4.14. The process of creating the fuzzy rules base includes incorporating physical conditions using the terms "IF," "and," and "THEN," as shown in Figure 4.15. The MATLAB software was used as the designated software for implementing the model.

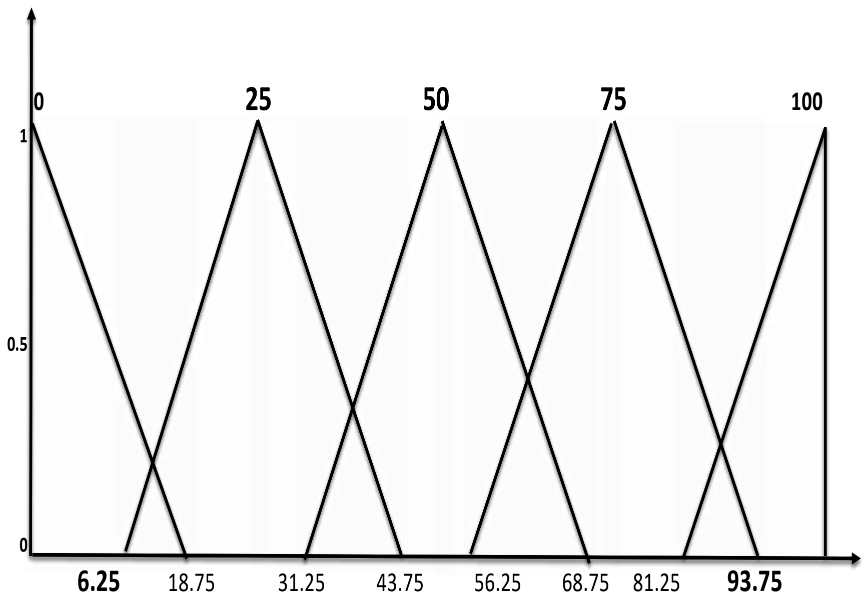

Figure 4.13 The key values of the land use MFs.

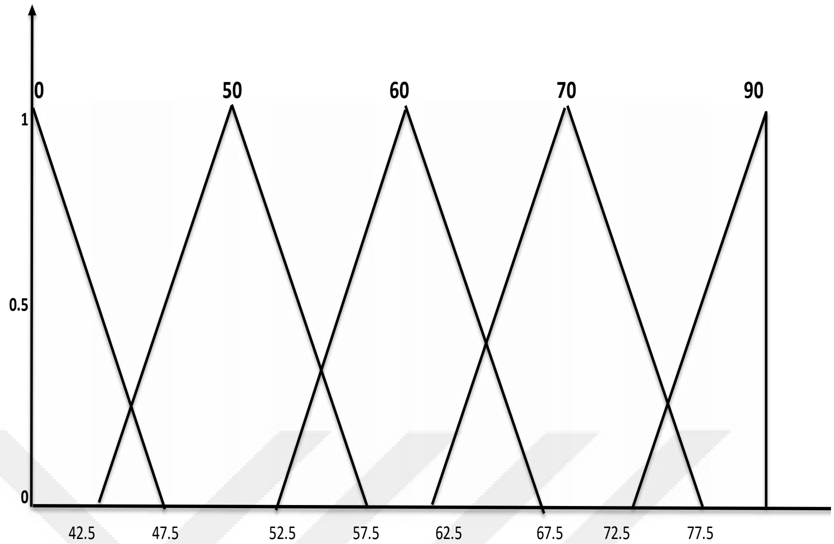

Figure 4.14 The key values of the slope MFs.

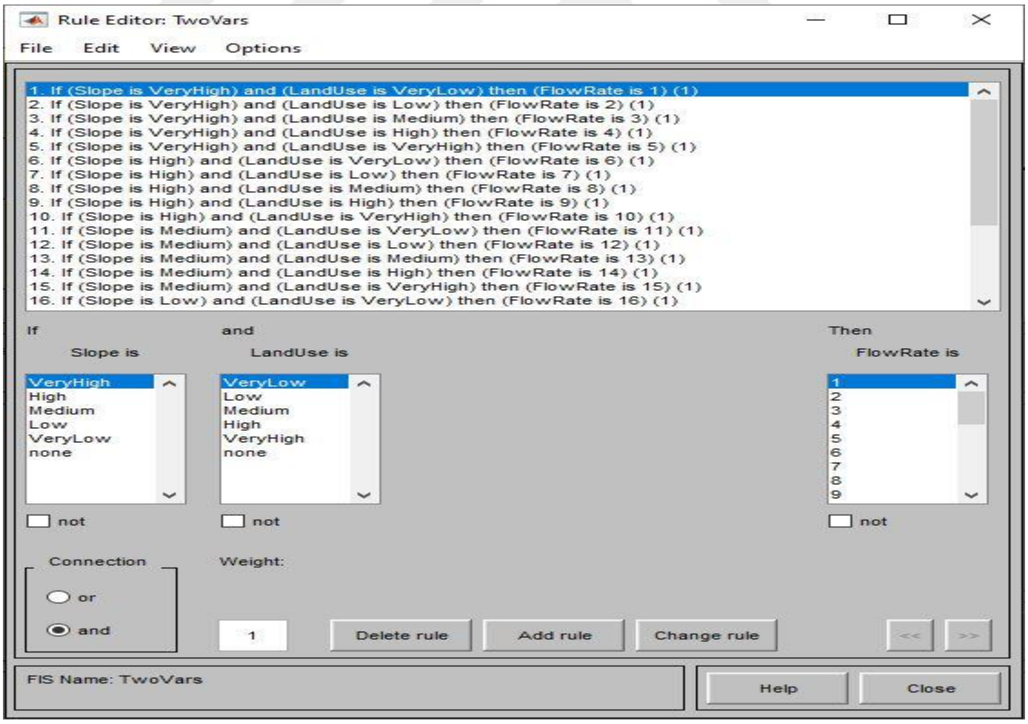

Figure 4.15 MATLAB view of the generated fuzzy rules.

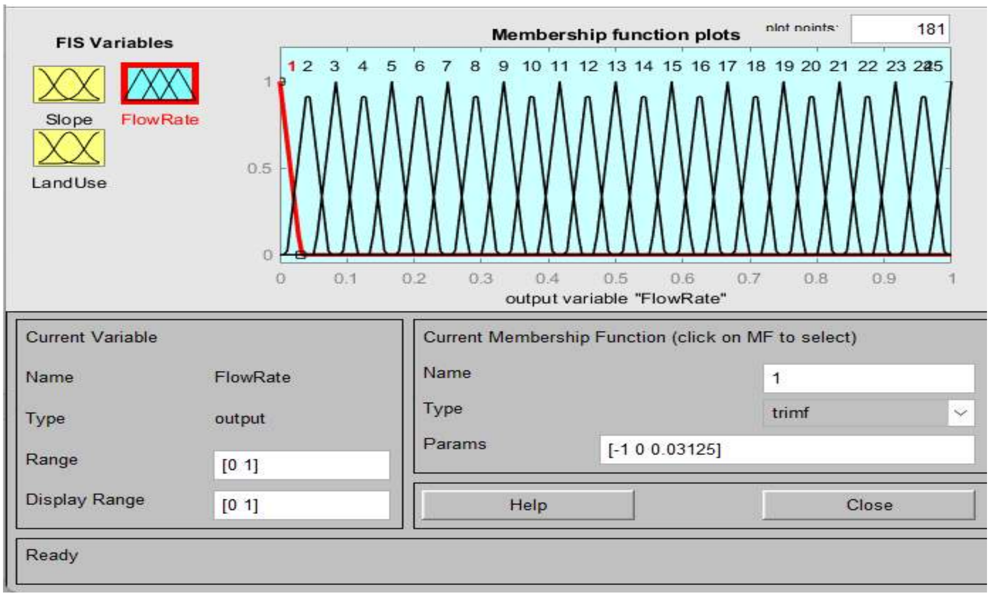

Figure 4.16 MFs of the output (flow coefficient).

Table 4.4 below displays the key values of each input variable, as determined by the equations provided in the preceding section. These key values were utilized as inputs for the model.

Table 4.4 key values of the input variables.

Key values	Input variables	K1	K2	K3	K4	K5
SMRGT-2	LU	6.25	25	50	75	100
	S	5.625	22.5	45	67.4	84.375

The SMRGT-2 model, characterized by its fuzzy nature, is implemented using MATLAB software, considered the most suitable software package for this study. The program has undergone an update to incorporate the integration of input and output files, which have been appropriately formatted with the (.dat) extension. Following this, the software denoted by the (.fis) file extension is loaded. The file denoted by the ".m" extension is designed for the execution of the prepared program. The model results can be obtained by executing the file with the (.m) extension. This procedure will efficiently reduce the need for trial and error in program preparation. Figures 4.17 and 4.18 depict the upper and lower limits of the flow coefficient, considering fluctuations in land utilization and incline. When the land utilization reaches its minimum threshold of 4.74%, and the slope is at 4.27%, it becomes evident that the flow coefficient achieves a value of 0.00832. When land utilization reaches its maximum limit of 98.2%, and the slope is 87.7%, the flow coefficient is calculated to be 0.992. The examples above serve as empirical support for the model's accurate functioning in both mathematical and physical domains. Moreover, a positive correlation can be observed between the output and inputs. Based on the premise that all precipitation adequately reaches the Earth's surface, it can be deduced that the flow coefficient will demonstrate a notable augmentation in regions where land coverage is higher, and slopes are steeper.

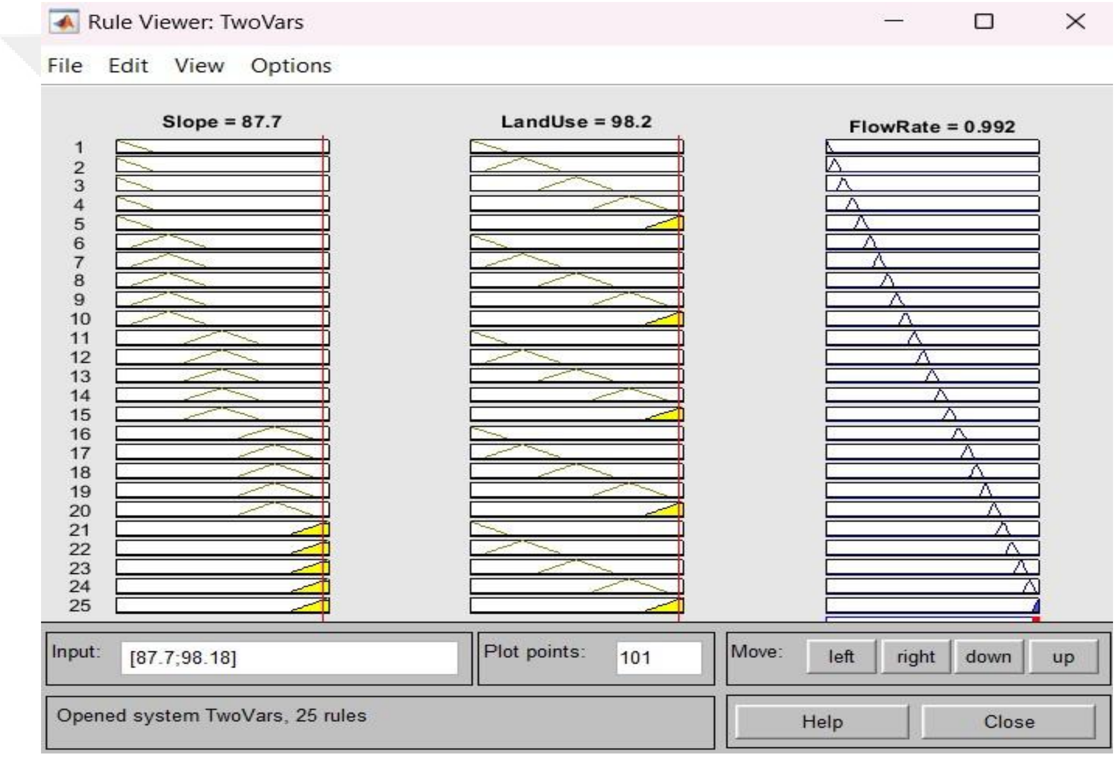

Figure 4.17 Graphical view of the rules (maximum value of output).

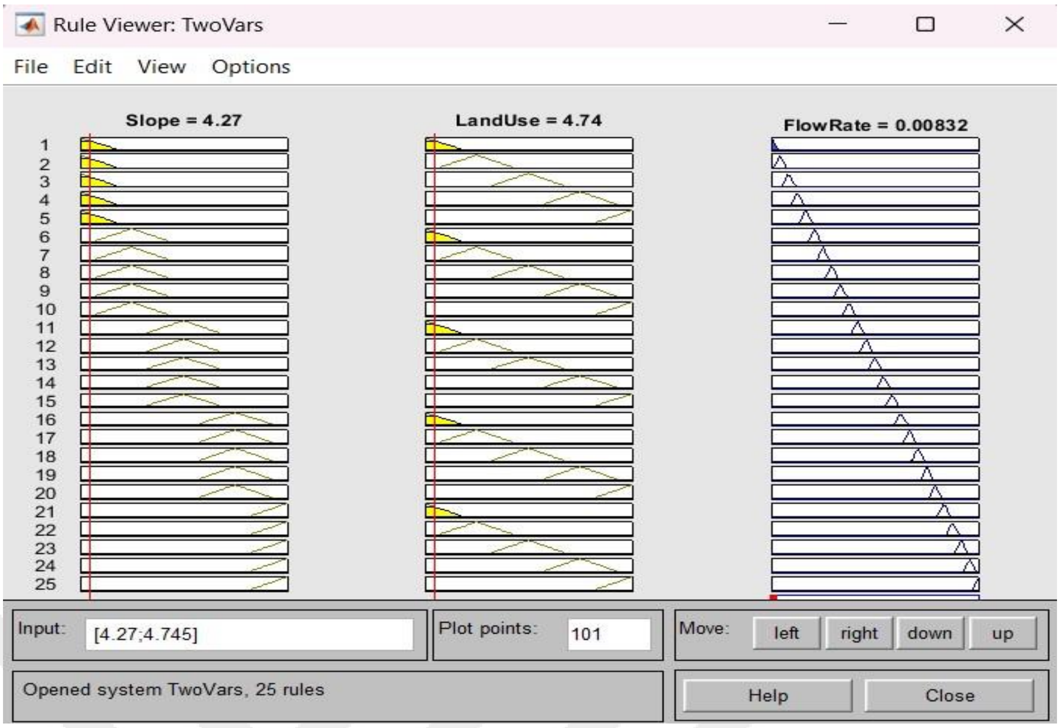

Figure 4.18 Graphical view of the rules (minimum value of output).

Table 4.5 displays key output values, the total number of fuzzy rules, and the creation of a fuzzy model.

Table 4.5 Generated fuzzy set

Rules No	Slope %		Land use %		Flow Coefficient (data)	Flow Coefficient (model)	MAPE
	Numerical	Verbal	Numerical	Verbal			
1	5.625	VL	6.25	VL	0.01	0.00869	0.000
2	5.625	VL	25	L	0.0345	0.044	0.138
3	5.625	VL	50	M	0.08	0.0835	0.707
4	5.625	VL	75	H	0.122	0.125	0.863
5	5.625	VL	93.75	VH	0.162	0.167	0.709
6	22.5	L	6.25	VL	0.2021	0.2	1.112
7	22.5	L	25	L	0.2412	0.25	1.000
8	22.5	L	50	M	0.28	0.29	0.462
9	22.5	L	75	H	0.325	0.33	0.179
10	22.5	L	93.75	VH	0.362	0.375	0.174
11	45	M	6.25	VL	0.4026	0.417	0.570

12	45	M	25	L	0.4487	0.46	0.404
13	45	M	50	M	0.489	0.5	0.283
14	45	M	75	H	0.525	0.542	0.130
15	45	M	93.75	VH	0.568	0.58	0.085
16	67.5	H	6.25	VL	0.613	0.625	0.355
17	67.5	H	25	L	0.652	0.663	0.321
18	67.5	H	50	M	0.675	0.7	0.148
19	67.5	H	75	H	0.7133	0.75	0.091
20	67.5	H	93.75	VH	0.75	0.79	0.068
21	84.375	VH	6.25	VL	0.8	0.83	0.545
22	84.375	VH	25	L	0.812	0.875	0.522
23	84.375	VH	50	M	0.855	0.917	0.409
24	84.375	VH	75	H	0.9444	0.958	0.306
25	84.375	VH	93.75	VH	1	0.996	0.036

The outcomes of the model are compared to the available data. In order to assess the predictive performance of the model, several statistical parameters were used. These included the minimum value (Xmin), mean value (Xm), maximum value (Xmax), standard deviation (σ), coefficient of variation (Cvx), coefficient of skewness (Csx), correlation coefficient (r), as well as metrics such as Mean Absolute Relative Error (MARE), Mean Square Error (MSE), Mean Absolute Error (MAE), and Root Mean Square Error (RMSE). The results of the statistical comparison are displayed in Table 4.6. Low error rates and a high correlation coefficient suggest the potential for mathematically representing the statistical association between the model and the data.

Table 4.6 Statistical comparison of the SMRGT-2 model and data

Statistical Parameters and Errors	**Data**	**Model**
Max.	1.00	1.00
Min.	0.01	0.01
Mean	0.48	0.50
Standard Deviation	0.289	0.299
Skewness	0.0175	0.0093
Coefficient of Variance (CV)	0.599	0.599
Correlation Coefficient (r)	0.98	

Mean Square Error (MSE)	0.05
Mean Absolute Error (MAE)	0.17
Mean Absolute Precentage Error (MAPE)	10
Root Mean Square Error (RMSE)	0.02

Furthermore, the comparison's visual representation was conducted through a scatter diagram and a series graph, as depicted in Figures 4.19 and 4.20. The scatter plot illustrates that the regression line intersects the horizontal axis at an approximate angle of 45 degrees. However, the model's predictions strongly correlate with the gathered data and do not exhibit substantial deviations. The scatter plot exhibits a pronounced positive correlation between the observed and predicted data. Figure 4.21 illustrates the intricate correlation between dependent and independent variables in a three-dimensional visual format.

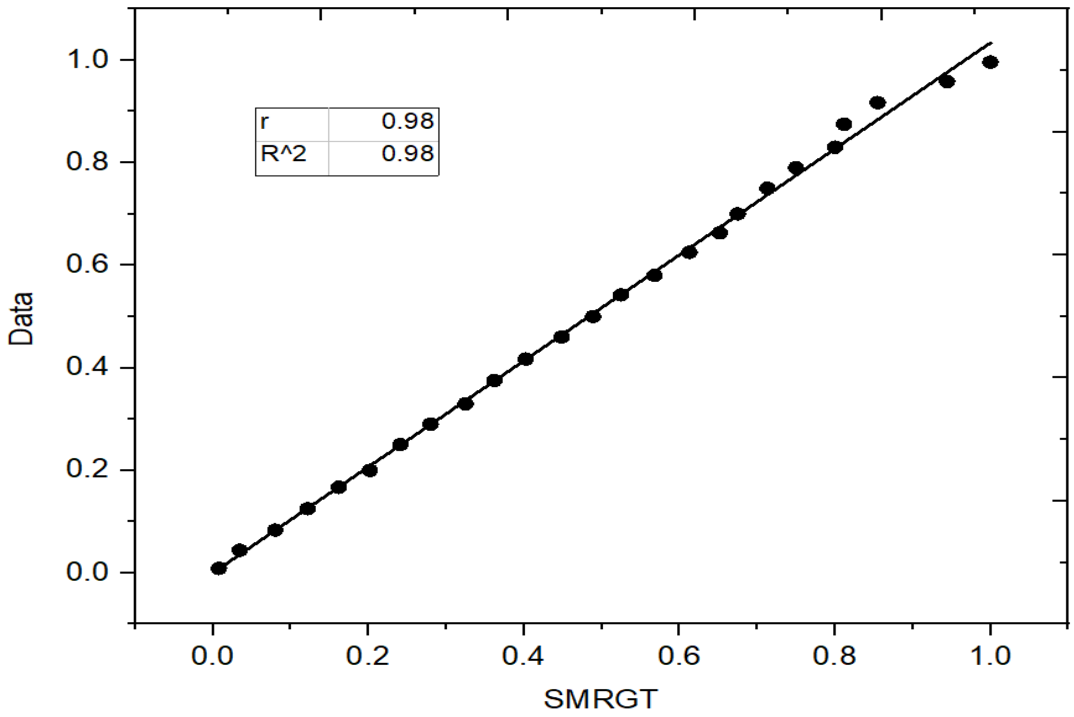

Figure 4.19 The series graph of the SMRGT-2 results.

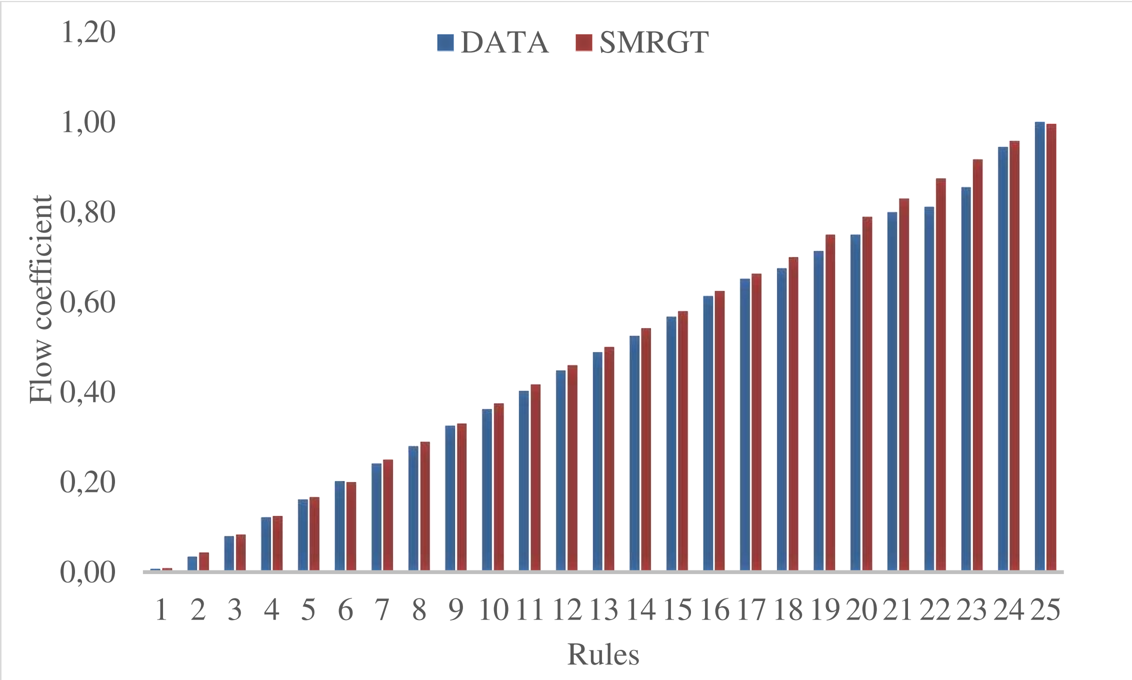

Figure 4.20 The series graph of the SMRGT-2 results.

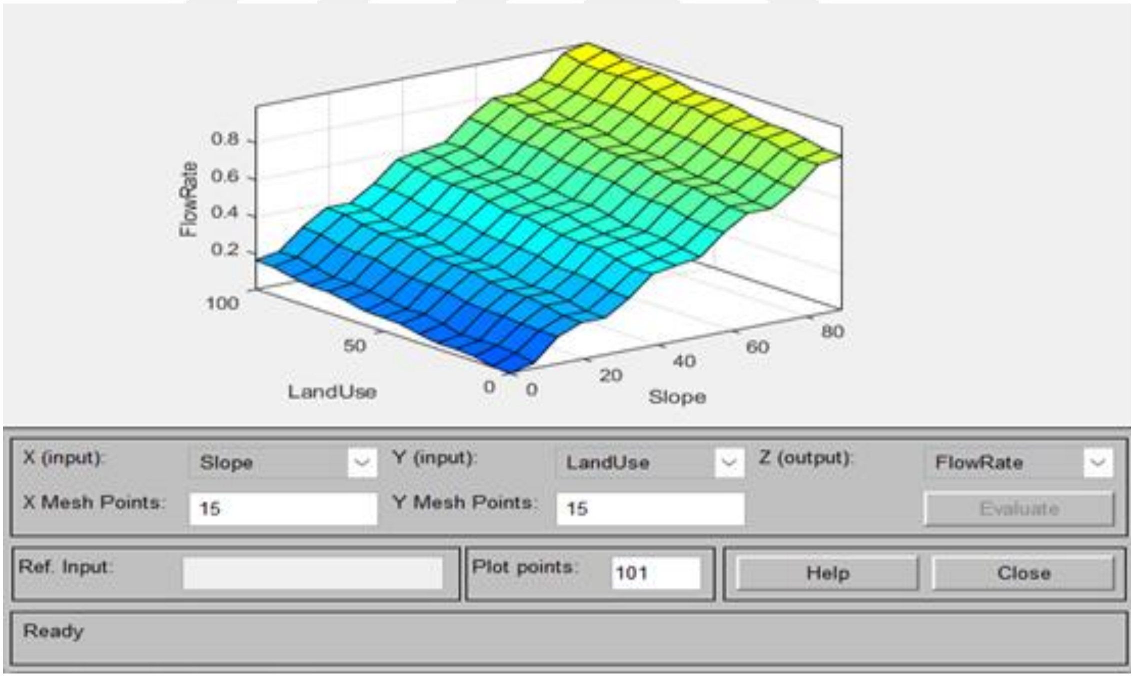

Figure 4.21 Variation of output as a function of inputs for SMRGT-2.

4.2.3 Model 3 : SMRGT-3 (Precipitation (P) mm, Temperature (T) °C, and Relative humidity (Rh) %:):

The flow coefficient was calculated by using the input variables of Precipitation (P) mm, Temperature (T) °C, and Relative humidity (Rh) % data. The SMRGT method has successfully identified the dependent and independent variables. The value that is commonly referred to as the flow coefficient is known as the dependent variable. The developed fuzzy model is illustrated in Figure 4.22.

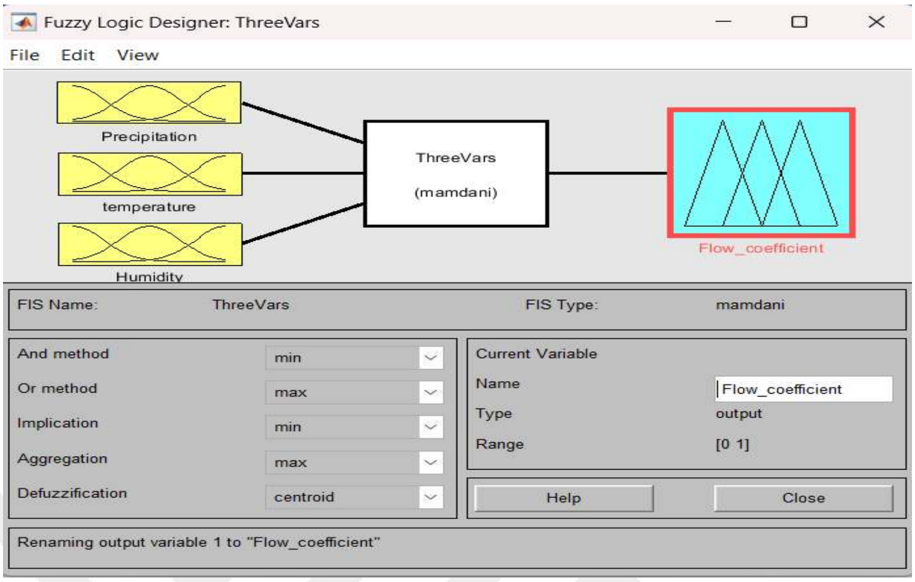

Figure 4.22 Inputs and output of the model.

Five membership functions were generated for each input variable. The key values for these membership functions were determined, as shown in Figures 4.23- 4.25. The process of creating the fuzzy rules base includes incorporating physical conditions using the terms "IF," "and," and "THEN," as shown in Figure 4.26. The MATLAB software was used as the designated software for implementing the model.

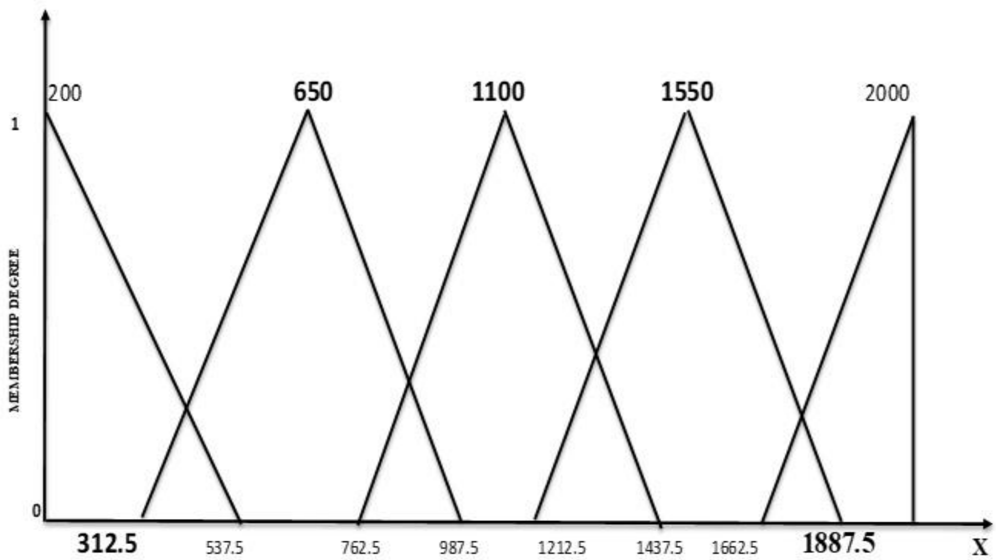

Figure 4.23 The key values of the precipitation MFs.

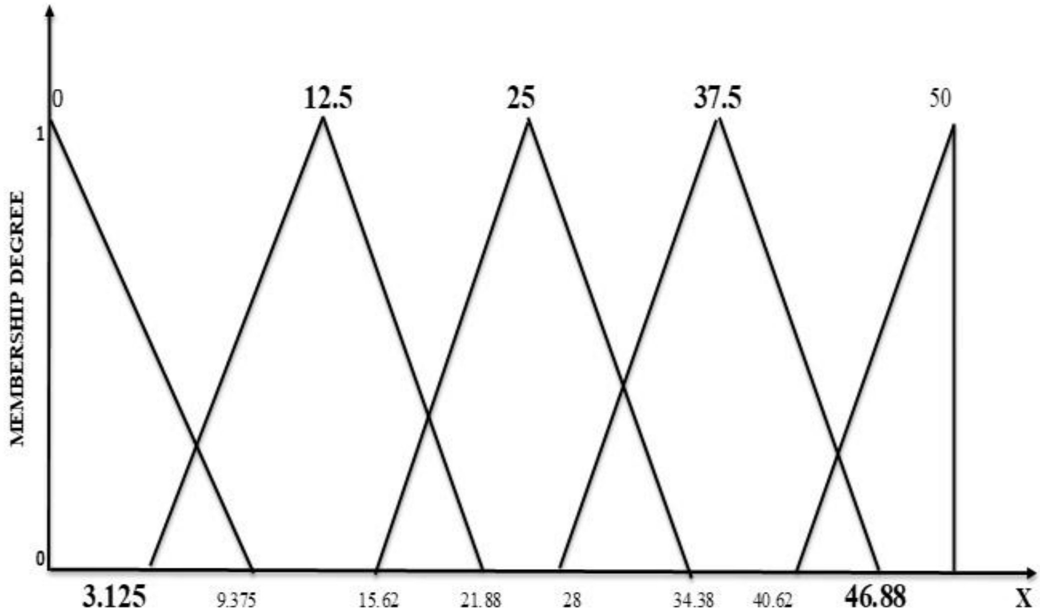

Figure 4.24 The key values of the temperature MFs.

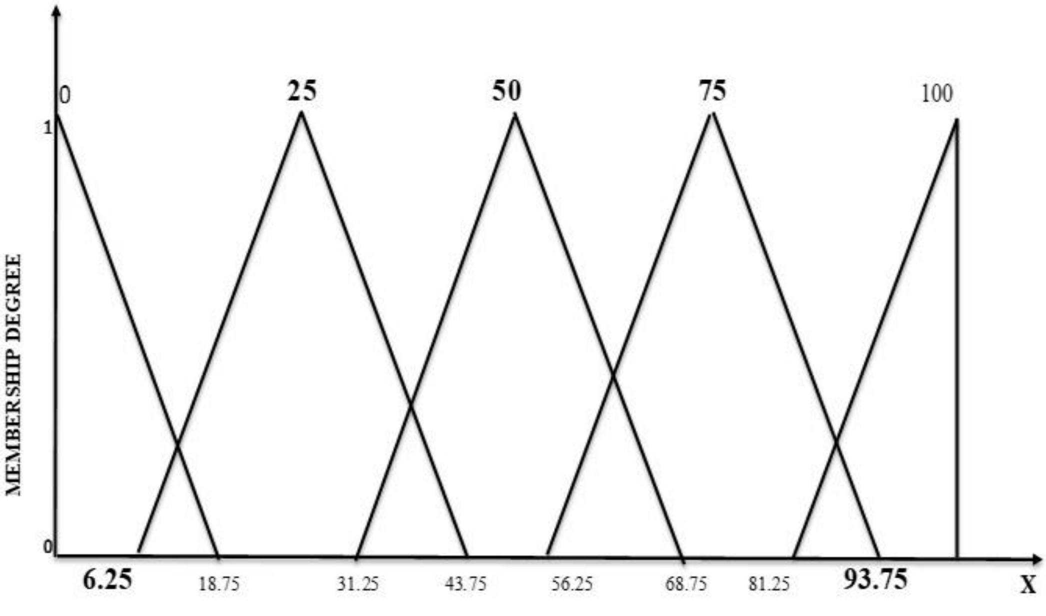

Figure 4.25 The key values of the relative humidity MFs.

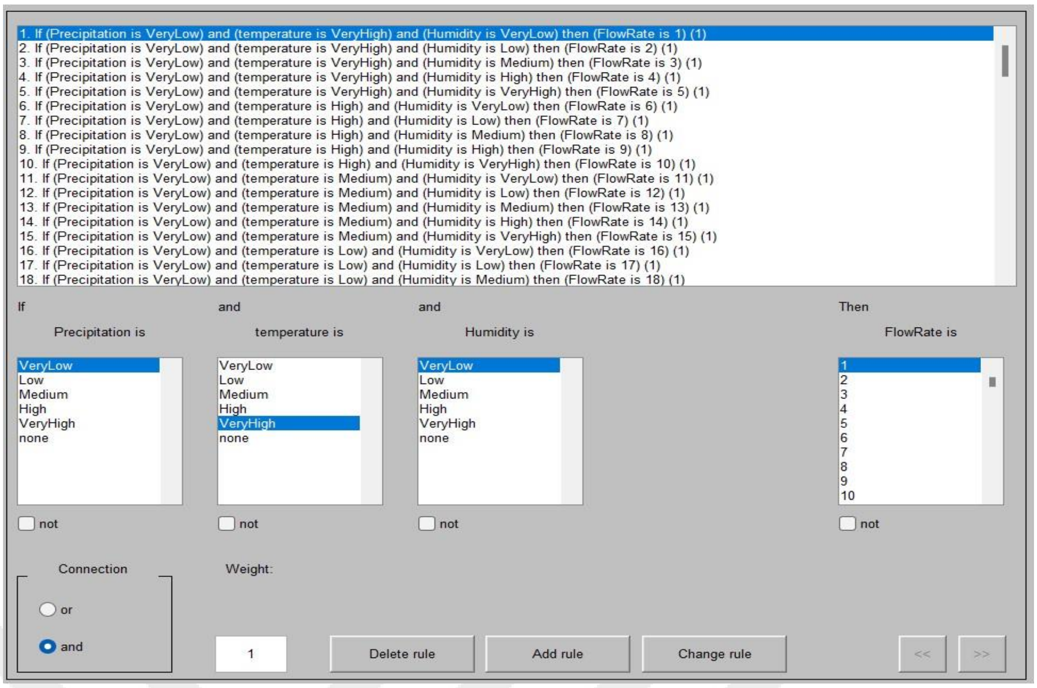

Figure 4.26 MATLAB view of the generated fuzzy rules.

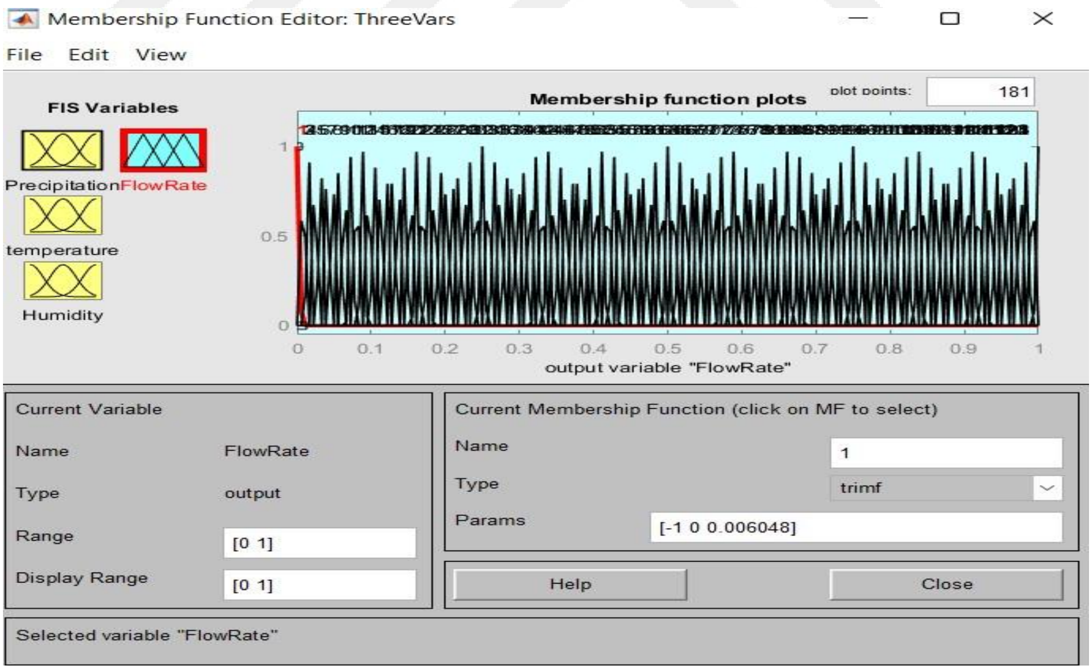

Figure 4.27 MFs of the output (flow coefficient).

Table 4.7 below displays the key values of each input variable, as determined by the equations provided in the preceding section. These key values were utilized as inputs for the SMRGT-3 model.

Table 4.7 Key values of the input variables.

Model	Input variables	K1	K2	K3	K4	K5
SMRGT-3	P	312.5	650	1100	1550	1887.5
	T	3.125	12.5	25	37.5	46.88
	Rh	6.25	25	50	75	93.75

Figures 4.28 and 4.29 illustrate the minimum and maximum values of the flow coefficient. Upon examination of the graphs, it is evident that the flow coefficient attains a value of zero under conditions of minimal precipitation and humidity, specifically at 200 mm and 0%, respectively, while the temperature is at an exceedingly elevated level of 50 C°. Furthermore, the flow coefficient attains a value of unity under conditions of maximum precipitation and humidity, i.e., 2000 mm and 100%, respectively, coupled with an extremely low temperature of zero degrees Celsius. The instances above prove that the model possesses mathematical precision and physical validity. This conclusion is supported by the research presented in (Toprak 2009), (Bayri 2018), (Sevgin 2021), (Unes et al. 2019), etc. The volume of water passing through a given area will be maximized under heavy precipitation and low temperature accompanied by elevated relative humidity. The analysis reveals the presence of a statistically significant positive and negative correlation between the output variable and the input variables. In other words, a positive correlation exists between the flow coefficient and the quantity of precipitation and humidity present in the atmosphere, while a negative correlation exists between the flow coefficient and temperature.

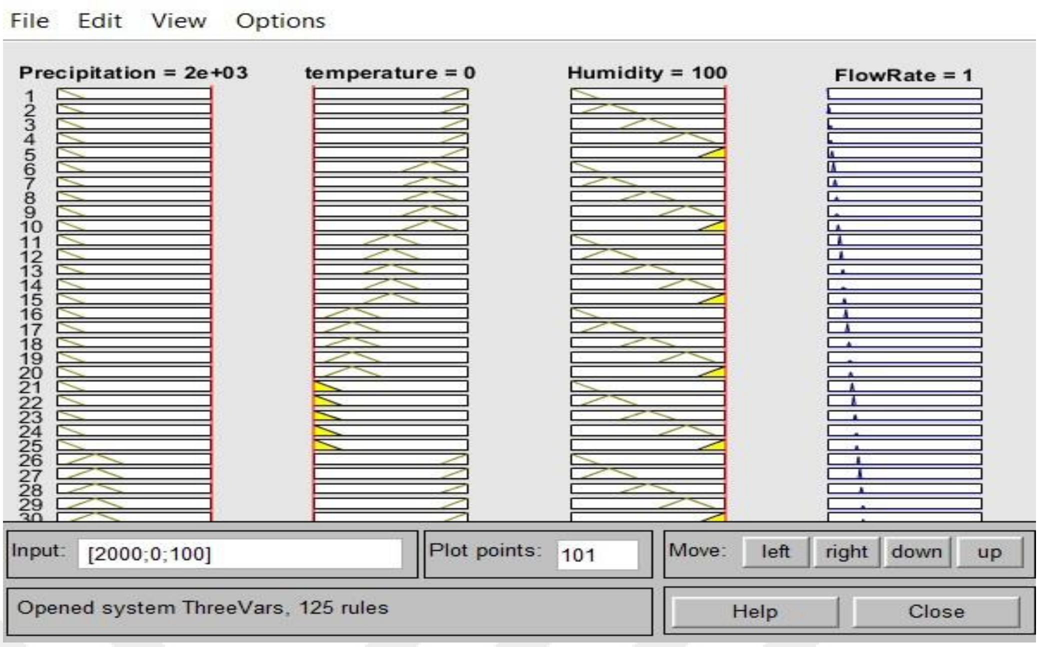

Figure 4.28 Graphical view of the rules (maximum value of output).

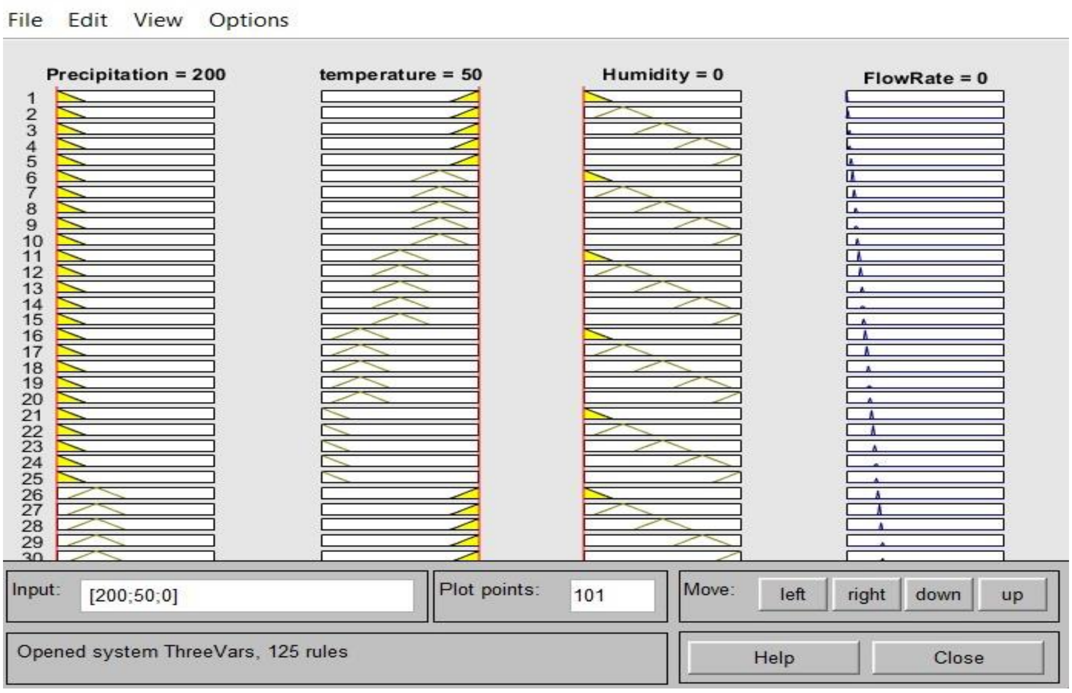

Figure 4.29 Graphical view of the rules (minimum value of output).

The generated fuzzy set table for this model is shown in (APPENDIX A). The statistical parameters minimum (X_{min}), mean (X_m), maximum (X_{max}), standard deviation (σ), coefficient of variation (C_{vx}), coefficient of skewness (C_{sx}), and correlation coefficient (r) were used to compare the model's output with the data to test the model's predictions. Error types also included Mean Absolute Precentage Error (MAPE), Mean Square Error (MSE), Mean Absolute Error (MAE), and Root

Mean Square Error (RMSE). The results of statistical comparisons are shown in Table 4.8. In addition, a scatter plot and series diagram (Figures 4.30 and 4.31) were used to illustrate the comparison. The scatter diagram reveals that the regression line intersects the horizontal axis at an angle of approximately 45 degrees. This means that the model is not skewed. In other words, the model does not produce consistently larger or smaller predictions than the observed data. The high coefficient of determination (R^2 = 0.963) indicates that the statistical relationship between the model and data outcomes can be expressed mathematically. In other words, the model identifies the trend in the data. Most points lie close to the regression line, indicating that the model results and actual data are numerically comparable.

Table 4.8 Statistical comparison of the SMRGT-3 model and data

Statistical Parameters and Errors	**Data**	**Model**
Max.	1.00	1.00
Min.	0.14	0.00
Mean	0.58	0.50
Standard Deviation	0.304	0.29
Skewness	0.00045	-0.0000029
Coefficient of Variance (CV)	0.527	0.582
Correlation Coefficient (r)	0.98	
Mean Square Error (MSE)	0.09	
Mean Absolute Error (MAE)	0.08	
Mean Absolute Precentage Error (MAPE)	15	
Root Mean Square Error (RMSE)	9.6	

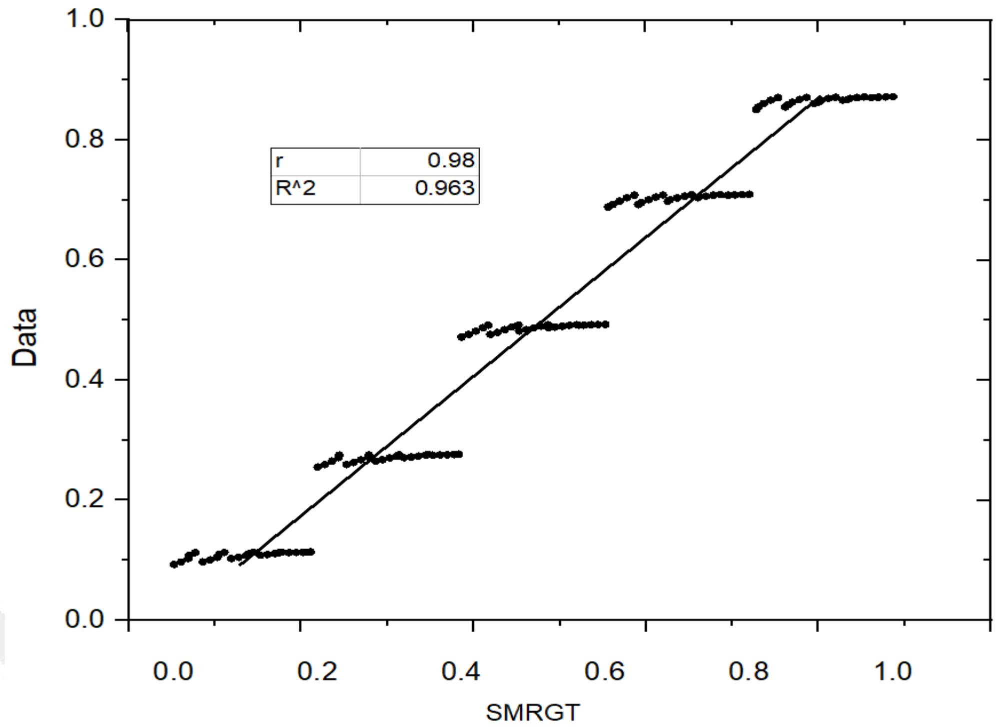

Figure 4.30 The scatter plot of the SMRGT-3 results.

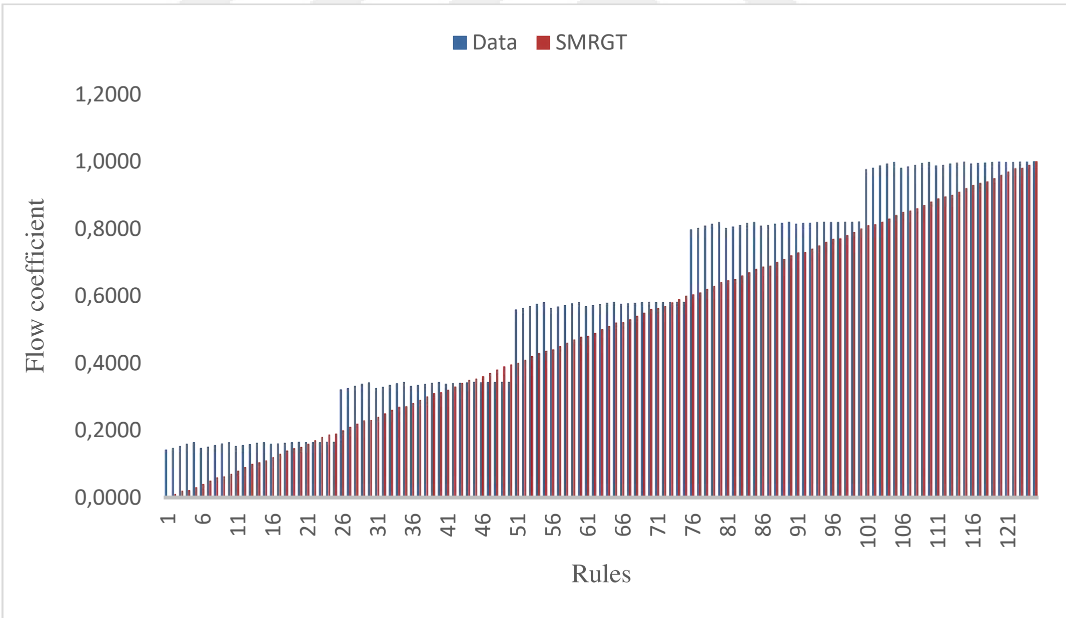

Figure 4.31. The series graph of the SMRGT-3 results.

Figures 4.32 – 4.34 show, respectively, how the model result (the dependent variable, the flow coefficient) varies in three dimensions 3D as a function of the variables that are considered independent (Precipitation, Temperature, and Humidity). Generating a 3-dimensional surface involves evaluating the membership functions of each input variable and then combining them using fuzzy inference rules to determine the degree of membership in the output fuzzy sets. The results are commonly articulated in a degree of membership with imprecision or a definite output quantity achieved via defuzzification. Each point on the surface represents a distinct combination of input variables and their corresponding output value, as the fuzzy inference process ascertains. The presence of complex patterns, associations that are not linear, or unclear boundaries is dependent on the membership functions and fuzzy inference rules that have been chosen. The analysis of the tridimensional surface can enhance understanding of the effects of modifications in the input parameters on the output, thus aiding in the creation of determinations or the establishment of management systems based on the fuzzy logic model.

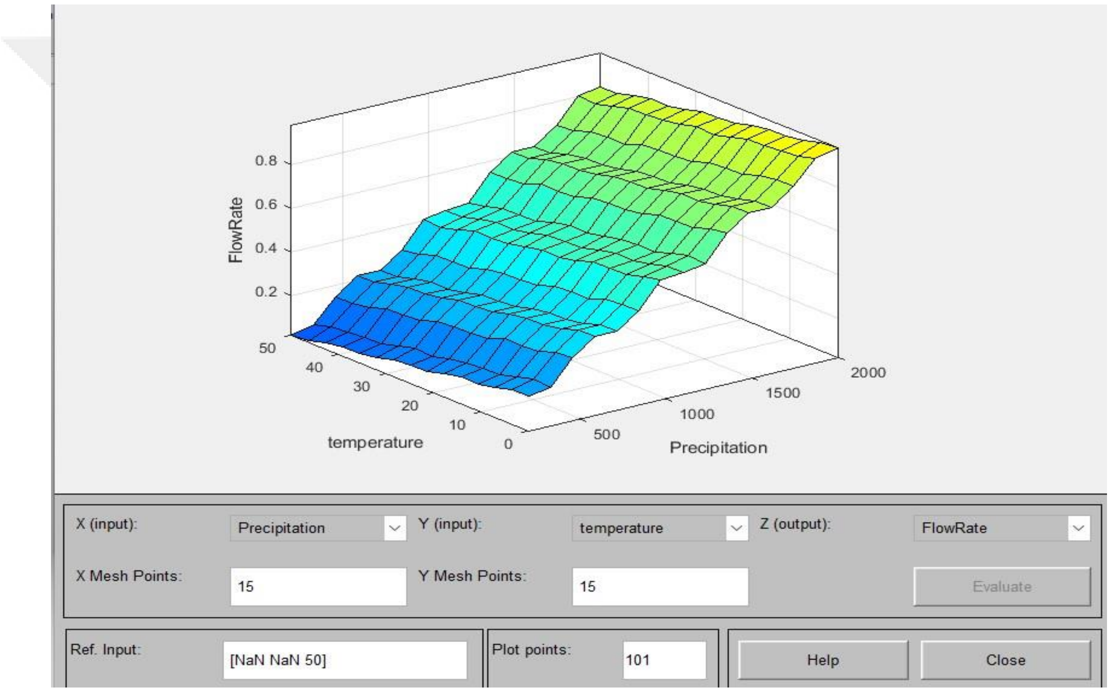

Figure 4.32 The 3D variation of the flow coefficient due to precipitation & temperature.

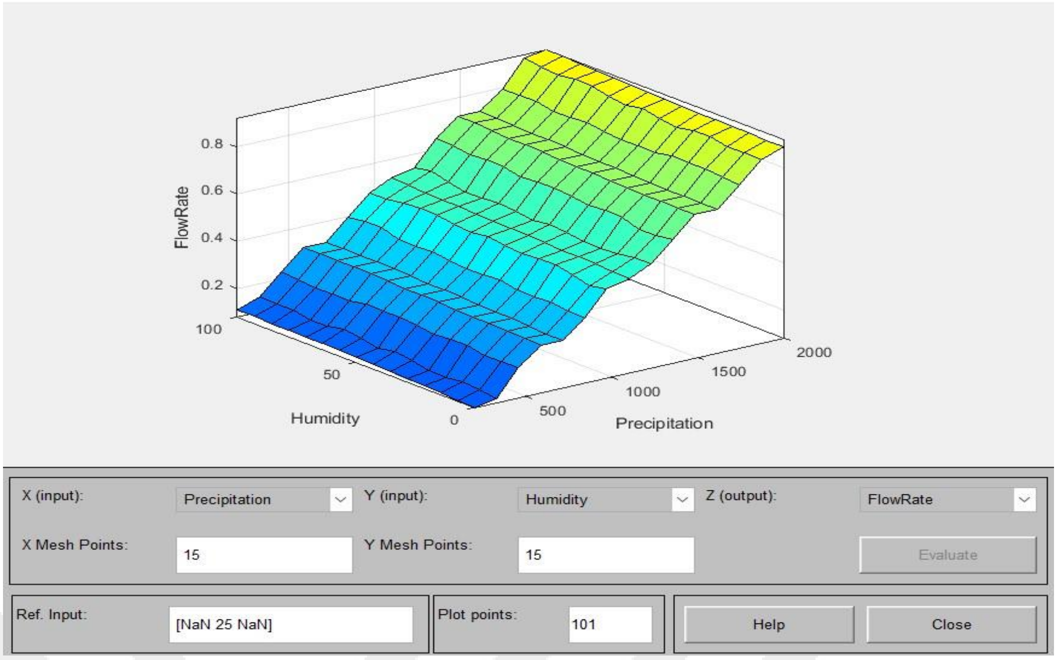

Figure 4.33 The 3D variation of the flow coefficient due to precipitation & humidity.

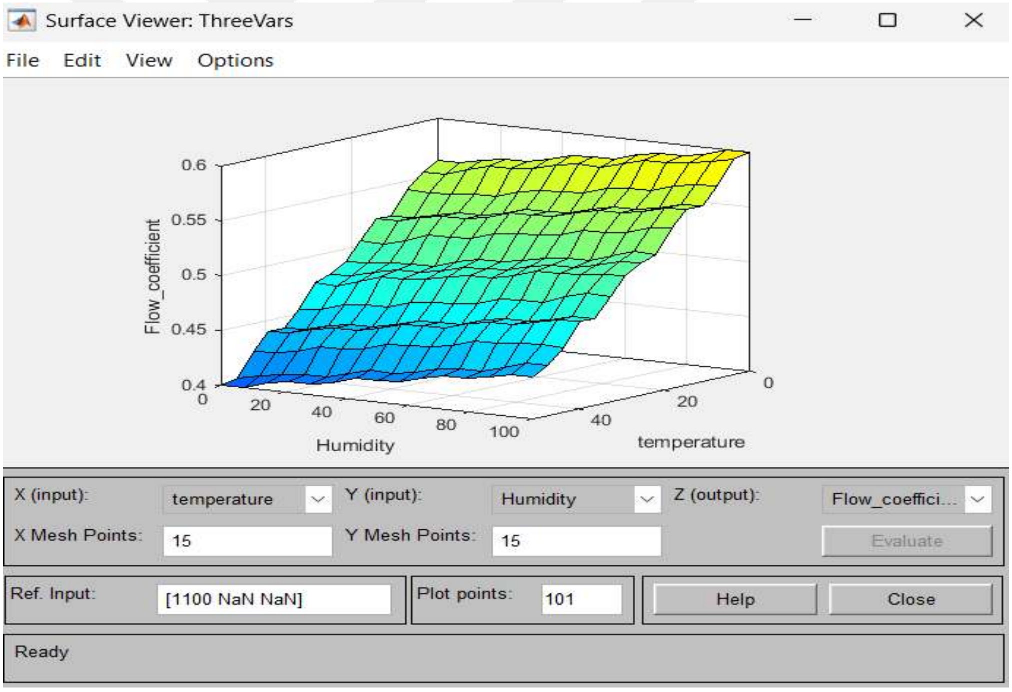

Figure 4.34 The 3D variation of the flow coefficient due to temperature & humidity.

4.2.4 Model-4 : SMRGT-4 (Precipitation (P), Land Use (LU), and Soil Permeability (Sp)):

The input variables for this model encompassed precipitation, soil type (as determined by permeability), and land use characteristics within the research area. The flow coefficient was obtained as the model's output, as depicted in Figure 4.35.

Five membership functions were generated and assigned labels for each independent variable, namely Very low (VL), Low (L), Medium (M), High (H), and Very High (VH).

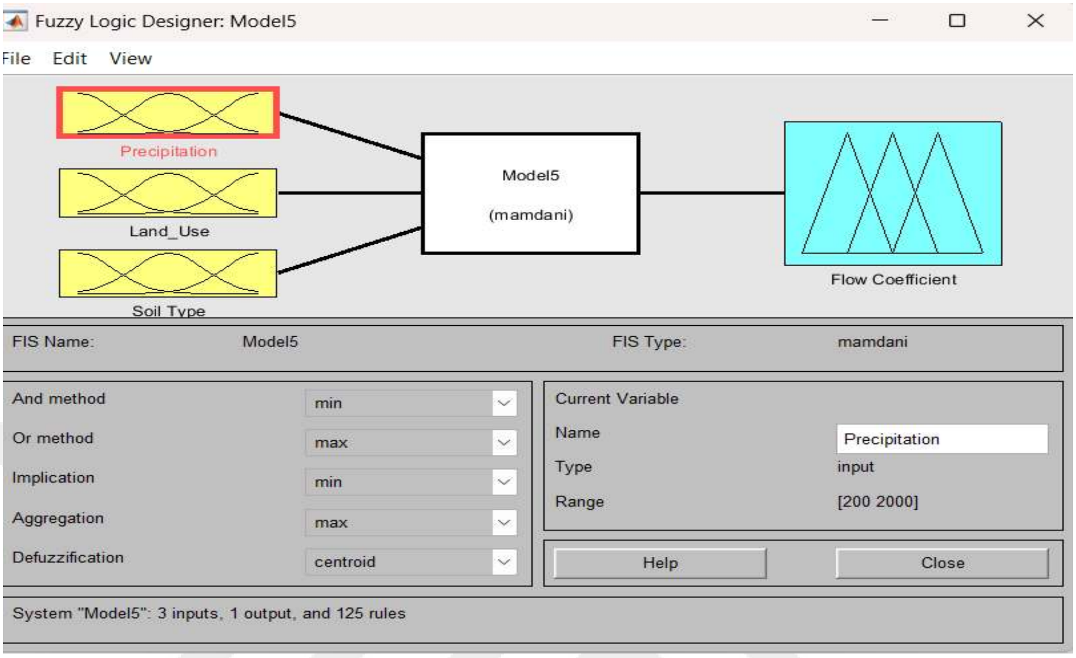

Figure 4.35 Configuration of the SMRGT-4 model.

The recommendation made by Toprak (2009) was followed, and a trapezoidal membership function shape was used. The boundaries for each membership function are shown in Figures 4.36-4.38. When evaluating the fundamental principles of input variables, it is common practice to seek the help of an expert in the field. The model takes the parameters as input. According to the SMRGT methodology, the model output, specifically the flow coefficient, must equal the number of rules used in the study. In this case, there are 125 rules employed.

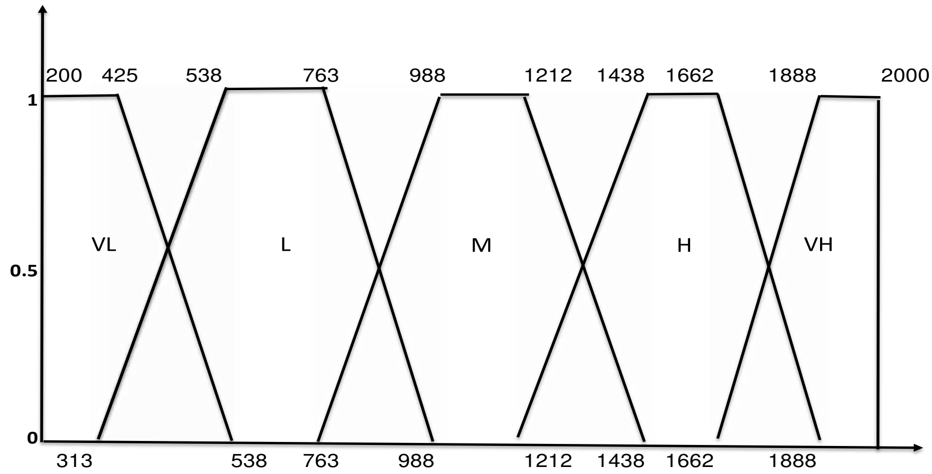

Figure 4.36 The trapezoidal MFs of the precipitation.

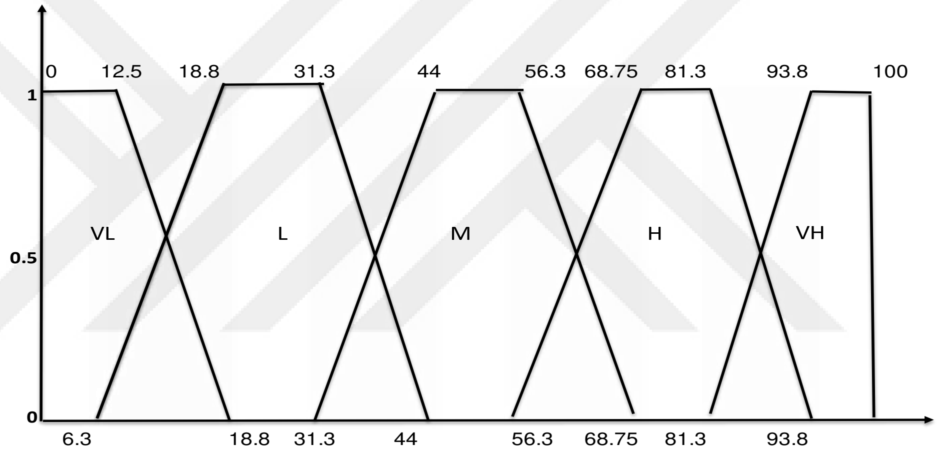

Figure 4.37 The trapezoidal MFs of the land use.

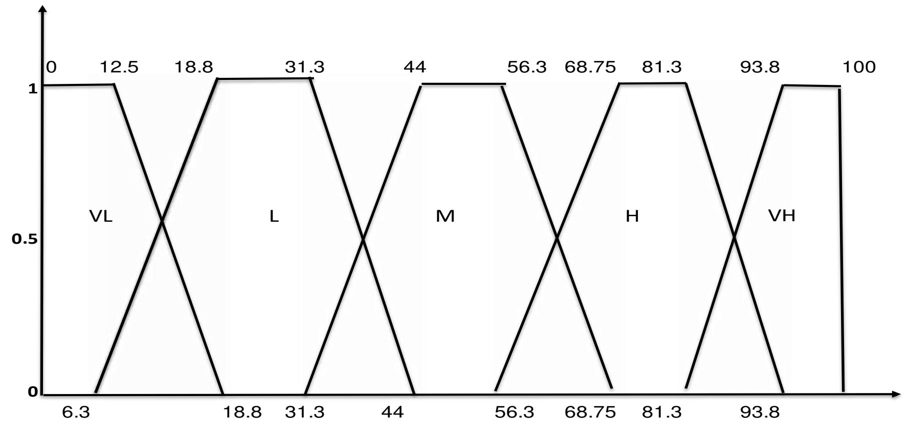

Figure 4.38 The trapezoidal MFs of the soil permeability

Table 4.9 below displays the key values of each input variable, calculated using the equations described in the previous section. The SMRGT-4 model utilized these key values as its inputs.

Table 4.9 Calculated key values of the SMRGT-4 model

Model	Input variables	K1	K2	K3	K4	K5
SMRGT-4	P	312.5	650	1100	1550	1887.5
	LU	6.25	25	50	75	93.75
	Sp	6.25	25	50	75	93.75

The model considers all possible probabilities of precipitation events to create a comprehensive framework, which creates a flow coefficient model. The flow coefficient ranges from a minimum value of 0 to a maximum value of 1. The generated model showed variations in precipitation, land use, and soil type effects on the flow coefficient. Each independent variable had a distinct influence. Figures 4.39 and 4.40 show the minimum and maximum values of the flow coefficient, respectively. According to the graphs, the flow coefficient reaches zero when the soil permeability is high (100%), precipitation is low (200 mm), and land use is minimal (0%). In cases where the soil's permeability is extremely low, reaching zero percent, the precipitation and land use levels are at their maximum values of 2000 mm and 100%, respectively, while the flow coefficient remains at one. The examples mentioned above demonstrate the model's mathematical and physical accuracy. The above finding is supported by scholarly research documented in references [Sevgin, 2021, Toprak, 2009, Karakaya, 2020].

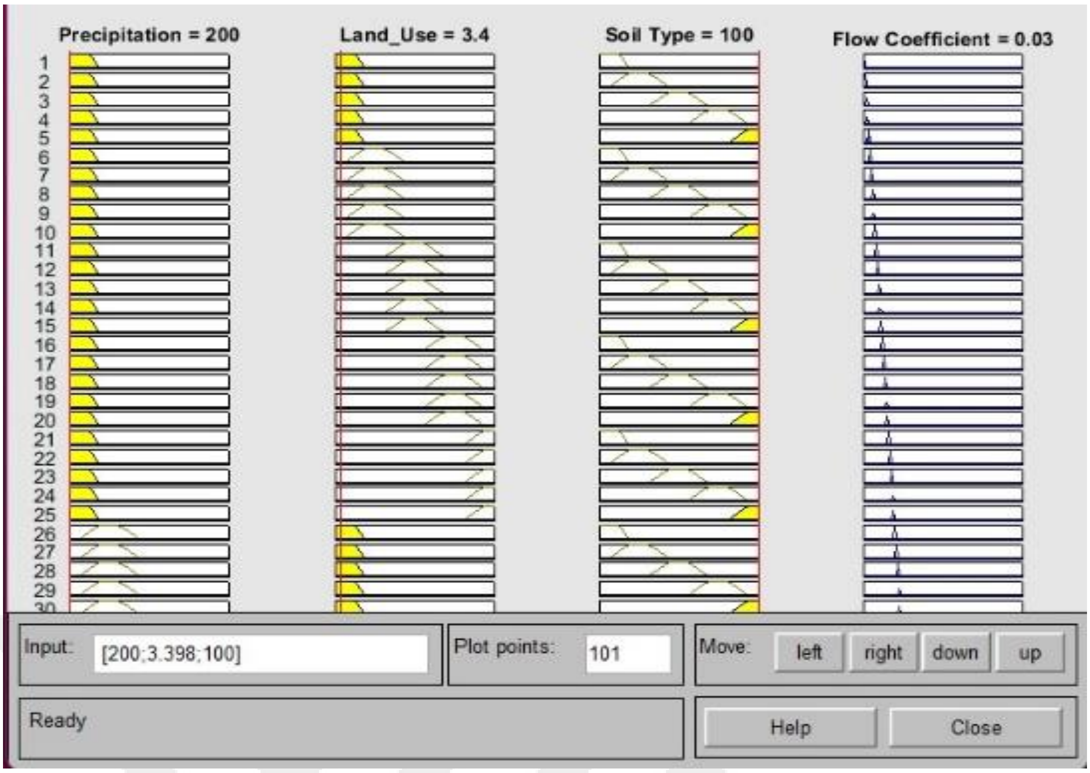

Figure 4.39 A graphic view of the output maximum value.

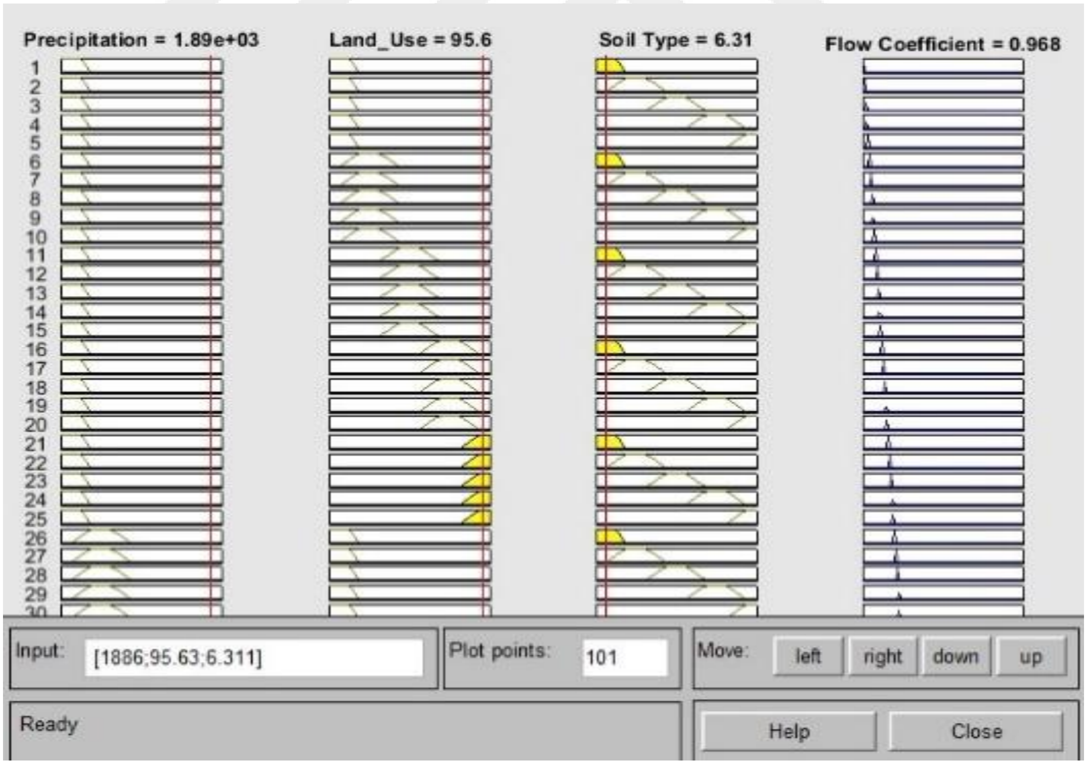

Figure 4.40 A graphic view of the output maximum value.

The evaluation of the model's predictive accuracy involved comparing the model's output to the actual data. Various statistical measures were computed, including the minimum (Xmin), mean (Xm), maximum (Xmax), standard deviation (σ), coefficient of variation (Cvx), coefficient of skewness (Csx), and correlation coefficient (R). The calculations for Mean Absolute Relative Error, Mean Square Error, Mean Absolute Error, and Root Mean Square Error were also conducted. The statistical results are displayed in Table 4.10.

Table 4.10 The statistical findings and rate of errors

Statistical Parameters and rate of Errors	**Data**	**Model**
Max.	1.00	1.00
Min.	0.002	0.006
Mean	0.55	0.50
Standard Deviation	0.324	0.291
Skewness	-0.141	0.0203
Coefficient of Variance (CV)	0.588	0.582
Correlation Coefficient (r)	0.98	
Mean Square Error (MSE)	0.59	
Mean Absolute Error (MAE)	0.06	
Mean Absolute Precentage Error (MAPE)	22	
Root Mean Square Error	7.74	

In addition, graphical representations in the form of a scatter diagram and series plot were utilized to depict the observed differences visually. These graphical representations can be observed in Figures 4.41 and 4.42, respectively. In a scatter diagram, the regression line intersects the horizontal axis at a 45-degree angle. This implies that the model does not exhibit any asymmetry. Put differently, the model does not generate estimations that exhibit a consistent bias towards either overestimation or underestimation compared to the actual data. The substantial coefficient of determination (R^2 = 0.98) suggests a robust mathematical relationship between the model and the observed data. In simple terms, the model is responsible for identifying the pattern or trajectory of the data. Most data points are directly on or close to the regression line, suggesting a robust quantitative agreement between the model's outcomes and the observed data.

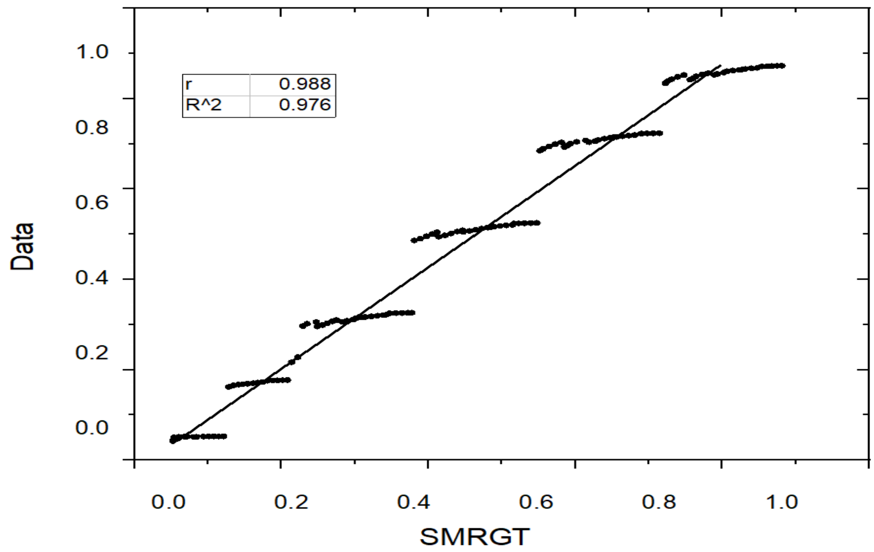

Figure 4.41 The scatter plot of the SMRGT-4 results.

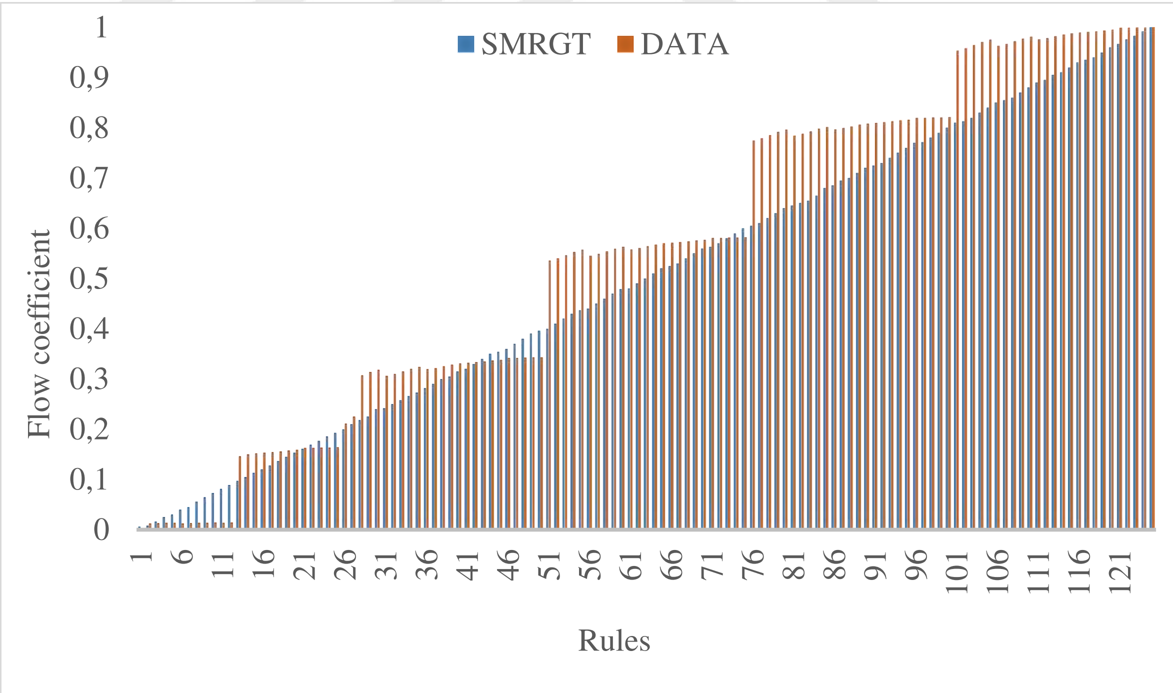

Figure 4.42 The series graph of the SMRGT-4 results.

Important output values, the total number of FRs, and the development of fuzzy rules for a fuzzy model are shown in APPENDIX 2.

The flow coefficient positively correlates with reduced soil cover, indicating decreased land use. It also suggests an increase in pore density, which implies a decrease in clay content. Soils with a high proportion of clay particles are known for their reduced permeability, making it challenging for water to infiltrate the soil. Unstable soil structures are prone to erosion and can impede the process of soil infiltration. The presence of soil characteristics significantly affects the flow characteristics within a basin. River floods occur when the amount of water flowing in a river exceeds its capacity to carry it.

Figures 4.43 – 4.45 depict the three-dimensional variation of the model's dependent variable, the flow coefficient, concerning the independent variables of Precipitation (P), Land use (LU), and Soil permeability. The process of generating a three-dimensional surface entails the assessment of the membership functions associated with each input variable. These membership functions are subsequently combined using fuzzy inference rules to ascertain the extent of membership in the output fuzzy sets. The examination of the three-dimensional surface can improve comprehension of the impacts of alterations in the input variables on the output, thereby facilitating the formulation of decisions or the development of management systems grounded in the fuzzy logic model.

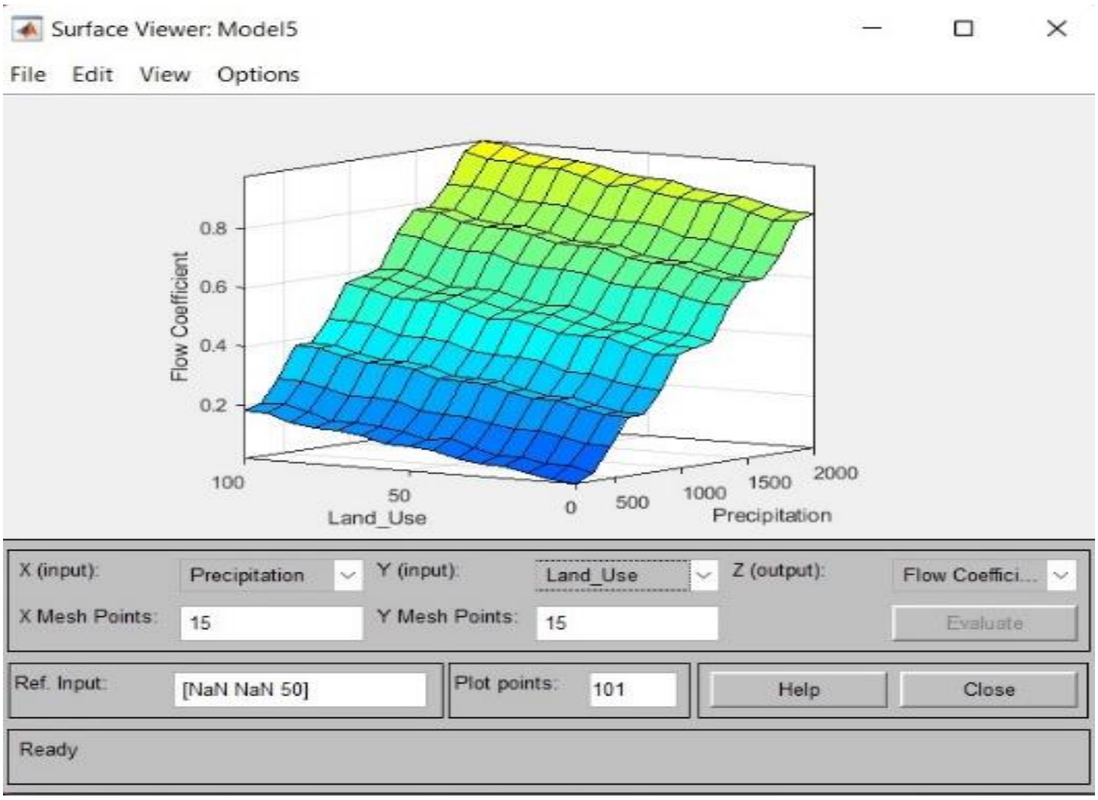

Figure 4.43 The 3D variation of output due to precipitation & land use.

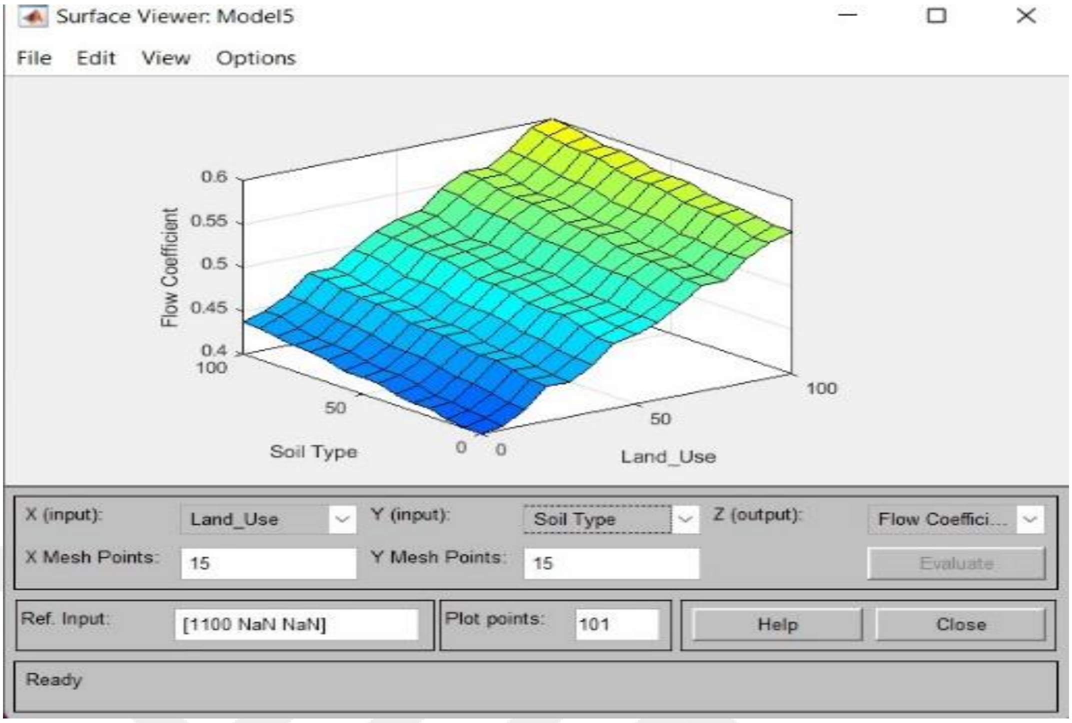

Figure 4.44 The 3D variation of output due to soil type & land use.

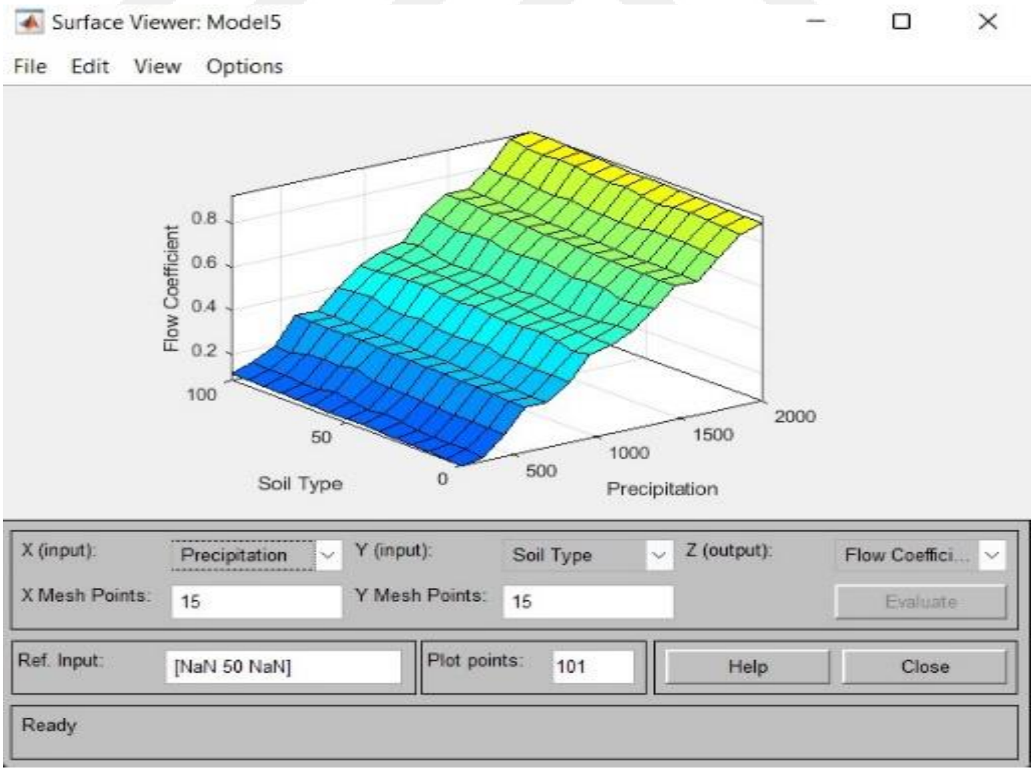

Figure 4.45 Tthe 3D variation of output due to precipitation & soil type.

4.2.5 Model-5: SMRGT-5

Precipitation (P), Temperature (T), Relative humidity (Rh %), Land Use (LU), and Slope (S %):

The input variables for this model encompassed precipitation, temperature, humidity, slope, and land use characteristics within the research area. The flow coefficient was calculated based on the model's output, as shown in Figure 4.46.

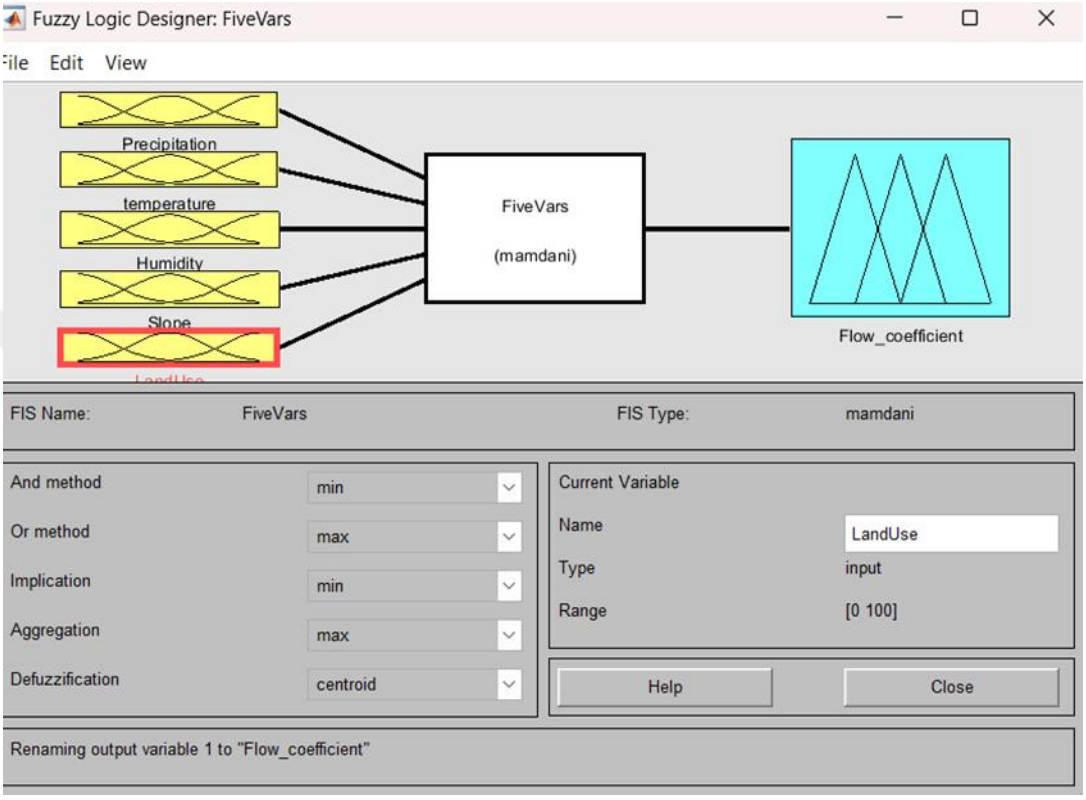

Figure 4.46 Framework of the SMRGT-5 model.

The suggestion put forth by Toprak (2009) was implemented, wherein a triangular membership function shape was employed. The delineations for each membership function are illustrated in Figures 4.47 - 4.51. Five membership functions were generated and designated with labels for each independent variable. The aforementioned labels encompass a range of values, namely Very Low (VL), Low (L), Medium (M), High (H), and Very High (VH). According to the SMRGT method, it is recommended that the membership functions for the model output, specifically the flow coefficient, in this study be assigned a quantity equal to the number of rules, which is 3125. This model is regarded as the initial attempt to utilize many fuzzy rules in the SMRGT technique.

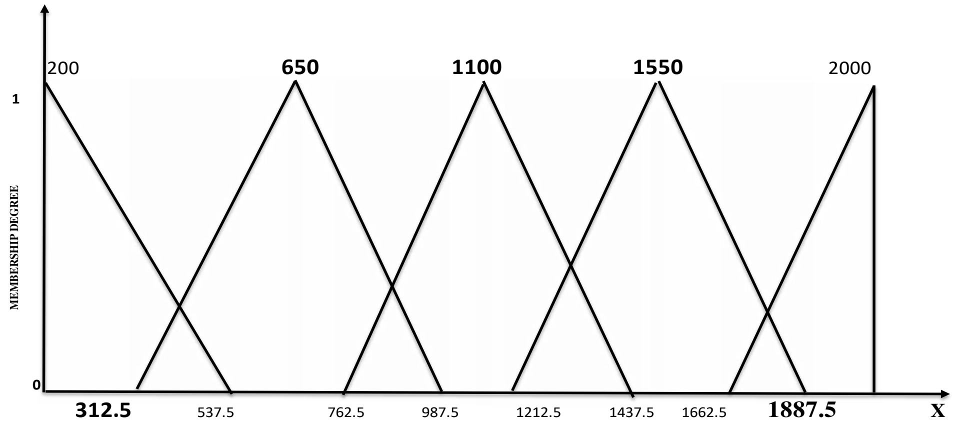

Figure 4.47 The triangular MFs of the precipitation

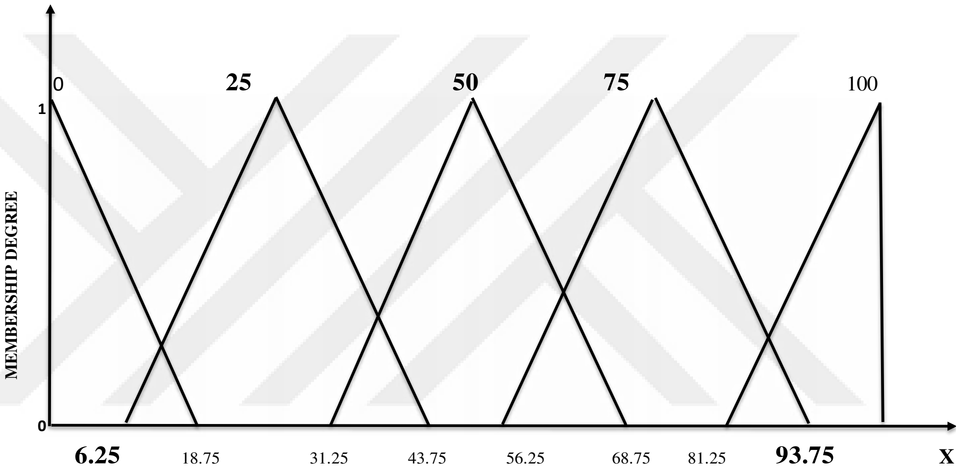

Figure 4.48 The triangular MFs of the relative humidity

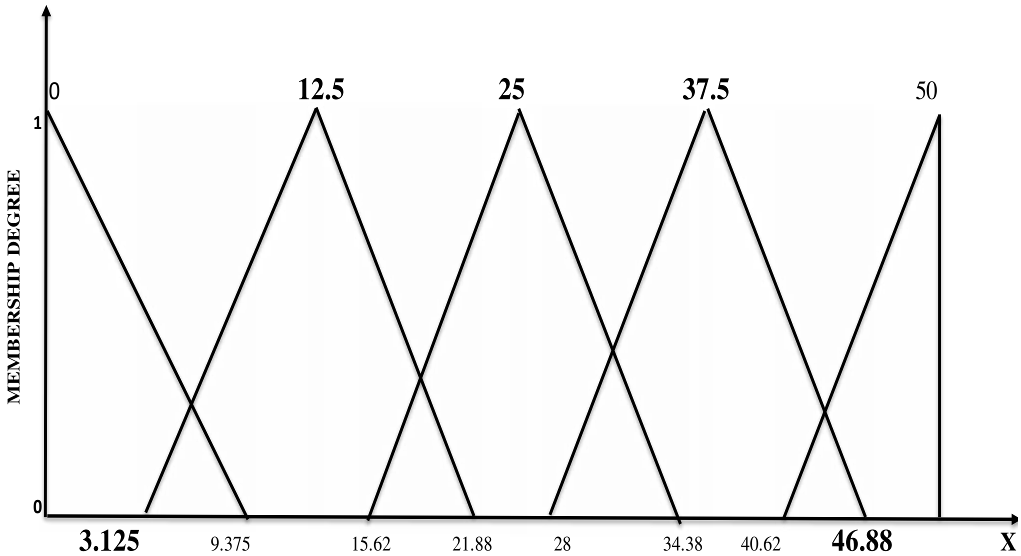

Figure 4.49 The triangular MFs of the temperature

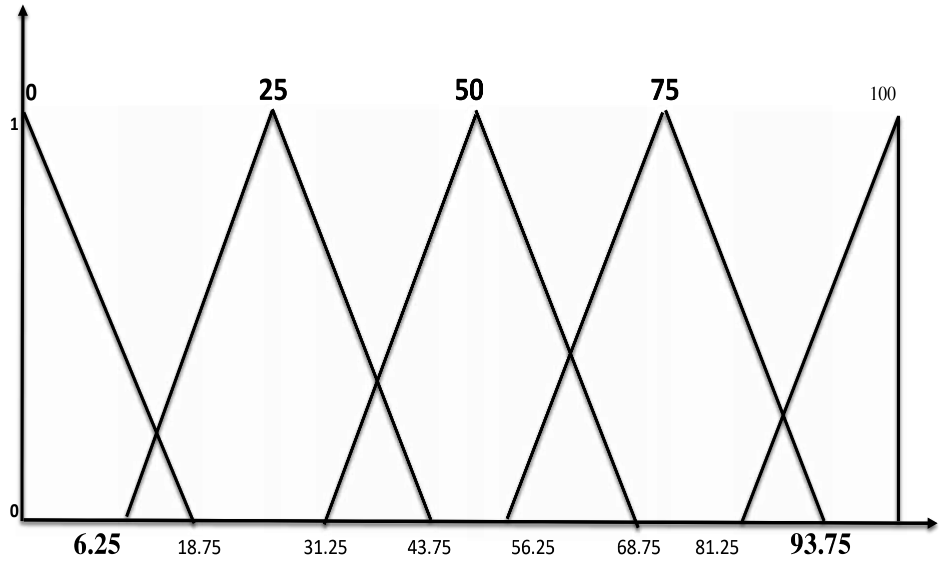

Figure 4.50 The triangular MFs of the land use

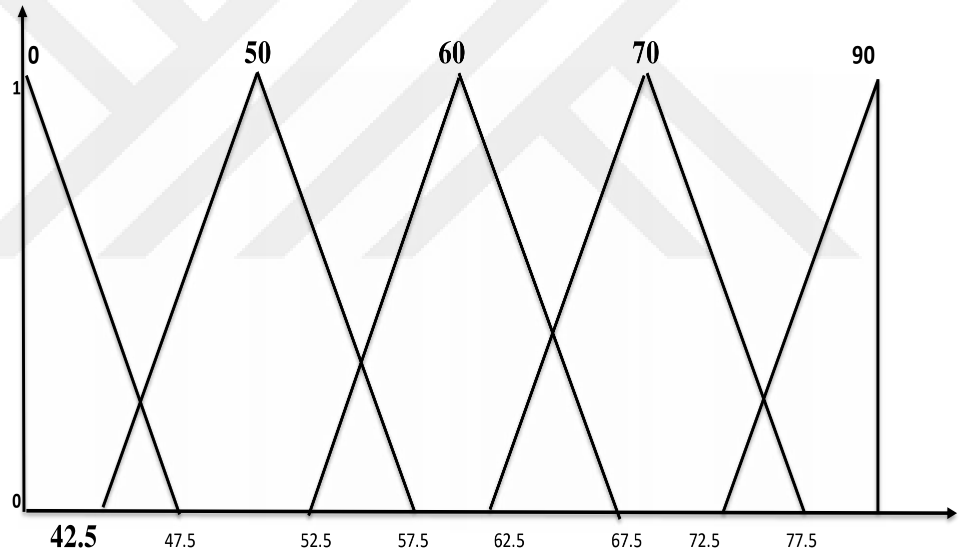

Figure 4.51 The triangular MFs of the slope

Table 4.12 below displays the key values of each input variable, calculated using the equations described in the previous section. The SMRGT-5 model utilized these key values as its inputs.

Table 4.12 Calculated key values of the SMRGT-5 model

Model	Input variables	K1	K2	K3	K4	K5
SMRGT-5	P	312.5	650	1100	1550	1887.5
	T	3.125	12.5	25	37.5	46.88
	Rh	6.25	25	50	75	93.75
	S	5.625	22.5	45	67.4	84.375
	LU	6.25	25	50	75	100

The flow coefficient attained its peak value of (1) under extreme conditions, with precipitation measuring 2000 mm (indicating a very high level), temperature at 0° C (indicating a deficient level), humidity at 100% (indicating a very high level), slope at 90° (indicating a very high level), and land use at 100% (indicating a very high level) as depicted in Figure 4.52. At a precipitation level of 200 millimeters, which can be considered significantly low, the temperature reached 50 degrees Celsius, indicating a considerably high value. The humidity, on the other hand, was recorded at 0%, indicating a deficient value. Similarly, the slope of the terrain was measured at 0 degrees, indicating a minimal incline. Lastly, land use was recorded at 0%, indicating a negligible percentage of land utilization. When there is no precipitation, the flow coefficient's minimum and maximum values are changed to 0 and 1, respectively. These values are used to calculate the flow coefficient. The impact of precipitation, temperature, humidity, slope, and land use on the flow coefficient was evaluated differently.

Recognizing that these environmental factors do not act independently but interact in complex ways to influence the flow coefficient is essential. Understanding these interactions and considering the variability of these factors across different landscapes is crucial in accurately assessing the flow coefficient and its implications for water management and environmental conservation.

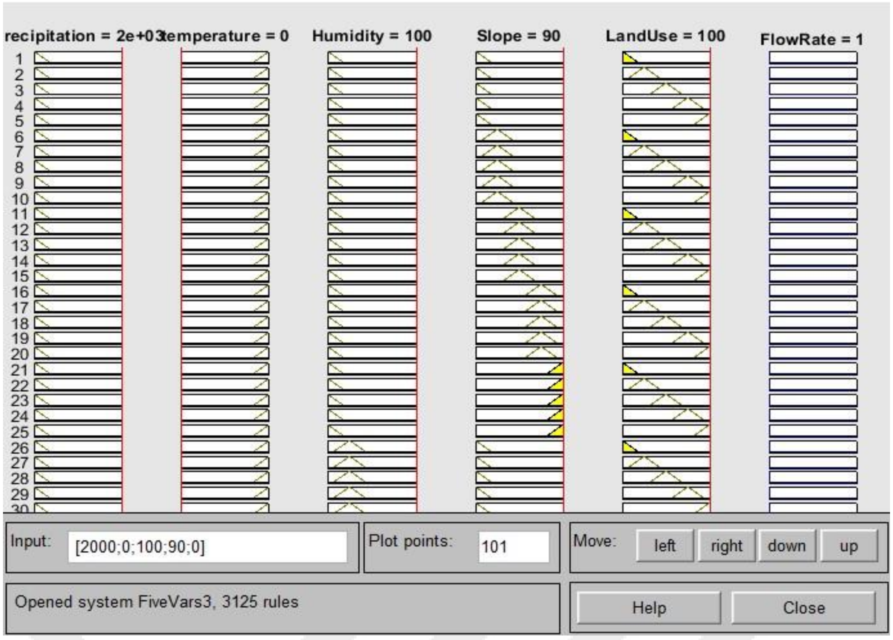

Figure 4.52 A graphic view of the output maximum value.

In order to assess the model's predictive accuracy for future events, various statistical parameters were employed, including the minimum value (Xmin), mean value (Xm), maximum value (Xmax), standard deviation (σ), coefficient of variation (Cvx), coefficient of skewness (Csx), and correlation coefficient (r). These parameters were utilized to compare the model's output with the available data. There are several types of errors commonly encountered in various fields, such as the Mean Absolute Precentage Error (MAPE), Mean Square Error (MSE), Mean Absolute Error (MAE), and Root Mean Square Error (RMSE). Table 4.13 displays the outcomes of the statistical comparison. Furthermore, the comparison was visually depicted through the utilization of a scatter diagram, as illustrated in Figure 4.53. The model generated a total of 3125 outputs. However, only 102 membership functions (MFs) were selected based on the recommendation by Toprak (2009). This decision was made to address the issue of excessive overlap observed in the output membership functions. The objective can be accomplished by merging multiple combined membership functions into a single function. Consequently, several interconnected MFs underwent a transformation and became individual MFs.

Table 4.13 the statistical results of the SMRGT-5

Statistical Parameters & Errors	**Data**	**Model**
Max.	1.00	1.00
Min.	0.10	0.00
Mean	0.57	0.50
Standard Deviation	0.304	0.288
Skewness	-0.008514	-0.00291
Coefficient of Variance	0.532	0.577
Correlation Coefficient	0.966	
Mean Square Error (MSE)	0.91	
Mean Absolute Error (MAE)	0.11	
Mean Absolute Precentage Error (MAPE)	18.3	
Root Mean Square Error (RMSE)	9.3	

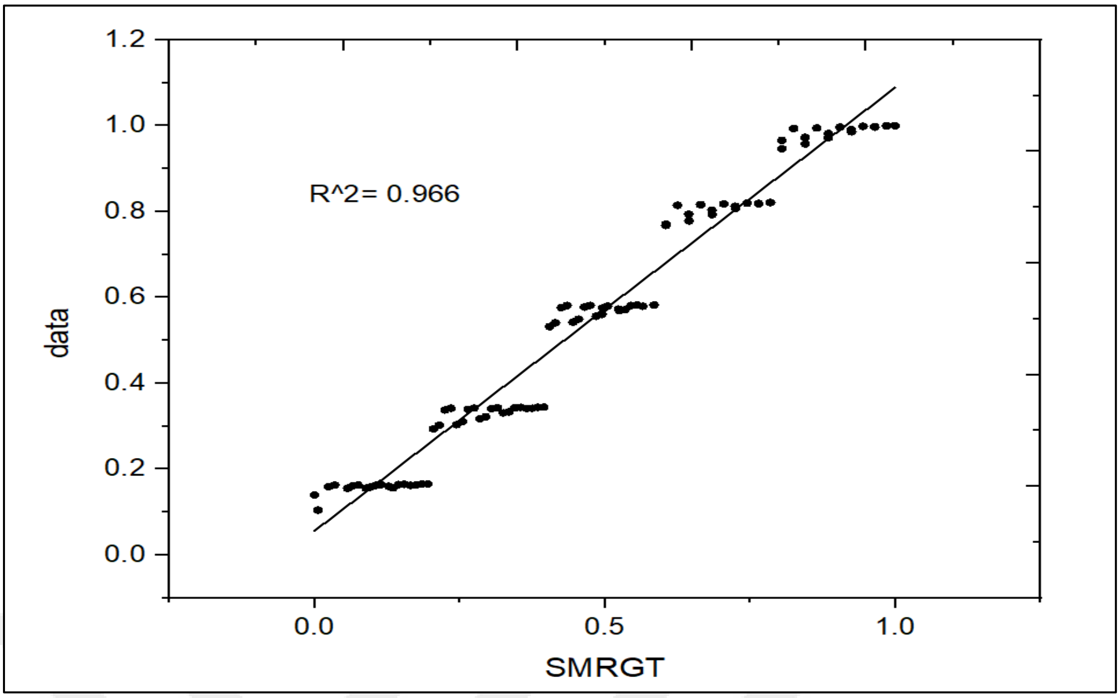

Figure 4.53 The scatter plot of the SMRGT-5 results.

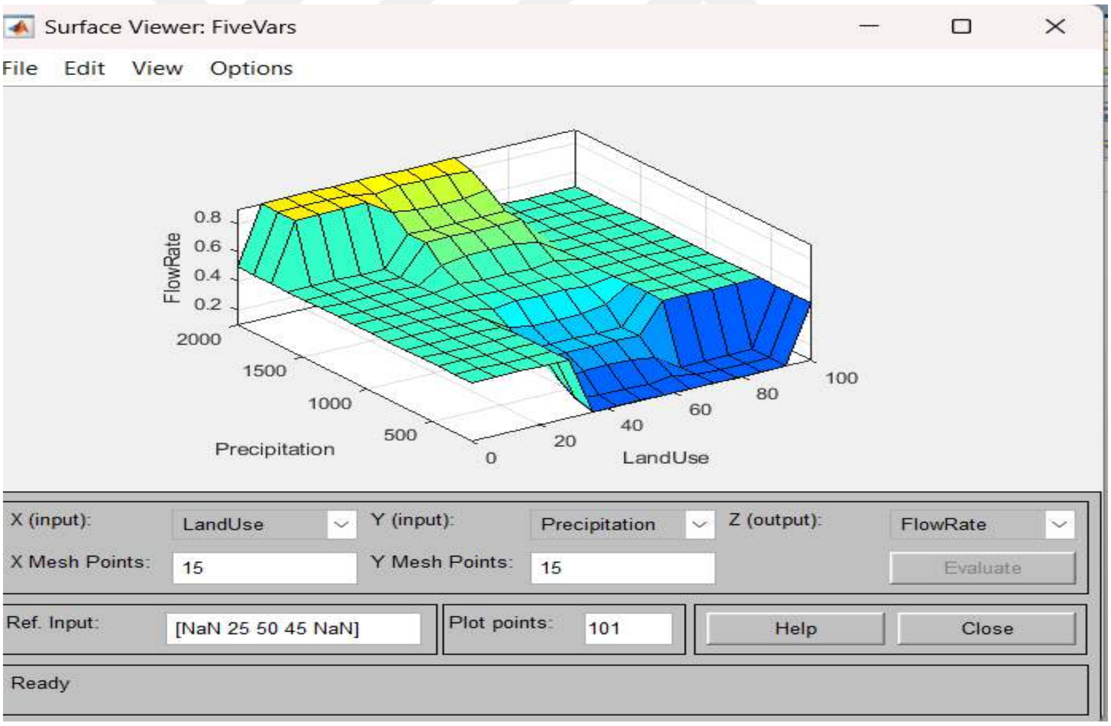

Figure 4.54 Variation of output as a function of inputs (P&LU).

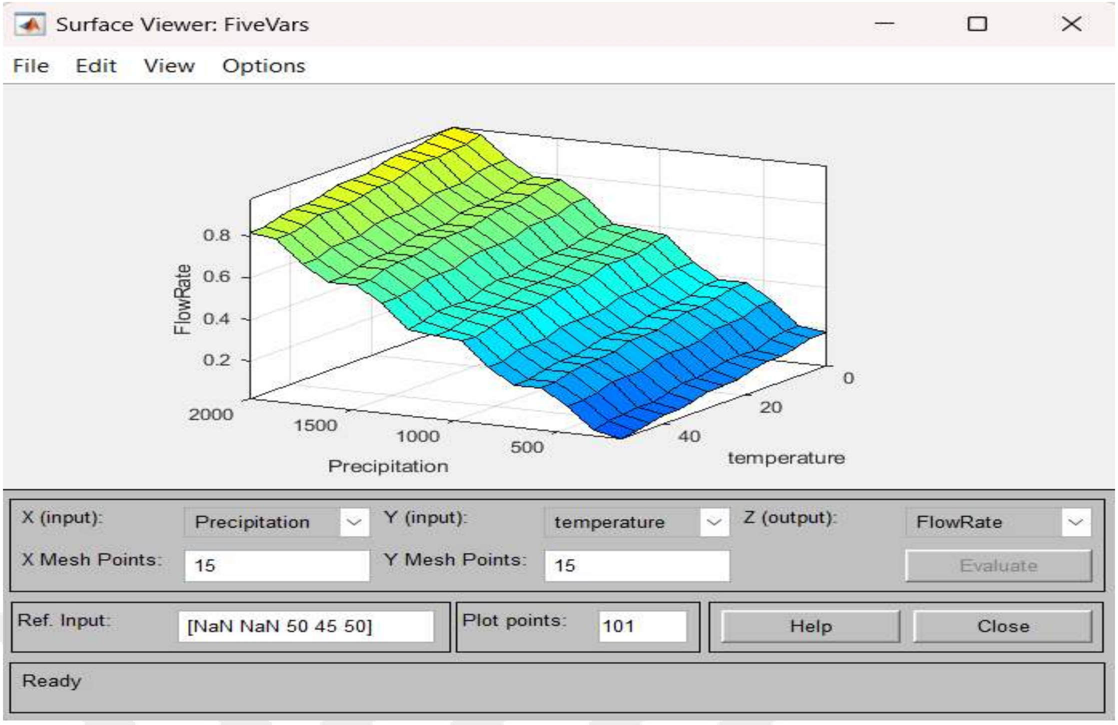

Figure 4.55 Variation of output as a function of inputs (P&T).

The dependence of the flow coefficient value on the input data serves as evidence for the model's mathematical and physical accuracy. The statistical analysis reveals a significant relationship between the output variable and the variables utilized in its creation, demonstrating significance in both directions. A positive correlation has been observed between the flow coefficient and various factors such as precipitation, humidity, slope, and land use. Conversely, an inverse correlation has been identified between the flow coefficient and temperature. The scatter plot exhibits a regression line intersecting the horizontal axis at an approximate angle of 45 degrees. In alternative terms, the model consistently produces predictions that align with the collected data. The high coefficient of determination ($R^2 = 0.966$) indicates a robust statistical relationship between the model and the data, implying that this relationship can be mathematically expressed.

Upon examination of the figures above, it was observed that the forecasted values yielded outcomes that were more proximate to the actual values almost in all combinations. The regression line of the scatter plot intersects the horizontal axis at a 45-degree angle, suggesting that the model produces inconsistent estimates that deviate from the actual data. In other words, the model does not tend to overestimate or underestimate the data, indicating its reliability and accuracy.

The models' statistical criteria were assessed and computed using the approach described in the preceding section. Based on RMSE, MAE, and R^2 parameters, the assessment found that the SMRGT framework produced excellent results. The obtained correlation coefficients for SMRGT-1, SMRGT-2, SMRGT-3, SMRGT-4, and SMRGT-5 were 0.99, 0.98, 0.963, 0.976, and 0.966, respectively.

4.3 Adaptive Neural Fuzzy Inference System Application Results

4.3.1 ANFIS-1:

The ANFIS analysis used Gaussian membership functions 20 x 15 MFs for training and generalized bell membership functions (gbellmf) for testing. The Grid partition section was performed with 100 iterations, assuming a linear output (see Fig 4.56).

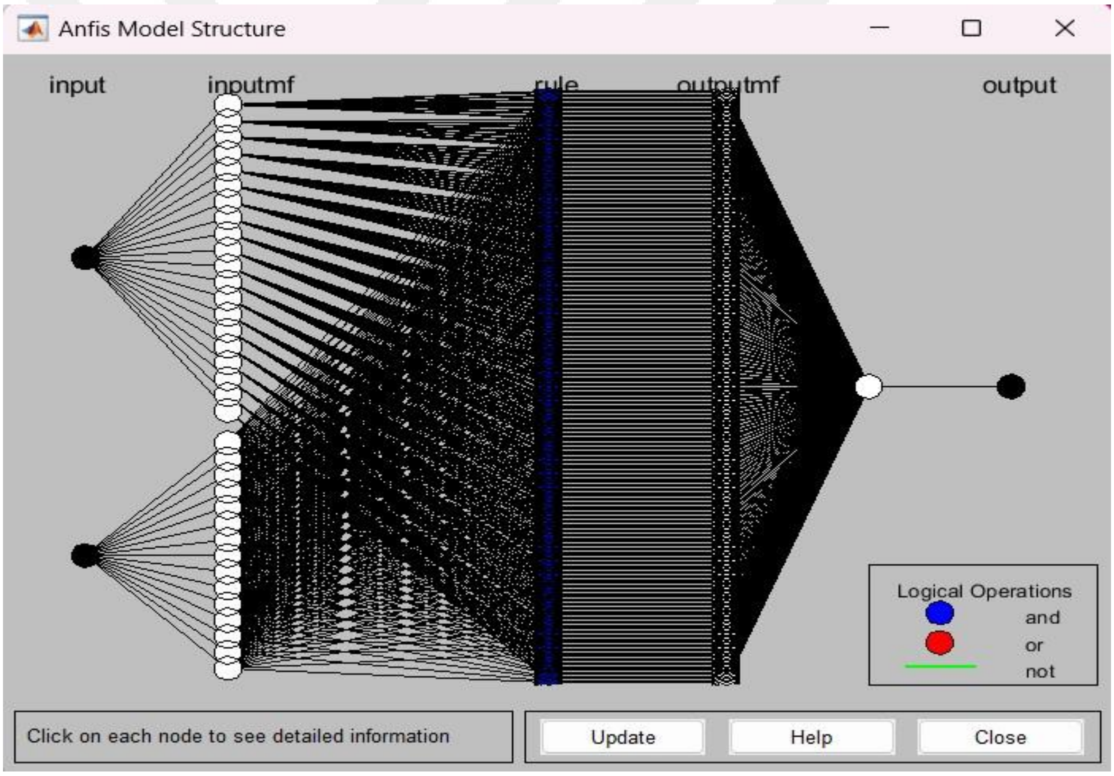

Figure 4.56 Structure of the created ANFIS model.

The dataset was partitioned into two distinct phases, namely the training and testing phases, with a split ratio of 60% for training and 40% for testing. To conduct the training, we selected the monthly average temperature and wind speed data spanning from 2010 to 2016. Subsequently, for the purpose of testing, we utilized data from the years 2017 to 2019. The results of the ANFIS method were visualized using variation and scatter graphs, as depicted in Figures 4.57- 4.62. The coefficient of determination for the training, testing, and all data sets were computed as follows: R^2 = 0.893 for the training data, R^2 = 0.656 for the testing data, and R^2 = 0.803 for the combined data. The researchers noted a moderate correlation. The figures below illustrate that the ANFIS model's results deviated from the actual values to a certain extent.

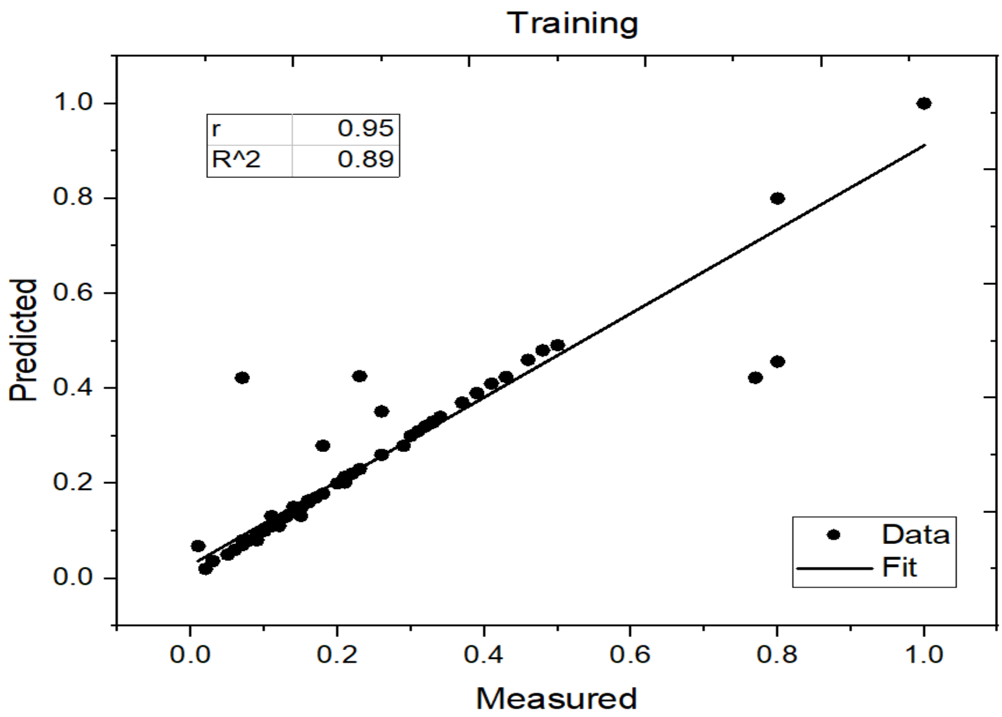

Figure 4.57 The scatter plot of the ANFIS-1 (training) result.

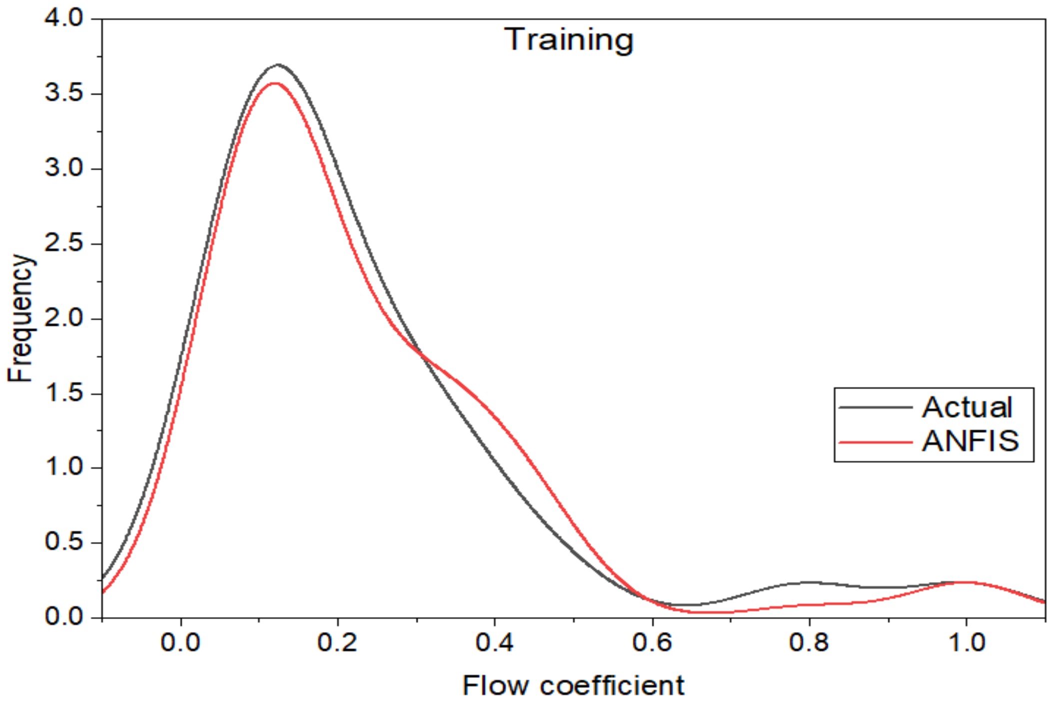

Figure 4.58 Time series graph for the actual and training data.

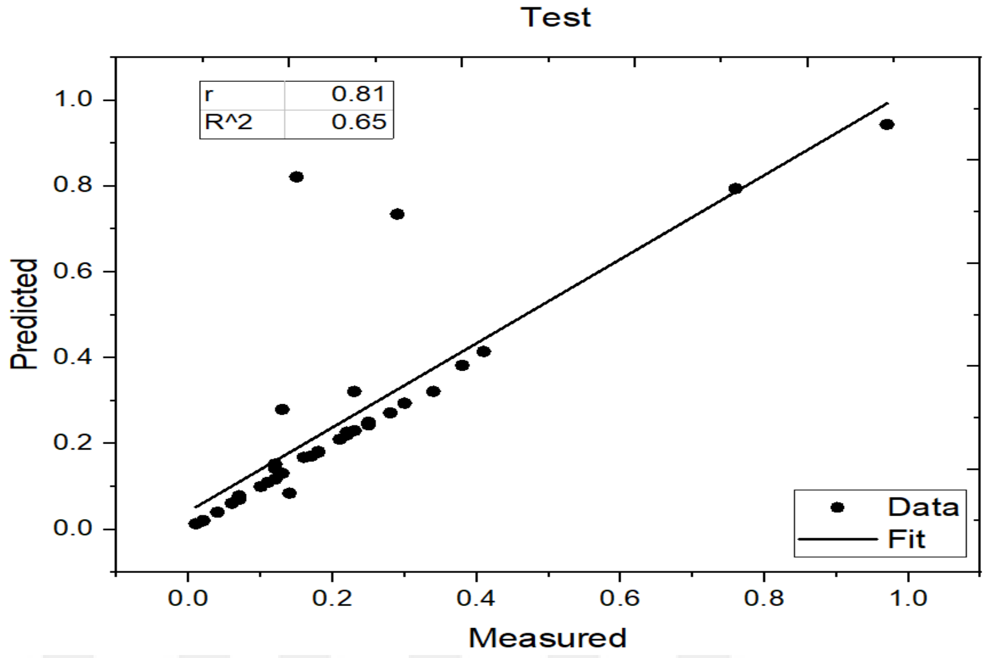

Figure 4.59 The scatter plot of the ANFIS-1 (test) result.

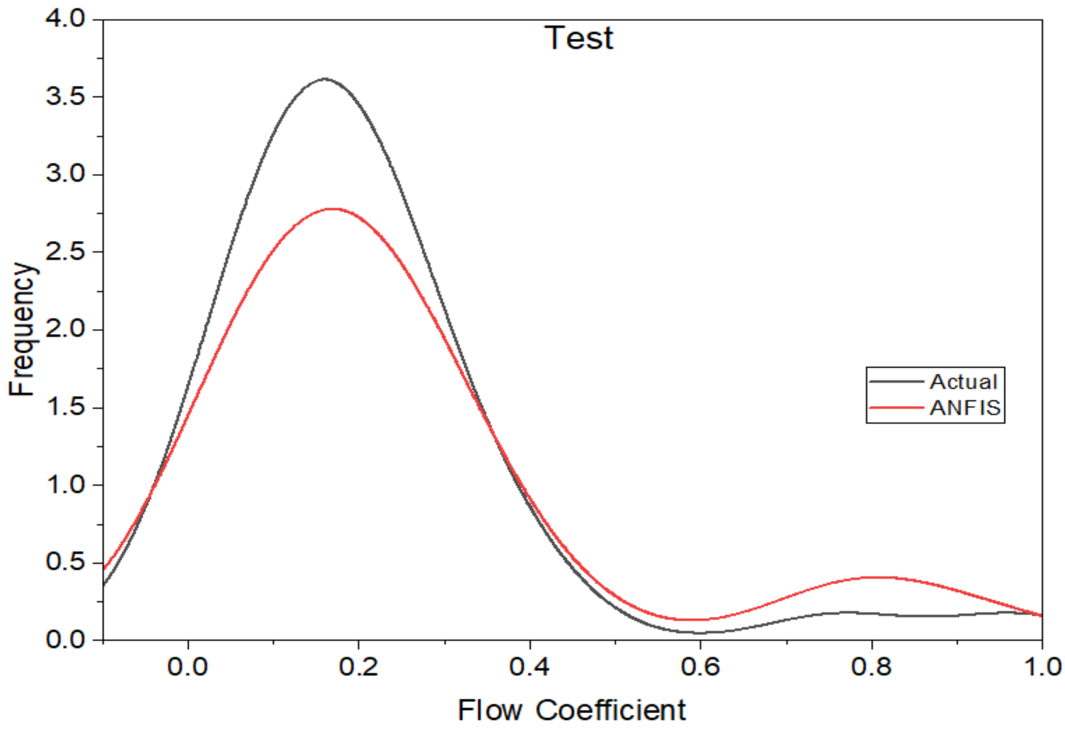

Figure 4.60 Time series graph for the actual and test data.

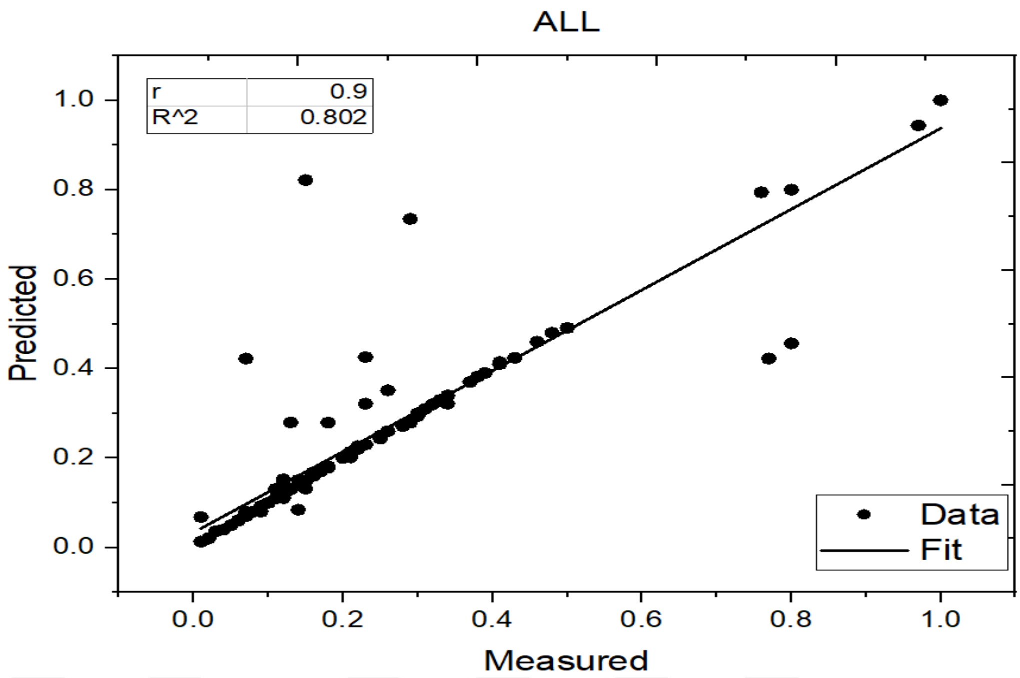

Figure 4.61 The scatter plot of the ANFIS-1 (all) result.

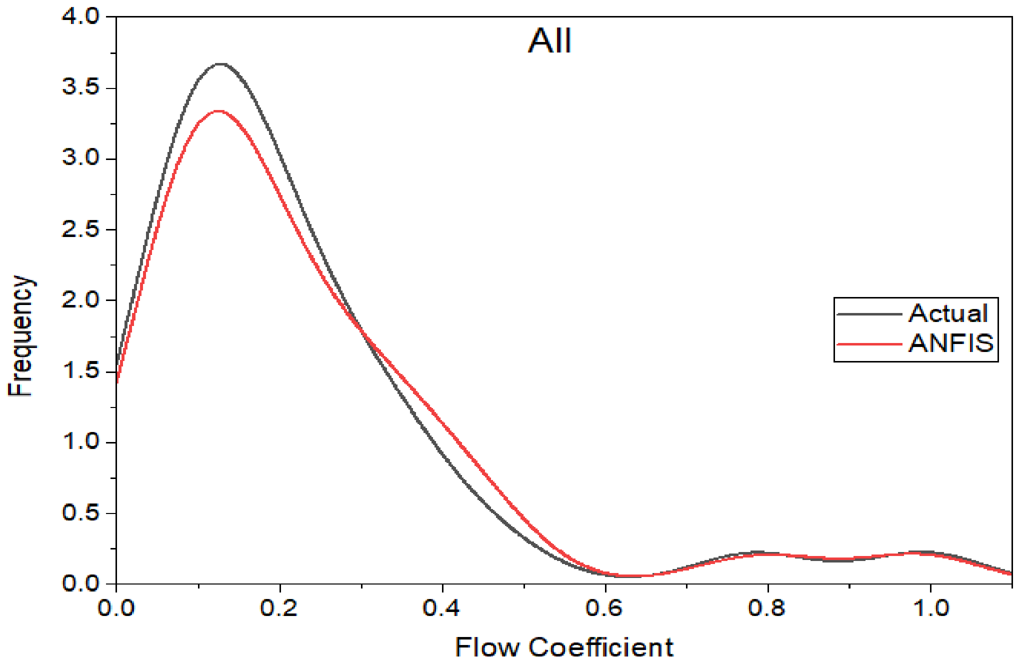

Figure 4.62 Time series graph for the actual and all data.

4.3.2 ANFIS-2

The ANFIS-2 analysis used Gaussian parabolic 5 × 5 × 5 Membership Functions (MFs) for the training and test phase, and the Grid partition section was analyzed with 100 iterations, assuming the output as linear (see Figure 4.63).

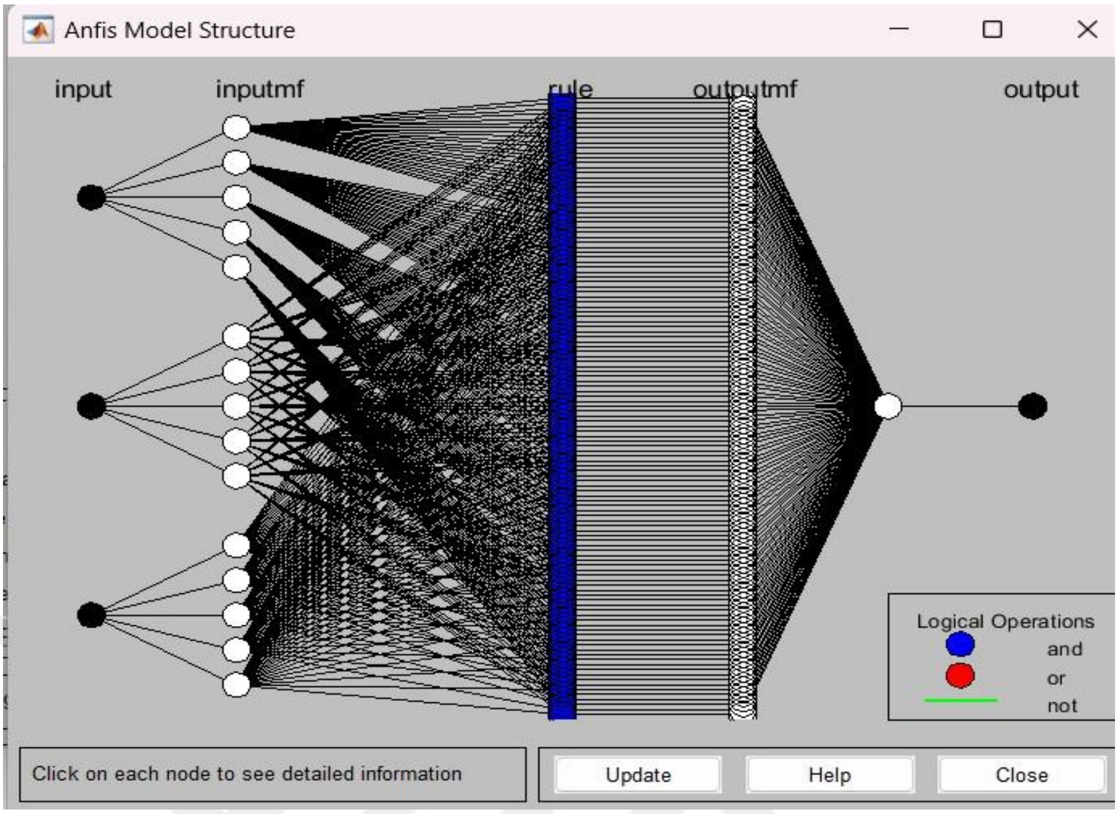

Figure 4.63 ANFIS-2 structure using three inputs and 5 MFs for each input with a type of gaussmf.

The dataset was divided into two distinct phases: the training phase and the testing phase. The split ratio used was 60% for training and 40% for testing. To conduct the training, we chose to use the monthly average precipitation, temperature, and relative humidity data from 2013 to 2017. For testing purposes, we used data from the years 2018 to 2019. The results obtained from the ANFIS method were presented in Figures 4.64 – 4.69 through the use of time series and scatter graphs. The coefficient of determination was computed for the training, testing, and all data sets, resulting in R^2 values of 0.993, 0.54, and 0.86, respectively. There appears to be a moderate correlation between the measured and predicted data. The figures below demonstrate that the results of the ANFIS model deviated to some extent from the actual values.

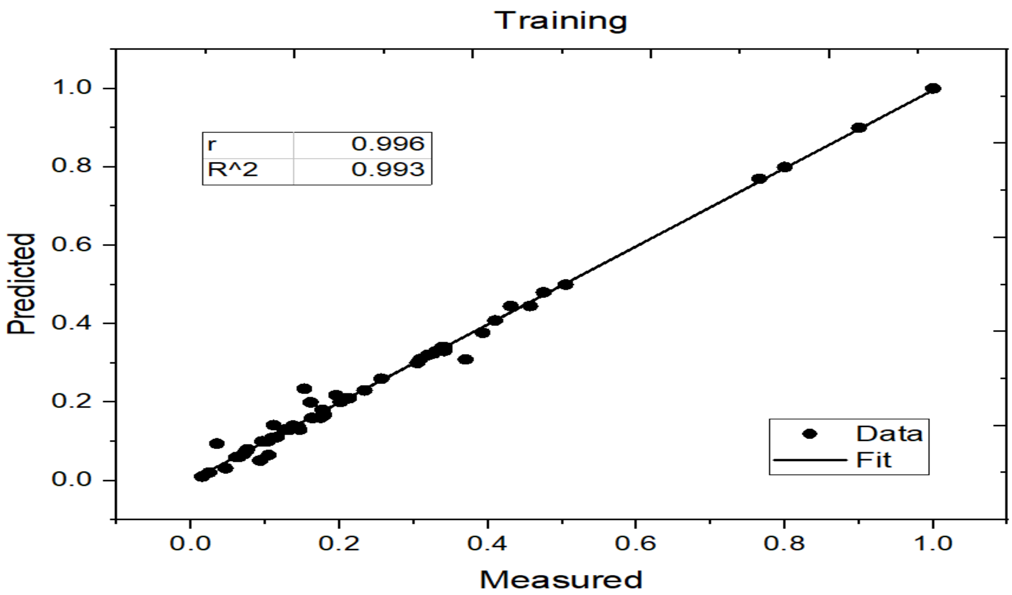

Figure 4.64 The scatter plot of the ANFIS-2 (training) result.

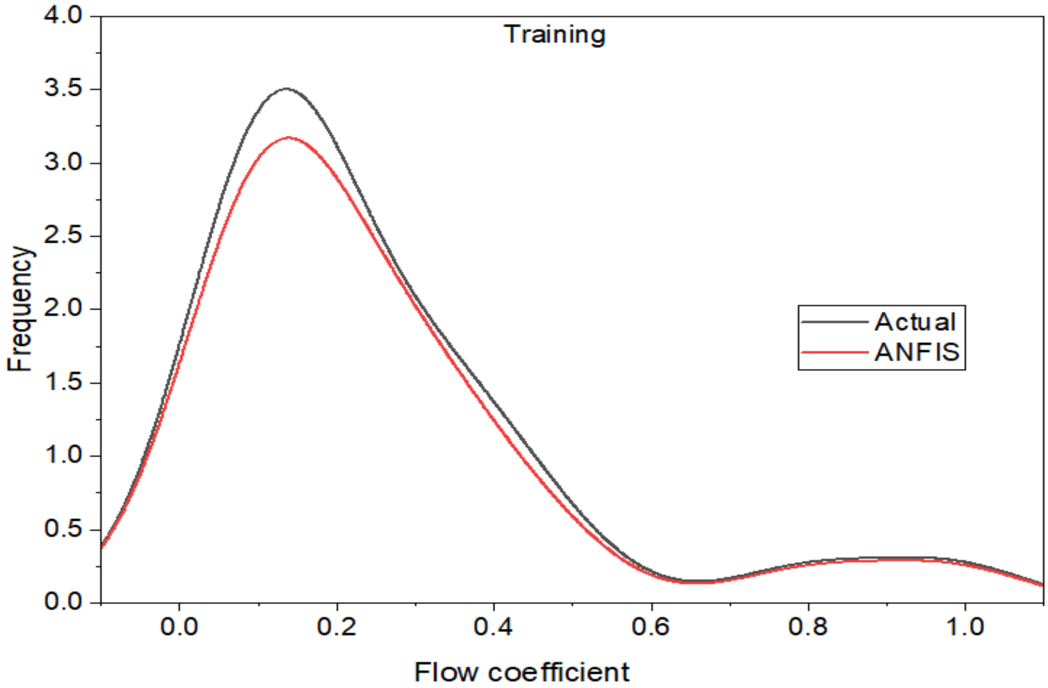

Figure 4.65 Time series graph for the actual and training data.

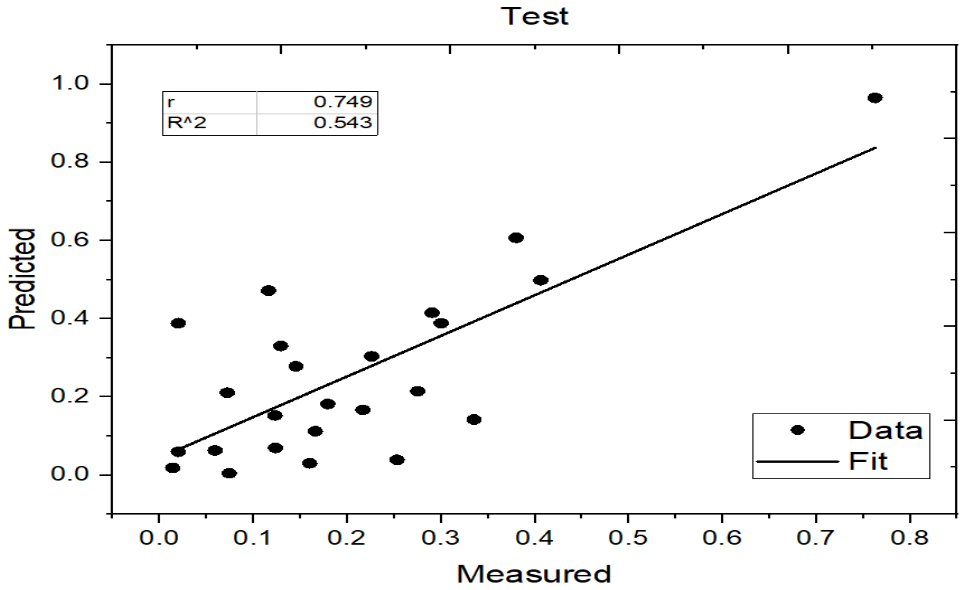

Figure 4.66 The scatter plot of the ANFIS-2 (test) result.

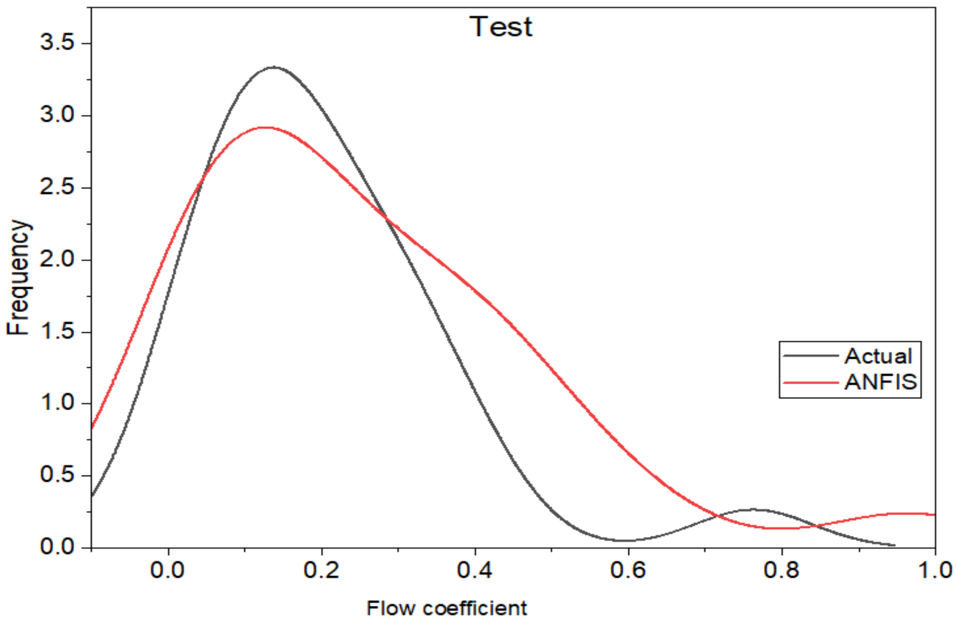

Figure 4.67 Time series graph for the actual and test data.

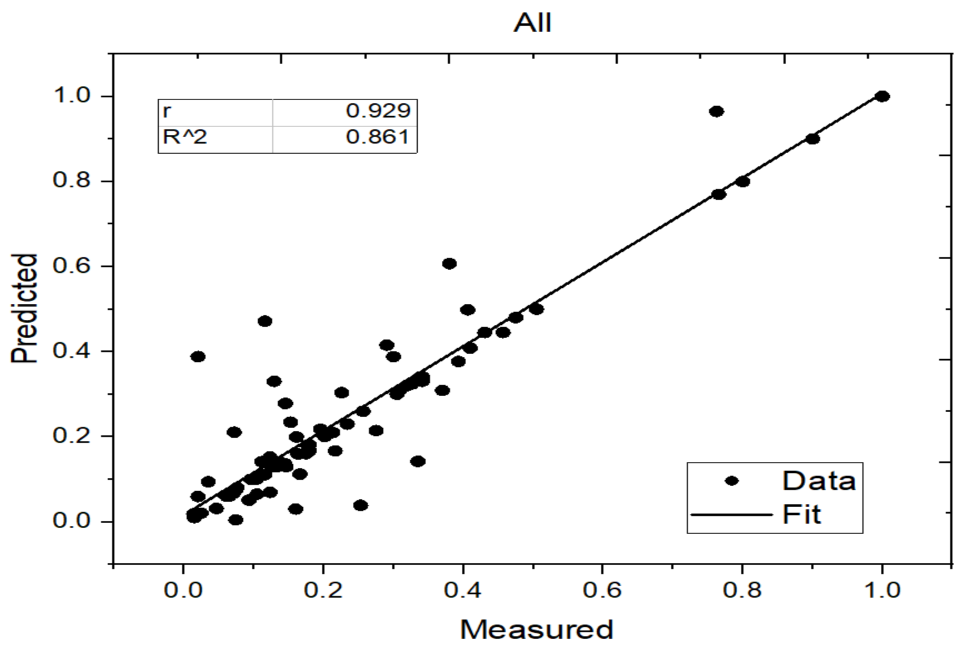

Figure 4.68 The scatter plot of the ANFIS-2 (all) result.

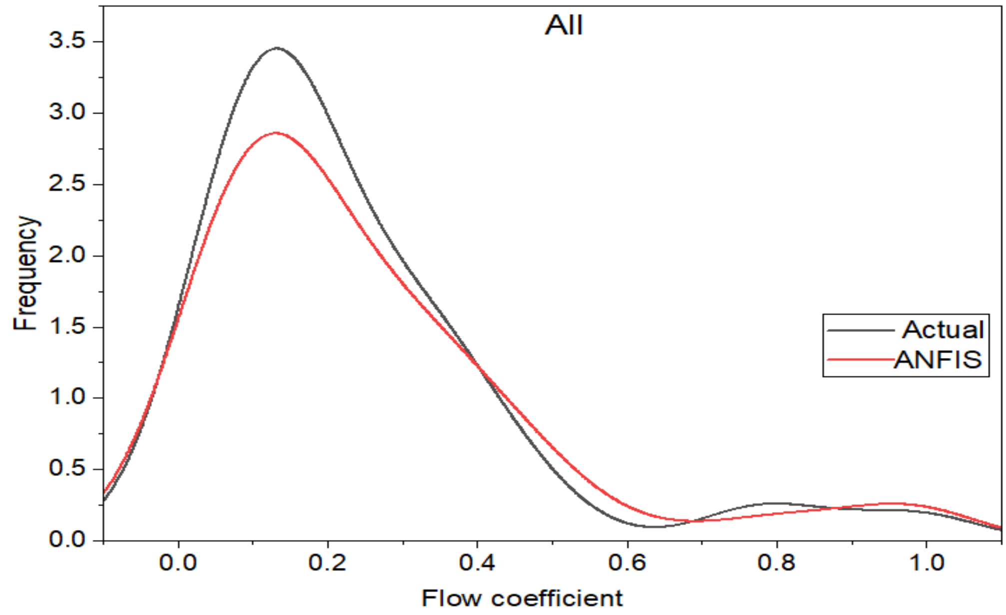

Figure 4.69 Time series graph for the actual and all data.

4.3.3 ANFIS-3

This model incorporated a dataset comprising fifteen years of climate data. The independent variables consisted of data pertaining to precipitation, temperature, wind velocity, and relative humidity. The study of the Adaptive Neuro-Fuzzy Inference System (ANFIS) utilised Gaussian membership functions (gaussmf) with a configuration of 4 x 4 x 4 x 4 for the training phase, as depicted in Figure 4.70. For the testing phase, a π shaped membership function (pimf) was employed. The Grid partition portion was executed with 50 iterations, assuming a linear output. The dataset was partitioned into two distinct phases, namely the training phase and the testing phase, with a distribution ratio of 60% for training and 40% for testing.

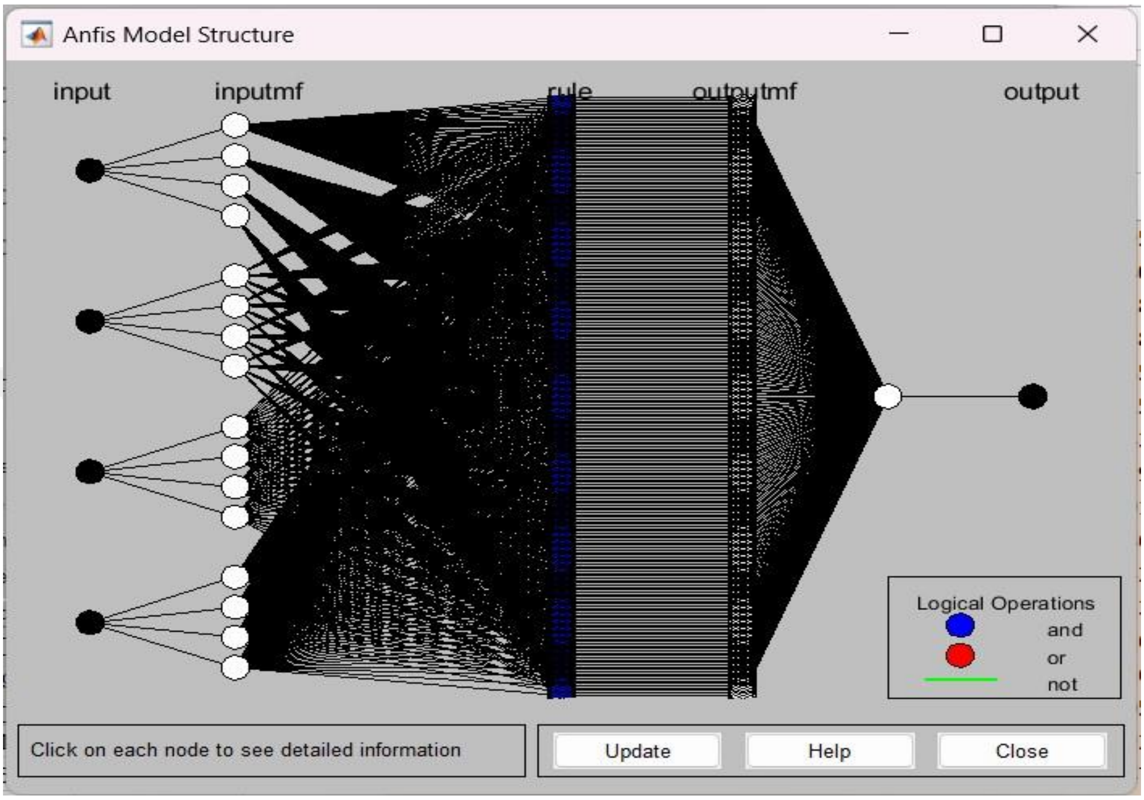

Figure 4.70 Structure of the ANFIS model.

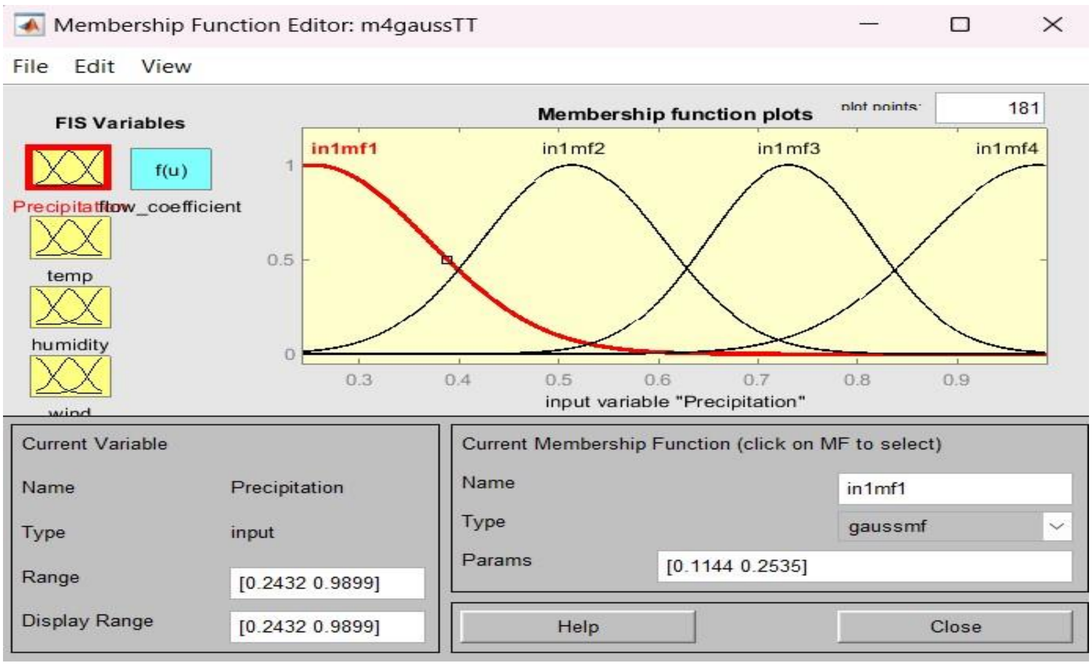

Figure 4.71 Gaussian membership function of the inputs.

The ANFIS outcomes were visualized using scatter and time series graphs, as depicted in Figures 4.72- 4.79. It was noted a strong correlation between the forecasted and observed data. The ANFIS-3 model's outcomes were found to be too closely aligned with the actual values.

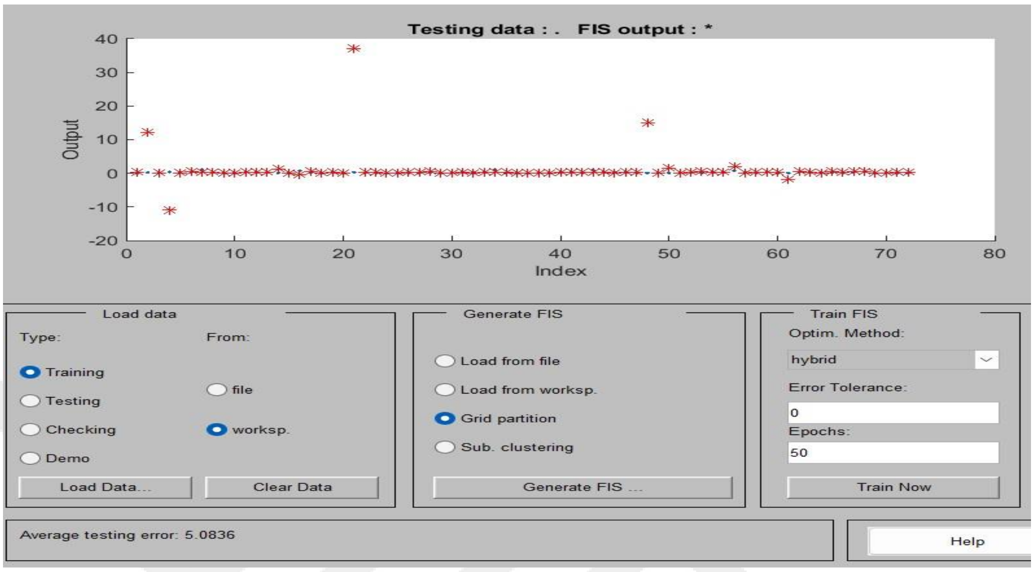

Figure 4.72 View of the testing phase.

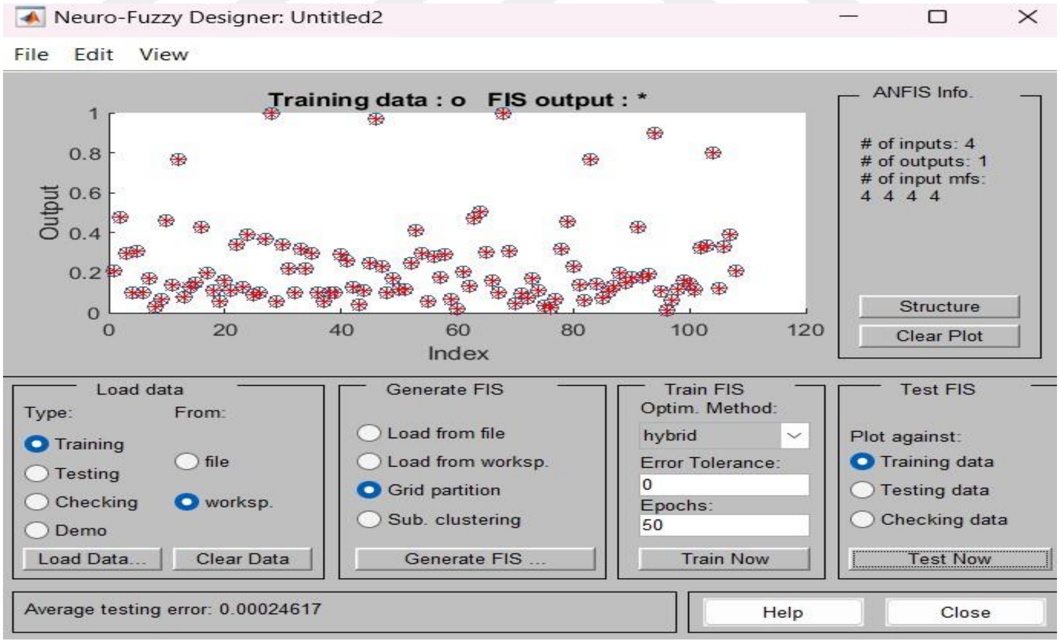

Figure 4.73 View of the training phase.

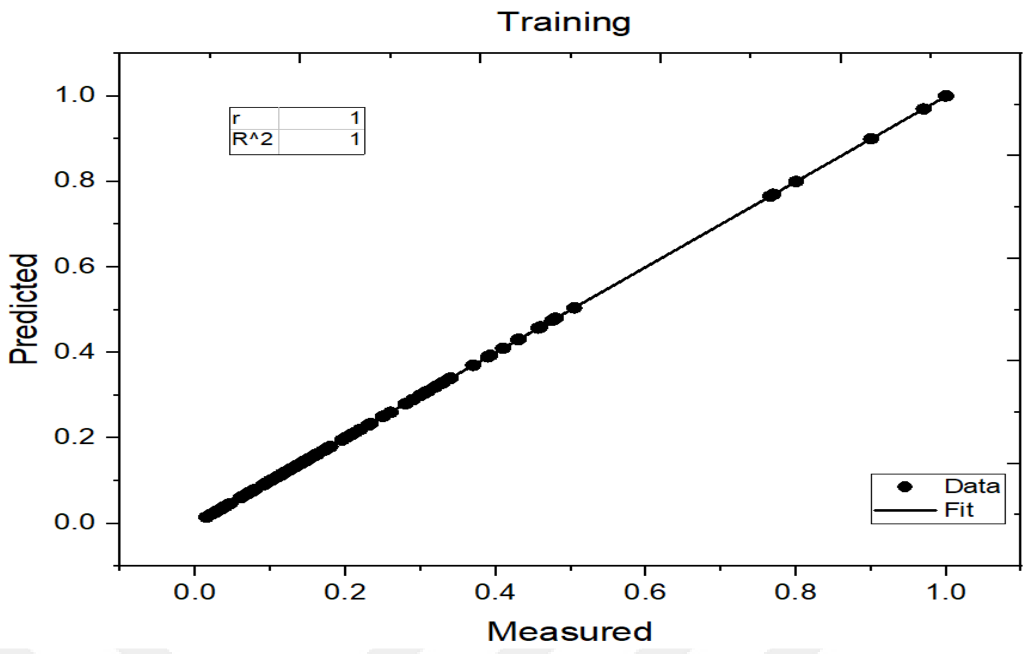

Figure 4.74 The scatter plot of the ANFIS-3 (training) result.

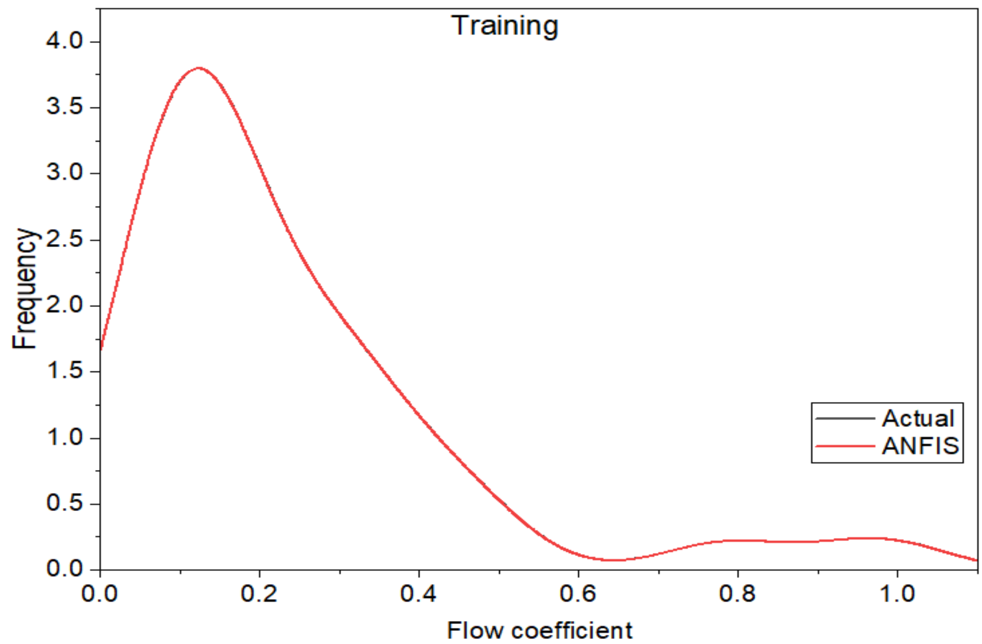

Figure 4.75 Time series graph for the actual and training data.

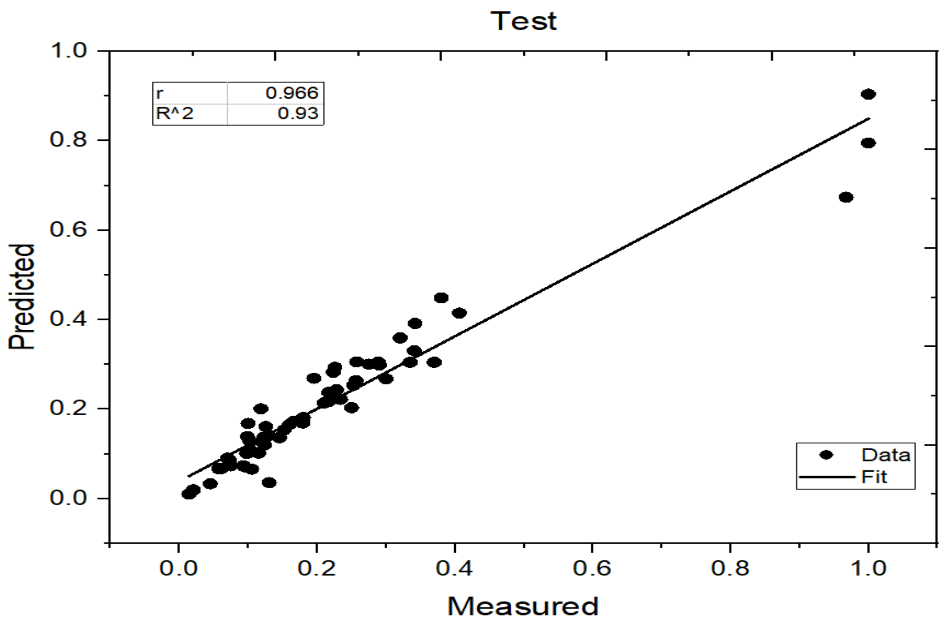

Figure 4.76 The scatter plot of the ANFIS-3 (test) result.

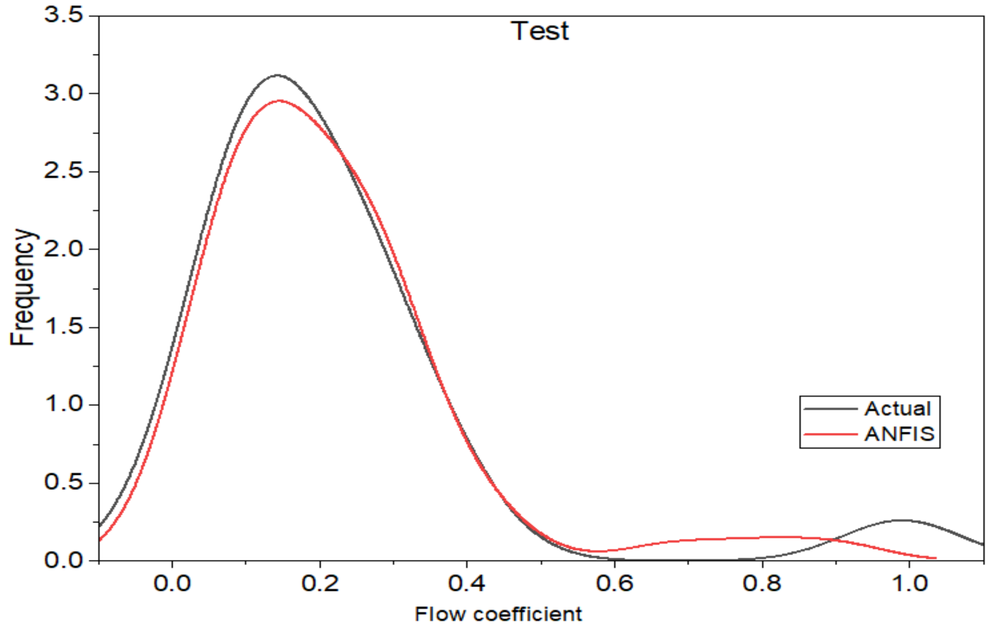

Figure 4.77 Time series graph for the actual and test data.

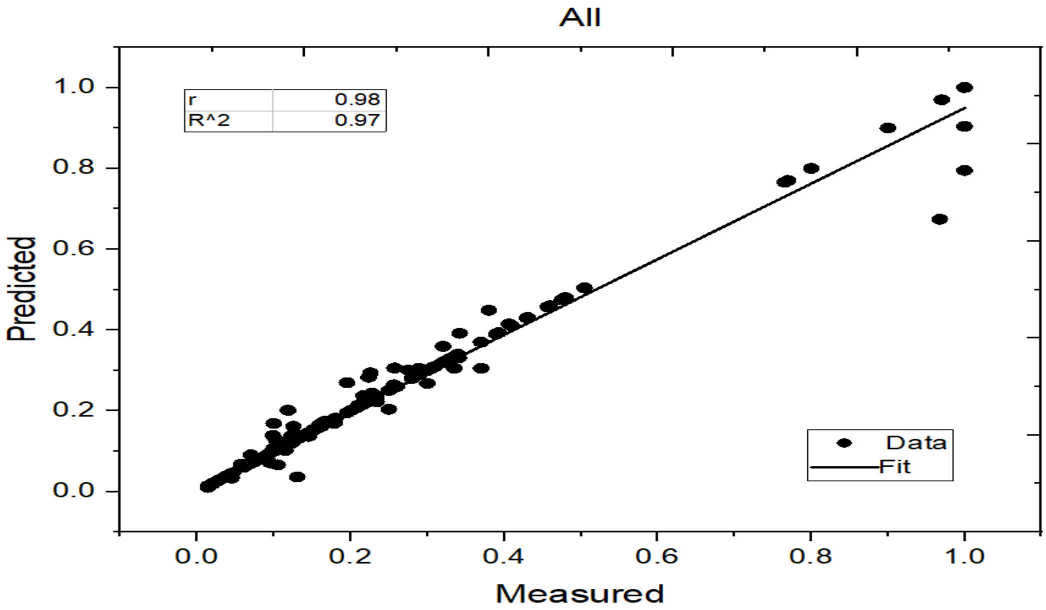

Figure 4.78 The scatter plot of the ANFIS-3 (all) result.

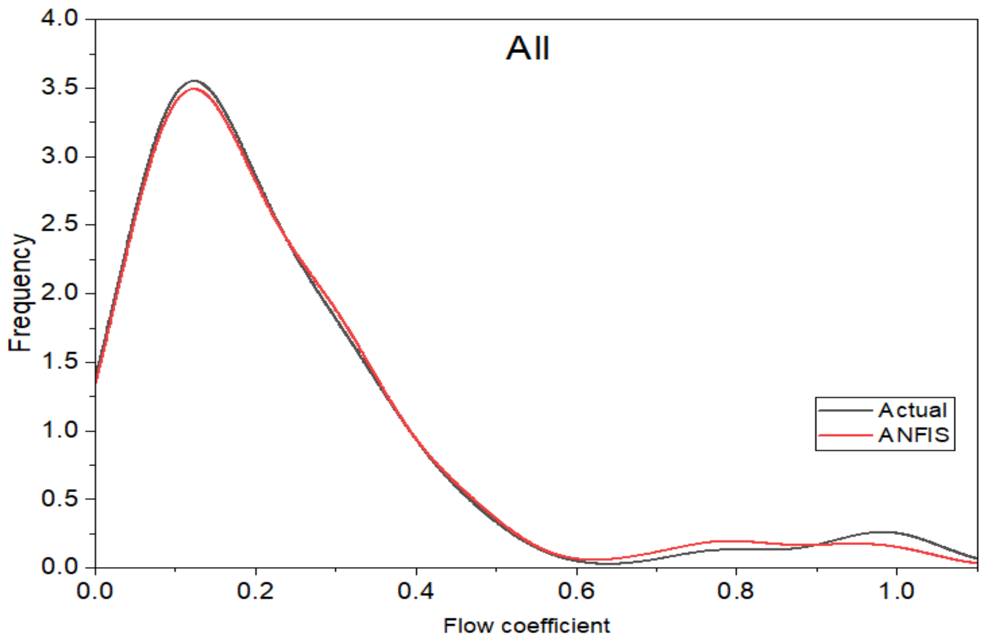

Figure 4.79 Time series graph for the actual and all data.

After analyzing the ANFIS-3 results, it was observed that the input parameters used provided accurate estimates of the flow coefficient in the studied basin with the determination coefficients of (R^2:1, R^2:0.935, and R^2:0.974) for training, testing, and all data, respectively.

The use of ANFIS to estimate the flow coefficient with climatic data has been shown to be reliable, effective, and applicable in similar projects. It is suggested that utilizing easily accessible climatic data to calculate the flow coefficient is a straightforward, practical, and sufficiently precise approach. However, the ANFIS-3 model showed a robust correlation between the actual and anticipated data, as seen in the table below. The statistical parameters for ANFIS-based prediction are given in Table 4.14. ANFIS-1 and ANFIS-2 models exhibit more significant error rates than ANFIS-3 and poorer NSE and R^2 values when the RMSE and MAE criteria are used. The results of the ANFIS-3 model demonstrated that the Adaptive Neural Fuzzy Inference System method could be successfully applied to establish accurate and reliable flow coefficient prediction.

Table 4.14 the ANFIS model's results

Models		**MAE**	**RMSE**	**NSE**	**R^2**
ANFIS-1	Training	1.95	7.11	0.862	0.893
	Test	4.47	1.38	0.55	0.561
	All	2.7	0.96	0.8	0.804
ANFIS-2	Training	1.01	1.92	0.99	0.993
	Test	12.15	15.67	0.56	0.561
	All	4.19	8.53	0.84	0.863
ANFIS-3	Training	0.1	0.2	1	1
	Test	3.1	5.7	0.92	0.935
	All	1.2	3.5	0.97	0.974

The diagrams presented in Figure 4.80 depict the variation of the flow coefficient, a dependent variable, in three dimensions concerning the model's independent variables, namely the amount of precipitation mm, temperature °C, relative humidity %, and wind speed m/s. This variation is depicted in a three-dimensional spatial context.

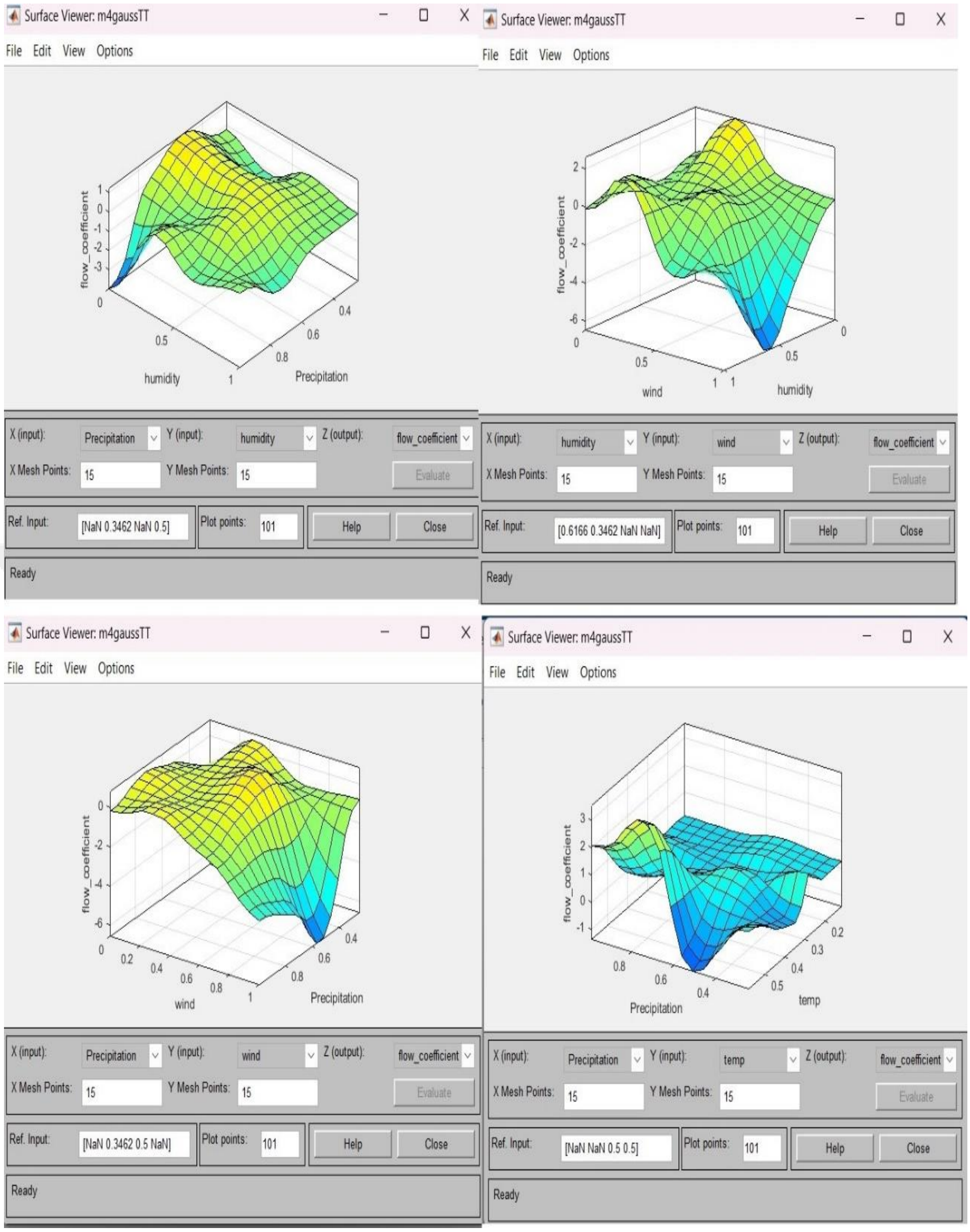

Figure 4.80 Variation **of** output as a function of inputs.

In summary, the ANFIS-3 model seems to have produced the most accurate predictions among the three models, as evidenced by its high R^2 values and the close agreement between the predicted and actual data points in the scatter plots. However, further analysis and validation may be required to understand the model's performance and potential limitations fully. Additionally, it is essential to interpret these results in the context of the specific problem and data at hand.

The inclusion of precipitation, temperature, humidity, and wind variables in the model can enhance the accuracy of predicting the flow coefficient. This is attributed to their physical significance, potential synergistic interactions, and improved depiction of the underlying dynamics of the system. Nevertheless, it is imperative to conduct comprehensive validation and testing of the model's performance to ascertain its superiority in comparison to less complex models that incorporate fewer variables.

4.4 Artificial Neural Network (ANN) Application Results

4.4.1 LMBP-ANN

The study used three different input combinations of neural network models that were assessed to forecast the flow coefficient of the Aksu River basin. Monthly climate data from 15 years (2005-2020) were selected for this study, and three Levenberg-Marquardt back-propagation (LMBP-NN) training algorithm functions in MATLAB were employed to determine the effect of individual parameters on output, following the selection of suitable input combinations. The artificial neural network (ANN) models were constructed utilizing an input layer comprising five neurons representing precipitation, temperature, humidity, and wind speed. A single hidden layer was employed, comprising 20 neurons. The determination of the optimal number of neurons in the hidden layer was achieved through a process of trial and error. The output layer consists of a solitary neuron that functions to forecast the flow coefficient. Three ANN models were conducted using Levenberg-Marquardt back-propagation training algorithms called TRAINLM function in MATLAB. The Levenberg-Marquardt algorithm is a modified iteration scheme of the Gauss-Newton method, as elaborated in references (Hagan & Menhaj, 1994; Reynaldi et al., 2012). The initial model, designated as ANN-1, underwent training utilizing two sets of inputs, namely temperature and wind speed. The subsequent model, ANN-2, was trained to utilize a set of three inputs: precipitation, temperature, and humidity. The third model, denoted as ANN-3 was trained utilizing four inputs: precipitation, temperature, wind speed, and humidity. The artificial neural network (ANN) model underwent training using a dataset of 16 years of meteorological observations. The dataset was partitioned into three subsets, with 70% of the data allocated for the training stage, 15% for the validation stage, and the remaining 15% for the test stage. The Min-Max scaling method standardized the training, test, and validation datasets.

The optimal input combination was selected based on the minimum score of (MAE, RMSE) and maximum score of (R^2, NSE). The study summarized the input parameters for the three models and their performance assessment criteria in Table 4.15. The correlation coefficient (R^2) between the observed and predicted flow coefficient was evaluated for each model, with ANN-1 (comprised of two input parameters) producing values of 0.723, 0.053, 0.098, and 0.515 for training, validation, test, and all data, respectively. For ANN-2 (comprised of three input parameters), the values were 0.837, 0.779, 0.684, and 0.76 for training, validation, test, and all data, respectively. Meanwhile, for ANN-3 (comprised of four input parameters), the values were 0.889, 0.869, 0.803, and 0.876 for training, validation, test, and all data, respectively.

Table 4.15 the results of the ANN model

Model	**Input variables**		**MAE**	**RMSE**	**NSE**	**R^2**
ANN-1	T	Training	10.1	13.6	0.49	0.723
	Ws	Validation	10.9	16.2	0.52	0.053
		Test	12.1	16.1	0.48	0.098
		All	11.3	15	0.47	0.515
ANN-2	T	Training	3.7	5	0.95	0.837
	Rh	Validation	5.5	7.7	0.89	0.779
	P	Test	11.4	15.3	0.34	0.684
		All	5.6	8.6	0.84	0.76
ANN-3	T	Training	2.6	4.4	0.971	0.889
	Rh	Validation	3.1	4.3	0.965	0.869

	P	Test	5.1	3.2	0.91	0.803
	Ws	All	3.1	4.4	0.955	0.876

It is seen that the parameters (precipitation, temperature, humidity, and wind speed) altogether have a significant effect on output (C). The plot of observed and predicted data for ANN-3 showed an excellent similarity (Figures 4.81 – 4.86). Therefore, it is considered the best-input combination for the ANN models and was considered for flow coefficient prediction in the Aksu River basin.

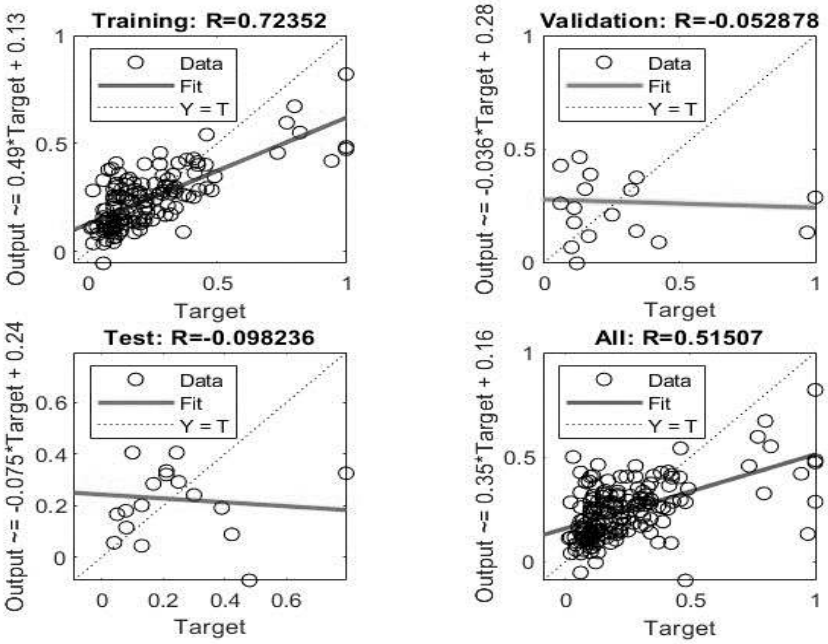

Figure 4.81 Result of ANN-1 model.

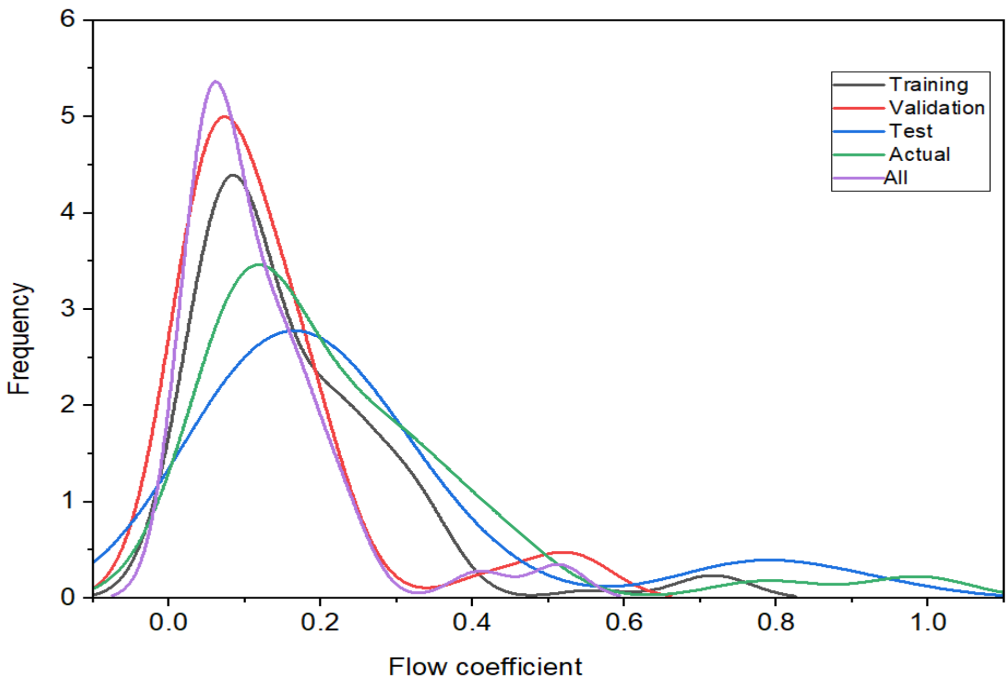

Figure 4.82 Time series graph of the ANN-1 model

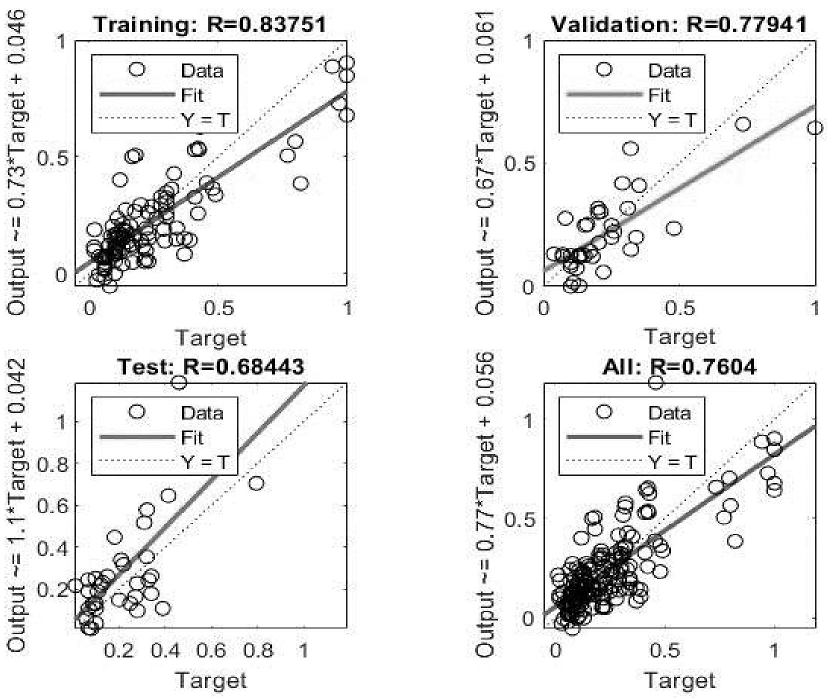

Figure 4.83 Result of ANN-2 model.

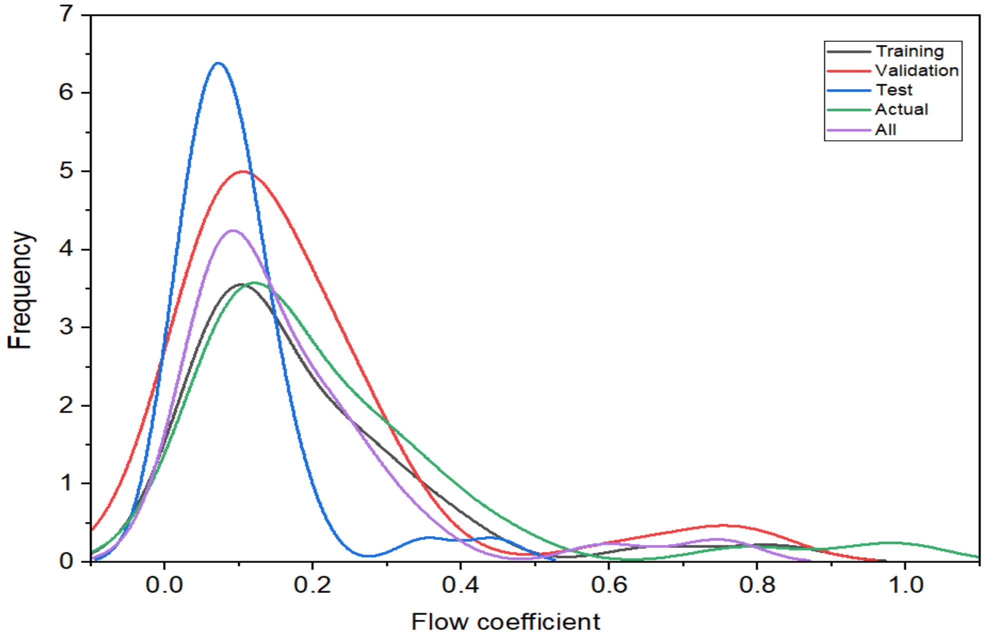

Figure 4.84 Time series graph of the ANN-2 model

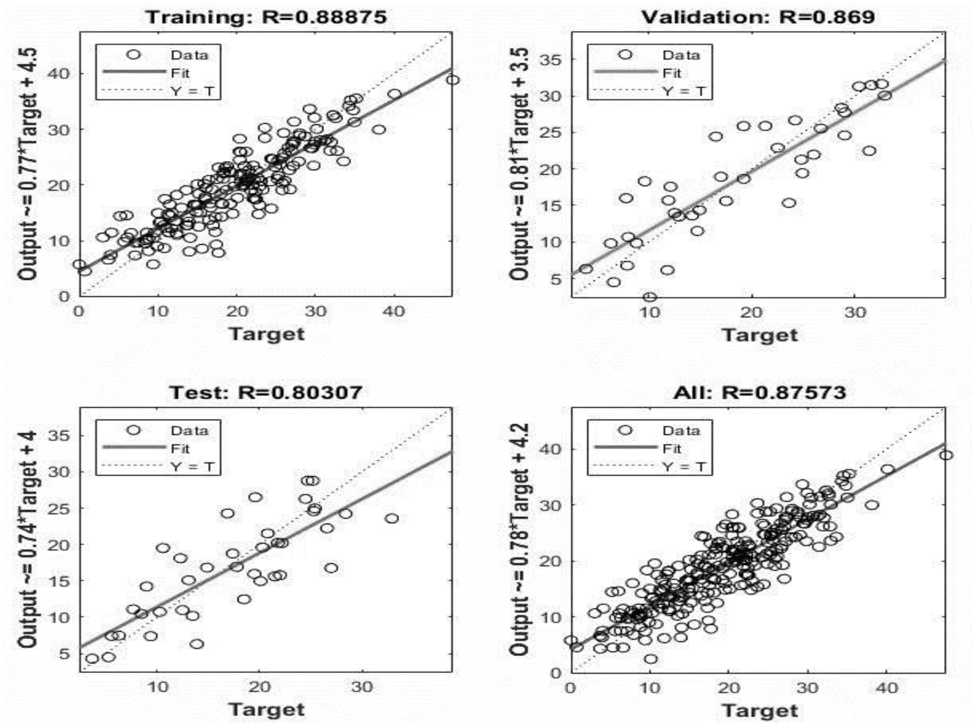

Figure 4.85 Result of ANN-3 model.

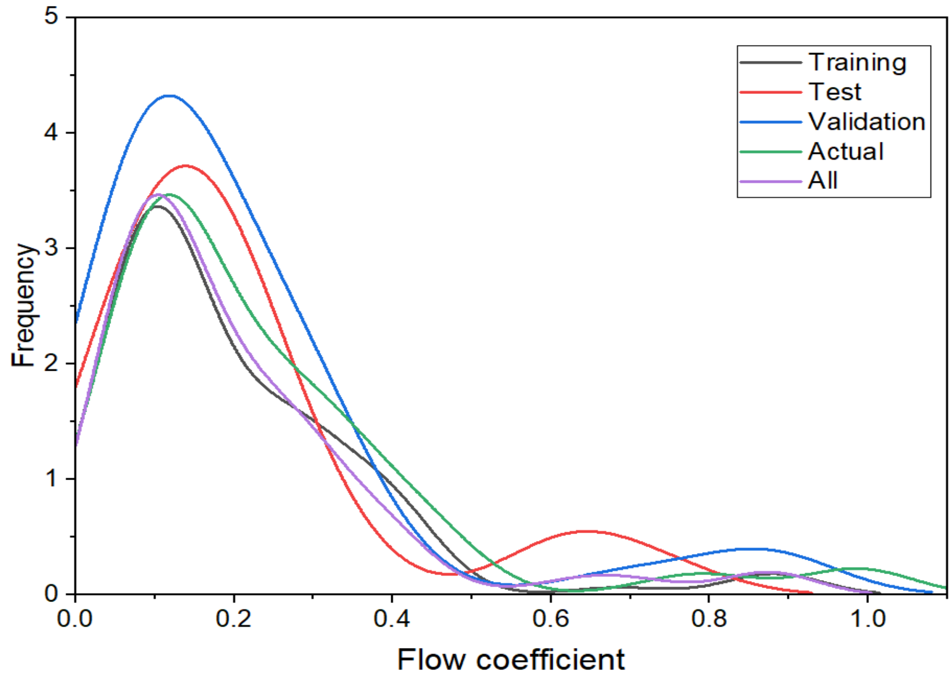

Figure 4.86 Time series graph of the ANN-3 model.

The overall results indicate that the SMRGT model performed better than the other models employed in this investigation. Upon comparison with all other models, it is evident that the SMRGT model exhibited the least error rates in terms of both Root Mean Square Error (RMSE) and Mean Absolute Error (MAE) while also displaying the highest correlation because physics-based models have the advantage of being able to function effectively with lesser quantities of data in comparison to solely data-driven approaches. This is due to their utilization of fundamental physical principles to formulate predictions and compensate for potential data sparsity. Through the integration of physical laws, these models possess the capability to extrapolate and interpolate the system's behavior, thereby mitigating the necessity for copious amounts of training data. Furthermore, it pertains to their robustness, which refers to their capacity to perform effectively in the face of noise, uncertainties, or perturbations. The SMRGT approach provides a notable level of interpretability due to its reliance on precisely defined fuzzy rules and expert knowledge.

Moreover, it is very clear from the ANN and ANFIS model result that neural network models are getting significantly more accurate as the number of input to the model increases. A low correlation coefficient indicates a weak linear relationship between the inputs and the target variable (Hahs-Vaughn, 2022). In this case, the inputs may not contain enough information or exhibit a strong enough pattern to predict the target variable accurately. The model's inability to capture this weak relationship can lead to high prediction errors. Moreover, neural networks are capable of learning complex patterns and relationships in data. However, with only two inputs, the model may struggle to represent and learn the underlying structure of the data accurately. The limited complexity of the model can result in high errors as it fails to capture the non-linear relationships or dependencies between the inputs and the target variable (Hahs-Vaughn, 2022).

4.5 Sensitivity analysis

Sensitivity analysis is essential to modeling and analysis in any field, including river basin management. In implementing fuzzy SMRTG, ANN, and ANFIS approaches for flow coefficient estimation in the Antalya river basin, sensitivity analysis help identify the most critical input parameters in the models and their impact on the model outputs (Li & Chen, 2020). In implementing fuzzy SMRTG, ANN, and ANFIS approaches for flow coefficient estimation in the Antalya river basin, sensitivity analysis help identify the most critical input parameters in the models and their impact on the accuracy of the coefficient estimation. The sensitivity analysis identifies which input parameters, such as precipitation, temperature, or land use, have the most significant impact on the flow coefficient estimation (Demirel et al., 2018). This information is used to refine the models and improve their accuracy by focusing on the most critical input parameters (Hajdu, 2019).

The sensitivity analysis using the OAT method applied to the ANN-1 model, ANFIS, and SMRGT for flow coefficient estimation, a crucial hydrological procedure for flood prediction, water resource management, and flood mitigation (Hajdu, 2019). The OAT method involves varying one input variable at a time while keeping the other inputs constant and evaluating the model's output for each set of input values (Li & Chen, 2020). Repeating this process for each input variable determines the model's sensitivity to changes in each input variable (Demirel et al., 2018).

The SMRGT model shows the critical input values (Rainfall: 0 mm to 500 mm based on the average annual rainfall in Antalya, Temperature: -10°C to 40°C based on the range of temperatures observed in Antalya throughout the year, Topography: 0 to 2000 meters based on the elevation range in the Antalya region, Land cover: 0% to

100% based on the percentage of each land cover type in the study area, such as forest, agriculture, urban, etc.) In addition, statistical parameters for each of the five models (SMRGT-1 to SMRGT-5). Using the OAT method, we vary each input variable while holding the others constant to determine the model's sensitivity to changes in that variable. To determine the sensitivity of the SMRGT model to changes in individual input variables using the OAT (One-At-A-Time) method, to investigate the sensitivity of the SMRGT-1 model to changes in temperature (T), fix the values of all other input variables (Ws), and vary T over a range of values (0°C to 50°C). They could then evaluate the model's output (e.g., flow coefficient) for each set of input values. By repeating this process for each input variable (K1 to K7), we determine the sensitivity of the SMRGT model to changes in each input variable.

Similarly, Tables 4.15 and 4.16 show the statistical parameters and critical input variables for the ANFIS and ANN models. The OAT method is used to evaluate the sensitivity of these models to changes in individual input variables, providing valuable insights into which variables have the most significant impact on the models' output. To determine the sensitivity of the ANFIS and ANN models to changes in individual input variables using the OAT method, to investigate the sensitivity of the ANN-1 model to changes in temperature (T), fix the values of all other input variables (Ws), and vary T over a range of values (e.g., 0°C to 50°C). Then evaluate the model's output (e.g., flow coefficient) for each set of input values. By repeating this process for each input variable, determine the sensitivity of the ANN and ANFIS models to changes in each input variable. This information is used to identify the most critical variables that significantly impact the model's output. This help to optimize the models and improve their accuracy in flow coefficient estimation, which has significant implications for flood prediction, water resource management, and flood mitigation.

To analyze the ANFIS and ANN model results to ascertain the model's sensitivity to changes in each input variable using the OAT method, using Table 4.15, investigate the sensitivity of the ANFIS-1 model to changes in wind speed (Ws) by fixing the values of all other input variables (T) and varying Ws over a range of values (e.g., 0 m/s to 10 m/s). Then evaluate the model's output (e.g., flow coefficient) for each set of input values.

By repeating this process for each input variable (K1 to K7), we determine the sensitivity of the SMRGT model to changes in each input variable. This information can be used to optimize the model's performance and improve its accuracy in flow coefficient estimation. Similarly, Tables 4.15 and 4.16 show the statistical parameters and critical input variables for the ANFIS and ANN models. The OAT method can be used to evaluate the sensitivity of these models to changes in individual input variables, providing valuable insights into which variables have the most significant impact on the models' output. To determine the sensitivity of the ANFIS and ANN models to changes in individual input variables using the OAT method and to investigate the sensitivity of the ANN-1 model to changes in temperature (T), hydrologists could fix the values of all other input variables (Ws), and vary T over a range of values (e.g., 0°C to 50°C). They could then evaluate the model's output (e.g., flow coefficient) for each set of input values.

The OAT method was employed to determine the sensitivity of the ANFIS and ANN models to changes in each input variable. By varying each input variable while keeping the others constant, the sensitivity of the models to changes in each variable was determined. This information can be used to identify the most critical variables that significantly impact the model's output, which can help optimize the models and improve their accuracy in flow coefficient estimation. To analyze the ANFIS and ANN model results using the OAT method, following similar steps. Using Table 4.15, the sensitivity of the ANFIS-1 model to changes in wind speed (Ws) can be investigated. They are fixing the values of all other input variables, such as temperature (T) and varying Ws over a range of values. Then, the model's output, such as the flow coefficient, can be evaluated for each set of input values by repeating this process for each input variable, determining the sensitivity of the ANFIS and ANN models to changes in each input variable.

Using the One-At-A-Time (OAT) method, we varied each input parameter while holding the others constant to determine the sensitivity of the models to changes in that parameter. For the SMRGT model, we used Tables to identify the critical input values and statistical parameters for each of the five models (SMRGT-1 to SMRGT-5). We varied each input parameter (K1 to K7) to determine the model's sensitivity to changes in each parameter. Similarly, we used all tables above to determine the critical input parameters for the ANFIS and ANN models. We conducted sensitivity analyses using the OAT method to identify each model's most significant input parameters. The sensitivity analysis results showed that changes in temperature, precipitation, and wind speed were the most significant input parameters in the models, with temperature having the most significant impact on the ANFIS-1 model's output and precipitation having the most significant impact on the ANN-2 model's output. These findings suggest that accurate measurements or estimates of temperature, precipitation, and wind speed are crucial for improving the accuracy of the models in flow coefficient estimation. Improving the accuracy of these input parameters can optimize the models and improve their performance in flood prediction, water resource management, and flood mitigation.

CHAPTER V

CONCLUSION AND RECOMMENDATIONS

5.1 Conclusion

The present study examines the feasibility and efficacy of neural networks and fuzzy logic methodologies to develop dependable models of flow coefficients. Monthly data sets from the Aksu River basin in Antalya, Turkey, were utilized for this investigation. The study's findings indicate that the SMRGT model exhibited superior performance based on the statistical parameters and correlation coefficients in the context of nonlinear modeling. Moreover, it was observed that the ANFIS-3 model exhibited superior performance in comparison to the artificial neural network (ANN) models.

The best input performance metrics model was found by applying a minimum score of (MAE, RMSE) and a maximum score of (R^2, NSE). The ANN-3 model has the best statistical performance. This model has the lowest Mean Absolute Error (MAE) and Root Mean Squared Error (RMSE) values among the three models, indicating that it has the most negligible average difference between observed and predicted values. In addition, the ANN-3 model has the highest Nash-Sutcliffe Efficiency (NSE) and correlation coefficient (R^2) values, suggesting that it best fits the data. The ANN-3 model uses a combination of four input variables (T, Rh, P, and Ws), which provides a more comprehensive representation of the factors affecting flow than the other models with fewer input variables. The superior performance of the ANN-3 model may also be due to the use of the Levenberg-Marquardt back-propagation (LMBP-NN) training algorithm, which is known for its ability to quickly converge to a solution and avoid getting stuck in local minima.

The ANFIS-3 model based on performance metrics has the best statistical performance. This model has the lowest Mean Absolute Error (MAE) and Root

Mean Squared Error (RMSE) values among the three models, indicating that it has the most negligible average difference between observed and predicted values.

In addition, the ANFIS-3 model has the highest Nash-Sutcliffe Efficiency (NSE) and correlation coefficient (R^2) values for both the training and test datasets, suggesting that it has the best overall fit to the data, with the lowest MAE and RMSE values for both the training and test datasets, Suggesting that it has the best overall fit to the data. The ANFIS-3 model combines four input variables, which provides a comprehensive representation of the factors affecting flow.

Based on the provided performance metrics in Table 2, ANFIS-2 has the worst results among the three ANFIS models. This model has the giant MAE and RMSE values for both the training and test datasets, indicating that it has the most considerable average difference between observed and predicted values. Additionally, ANFIS-2 has relatively low NSE and R^2 values for both the training and test datasets, suggesting that it may not have a good overall fit for the data.

ANFIS-1 also performs relatively poorly on the test dataset, with larger MAE and RMSE values than ANFIS-3. However, ANFIS-1 has a lower NSE and R^2 value for the training dataset than ANFIS-3.

Based on the performance metrics, SMRGT-1 has the best statistical parameters among the five models. This model has the most petite MAE and RMSE values, indicating the most negligible average difference between observed and predicted values. Additionally, SMRGT-2 has a relatively high R^2 value, suggesting an excellent overall fit to the data. The MAPE value for SMRGT-1 is also relatively low compared to the other models.

SMRGT-4 also has relatively good statistical parameters, with low MAE and RMSE values and high R^2 values. However, SMRGT-4 has a relatively high MAPE value, indicating that the model may not be as accurate in predicting flow coefficient values for certain input variables.

SMRGT-3 and SMRGT-5 have the worst results among the five models. These models have giant MAE and RMSE values, indicating the highest average difference between observed and predicted values. Additionally, SMRGT-3 and SMRGT-5 have a relatively low R^2 value, suggesting they may not have a good overall fit to the data. The MAPE value for SMRGT-3 and SMRGT-5 is also relatively high compared to the other models.

Fuzzy logic theory can potentially evaluate traditional systems with relatively moderate levels of complexity and no significant uncertainties or problems. The ANFIS and SMRGT fuzzy approaches have been widely used in various hydrological applications. The ANFIS approach is based on adaptable neural networks and fuzzy inference systems, which can effectively manage complex and nonlinear data connections. The SMRGT approach, on the other hand, employs simple membership functions and fuzzy rules to recognize ambiguous and imprecise information features. The choice of a method is determined by the specific characteristics of the river basin and the data available, as each method has advantages and limitations. Both approaches have shown promising results in accurately estimating the flow coefficient. SMRGT's results, on the other hand, outperformed ANFIS. The scatter plot, high coefficient of determination, and low MAE and RMSE values demonstrate the SMRGT model's neutrality and linearity. These findings suggest that the model is reliable, exact, and appropriate for flow coefficient calculations, a critical parameter in hydrological modeling and water resource management, and that further research is required.

The study's findings suggest that the SMRGT methodology is based on physical principles. This conclusion is based on the results obtained from the SMRGT-1 model. The analysis of meteorological data indicates that temperature and wind are the parameters that impact the flow coefficient value in the study region. Integrating temperature and wind speed data into the SMRGT method was the most favorable outcome. The researchers are provided with a simplified form of occurrences characterized by natural ambiguity.

5.2 Recommendations

The present investigation centered on the use of neural networks and fuzzy logic methodologies to construct reliable models of flow coefficients. This study has provided insights into the possibilities of these techniques in hydrological applications. Drawing upon the discoveries and knowledge acquired via this investigation, there exist numerous prospective routes for forthcoming study endeavors that can augment our comprehension and use of AI-based models in the domain of flow coefficient modeling.

1. This study may include datasets obtained from different geographical regions and hydrological contexts. Additionally, this study aims to assess the ability of artificial intelligence (AI) models, specifically the SMRGT and ANFIS methodologies, to exhibit generalizability across various basins, climatic conditions, and land utilization patterns.
2. The integration of various artificial intelligence (AI) models, such as neural networks and fuzzy logic, into ensemble frameworks. Ensemble models can enhance forecast accuracy by incorporating a broader range of data patterns and uncertainties.
3. Analyze the performance of AI models, especially the SMRGT model, across various temporal scales, such as daily and seasonal, as well as different spatial scales, including sub-basins. Moreover, an investigation may conduct to determine if the models maintain their accuracy when applied to different levels of resolution, whether finer or coarser.
4. Real-time predictive model development could utilize AI algorithms for short-term flow coefficient forecasting. This can be valuable for flood forecasting, emergency response, and water management during extreme weather events.
5. Incorporation of uncertainty quantification techniques to assess the reliability of AI-based predictions. This can involve sensitivity analysis, Monte Carlo simulations, and probabilistic modeling to account for input parameter variability.
6. More comparative studies may be done that evaluate the performance of AI models against other advanced modeling techniques, such as physics-based models or hybrid approaches that combine data-driven and process-based methods.

The present investigation has yielded significant findings regarding the viability and effectiveness of artificial intelligence approaches in modeling flow coefficients. Subsequent investigations should expand upon the existing groundwork to examine diverse facets of model performance, applicability, and adaptability. These endeavors will ultimately contribute to the progression of hydrology, water resource management, and predictive modeling in response to evolving environmental circumstances.

REFERENCES

Ahamad, A., Madhav, S., Singh, P., Pandey, J., & Khan, A.H. (2018). Assessment of groundwater quality with special emphasis on nitrate contamination in parts of Varanasi City, Uttar Pradesh, India. Applied Water Science, 8(4), 1-13. doi:10.1007/s13201-018-0846-7

Akhtar, A. (2013). Indus Basin Floods Mechanism, Impacts, and Management. Metro Manila, Philippines: Asian Development Bank.

Alley, H., Bacinello, C.P., & Hipel, K.W. (1979). Fuzzy set approaches to planning in the Grand River Basin. Adv. in Water Resources, 2, 3-12.

Altaş, E., Aydın, M. C., & Toprak, Z. F. (2017). Determination of Water Surface profile in Open Canal Using a New Fuzzy Modeling Technique (SMRGT). International Conference on Water Resource and Environmental (WRE 2017), Qingdao, China.

Altaş, E., Aydın, M. C., & Toprak, Z. F. (2018). Açık kanal akımlarında su yüzü profilinin bulanık SMRGT yöntemiyle modellenmesi. Dicle Üniversitesi Mühendislik Fakültesi Mühendislik Dergisi, 9(2), 975-981.

Alvi, I. A., & Ayyub, B. M. (1990). Analysis of system performance under stochastic and fuzzy uncertainty. North American Fuzzy Information Processing Society, NAFIPS 1990, University of Toronto.

Angelidis, P., Kotsikas, M., & Kotsovinos, N. (2010). Management of upstream dams and flood protection of the transboundary river Evros/Maritza. Water Resources Management, 24(11), 2467-2484.

Ansari, A., Noorzad, A., & Zanjani, M. (2004). Calculation of probabilistic fuzzy response spectra of earthquake. In 13th World Conference on Earthquake Engineering, Vancouver, B.C., Canada, August 1-6, Paper No. 1154.

Anusree, K., ve Varghese, K.O. (2016). ANFIS, YSA ve MNLR modelleri kullanılarak Karuvannur Nehir havzasının akış tahmini. Prosedür Teknolojisi, 24, 101-108.

Aşıkoğlu, Ö. L. (2017). Frekans analizinde alternatif bir parametre tahmin metodu. Selçuk Üniversitesi Mühendislik, Bilim ve Teknoloji Dergisi, 5(4), 445-459.

Atik, I. (2022). A New CNN-Based Method for Short-Term Forecasting of Electrical Energy Consumption in the Covid-19 Period: The Case of Turkey. IEEE Access, 10, 22586-22598.

Ayyub, B.M. & Ibrahim, A. (1990). Risk-based inspection with uncertainty considerations. Department of Civil Engineering, University of Maryland, College Park, MD, 26 p.

Badrzadeh, H., Sarukkalige, R., ve Jayawardena, A. W. (2018). Hibrit dalgacık nöro-bulanık model ile aralıklı akış akışı tahmini ve modellemesi. Hidroloji Araştırması, 49 (1), 27-40.

Bagarello, V., & Ferro, V. (2010). Analysis of soil loss data from plots of differing lengths for the Sparacia experimental area, Sicily, Italy. Biosystems Engineering, 105(3), 411-422.

Bai, Y. Y., Zhuang, H., & Wang, D. (2006). Advanced Fuzzy Logic Technologies in Industrial Applications. Springer.

Barnett, T. P., Adam, J. C., & Lettenmaier, D. P. (2005). Potential impacts of a warming climate on water availability in snow-dominated regions. Nature, 438(7066), 303-309. doi: 10.1038/nature04141.

Barnett, T.P., Adam, J.C., & Lettenmaier, D.P. (2005). Potential impacts of a warming climate on water availability in snow-dominated regions. Nature, 438(7066), 303-309. doi:10.1038/nature04141

Bayri, G. (2018). Classification of Soils with Simple Membership Functions and Fuzzy Rules Generation Technique (SMRGT). Master Thesis, Institute of Science and Technology, Bitlis Eren University.

Bedient, P. B., Huber, W. C., & Vieux, B. E. (2008). Hydrology and floodplain analysis (Vol. 816). Upper Saddle River, NJ: Prentice Hall.

Belvederesi, C., Dominic, J. A., Hassan, Q. K., Gupta, A., ve Achari, G. (2020). Yapay zeka tabanlı sıralı uyarlanabilir nöro-bulanık çıkarım sistemi kullanarak nehir akışını tahmin etme. Su, 12(6), 1622.

Ben-Haim, Y. (2006). Info-gap decision theory: Decisions under severe uncertainty (2nd ed.).London: Academic Press.

Beurton, S., & Thieken, A. H. (2009). Seasonality of Floods in Germany. Hydrological Sciences Journal, 54, 62–76.

Bih, J. (2006). Paradigm shift - an introduction to fuzzy logic. IEEE Potentials, 25(1), 6-21.

Bisht, D. C., ve Jangid, A. (2011). Discharge modelling using adaptive neuro-fuzzy inference system. International Journal of Advanced Science and Technology. 31(1), 99-114.

Brown, C. B., Chameau, J.-L., Palmer, R. N., & Yao, J. T. P. (1985). Proceedings of Workshop on Civil Engineering Applications of Fuzzy Sets. School of Civil Engineering, Purdue University.

Brown, C.B. (1979). A fuzzy safety measure. Journal of Engineering Mechanics, 105(5), 855-872.

Brown, C.B. (1980). The merging of fuzzy and crisp information. Journal of Engineering Mechanics, 106(1), 123-133.

Çakır Aydın, D. (2017). İşitsel Peyzajda Ses Çevresi Memnuniyet Düzeyinin Bulanık Mantık ile Tahmin Edilmesi: Diyarbakır Suriçi Uygulaması. (Yayımlanmamış Doktora Tezi). İstanbul Teknik Üniversitesi Fen Bilimleri Enstitüsü.

Campos, M. De R., & Machado, R. E. (2018). Time distribution of intense rainfalls at Campinas, Brazil. International Journal of Advanced Engineering Research and Science (IJAERS), 5(Issue-11). https://doi.org/10.22161/ijaers. Nov-.

Çelekli, A., Lekesiz, Ö., & Çetin, T. (2022). Eco-assessment of least disturbed areas of the Antalya River basin: application of diatom indices from different ecoregions. Environmental Science and Pollution Research, 29, 790-804. https://doi.org/10.1007/s11356-021-15394-0

Celestin, S., Qi, F., Li, R., Yu, T., & Cheng, W. (2020). Evaluation of 32 Simple Equations against the Penman–Monteith Method to Estimate the Reference Evapotranspiration in the Hexi Corridor, Northwest China. Water Journal, 12(10), 1-22.

Chaudhry, M. H. (1993). Open-Channel Flow. Prentice-Hall, Inc., Englewood Cliffs.

Chow, V.T. (1962). Hydrologic determination of waterway areas for the design of drainage structures in small drainage basins. University of Illinois, Engineering Experimental Station Bulletin.

Che, D., Liang, A., Li, X., & Ma, B. (2018). Remote sensing assessment of safety risk of iron tailings pond based on runoff coefficient. Sensors, 18, 4373. https://doi.org/10.3390/s18124373

Chow, V.T., Maidment, D.R., & Mays, L.W. (1988). Applied Hydrology. McGraw-Hill Book Company.

Cimen, O. (2002). Killi zeminlerin şişme ve emme özelliklerinin belirlenmesinde bulanık model yaklaşımı. S.D.Ü. Doktora Tezi, 130s, Isparta.

Coskun, C. (2014). Automated Fuzzy Model Generation and an Analysis of the Proposed Method. International Journal of Open Problems in Computer Science and Mathematics, 7(2), 1998-6262.

Crouzeilles, R., & Curran, M. (2016). Which landscape size best predicts the influence of forest cover on restoration success? A global meta-analysis on the scale of effect. Journal of Applied Ecology, 53(2), 440-448. https://doi.org/10.1111/1365-2664.12590

Date, C. J. (2004). An introduction to database systems. Addison-Wesley Professional.

Dooge, J.C.I. (1957). The rational method for estimating flood peaks, Engineering, 184, 311- 313, 347-377.

Demirel, M. C., Koch, J., Mendiguren, G., & Stisen, S. (2018). Spatial pattern oriented multicriteria sensitivity analysis of a distributed hydrologic model. Water, 10(9), 1188.

Demirel, M. C., Koch, J., Mendiguren, G., & Stisen, S. (2018). Spatial pattern oriented multicriteria sensitivity analysis of a distributed hydrologic model. Water, 10(9), 1188.

Demirpençe, H. (2001). Dolgu Barajların Yıkılmasıyla Oluşan Maksimum Taşkın Debisinin Bulanık Mantık ile Modellenmesi. İ.T.Ü. Mühendislikte Modern Yöntemler Sempozyumu, 150s, İstanbul.

Dikici, M., & Kazezyılmaz-Alhan, C. M. (2018). Alibeyköy havzası için farklı hidrolojik modelleme yöntemleri ile taşkın debilerinin belirlenmesi. DÜMF Mühendislik Dergisi, 9(2), 919-928.

EM-DAT. (2016). The OFDA/CRED-International Disaster Database. Université catholique de Louvain, Brussels, Belgium.

Esendal, H. (2007). Eğirdir Gölü Su Seviyesi Mevsimsel Değişiminin Bulanık Mantık Metoduyla Modellenmesi. (Master's Thesis). Süleyman Demirel Üniversitesi Fen Bilimleri Enstitüsü İnşaat Mühendisliği Anabilim Dalı.

Farboudfam, N., Ghorbani, M. A., & Alami, M. T. (2009). Genetik programlama kullanarak nehir akış tahmini. Su ve Toprak Bilimi, 19(1), 107-123.

Fernando, D. A. K., & Jayawardena, A. W. (1998). Runoff forecasting using RBF networks with OLS algorithm. Journal of Hydrol. Eng., 3, 203–209.

Fırat, M. (2007). Artificial intelligence techniques for river flow forecasting in the Seyhan river catchment-Turkey. Hydrology and Earth System Sciences Discussions, 4(3), 1369-1406.

Fırat, M. (2007). Artificial intelligence techniques for river flow forecasting in the Seyhan river catchment, Turkey. Hydrology and Earth System Sciences Discussions, 4 (3), 1369-1406.

Franchini, M., & Mannucci, P. M. (2012). Past, Present and Future of Hemophilia: A Narrative Review. Orphanet Journal of Rare Diseases, 7, 24. https://doi.org/10.1186/1750-1172-7-24.

Freksa, C. (1992). Temporal reasoning based on semi-intervals. Artificial Intelligence, 54, 199–227.

Gilbert, R. O. (1987). Statistical Methods for Environmental Pollution Monitoring. Wiley.

Gkountakou, F., Papadopoulos, B. (2020). The use of fuzzy linear regression and ANFIS methods to predict the compressive strength of cement. Symmetry, 12(8), 1295.

Gökay, M. K. (1998). Bulanık Mantık Yaklaşımının Kaya Kütlesi Sınıflandırmalarında Kullanılması. Madencilik, 37(4), 3-11.

Gürer, I., Uçar, I. (2009). Flood disasters' inventory in Turkey. In Elevation International Symposium on Water Management and Hydraulics Engineering (pp. 371–380). Ohrid, Macedonia, vol. 2009.

Gürer, I., & Uçar, I. (2009). Flood disasters' inventory in Turkey. In Elev. Int. Symp. Water Manag. Hydraul. Eng., Ohrid, Macedonia, vol. 2009 (pp. 371–380).

Hagan, M. T., Menhaj, M. B. (1994). Training feedforward networks with the Marquardt algorithm. IEEE transactions on Neural Networks, 5(6), 989-993.

Haghighi, A., Fijani, E., Kisi, O., Zarghami, M. (2018). Groundwater level prediction using ANFIS and M5 model tree algorithms. Environmental Earth Sciences, 77(11), 417.

Haan, C.T., Barfield, B.J., Hayes, J.C. (1994). design Hydrology and Sedimentology for Small Catchments. Academic Press: San Diego CA.

Hahs-Vaughn, D. L. (2022). Foundational methods: descriptive statistics: bivariate and multivariate data (correlations, associations). In International Encyclopedia of Education (Fourth Edition), pp 734-750. https://doi.org/10.1016/B978-0-12-818630-5.10084-3.

Hajdu, F. (2019). Sensitivity study of a nonlinear semi-active suspension system. Acta Technica Jaurinensis, 12(3), 205-217.

Hajdu, F. (2019). Sensitivity study of a nonlinear semi-active suspension system. Acta Technica Jaurinensis, 12(3), 205-217.

Haltas, I., Demir, I. (2014). Toward a flood information system for Turkey. In 11th International Conference on Hydroinformatics. CUNY Academic Works, New York City, USA. Retrieved from https://academicworks.cuny.edu/cc_conf_hic/432

Haltas, I., Demir, I. (2014). Toward a flood information system for Turkey. In 11th Int. Conf. Hydroinformatics. CUNY Academic Works, New York City, USA. https://academicworks.cuny.edu/cc_conf_hic/432

Hankin, B.G., Beven, K.J. (1998). Modeling dispersion in complex open channel flows: Fuzzy calibration. Stochastic Hydrology and Hydraulics, 12(6), 377-396.

Hartley, R. V. L. (1928). Transmission of information. Bell System Technical Journal, 7, 535-563.

Haykin, S. (1994). Neural Networks: A Comprehensive Foundation. Prentice-Hall.

He, Z., Wen, X., Liu, H., and Du, J. (2014). A comparative study of artificial neural network, adaptive neuro fuzzy inference system and support vector machine for forecasting river flow in the semiarid mountain region. Journal of Hydrology, 509, 379-386.

Henderson, F. M. (1966). Open Channel Flow. Macmillan Publishing Company, Inc.

Hollander, M., Wolf, D. A. (1973). Nonparametric Statistical Methods. Wiley.

Hu, T. S., Lam, K. C., Ng, S. T. (2001). River flow time series prediction with a range-dependent neural network. Hydrological Science Journal, 46(5), 729-745.

Huff, D. D., Hargrove, B., Tharp, M. L., Graham, R. (2000). Managing Forests for WATER Yield: The Importance of Scale. Journal of Forestry, 98(12), 15-19.

Huntington, T. G. (2006). Evidence for intensification of the global water cycle: Review and synthesis. Journal of Hydrology, 319(1-4), 83-95. doi:10.1016/j.jhydrol.2005.07.003

Huntington, T. G. (2006). Evidence for intensification of the global water cycle: Review and synthesis. Journal of Hydrology, 319(1-4), 83-95. doi: 10.1016/j.jhydrol.2005.07.003.

Immerzeel, W. W., Van Beek, L. P. H., Bierkens, M. F. P. (2010). Climate change will affect the Asian water towers. Science, 328(5984), 1382-1385. doi:10.1126/science.1183188

Immerzeel, W. W., Van Beek, L. P. H., Bierkens, M. F. P. (2010). Climate change will affect the Asian water towers. Science, 328(5984), 1382-1385. doi: 10.1126/science.1183188.

IPCC. (2014). Climate Change 2014: Impacts, Adaptation, and Vulnerability. Part A: Global and Sectoral Aspects. Contribution of Working Group II to the Fifth Assessment Report of the Intergovernmental Panel on Climate Change. Cambridge University Press.

Jang, J. S. R. (1993). ANFIS: adaptive-network-based fuzzy inference system. IEEE Transactions on Systems, Man, and Cybernetics, 23(3), 665-685.

Jiang, W. G., Li, J., Li, Z. W. (2008). Fuzzy assessment of the population risk of the food disaster. J Hunan Univ [Nat Sci], 35(9), 84–87. [in Chinese]

Johnson, E. A., Ramallo, J., Spencer, B. F., Sain, M. K. (1998). Intelligent base isolation systems. In: Proc 2nd world conf on structural control. Wiley, New York.

Jonsson, G. (2010). The Environmental Factor in Migration Dynamics - A Review of African Case Studies. Oxford, U.K.

Júnior, A. R. (2022). Elementos de Hidrologia aplicada. Editora Blucher.

Karahoca, D., Karahoca, A.,   Yavuz, Ö. (2013). An early warning system approach for the identification of currency crises with data mining techniques. Neural Computing and Applications, 23(7), 2471-2479.

Karakaya, D. (2018). Modelling of flow coefficient with fuzzy SMGRT method. Master Thesis. Dicle University, Institute of Science and Technology, Diyarbakır.

Karakaya, D. (2018). Modelling of flow coefficient with fuzzy SMGRT method. Master Thesis. Dicle University, Institute of Science and Technology, Diyarbakır, 101.

Karataş, İ. (2018). Bulanık mantık ile klasik ve sembolik mantık ilişkisi Karşılaştırılması. European Journal of Educational and Social Sciences, 3(2), 144-163.

Kuichling, E. (1889). The relation between the rainfall and the discharge of sewers in populous district. Transactions, ASCE 20: 1-56.

Karataş, İ. (2018). Bulanık Mantık ile Klasik ve Sembolik Mantık İlişkisi (Karşılaştırılması). European Journal of Educational and Social Sciences, 3(2), 144-163.

Kaufmann, A. (1975). Introduction to the Theory of Fuzzy Subsets (translated by D.L. Swanson). Academic Press.

Kazeminezhad, M. H., et al. (2005). Ocean Engineering, 32(14-15), 1709-1725.

Kendall, M. G. (1975). Rank Correlation Methods (4th ed.). Charles Griffin.

Keskin, M. E. ve Taylan, D. (2009). Türkiye'nin güneyinde havzalar arası akış tahmini için yapay modeller. Hidrolojik Mühendislik Dergisi, 14 (7), 752-758.

Keskin, M. E., Terzi, O. (2006). Artificial Neural Network Models of Daily Pan Evaporation. Journal of Hydrologic Engineering, 11, 65–70.

Keskin, M. E., Terzi, O., Taylan, D. (2004). Estimating daily pan evaporation for Turkey by using artificial neural networks and multiple linear regression. Journal of Irrigation and Drainage Engineering, 130(5), 391-397.

Khatib, T., et al. (2011). Modelling of daily solar energy on a horizontal surface for five main sites in Malaysia. International Journal of Green Energy, 8(8), 795-819.

Kisi, E., Shiri, M. (2009). Fuzzy logic-based prediction of runoff coefficient in humid regions. Journal of Hydrology, 372(1-4), 36-45.

Kisi, O., Sanikhani, H. (2018). Application of the deep learning models for prediction of runoff coefficient. Journal of Hydrology, 564, 276-287. doi: 10.1016/j.jhydrol.2018.07.045.

Kisi, O., Sanikhani, H. (2018). Flow coefficient prediction using deep learning models. Water Resources Management, 32(8), 2831-2847. https://doi.org/10.1007/s11269-018-1977-9.

Koç, G., Thieken, A. H. (2018). The relevance of flood hazards and impacts in Turkey: What can be learned from different disaster loss databases? Natural Hazards, 91, 375–408.

Kumar, A. R. S., Sudheer, K. P., Jain, S. K., Agarwal, P. K. (2005). Rainfall-runoff modelling using artificial neural networks: comparison of network types. Hydrological Processes, 19, 1277–1291.

Kundzewicz, Z. W., Nohara, D., Tong, J., Oki, T., Buda, S., Takeuchi, K. (2009). Discharge of large Asian rivers – Observations and projections. Quaternary International, in print.

Lallahem, S., Mania, J., Hani, A., Najjar, Y. (2005). On the use of neural networks to evaluate groundwater levels in fractured media. Journal of Hydrology, 307, 92-111.

Li, H., Chen, Y. (2020). The spatial sensitivity analysis of land irrigation suitability evaluation based on groundwater data of Xinjiang inland river basin. Computers and Electronics in Agriculture, 177, 105680.

Li, H., Chen, Y. (2020). The spatial sensitivity analysis of land irrigation suitability evaluation based on groundwater data of Xinjiang inland river basin. Computers and Electronics in Agriculture, 177, 105680.

Liong, S. Y., Lim, W. H., Kojiri, T., Hori, T. (2000). Advance Flood forecasting for Flood stricken Bangladesh with a fuzzy reasoning method. Hydrological Process, 14, 431-448.

Lippmann, R. P. (1987). An introduction to computing with neural nets. IEEE ASSP Magazine, 4-22.

Macedo, M. N. Q., Galo, J. J. M., Almeida, L. A. L., Lima, A. C. C. (2016). Methodology for the calculation of the factor of priority for smart grid implantation using fuzzy logic. International Journal of Electrical Power Energy Systems, 78, 563–568.

Mahabir, C., Hicks, F. E., Fayek, A. R. (2003). Application of fuzzy logic to the seasonal runoff. Hydrological Process, 17, 3749–3762.

Maier, H. R., Dandy, G. C. (1996). The use of artificial neural network for the prediction of quality water parameters. Water Resources Research, 32(4), 1013-1022.

Mamdani, E. H., Assilian, S. (1975). An experiment in linguistics thesis with a fuzzy logic controller. International Journal of Man-Machine Studies, 7(1), 1-13.

Mann, H. B. (1945). Non-parametric tests against trend. Econometrica, 13, 163-171.

Mao, D. H., Wang, L. H. (2002). Diagnosis and an assessment on the vulnerability of the urban food-waterlogged disaster in the human province. Resour Environ Yangtze Basin, 11(1), 89–93 [in Chinese]

McCulloch, W. S., Pitts, W. (1943). A logical calculus of the ideas imminent in nervous activity. Bulletin of Mathematical Biology, 5, 115-133.

McCulloch, W. S., Pitts, W. (1943). A logical calculus of the ideas imminent in nervous activity. Bulletin of Mathematical Biology, 5, 115-133.

Merz, R., Blöschl, G. (2003). A Process Typology of Regional Floods. Water Resources Research, 39.

Merz, R., Blöschl, G. (2003). A Process Typology of Regional Floods. Water Resources Research, 39.

Metropolis, N., Rosenbluth, A. W., Rosenbluth, M. N., Teller, A. H., Teller, E. (1953). Equation of state calculation by fast computing machines. The Journal of Chemical Physics, 21(6), 1087-1092.

Metropolis, N., Rosenbluth, A. W., Rosenbluth, M. N., Teller, A. H., Teller, E. (1953). Equation of state calculation by fast computing machines. The Journal of Chemical Physics, 21(6), 1087-1091.

Mimikou, M., Rao, A.R. (1983). Regional monthly rainfall-runoff model. Journal of Water Resources Planning and Management, 109(1), 75-93.

Minns, A. W., Hall, M. J. (1996). Artificial Neural Networks as Rainfall-Runoff Models. Hydrological Sciences Journal, 41, 399-417.

Minns, A. W., Hall, M. J. (1996). Artificial neural networks as rainfall-runoff models. Hydrological Sciences Journal, 41(3), 399-418.

Mohammadi, K., Eslami, H. R., Kahawita, R. (2006). Parameter estimation of an ARMA model for river flow forecasting using goal programming. Journal of Hydrology, 331(1-2), 293-299.

N. J. Sairamya, L. Susmitha, S. Thomas George, M. S. P. Subathra (2019). Hybrid Approach for Classification of Electroencephalographic Signals Using Time–Frequency Images With Wavelets and Texture Features. In Intelligent Data-Centric Systems, Intelligent Data Analysis for Biomedical Applications, (Eds. N. Chaki, R. S. S. Yadav, M. S. Obaidat), Academic Press, Pages 253-273.

Nayak, P. C., Sudheer, K. P., Ramasastri, K. S. (2004). Fuzzy computing based rainfall-runoff model for real-time flood forecasting. Hydrological Process, 17, 3749–3762.

Nayak, P. C., Sudheer, K. P., Ramasastri, K. S. (2005). Fuzzy Computing Based Rainfall-runoff Model for Real Time Flood Forecasting. Hydrological Process, 19, 955–968.

Onur, F. (2015). Baraj Gölü Doluluk Tahmininde Bulanık Mantık Yaklaşımı. (Yüksek Lisans Tezi). Gebze Teknik Üniversitesi Fen Bilimleri Enstitüsü Jeodezi ve Fotogrametri Anabilim Dalı.

Onur, F., Ergun, B., Şahin, C. (2016). Bulanık Mantık Yaklaşımıyla Baraj Gölü Doluluk Tahmini Çalışması. In 6. Uzaktan Algılama-CBS Sempozyumu (UZAL-CBS 2016), 5-7 Ekim, Adana.

Onur, F., Ergun, B., Şahin, C. (2016). Bulanık Mantık Yaklaşımıyla Baraj Gölü Doluluk Tahmini Çalışması. 6. Uzaktan Algılama-CBS Sempozyumu (UZAL-CBS 2016), 5-7 Ekim, Adana.

Ozdemir, H. (2007). SCS CN Yağış-Akış Modelinin CBS ve Uzaktan Algılama Yöntemleriyle Uygulanması: Havran Çayı Havzası Örneği (Balıkesir). Coğrafi Bilimler Dergisi, 5(2), 1-12. DOI: 10.1501/Cogbil_0000000078

Özdemir, H. (2007). SCS CN Yağış-Akış Modelinin CBS ve Uzaktan Algılama Yöntemleriyle Uygulanması: Havran Çayı Havzası Örneği (Balıkesir). Coğrafi Bilimler Dergisi, 5(2), 1-12. DOI: 10.1501/Cogbil_0000000078.

Özger, M. (2009). Akış tahmini için bulanık çıkarım sistemlerinin karşılaştırılması. Hidrolojik Bilimler Dergisi, 54(2), 261-273.

Pagano, T.C., Hartmann, H.C., Sorooshian, S. (2002). Use of climate forecasts for water management in Arizona: a case study of the 1997-98 El Niño. Climate Research, 21, 59–269.

Palanisamy, K., Sundaravadivelu, R. (2000). Fuzzy logic approach for wave prediction. Ocean Engineering, 27(1), 1-20.

Prudhomme, C., Crooks, S., Kay, A. L., Reynard, N. (2013). Climate change and river flooding: Part 1 classifying the sensitivity of British catchments. Climatic Change, 119, 933–948.

Prudhomme, C., Crooks, S., Kay, A.L., Reynard, N. (2013). Climate change and river flooding: Part 1 classifying the sensitivity of British catchments. Climatic Change, 119, 933–948.

Reynaldi, A., Lukas, S., Margaretha, H. (2012). Backpropagation and Levenberg-Marquardt algorithm for training finite element neural network. In 2012 Sixth UKSim/AMSS European Symposium on Computer Modeling and Simulation (pp. 89-94). IEEE.

Rezaei, M., Motlaq, A. A. A., Mahmouei, A. R., Mousavi, S. H. (2015). Yapay sinir ağı kullanarak nehir akışı tahmini. Ciência e Natura, 37(6-1), 207-215.

Riad, S., Mania, J., Bouchaou, L., Najjar, Y. (2004). Rainfall-Runoff Model Using an Artificial Neural Network Approach. Mathematical and Computer Modelling, 40, 839-846.

Rumelhart, D. E., Hinton, G. E., Williams, R. J. (1986). Learning representations by backpropagation error. Nature, 323, 533-536.

Rustum, R., Kurichiyanil, R., Forrest, S., Sommariva, C., Adeloye, A., Zounemat-Kermani, M., Scholz, M. (2020). Sustainability Ranking of Desalination Plants Using Mamdani Fuzzy Logic Inference Systems. Sustainability, 12(2), 631. https://doi.org/10.3390/su12020631

Saka, S. (1999). Bulanık kontrol ve uygulamaları. İ.T.Ü. Y.Lisans Tezi, 100s, İstanbul.

Samanataray, S., Sahoo, A. (2021). A Comparative Study on Prediction of Monthly Streamflow Using Hybrid ANFIS-PSO Approaches. KSCE Journal of Civil Engineering, 25(10), 4032-4043.

Saplıoğlu, K., Çimen, M. (2010). Yapay sinir ağlarını kullanarak günlük yağış miktarının tahmini. Mühendislik Bilimleri ve Tasarım Dergisi, 1(1), 14-21.

Schröter, K., Kunz, M., Elmer, F., Mühr, B., Merz, B. (2015). What made the June 2013 flood in Germany an exceptional event; a hydro-meteorological evaluation. Hydrology and Earth System Sciences, 19, 309–327.

Schröter, K., Kunz, M., Elmer, F., Mühr, B., Merz, B. (2015). What made the June 2013 flood in Germany an exceptional event: A hydro-meteorological evaluation. Hydrology and Earth System Sciences, 19, 309–327.

Schultz, G. (1993). Application of GIS and Remote Sensing in Hydrology. In Hydro GIS 93: Application of Geographic Information Systems in Hydrology and Water Resources, Proceedings of the Vienna Conference, April 1993, IAHS Publication No. 211, pp. 127–142.

Sen, Z. (2002). Fuzzy (fuzzy) Logic and Modeling Principles. Bilge Art Production Publications, Istanbul.

Sen, Z. (2002). Fuzzy (fuzzy) Logic and Modeling Principles. Bilge Art production Publications, Istanbul.

Sen, Z. (2004). Fuzzy Logic and System Models in Water Sciences. Turkish Water Foundation, Bilge Press, Istanbul.

Sen, Z. (2009). Fuzzy logic and hydrological modeling. CRC Press.

Şen, Z., Altunkaynak, A. (2006). A comparative fuzzy logic approach to runoff coefficient and runoff estimation. Hydrological Process, 20, 1993–2009.

Sevgin, F. (2021). Determination of Meteorological Flow Coefficient by Fuzzy SMRGT Method: The Case of Murat Basin. DUMF Engineering Journal. https://doi.org/10.24012/dumf.844325.

Shannon, C. E. (1948). The mathematical theory of communication. Bell System Technical Journal, 27, 379-423, 623-656.

Sharaf, A. M., Lie, T. T. (1997). An Artificial Neural Network Coordinated Excitation/Governor Controller For Synchronous Generators. Electric Machines Power Systems, 25(1), 1-14. doi:10.1080/07313569708955720

Shrivastava, P., Gupta, N. (2021). ANFIS: an overview of applications in various fields. Journal of Ambient Intelligence and Humanized Computing, 12(2), 1867-1879.

Singh, Aditya, Singh, Arvind. (2021). Climatic controls on water resources and its management: challenges and prospects of sustainable development in the Indian perspective. In: Intelligent Data-Centric Systems, Intelligent Data Analysis for Biomedical Applications, (Eds. N. Chaki, R. S. S. Yadav, M. S. Obaidat). Academic Press, 253-273. doi: 10.1016/B978-0-12-820200-5.00015-4.

Sen, Z., Altunkaynak A. (2004). Fuzzy awakening in rainfall-runoff modeling. Nordic Hydrology, 35(1), 31-45.

Singh, V.P. (1995). Elementary Hydrology. Prentice Hall.

Smith, I., Eli, R. N. (1995). Neural-network models of rainfall-runoff process. Journal of Water Resources Planning and Management, 121(6), 499-508.

Sönmez, O., Çeribaşı, G., Doğan, E. (2016). Farklı sinir ağı yaklaşımları ve trend analizi yöntemleriyle kısa ve uzun vadeli akış tahmini: Sakarya Nehri vaka çalışması, Türkiye. Fresen. Environ. Bull, 25, 565-579.

Srinivasan, K., Neelakantan, T. R., Narayan, P. S., Nagarajukumar, Compolo. (1999). Mixed-integer programming model for reservoir performance optimization. Journal of Water Resources Planning and Management, 125(5), 298-301.

Sudheer, K. P., Gosain, A. K., Mohana Rangan, D., Saheb, S. M. (2002). Modelling evaporation using an artificial neural network algorithm. Hydrol. Process., 16, 3189-3202.

Sudheer, K. P., Gosain, A. K., Rangan, D. M., Saheb, S. M. (2002). Modelling evaporation using an artificial neural network algorithm. Hydrological Processes, 16, 3189–3202.

Sui, D. Z., Maggio, R. C. (1999). Integrating GIS with Hydrological Modeling: Practices, Problems, and Prospects. Computers, Environment and Urban Systems, 23, 33-51. https://doi.org/10.1016/S0198-9715(98)00052-0.

Sui, D.Z., Maggio, R.C. (1999). Integrating GIS with Hydrological Modeling: Practices, Problems, and Prospects. Computers, Environment and Urban Systems, 23, 33-51. https://doi.org/10.1016/S0198-9715(98)00052-0

Taşar, B., Unes, F., Varcin, H. (2019). Prediction of the rainfall–runoff relationship using neuro fuzzy and support vector machines. In 2019 ‘’Air and Water–Components of the Environment” Conference Proceedings, 237-246.

Tayfur, G., Vijay P. Singh, Tommaso Moramarco, Silvia Barbetta. (2018). Flood Hydrograph Prediction Using Machine Learning Methods. Water, 10(8), 968. https://doi.org/10.3390/w10080968

THERESA BLUME, ERWIN ZEHE AXEL BRONSTERT (2007) Rainfall—runoff response, event-based runoff coefficients and hydrograph separation, Hydrological Sciences Journal, 52:5, 843-862, DOI: 10.1623/hysj.52.5.843

Tokar, A. S., Johnson, P. A. (1999). Rainfall-runoff modeling using artificial neural networks. Journal of Hydrol. Eng., 4, 232–239.

Toprak, Z. F. (2009). Flow discharge modeling in open canals using a new fuzzy modeling technique (SMRGT). CLEAN–Soil, Air, Water, 37(9), 742-752.

Toprak, Z. F. (2009). Flow discharge modeling in open canals using a new fuzzy modeling technique (SMRGT). CLEAN–Soil, Air, Water, 37(9), 742-752.

Toprak, Z. F., Akkoyun, Ö. (2008). Mermer Blok Kalitelerinin Bulanık Mantık Yöntemi ile Belirlenmesi. Bilimde Modern Yöntemler Sempozyumu, BMYS'2008, 15–17 Ekim 2008, Eskişehir Osmangazi Üniversitesi.

Toprak, Z. F., Songur, M., Hamidi, N., Gulsever, H. (2013). Determination of Losses in Water Networks Using a New Fuzzy Technique (SMRGT). Global Journal on Technology, 3, 833-840.

Topraksu, Susurluk Havzası Toprakları, T.C. Köy İşleri Bakanlığı Yayınları 174, Topraksu Genel Müdürlüğü Yayınları 258, Raporlar Serisi: 46, Ankara, 1971.

Tucci, C. E. M. (2000). Coeficiente de escoamento e vazão máxima de bacias urbanas. RBRH: Revista Brasileira de Recursos Hídricos, 5(1), 61-68.

Turkington, T., Breinl, K., Ettema, J., Alkema, D., Jetten, V. (2016). A new flood type classification method for use in climate change impact studies. Weather and Climate Extremes, 14, 1–16.

Turkish State Meteorological Service. (n.d.). Historical weather data for Antalya. Retrieved from http://www.meteor.gov.tr/veridegerlendirme/il-ve-ilceler-istatistik.aspx?m=ANTALYA

UN Water. (2019). Water and energy. Retrieved from https://www.unwater.org/water-facts/water-and-energy/

UNESCO. (n.d.). Hydrology: The water cycle. Retrieved from https://en.unesco.org/themes/water-security/hydrology-water-cycle

United States Environmental Protection Agency (EPA). (2009). Statistical Analysis of Groundwater Monitoring Data at RCRA Facilities: Unified Guidance. EPA-530-R-09-007. Office of Resource Conservation and Recovery, U.S. Environmental Protection Agency. March.

USDA Natural Resources Conservation Service. (1986). Urban Hydrology for Small Watersheds. TR-55.

Van Leekwijck, W., Kerre, E. E. (1999). Defuzzification: criteria and classification. Fuzzy Sets and Systems, 108(2), 159–178. doi:10.1016/S0165-0114(97)00337-0.

Vaziri, M. (1997). Predicting Caspian Sea surface water level by ANN and ARIMA models. Journal of Waterway, Port, Coastal, and Ocean Engineering, 123(4), 158-162.

Vernieuwe, H., Georgieva, O., De Baets, B., Pauwels, V. R. N., Verhoest, N. E. C., De Troch, F. P. (2005). Comparison of data-driven Takagi–Sugeno models of rainfall–discharge dynamics. Journal of Hydrology, 302(1-4), 173-186.

Vieux, B. E. (2001). Distributed hydrologic modeling using GIS. Kluwer Academic, Dordrecht, The Netherlands, 1–17.

Vieux, B., Needham, S. (1993). Nonpoint-Pollution Model Sensitivity to Grid-Cell Size. Journal of Water Resources Planning and Management, 119(2), 141–157.

Wei, Y., Xu, W., Fan, Y., Tasi, H. T. (2002). Artificial neural network based predictive method for flood disaster. Computers Industrial Engineering, 42, 383-390.

World Weather Online. (n.d.). Antalya weather averages. Retrieved from https://www.worldweatheronline.com/lang/en/tr/antalya-weather-averages/antalya/tr.aspx

Yadav, A., Prasad, B. B. V. S. V., Mojjada, R. K., Kothamasu, K. K., Joshi, D. (2020). Application of artificial neural network and genetic algorithm based artificial neural network models for river flow prediction. Rev, d'Intelligence Artif., 34(6), 745-751.

Yalaz, S., Atay, A., Toprak, Z. F. (2013). Fuzzy Linear Regression for Time-Related Data with Fuzzy SMRGT Method. Mathematics Symposium, Diyarbakır, 1-7.

Yenigün, K., Gümüş, V. (2009). İnşaat Mühendisliği Bölümü Hidroloji Ders Notları (1. Baskı). Harran Üniversitesi.

Yenigün, K., Gümüş, V. (2009). İnşaat Mühendisliği Bölümü Hidroloji Ders Notları (1. Baskı). Harran Üniversitesi.

Yıldırım, E., Doğan, E., Karavul, C., Aşçı, M., Özçep, F., Arman, H. (2007). Bulanık mantık modeli ile zeminlerin sınıflandırılması. Uluslar Arası Deprem Sempozyumu, Kocaeli, Türkiye, s: 578-582.

Yılmaz, N. A. S. (2003). A Temporal Neuro-Fuzzy Approach for Time Series Analysis. Doctor of Philosophy, Thesis submitted to the Department of Computer Engineering, METU, Ankara.

Zadeh, L.A. (1965). Fuzzy sets. Inform. And Control, 8, 338-353.

Zhao, W., Chen, W., Zhu, Y., & Yu, X. (2014). Rainfall-runoff modeling using adaptive neuro-fuzzy inference system with differential evolution algorithm. The Scientific World Journal, 2014, 1-11.

Zurada, J. M. (1992). Introduction to Artificial Neural Systems. West Publishing Company.

APPENDIX

Appendix A The generated fuzzy set for SMRGT-3 model.

Rules No.	Precipitation		Temperature		Humidity		Flow Coefficient	Flow Coefficient	MAPE
	Numerical	Verbal	Numerical	Verbal	Numerical	Verbal	(data)	(model)	
1	312.5	VL	46.88	VH	6.25	VL	0.1423	0	0.80
2	312.5	VL	46.88	VH	25	L	0.1469	0.01	0.75
3	312.5	VL	46.88	VH	50	M	0.1531	0.02	0.70
4	312.5	VL	46.88	VH	75	H	0.1593	0.0212	0.69
5	312.5	VL	46.88	VH	93.75	VH	0.1640	0.03	0.65
6	312.5	VL	37.5	H	6.25	VL	0.1469	0.04	0.58
7	312.5	VL	37.5	H	25	L	0.1506	0.05	0.53
8	312.5	VL	37.5	H	50	M	0.1556	0.06	0.49
9	312.5	VL	37.5	H	75	H	0.1606	0.0627	0.49
10	312.5	VL	37.5	H	93.75	VH	0.1643	0.07	0.46
11	312.5	VL	25	M	6.25	VL	0.1531	0.08	0.38
12	312.5	VL	25	M	25	L	0.1556	0.09	0.34
13	312.5	VL	25	M	50	M	0.1589	0.1	0.30
14	312.5	VL	25	M	75	H	0.1622	0.104	0.29
15	312.5	VL	25	M	93.75	VH	0.1647	0.11	0.27
16	312.5	VL	12.5	L	6.25	VL	0.1593	0.12	0.20
17	312.5	VL	12.5	L	25	L	0.1606	0.13	0.15
18	312.5	VL	12.5	L	50	M	0.1622	0.14	0.11
19	312.5	VL	12.5	L	75	H	0.1639	0.146	0.09
20	312.5	VL	12.5	L	93.75	VH	0.1651	0.15	0.07
21	312.5	VL	3.125	VL	6.25	VL	0.1640	0.16	0.02
22	312.5	VL	3.125	VL	25	L	0.1643	0.17	0.03
23	312.5	VL	3.125	VL	50	M	0.1647	0.18	0.07
24	312.5	VL	3.125	VL	75	H	0.1651	0.187	0.11

CONT.

Appendix A the generated fuzzy set for SMRGT-3 model.

Rules No.	Precipitation mm		Temperature C		Humidity%		Flow Coefficient	Flow Coefficient	MAPE
	Numerical	Verbal	Numerical	Verbal	Numerical	Verbal	(data)	(model)	
25	312.5	VL	3.125	VL	93.75	VH	0.1654	0.19	0.12
26	650	L	46.88	VH	6.25	VL	0.3210	0.2	0.30
27	650	L	46.88	VH	25	L	0.3257	0.21	0.28
28	650	L	46.88	VH	50	M	0.3319	0.22	0.27
29	650	L	46.88	VH	75	H	0.3381	0.229	0.26
30	650	L	46.88	VH	93.75	VH	0.3428	0.23	0.26
31	650	L	37.5	H	6.25	VL	0.3257	0.24	0.21
32	650	L	37.5	H	25	L	0.3294	0.25	0.19
33	650	L	37.5	H	50	M	0.3344	0.26	0.18
34	650	L	37.5	H	75	H	0.3393	0.27	0.16
35	650	L	37.5	H	93.75	VH	0.3431	0.271	0.17
36	650	L	25	M	6.25	VL	0.3319	0.28	0.13
37	650	L	25	M	25	L	0.3344	0.29	0.11
38	650	L	25	M	50	M	0.3377	0.3	0.09
39	650	L	25	M	75	H	0.3410	0.31	0.07
40	650	L	25	M	93.75	VH	0.3435	0.313	0.07
41	650	L	12.5	L	6.25	VL	0.3381	0.32	0.04
42	650	L	12.5	L	25	L	0.3393	0.33	0.02
43	650	L	12.5	L	50	M	0.3410	0.34	0.00
44	650	L	12.5	L	75	H	0.3427	0.35	0.02
45	650	L	12.5	L	93.75	VH	0.3439	0.354	0.02
46	650	L	3.125	VL	6.25	VL	0.3428	0.36	0.04
47	650	L	3.125	VL	25	L	0.3431	0.37	0.06

CONT.

Appendix A the generated fuzzy set for SMRGT-3 model.

Rules No.	Precipitation mm		Temperature C		Humidity%		Flow Coefficient (data)	Flow Coefficient (model)	MAPE
	Numerical	Verbal	Numerical	Verbal	Numerical	Verbal			
48	650	L	3.125	VL	50	M	0.3435	0.38	0.09
49	650	L	3.125	VL	75	H	0.3439	0.39	0.11
50	650	L	3.125	VL	93.75	VH	0.3442	0.396	0.12
51	1100	M	46.88	VH	6.25	VL	0.5594	0.4	0.23
52	1100	M	46.88	VH	25	L	0.5641	0.41	0.22
53	1100	M	46.88	VH	50	M	0.5703	0.42	0.21
54	1100	M	46.88	VH	75	H	0.5765	0.43	0.20
55	1100	M	46.88	VH	93.75	VH	0.5811	0.437	0.20
56	1100	M	37.5	H	6.25	VL	0.5641	0.44	0.18
57	1100	M	37.5	H	25	L	0.5678	0.45	0.17
58	1100	M	37.5	H	50	M	0.5728	0.46	0.16
59	1100	M	37.5	H	75	H	0.5777	0.47	0.15
60	1100	M	37.5	H	93.75	VH	0.5814	0.479	0.14
61	1100	M	25	M	6.25	VL	0.5703	0.48	0.13
62	1100	M	25	M	25	L	0.5728	0.49	0.12
63	1100	M	25	M	50	M	0.5761	0.5	0.11
64	1100	M	25	M	75	H	0.5794	0.51	0.10
65	1100	M	25	M	93.75	VH	0.5819	0.52	0.09
66	1100	M	12.5	L	6.25	VL	0.5765	0.521	0.08
67	1100	M	12.5	L	25	L	0.5777	0.53	0.07
68	1100	M	12.5	L	50	M	0.5794	0.54	0.05
69	1100	M	12.5	L	75	H	0.5810	0.55	0.04
70	1100	M	12.5	L	93.75	VH	0.5823	0.56	0.03

CONT.

Appendix A the generated fuzzy set for SMRGT-3 model.

Rules No.	Precipitation mm		Temperature C		Humidity%		Flow Coefficient	Flow Coefficient	MAPE
	Numerical	Verbal	Numerical	Verbal	Numerical	Verbal	(data)	(model)	
71	1100	M	3.125	VL	6.25	VL	0.5811	0.563	0.02
72	1100	M	3.125	VL	25	L	0.5814	0.57	0.02
73	1100	M	3.125	VL	50	M	0.5819	0.58	0.00
74	1100	M	3.125	VL	75	H	0.5823	0.59	0.01
75	1100	M	3.125	VL	93.75	VH	0.5826	0.6	0.02
76	1550	H	46.88	VH	6.25	VL	0.7978	0.604	0.19
77	1550	H	46.88	VH	25	L	0.8024	0.61	0.19
78	1550	H	46.88	VH	50	M	0.8086	0.62	0.19
79	1550	H	46.88	VH	75	H	0.8149	0.63	0.18
80	1550	H	46.88	VH	93.75	VH	0.8195	0.64	0.18
81	1550	H	37.5	H	6.25	VL	0.8024	0.646	0.16
82	1550	H	37.5	H	25	L	0.8062	0.65	0.15
83	1550	H	37.5	H	50	M	0.8111	0.66	0.15
84	1550	H	37.5	H	75	H	0.8161	0.67	0.14
85	1550	H	37.5	H	93.75	VH	0.8198	0.68	0.14
86	1550	H	25	M	6.25	VL	0.8086	0.687	0.12
87	1550	H	25	M	25	L	0.8111	0.69	0.12
88	1550	H	25	M	50	M	0.8144	0.7	0.11
89	1550	H	25	M	75	H	0.8177	0.71	0.11
90	1550	H	25	M	93.75	VH	0.8202	0.72	0.10
91	1550	H	12.5	L	6.25	VL	0.8149	0.729	0.08
92	1550	H	12.5	L	25	L	0.8161	0.73	0.08
93	1550	H	12.5	L	50	M	0.8177	0.74	0.08

CONT.

Appendix A the generated fuzzy set for SMRGT-3 model.

Rules No.	Precipitation mm		Temperature C		Humidity%		Flow Coefficient (data)	Flow Coefficient (model)	MAPE
	Numerical	Verbal	Numerical	Verbal	Numerical	Verbal			
94	1550	H	12.5	L	75	H	0.8194	0.75	0.07
95	1550	H	12.5	L	93.75	VH	0.8206	0.76	0.06
96	1550	H	3.125	VL	6.25	VL	0.8195	0.77	0.05
97	1550	H	3.125	VL	25	L	0.8198	0.771	0.05
98	1550	H	3.125	VL	50	M	0.8202	0.78	0.04
99	1550	H	3.125	VL	75	H	0.8206	0.79	0.03
100	1550	H	3.125	VL	93.75	VH	0.8210	0.8	0.02
101	1887.5	VH	46.88	VH	6.25	VL	0.9768	0.81	0.14
102	1887.5	VH	46.88	VH	25	L	0.9815	0.813	0.14
103	1887.5	VH	46.88	VH	50	M	0.9877	0.82	0.14
104	1887.5	VH	46.88	VH	75	H	0.9939	0.83	0.13
105	1887.5	VH	46.88	VH	93.75	VH	0.9986	0.84	0.13
106	1887.5	VH	37.5	H	6.25	VL	0.9815	0.85	0.11
107	1887.5	VH	37.5	H	25	L	0.9852	0.854	0.11
108	1887.5	VH	37.5	H	50	M	0.9902	0.86	0.11
109	1887.5	VH	37.5	H	75	H	0.9951	0.87	0.10
110	1887.5	VH	37.5	H	93.75	VH	0.9989	0.88	0.10
111	1887.5	VH	25	M	6.25	VL	0.9877	0.89	0.08
112	1887.5	VH	25	M	25	L	0.9902	0.896	0.08
113	1887.5	VH	25	M	50	M	0.9935	0.9	0.08
114	1887.5	VH	25	M	75	H	0.9968	0.91	0.07
115	1887.5	VH	25	M	93.75	VH	0.9993	0.92	0.06
116	1887.5	VH	12.5	L	6.25	VL	0.9939	0.93	0.05

CONT.

Appendix A the generated fuzzy set for SMRGT-3 model.

Rules No.	Precipitation mm		Temperature C		Humidity%		Flow Coefficient	Flow Coefficient	MAPE
	Numerical	Verbal	Numerical	Verbal	Numerical	Verbal	(data)	(model)	
117	1887.5	VH	12.5	L	25	L	0.9951	0.937	0.05
118	1887.5	VH	12.5	L	50	M	0.9968	0.94	0.05
119	1887.5	VH	12.5	L	75	H	0.9984	0.95	0.04
120	1887.5	VH	12.5	L	93.75	VH	0.9997	0.96	0.03
121	1887.5	VH	3.125	VL	6.25	VL	0.9986	0.97	0.02
122	1887.5	VH	3.125	VL	25	L	0.9989	0.979	0.02
123	1887.5	VH	3.125	VL	50	M	0.9993	0.98	0.02
124	1887.5	VH	3.125	VL	75	H	0.9997	0.99	0.01
125	1887.5	VH	3.125	VL	93.75	VH	1.0000	1	0.00

Appendix B

The generated fuzzy set for the SMRGT-4 model

Rules No.	Precipitation		Land Use		Soil Permeability		Flow Coefficient	Flow Coefficient
	Numerical	Verbal	Numerical	Verbal	Numerical	Verbal	(data)	(model)
1	312.5	VL	46.88	VH	6.25	VL	0.0020	0.006
2	312.5	VL	46.88	VH	25	L	0.0122	0.008
3	312.5	VL	46.88	VH	50	M	0.0129	0.016
4	312.5	VL	46.88	VH	75	H	0.0135	0.025
5	312.5	VL	46.88	VH	93.75	VH	0.0139	0.03
6	312.5	VL	37.5	H	6.25	VL	0.0127	0.04
7	312.5	VL	37.5	H	25	L	0.0130	0.045
8	312.5	VL	37.5	H	50	M	0.0139	0.056
9	312.5	VL	37.5	H	75	H	0.0140	0.0645
10	312.5	VL	37.5	H	93.75	VH	0.0145	0.073
11	312.5	VL	25	M	6.25	VL	0.0140	0.081
12	312.5	VL	25	M	25	L	0.0143	0.0887
13	312.5	VL	25	M	50	M	0.1460	0.097
14	312.5	VL	25	M	75	H	0.1500	0.105
15	312.5	VL	25	M	93.75	VH	0.1520	0.113
16	312.5	VL	12.5	L	6.25	VL	0.1530	0.12
17	312.5	VL	12.5	L	25	L	0.1542	0.128
18	312.5	VL	12.5	L	50	M	0.1559	0.137
19	312.5	VL	12.5	L	75	H	0.1576	0.145
20	312.5	VL	12.5	L	93.75	VH	0.1588	0.153

CONT.

The generated fuzzy set for the SMRGT-4 model

Rules No.	Precipitation		Land Use		Soil Permeability		Flow Coefficient	Flow Coefficient
	Numerical	**Verbal**	**Numerical**	**Verbal**	**Numerical**	**Verbal**	**(data)**	**(model)**
1	312.5	VL	46.88	VH	6.25	VL	0.0020	0.006
2	312.5	VL	46.88	VH	25	L	0.0122	0.008
3	312.5	VL	46.88	VH	50	M	0.0129	0.016
4	312.5	VL	46.88	VH	75	H	0.0135	0.025
5	312.5	VL	46.88	VH	93.75	VH	0.0139	0.03
6	312.5	VL	37.5	H	6.25	VL	0.0127	0.04
7	312.5	VL	37.5	H	25	L	0.0130	0.045
8	312.5	VL	37.5	H	50	M	0.0139	0.056
9	312.5	VL	37.5	H	75	H	0.0140	0.0645
10	312.5	VL	37.5	H	93.75	VH	0.0145	0.073
11	312.5	VL	25	M	6.25	VL	0.0140	0.081
12	312.5	VL	25	M	25	L	0.0143	0.0887
13	312.5	VL	25	M	50	M	0.1460	0.097
14	312.5	VL	25	M	75	H	0.1500	0.105
15	312.5	VL	25	M	93.75	VH	0.1520	0.113
16	312.5	VL	12.5	L	6.25	VL	0.1530	0.12
17	312.5	VL	12.5	L	25	L	0.1542	0.128
18	312.5	VL	12.5	L	50	M	0.1559	0.137
19	312.5	VL	12.5	L	75	H	0.1576	0.145
20	312.5	VL	12.5	L	93.75	VH	0.1588	0.153

CONT.

The generated fuzzy set for the SMRGT-4 model

Rules No.	**Precipitation**		**Land Use**		**Soil Permeability**		**Flow Coefficient**	**Flow Coefficient**
	Numerical	**Verbal**	**Numerical**	**Verbal**	**Numerical**	**Verbal**	**(data)**	**(model)**
21	312.5	VL	3.125	VL	6.25	VL	0.1626	0.161
22	312.5	VL	3.125	VL	25	L	0.1630	0.169
23	312.5	VL	3.125	VL	50	M	0.1634	0.177
24	312.5	VL	3.125	VL	75	H	0.1638	0.1855
25	312.5	VL	3.125	VL	93.75	VH	0.1641	0.193
26	650	L	46.88	VH	6.25	VL	0.2113	0.2
27	650	L	46.88	VH	25	L	0.2250	0.21
28	650	L	46.88	VH	50	M	0.3077	0.218
29	650	L	46.88	VH	75	H	0.3139	0.225
30	650	L	46.88	VH	93.75	VH	0.3185	0.24
31	650	L	37.5	H	6.25	VL	0.3064	0.242
32	650	L	37.5	H	25	L	0.3101	0.25
33	650	L	37.5	H	50	M	0.3151	0.258
34	650	L	37.5	H	75	H	0.3201	0.266
35	650	L	37.5	H	93.75	VH	0.3238	0.273
36	650	L	25	M	6.25	VL	0.3193	0.282
37	650	L	25	M	25	L	0.3218	0.29
38	650	L	25	M	50	M	0.3251	0.3
39	650	L	25	M	75	H	0.3284	0.305

CONT.

The generated fuzzy set for the SMRGT-4 model

Rules No.	Precipitation		Land Use		Soil Permeability		Flow Coefficient	Flow Coefficient
	Numerical	Verbal	Numerical	Verbal	Numerical	Verbal	(data)	(model)
40	650	L	25	M	93.75	VH	0.3309	0.315
41	650	L	12.5	L	6.25	VL	0.3321	0.32
42	650	L	12.5	L	25	L	0.3334	0.33
43	650	L	12.5	L	50	M	0.3350	0.34
44	650	L	12.5	L	75	H	0.3367	0.35
45	650	L	12.5	L	93.75	VH	0.3379	0.354
46	650	L	3.125	VL	6.25	VL	0.3418	0.36
47	650	L	3.125	VL	25	L	0.3421	0.37
48	650	L	3.125	VL	50	M	0.3425	0.38
49	650	L	3.125	VL	75	H	0.3429	0.39
50	650	L	3.125	VL	93.75	VH	0.3432	0.396
51	1100	M	46.88	VH	6.25	VL	0.5356	0.4
52	1100	M	46.88	VH	25	L	0.5403	0.41
53	1100	M	46.88	VH	50	M	0.5465	0.42
54	1100	M	46.88	VH	75	H	0.5527	0.43
55	1100	M	46.88	VH	93.75	VH	0.5574	0.437
56	1100	M	37.5	H	6.25	VL	0.5452	0.44
57	1100	M	37.5	H	25	L	0.5490	0.45
58	1100	M	37.5	H	50	M	0.5540	0.46

CONT.

The generated fuzzy set for the SMRGT-4 model

Rules No.	Precipitation		Land Use		Soil Permeability		Flow Coefficient	Flow Coefficient
	Numerical	**Verbal**	**Numerical**	**Verbal**	**Numerical**	**Verbal**	**(data)**	**(model)**
59	1100	M	37.5	H	75	H	0.5589	0.47
60	1100	M	37.5	H	93.75	VH	0.5627	0.479
61	1100	M	25	M	6.25	VL	0.5581	0.48
62	1100	M	25	M	25	L	0.5606	0.49
63	1100	M	25	M	50	M	0.5639	0.5
64	1100	M	25	M	75	H	0.5672	0.51
65	1100	M	25	M	93.75	VH	0.5697	0.52
66	1100	M	12.5	L	6.25	VL	0.5710	0.525
67	1100	M	12.5	L	25	L	0.5722	0.53
68	1100	M	12.5	L	50	M	0.5739	0.54
69	1100	M	12.5	L	75	H	0.5755	0.55
70	1100	M	12.5	L	93.75	VH	0.5768	0.56
71	1100	M	3.125	VL	6.25	VL	0.5806	0.563
72	1100	M	3.125	VL	25	L	0.5809	0.57
73	1100	M	3.125	VL	50	M	0.5813	0.58
74	1100	M	3.125	VL	75	H	0.5817	0.59
75	1100	M	3.125	VL	93.75	VH	0.5820	0.6
76	1550	H	46.88	VH	6.25	VL	0.7744	0.605
77	1550	H	46.88	VH	25	L	0.7791	0.61

CONT.

The generated fuzzy set for the SMRGT-4 model

Rules No.	Precipitation		Land Use		Soil Permeability		Flow Coefficient	Flow Coefficient
	Numerical	**Verbal**	**Numerical**	**Verbal**	**Numerical**	**Verbal**	**(data)**	**(model)**
78	1550	H	46.88	VH	50	M	0.7853	0.62
79	1550	H	46.88	VH	75	H	0.7915	0.63
80	1550	H	46.88	VH	93.75	VH	0.7962	0.64
81	1550	H	37.5	H	6.25	VL	0.7841	0.645
82	1550	H	37.5	H	25	L	0.7878	0.65
83	1550	H	37.5	H	50	M	0.7928	0.655
84	1550	H	37.5	H	75	H	0.7978	0.665
85	1550	H	37.5	H	93.75	VH	0.8015	0.68
86	1550	H	25	M	6.25	VL	0.7969	0.685
87	1550	H	25	M	25	L	0.7994	0.695
88	1550	H	25	M	50	M	0.8027	0.7
89	1550	H	25	M	75	H	0.8061	0.71
90	1550	H	25	M	93.75	VH	0.8085	0.72
91	1550	H	12.5	L	6.25	VL	0.8098	0.725
92	1550	H	12.5	L	25	L	0.8110	0.73
93	1550	H	12.5	L	50	M	0.8127	0.74
94	1550	H	12.5	L	75	H	0.8143	0.75
95	1550	H	12.5	L	93.75	VH	0.8156	0.76
96	1550	H	3.125	VL	6.25	VL	0.8194	0.77

CONT.

The generated fuzzy set for the SMRGT-4 model

Rules No.	Precipitation		Land Use		Soil Permeability		Flow Coefficient	Flow Coefficient
	Numerical	**Verbal**	**Numerical**	**Verbal**	**Numerical**	**Verbal**	**(data)**	**(model)**
97	1550	H	3.125	VL	25	L	0.8197	0.771
98	1550	H	3.125	VL	50	M	0.8202	0.78
99	1550	H	3.125	VL	75	H	0.8206	0.79
100	1550	H	3.125	VL	93.75	VH	0.8209	0.8
101	1887.5	VH	46.88	VH	6.25	VL	0.9536	0.81
102	1887.5	VH	46.88	VH	25	L	0.9582	0.813
103	1887.5	VH	46.88	VH	50	M	0.9644	0.82
104	1887.5	VH	46.88	VH	75	H	0.9707	0.83
105	1887.5	VH	46.88	VH	93.75	VH	0.9753	0.84
106	1887.5	VH	37.5	H	6.25	VL	0.9632	0.85
107	1887.5	VH	37.5	H	25	L	0.9669	0.855
108	1887.5	VH	37.5	H	50	M	0.9719	0.86
109	1887.5	VH	37.5	H	75	H	0.9769	0.87
110	1887.5	VH	37.5	H	93.75	VH	0.9806	0.88
111	1887.5	VH	25	M	6.25	VL	0.9761	0.89
112	1887.5	VH	25	M	25	L	0.9785	0.895
113	1887.5	VH	25	M	50	M	0.9819	0.905
114	1887.5	VH	25	M	75	H	0.9852	0.91
115	1887.5	VH	25	M	93.75	VH	0.9877	0.92

CONT.

The generated fuzzy set for the SMRGT-4 model

Rules No.	Precipitation		Land Use		Soil Permeability		Flow Coefficient	Flow Coefficient
	Numerical	**Verbal**	**Numerical**	**Verbal**	**Numerical**	**Verbal**	**(data)**	**(model)**
116	1887.5	VH	12.5	L	6.25	VL	0.9889	0.93
117	1887.5	VH	12.5	L	25	L	0.9902	0.935
118	1887.5	VH	12.5	L	50	M	0.9918	0.94
119	1887.5	VH	12.5	L	75	H	0.9935	0.95
120	1887.5	VH	12.5	L	93.75	VH	0.9947	0.96
121	1887.5	VH	3.125	VL	6.25	VL	0.9985	0.967
122	1887.5	VH	3.125	VL	25	L	0.9989	0.976
123	1887.5	VH	3.125	VL	50	M	0.9993	0.983
124	1887.5	VH	3.125	VL	75	H	0.9997	0.992
125	1887.5	VH	3.125	VL	93.75	VH	1.0000	1

CURRICULUM VITAE

Ruya Mehdi Zainalabdeen ZAINALABDEEN

EDUCATION

09/2019 - 08/2023 **Doctor of Philosophy Degree in Civil Engineering**

Gaziantep University, Gaziantep, Turkey.

09/2016 - 01/2019 **Master's Degree in Civil Engineering**

Gaziantep University, Gaziantep, Turkey

09/2009- 06/2013 **Bachelor's Degree in Civil Engineering**

University of Kirkuk Iraq, Kirkuk.

ACHIEVEMENTS OF THE THESIS

1. The study of land use and slope role in flow coefficient determination (5th Advanced Engineering Days (AED) – 21 September 2022 – Mersin, Türkiye).
2. A Comparative Study of Using Adaptive Neural Fuzzy Inference System (ANFIS), Gaussian Process Regression (GPR), And SMRGT Models in Flow Coefficient Estimation(https://doi.org/10.17993/3ctecno.2023.v12n2e44.125-146).
3. Forecasting the Flow Coefficient of the River Basin Using Adaptive Fuzzy Inference System and Fuzzy SMRGT Method https://doi.org/10.12911/22998993/163367.
4. Flow Coefficient Determination in Catchment Based on Analysis of Temperature and Wind Speed Data Using the Fuzzy SMRGT Method https://doi:10.1088/1755-1315/1222/1/012014.
5. Prediction of Runoff Coefficient under Effect of Climate Change Using Adaptive Neuro Inference System (Journals of the University of Babylon, ISSN: 2616 - 9916).

6. Application of a New Fuzzy Logic Model Known as "SMRGT" for Estimating Flow Coefficient Rate (Turkish Journal of Engineering, 8(1), 2024).
7. Computation of Flow Coefficient via Non-Deterministic Approach of Fuzzy Logic Called "SMRGT" Based on Meteorological Properties (Jordan Journal of Civil Engineering, Volume 17, No. 4, 2023).
8. The Impact of Land Use and Slope Change in Flow Coefficient Estimation (Engineering Applications, 2023,2(4), part of the study was published in 5th Advanced Engineering Days (AED))
9. A New Fuzzy Model for Predicting Flow Coefficient Rate Based on Soil Properties and Land Use Information A Case Study of Aksu River Basin (International Journal of Fuzzy Logic and Intelligent Systems (pISSN 1598-2645, eISSN 2093-744X) (The study is under review).
10. Implementation of Back Propagation (BP) Based Artificial Neural Network (BP-ANN), ANFIS, and Fuzzy SMRGT Techniques for Flow Coefficient Estimation of the River Basin: An application to Aksu River Basin- Turkey (MDPI-Sustainability), (The study is accepted with revision).